



**NOAA Educational Partnership
Program
with Minority Serving Institutions**

8TH BIENNIAL EDUCATION AND SCIENCE FORUM

Host

**City College of the City University of New York
NOAA-Cooperative Remote Sensing Science & Technology Center**

through a

**National Oceanic and Atmospheric Administration
Cooperative Agreement Award**

***Advancing NOAA-Mission STEM Fields through Education
and Research Collaborations: Building on a Successful
15-Year Partnership with
Minority Serving Institutions***

Forum Proceedings

Edited By

Reza Khanbilvardi, PhD and Shakila Merchant, PhD

**August 28-31, 2016
New York, NY 10031**

Foreword

After 15 years of successful partnership with Federal–Minority Serving Institutions and the National Oceanic and Atmospheric Administration (NOAA), it's time to celebrate our collective achievements and advancements!

In 2016, the NOAA Cooperative Remote Sensing Science and Technology Center (CREST) at the City University of New York will host the **NOAA Educational Partnership Program with Minority Serving Institutions (EPP/MSI) 8th Biennial Education and Science Forum**. NOAA and CREST will convene representatives from the Federal government, academia and the public/private sectors. This Forum will showcase education and research results supported through EPP/MSI cooperative agreements to four Cooperative Science Centers and student scholarship programs.

I am particularly proud that the education and research conducted by students and faculty at the Cooperative Science Centers, in collaboration with NOAA scientists and managers, is in direct support of NOAA's goals and its mission of science, service and stewardship. It's important that the Forum also expand opportunities to foster professional development through a series of student-focused engagement activities. Through this partnership, we have successfully built, and will continue to build, a diverse talent pool of graduates for NOAA mission fields in science, technology engineering and mathematics.

I am grateful for the co-sponsorship and participation from the private sector and to our academic partners for their support for this Forum. The shared engagement in advancing opportunities is essential to building a more diverse and inclusive America environmental intelligence community.

Sincerely,

A handwritten signature in blue ink, appearing to read 'K. Sullivan', with a long horizontal flourish extending to the right.

Kathryn D. Sullivan, Ph.D.

Under Secretary of Commerce for Oceans and Atmosphere
and NOAA Administrator

Table of Content

THEME I:	1
Climate Adaptation and Mitigation	
Precipitation variations during the recent Sea Surface Temperature warming period in the Intra-Americas Region, 1982–2012	2
<i>E. Glenn, M. Angeles, J. González and T. Smith</i>	
Mapping Field-Scale Soil Moisture Using Ground-Based L-band Passive Microwave Observations in Western Puerto Rico	5
<i>Jonathan Nunez-Olivieri, Jonathan Munoz-Barreto, Rebecca Tirado-Corbala, and Tarendra Lakhankar</i>	
Development of a Mid-Infrared Sea and Lake Ice Index (MISI) using the GOES Imager	7
<i>Peter Dorofy, Rouzbeh Nazari, Peter Romanov, Jeffrey Key</i>	
Drought Response Timescales from Thermal Emission versus Shortwave Remote Sensing	10
<i>Erika Andujar, Nir Krakauer, Chuixiang Yi, and Felix Kogan</i>	
Absorption of Near UV Light by HNO₃/NO₃ on Sapphire Surfaces	12
<i>Manuvesh Sangwan, William R. Stockwell, Devoun Stewart and Lei Zhu</i>	
The Structure and Evolution of the Urban Boundary Layer	14
<i>D. Melecio-Vazquez, J.E. Gonzalez-Cruz, P. Ramamurthy, M. Arend</i>	
Climatology analysis of cirrus cloud in Three different ARM sites	17
<i>K.Olayinka, S.Li(Dr.), E. Joseph(Dr.)</i>	
Observations of Saharan dust long-range transport and optical properties at the Caribbean area	19
<i>Wilson Pena *, Nathan Hosannah , Jorge Gonzalez , Yonghua Wu , Fred Moshary , R. Solis, H. Parsiani, M. Angeles, L. Aponte, R. Armstrong, B. Bornstein, E. Harmsen, L. Leon, D. Niyogi, P. Ramamurthy, M. Angeles, N. Ramirez.</i>	
Atmospheric Ozone and Ultraviolet B Radiation Coupling Impact on Sensitive Crops Production, at Beltsville, Maryland	21
<i>Lekealem Taku,Ricardo Sakai,Everette Joseph</i>	
An Environmental Perspective on the Water Management Policies of the Upper Delaware River Basin	24
<i>A. Arun Ravindranath, B. Naresh Devineni, and C. Peter Kolesar</i>	
Development of a Demand Sensitive Drought Index and its Application for Agriculture over the Conterminous United States	27
<i>E. Etienne, N. Devineni, R. Khanbilvardi, and U. Lall</i>	
Remote Sensing of Snow Estimation: Satellites, Models and Field Experiment	30
<i>Tarendra Lakhankar, Peter Romanov, Carlos Perez, and Reza Khanbilvardi</i>	
Characterizing Aerosol Impacts on the Distribution of Water in the Tropospheric Column During the Monsoon Season in the Philippines	33
<i>Kar’retta Venable and Vernon Morris</i>	
Biophysical Impacts of Sea Level Rise Coastal Policies in Galveston Bay, Texas	34
<i>Rachel Edwards*, James Gibeaut, Marissa Dotson, Mukesh Subedee, and Richard McLaughlin</i>	
Examining the Energetic Importance of Two Gulf Coast Barrier Islands for Transient Birds During Spring Migration	37
<i>Melanie L. Mancuso, Alan H. Kneidel, Armando A. Aispuro, Lori A. Lester, Christopher M. Heckscher</i>	
Global Trends in Mean and Extreme Runoff and Streamflow Simulations Based on Observations and Climate Models	39
<i>Behzad Asadiieh *, Nir Y. Krakauer , Balazs M. Fekete</i>	
Toxic Tides (or A Fatal Coupling of Climate Change & Legacy Pollution)	42
<i>Lemir Teron</i>	
The Relationship between Global Crop Yield and Climatic Trends and Technology Enhancement	43
<i>Ehsan Najafi, Naresh Devineni, Reza Khanbilvardi</i>	
Hydro-climatological Assessment of New York City Water Supply Management: Towards a Sustainable Seasonal Inflow Forecast Based on Climate Indices and Water Releases and Storages	46
<i>Nasser Najibi and Naresh Devineni</i>	

Legal and Policy Aspects of Adapting to Sea-Level Rise Along the Texas Coast.....49
Richard J. McLaughlin

Understanding the Risk to Recreational Fishers and Harvesters in Lee County, Florida from Exposure to Red Tides51
Krystal Pree, Dr. Elijah Johnson, Theresa Goedeke, Larry Robinson, Richard Gragg, and Torhonda Lee

Satellite-based microwave global land emissivity estimation and its application for freeze/thaw detection54
Satya Prakash, Hamid Norouzi, and Christian Campo

The 2016 CREST Undergraduate Research Experience (CURE) at Hampton University57
Baseemah Rucker, Maurice Roots, Kamali Lowe, Millan Robinson and John Anderson

Mapping Building Energy Consumption in New York City59
Yoribaldis Olivo, Prathap Ramamurthy, and Gehovanny Baez

A Delayed-Action Oscillator Model for El Niño.....61
Nour Hadjih, Hassebo, and Frank Wang

THEME II: Weather Ready Nation 63

The Impact of Lightning on Intensity Forecasts Using the HWRf Model64
Keren Rosado, Vijay Tallapragada, Gregory Jenkins

The Validation of Suomi NPP OMPS Limb Profiler Ozone Measurements.....67
S. Buckner, L. Flynn, and D. Barnes

Towards a unified representation of the planetary boundary layer and shallow cumulus convection in numerical climate models70
David A. New

Urban Impacts on New York City Weather During a Heat Wave72
Luis E. Ortiz, Jorge E. Gonzalez, Wei Wu, Robert Bornstein, Martin Schoonen, and Jeffrey Tongue

Remote Sensing Monitoring of Canadian Wildfire Smoke and its Impact on Baltimore Air Quality...75
Shelbi Tippet, Ruben Delgado

Remote sensing of river ice and ice jams using an automated algorithm with local cloud mask for MODIS and VIIRS: Application over the Lower Susquehanna River (2001-2016).....77
S. Kraatz, P. Romanov, and R. Khanbilvardi*

A Complete Picture of Boundary Layer Events in the Plains Elevated Convection at Night (PECAN) Campaign Including Low-level Jet Vertical Winds79
Brian Carroll, Belay Demoz, Ruben Delgado, Bruce Gentry*

Weather: An Exploration of Public Engagement and Understanding of Science through NOAA’S Twitter81
L. Williams

Use of LIDARs in Atmospheric Sciences.....83
Richard Medina

The Continuing Convection, Aerosol, and Synoptic-Effects in the Tropics (CAST) Field Experiment.85
Nathan Hosannah, Jorge González, Rafael Rodriguez-Solis, Hamed Parsiani, Fred Moshary, Luis Aponte, Roy Armstrong, Eric Harmsen, Prathap Ramamurthy, Moises Angeles, Leyda León, Robert Bornstein, Nazaro Ramirez, Robert Davis, Wilson Peña, Chris Lunger, and Dev Niyogi

Evaluation of MODIS land surface temperature with in situ snow surface temperature from CREST-SAFE.....88
Carlos Perez, Tarendra Lakhankar, Peter Romanov, Jonathan Muñoz, Reza Khanbilvardi, and Yunyue Yu

A multilevel Poisson regression model to detect trends in frequency of extreme rainfall events.....91
Saman Armal, Naresh Devineni, Reza Khanbilvardi

Classifying Vertical Wind Speed Profiles for Offshore Wind Resource and Power Assessment.....95
Alexandra St.Pé, Shelbi Tippet, Scott Rabenhorst, Ruben Delgado*

Determination of Planetary Boundary Layer Heights from Doppler Wind Lidar Measurements98
Benjamin Tucker, Ruben Delgado, Brian Carroll, Belay Demoz, Thomas Rieutord, Alan Brewer, Aditya Choukulkar, Timothy Bonin

Investigating the Effects of Saharan Dust on Tropical Deep Convection using Spectral Bin Microphysics101
Matthew Gibbons, Qilong Min, and Jiwen Fan

Determining Planetary Boundary Layer Heights from NWS ASOS Ceilometer Network105
Kweku Mills-Robertson, Ruben Delgado, Kevin Vermeesch, Ricardo Sakai, Dennis Atkinson, Michael Hicks, Belay Demoz

Study of Photolysis Rate Coefficients to Improve Air Quality Models	107
<i>Suhail Mahmud, Pema Wangchuk, Rosa Fitzgerald, Dr. William Stockwell, Dr. Duanjun Lu</i>	
Risk Analysis of New York City Extreme Rainfalls Applying Nonparametric Simulation on Radar Rainfall Data	109
<i>Ali Hamidi, Naresh Devineni, Reza Khanbilvardi</i>	
Tracking Volcanic Aerosols Using CALIPSO and HYSPLIT	112
<i>Sean Leavor, and Michael Hill</i>	
Modeling Regional & Global Atmospheric Chemistry Mechanisms: Observing Adverse Respiratory Health Effects due to Air Pollution from Modeling Output Data.....	114
<i>A. Saunders, Emily M. & B. Stockwell, William R.</i>	
Episodic Rainfall and Saharan Dust Events Analysis Using Ceilometers CL31 and CL51, Satellite and Surface Measurements	116
<i>M.J. Santiago, R.A. Armstrong, and N. Hosannah</i>	
Tracking and Characterizing Stratospheric Aerosols from the Nabro Volcanic Eruption of 2011	118
<i>Ariana Atwell</i>	
Applying The Deep Atmospheric Concept to The NCEP Mesoscale Spectrum Model. The First Part: Implementation of The Generalized Hybrid Coordinate.....	122
<i>Jia-Fong Fan, Hann-Ming Henry Juang and Tsann-Wang Yu</i>	
Aerosols and trace gases modeling in the tropical Atlantic during the summer of 2009	125
<i>A. Jose M Tirado, B. Vernon R Morris</i>	
NCAS-CAREERS Puerto Rico Weather Camp: a decade of achievements, challenges, and opportunities to foster diversity in STEM fields.....	128
<i>Y. Detrés and R. Armstrong</i>	
Active standoff detection of CH₄ and N₂O leaks using hard-target backscattered light using an open-path quantum cascade laser sensor	130
<i>A. Diaz, B. Thomas, P. Castillo, B. Gross and F. Moshary</i>	
Perceptions of Safety and its Gendered Differences: An Exploratory Analysis of Severe Weather Reactions	134
<i>A. Shadya Sanders, B. Terri Adams-Fuller, and C. Everette Joseph</i>	
Inter-annual Variability in Urban Heat Island Intensity Over 10 Major Cities in The United States.....	136
<i>A.Prathap Ramamurthy and B. Michael Sangobanwo</i>	
Guidance Index for Shallow Landslide Hazard Analysis	138
<i>C Avalon Culler, Rafa Al-Suhili, and R. Khanbilvardi,</i>	
Aerosol modeling of volatile organic compounds and sulfur dioxide during particle growth events at Beltsville, MD.....	140
<i>Megan K. Payne, Everette Joseph, William R. Stockwell, and Fangqun Yu</i>	
On the Creation of an Urban Boundary Layer Product Using the Radar Wind Profiler of the New York City Meteorological Network.....	142
<i>Mark J. Dempsey, James F. Booth, Mark Arend and David Melecio-Vazquez</i>	
K-Nearest Neighbor Approach for Developing Gridded Snow Product in Russia	144
<i>Lawrence Vulis, Naresh Devineni, Sean R. Helfrich and Cezar Kongoli</i>	
Planetary Boundary Layer Turbulence Characterization	146
<i>Ivan Valerio, Mark Arend, Fred Moshary, Stephen Nufeld</i>	
The Dynamics of Water Storage Over Lake Eyre, Australia Observed by Satellite Data	148
<i>Obeng Kwaku Buo, Kibrewossen Tesfagiorgis</i>	
THEME III: HEALTHY OCEANS	151
Using the position of digestive contents relative to chlorinated hydrocarbon (CHC) concentrations in the liver to map CHC movement through the smooth dogfish (<i>Mustelus canis</i>)	152
<i>Tyler Plum, Olivia Skeen, and Eric May</i>	
Zooplankton Composition in Hampton Roads, VA: Spatio-temporal Variability and DNA Barcoding of Copepoda	155
<i>Alexandra Salcedo Bauzá, Áurea E. Rodríguez and Deidre M. Gibson</i>	
A molecular approach to study the in situ diet of the pelagic tunicate <i>Thalia democratica</i> (Salpida, Thaliacea) in the South Atlantic Bight (SAB).....	157
<i>A. Natalia B. López-Figueroa, B. Deidre M. Gibson, C. Aurea E. Rodríguez-Santiago, D. Tina Walters and E. Marc Frisher</i>	

Effect of benzo[<i>a</i>]pyrene exposure on clutch size and embryonic development of the daggerblade grass shrimp <i>Palaemonetes pugio</i>	160
<i>Coral Thompson, and Sue C. Ebanks</i>	
Population Ecology of Weakfish in the Maryland Coastal Bays.....	163
<i>Shynna Dale, Rebecca Peters, and Paulins Chigbu</i>	
Analysis of Stranding Demographics, Inorganic Contaminants and Cytotoxicity in Bottlenose Dolphins (<i>Tursiops truncatus</i>) from Coastal Maryland	166
<i>Audy Peoples, Cindy Driscoll, Amanda Wechsler, and Maurice Crawford</i>	
The Use of Probiotics in Shrimp Production	168
<i>Jasmine Smalls*, and Dr. Dennis McIntosh</i>	
The Effects of Hypoxia and Increased Temperature on the Behavior of Larval Estuarine Fish.....	171
<i>Keith Leonard, Gulnihal Ozbay, and Stacy Smith</i>	
Investigating the Application of Multibeam Sonar and Remotely Operated Vehicles in Fish Population Monitoring on Artificial Reefs	173
<i>R. Figueroa-Downing and David Hicks</i>	
Survival of red deepsea crab <i>Chaceon quinquegens</i> Smith, 1879, larvae in cultivation: effects of diet and temperature	175
<i>Nivette M. Pérez-Pérez, Matthew Poach, Bradley Stevens, Stacy Smith, and Gulnihal Ozbay</i>	
Condos and Connectivity: Developing an Interdisciplinary Approach to Guide Caribbean Spiny Lobster (<i>Panulirus argus</i>) Fisheries Management within The Bahamas.....	178
<i>K. Callwood</i>	
Water Quality Monitoring and Validation from NOAA operational satellite sensor (VIIRS) Data Products in Coral Reef Environments.....	181
<i>William J. Hernandez, Roy A. Armstrong, Alan E. Strong, Robert A. Warner, Erick F. Geiger, C. Mark Eakin, Menghua Wang, Maria A. Cardona-Maldonado, Suhey Ortiz-Rosa, Jeremy Kravitz, Myrna J. Santiago.</i>	
Pharmaceuticals and Personal Care Products: Local, National, and Global Challenges.....	183
<i>Zakiya Hoyett*, Marcia Allen Owens, Clayton Clark II, Michael Abazinge</i>	
Protocol Development for Environmental Stressors on Reproduction and Larval Development in the Daggerblade Grass Shrimp <i>Palaemonetes pugio</i>	186
<i>Vanessa Foster, Coral Thompson, and Sue C. Ebanks</i>	
Post-nesting movement patterns of the green sea turtle from the East End beaches of St. Croix, USVI	189
<i>E. Schultz and D. Hoskins</i>	
Satellite retrievals of <i>Karenia brevis</i> harmful algal blooms in the West Florida Shelf using neural networks and comparisons with other techniques.....	191
<i>Ahmed El-habashi and Samir Ahmed*</i>	
Diet analysis of Red Snapper, <i>Lutjanus campechanus</i>, on natural and artificial reefs in the western Gulf of Mexico.....	195
<i>Charles H. Downey, Rachel A. Brewton, Jennifer J. Wetz, Matthew J. Ajemian, and Gregory W. Stunz</i>	
Reducing Discard Mortality in the Northwestern Gulf of Mexico Red Snapper Fishery.....	197
<i>Alex Tompkins, Judd Curtis, Greg Stunz</i>	
Salinity Responses of Oyster Reefs to Freshwater Inflow in Apalachicola Bay NERR, Florida	199
<i>Duc N Le, and Wenrui Huang</i>	
Persistent Impacts to the Deep Soft-Bottom Benthos four years after the Deepwater Horizon Event.....	201
<i>Paul A. Montagna, Jeffery G. Baguley, Jeffery L. Hyland, Cynthia Cooksey</i>	
Carbon Storage in Northern Gulf of Mexico Salt Marshes and Mangroves	204
<i>Lauren Hutchison*, David Yoskowitz, Just Cebrian, and Aaron Macy</i>	
A Study of Nutrient Impacts on HAB Biotxin Concentrations in Apalachicola Bay and Grand Bay National Estuarine Research Reserve.....	206
<i>Shareena Cannonier</i>	
Assessment of fish health parameters of <i>Morone americana</i> (White Perch): A fish health index in the Choptank River, MD.....	208
<i>D. Bell, Dr. M. Abazinge, Dr. C. Jagoe, Dr. L. Gonsalves, M. Matsche</i>	
High resolution measurements of changes in molecular composition of crude oil undergoing degradation by native microbes from the Gulf of Mexico	210
<i>G. Hitz, C. Jagoe, A. Chauhan, E. Hilinski, E. Johnson, and R. Gragg</i>	
Effects of light on vertical migration patterns of <i>Chrysaora quinquecirrha</i> Ciara C. Schnyder	213

<i>Margaret Sexton</i>	
Can Other Crustaceans be a Host to a Fatal Blue Crab Virus?	215
<i>Chiamaka Nnah, Eric Schott</i>	
More Regulation for Healthier Oceans: A look at the Magnuson- Stevens Fishery Conservation and Management Act (MSA)	217
<i>Leara Morris-Stokes</i>	
THEME IV: Resilient Coastal Communities and Economies	219
Simulating Dust Emission and Biota Transport from Playa Systems using a Wind Tunnel	220
<i>Jose Rivas, Thomas E. Gill, Elizabeth J. Walsh, R. Scott Van Pelt</i>	
Benthic Invertebrate Communities at Five South Texas Banks	223
<i>M. Cooksey and D. Hicks</i>	
Improved Remote Sensing Tools for Monitoring Marine Ecosystem Health	225
<i>R. Foster, A. Ibrahim, A. Gilerson, A. McGilloway, A. El-habashi, C. Carrizo, M. Ottaviani, S. Ahmed</i>	
A Survey of Arm Length and Regeneration Abundance in the Forbes Sea Star <i>Asterias forbesi</i> in Wassaw Inlet, GA, USA	228
<i>Rebecca Noel Thublin_1 and Sue C. Ebanks_2</i>	
Wetland Land Use/ Land Cover (LULC) Changes: Case Study from Grand Bay National Estuarine Research Reserve (NERR)	231
<i>Eric M. Gulledege, Ranjani W. Kulawardhana, Taimei T. Harris, Fengxiang X. Han & Paul B. Tchounwou</i>	
Decomposition of Black Mangrove (<i>Avicennia germinans</i>) leaf litter: calibrating estuarine indicators of functional recovery	233
<i>Leticia Contreras*, Alejandro Fierro-Cabo, and Carlos E. Cintra Buenrostro</i>	
Impacts of natural- and human-induced disturbances on Estuarine Wetland Ecosystems: Case study from Grand Bay National Estuarine Research Reserve (NERR), Mississippi, USA	235
<i>Ranjani W. Kulawardhana, Taimei T. Harris, Eric M. Gulledege, Fengxiang X. Han, & Paul B. Tchounwou</i>	
Spatial Patterns and Temporal Dynamics of <i>Juncus roemerianus</i> Dominated Wetland Vegetation Characteristics and Carbon Stocks of Grand Bay National Estuarine Research Reserve (GBNERR), Mississippi, USA	237
<i>Taimei T. Harris, Ranjani W. Kulawardhana, Eric M. Gulledege, Fengxiang X. Han,</i>	
A framework for conducting riverscape genetics studies	241
<i>Chanté Davis, Flitcroft, R.L, and Banks, M.A.</i>	
New VIIRS Satellite Ocean Color Products for Management of Land-Based Sources of Pollution over Coral Reefs	245
<i>Alan E. Strong, Menghua Wang, C. Mark Eakin, Erick F. Geiger, Robert A. Warner, William Skirving, Gang Liu, Scott F. Heron, Kyle V. Tirak, Michael Ondrusek, William J. Hernandez, Maria Cardona-Maldonado, *Roy A. Armstrong, and Jacqueline L. De La Cour</i>	
Satellite Data Products for Coral Reefs in Southwestern Puerto Rico: In Situ Water Quality Measurements for Data Validation	246
<i>*Suhey Ortiz-Rosa, William J. Hernandez, Roy A. Armstrong, Maria A. Cardona-Maldonado, Jeremy Kravitz and Myrna J. Santiago</i>	
Improving coral reef science and management through collaborative efforts from NOAA Educational Partnership Program	249
<i>William J. Hernandez, Maria Cardona-Maldonado, Roy Armstrong, Portia Caldwell, Endia Casely, Charles Jagoe, Marlene Kaplan, William Skirving, Alan E. Strong, Robert A. Warner.</i>	
Evaluation of Oyster (<i>Crassostrea virginica</i>) Density and Slope at Natural and Restored Oyster Reefs in Coastal Georgia	251
<i>P. Clower, T. Taubenheim, D. Hoskins</i>	
The 2014-2016 Global Coral Bleaching Event: Preliminary Comparisons Between Thermal Stress and Bleaching Timing and Intensity	253
<i>Andrea M. Gomez, C. Mark Eakin, Jacqueline L. De La Cour, Gang Liu, Erick F. Geiger, Scott F. Heron, William J. Skirving, Kyle V. Tirak, Alan E. Strong, Kyle C. McDonald, Ana Carnaval</i>	
Offshore Oil Rig Decommissioning and Rigs-to-Reefs Programs in the Gulf of Mexico: Current Status and Strategies, and a Review of Decommissioning Cost Estimation	256
<i>Elena Kobrinski</i>	
Evaluating the Eastern Mosquitofish (<i>Gambusia holbrooki</i>) as a bioindicator species for endocrine disrupting chemicals	259
<i>Queria Simpson and Paulette C. Reneau</i>	

Polarization characteristics of light in water and their impact on the TOA radiances.261
Carlos Carrizo, Gilerson, A., Foster R., Al-Habashi, A., Ottaviani, M.

Urban Flooding Index Based on NYC311 Reporting Database263
Sina Kashuk, PhD; Michael Grossberg, PhD; Masoud Ghandehari, PhD; and Reza Khanbilvardi, PhD

High Temporal and Spatial Resolution Study of Morphological Response to Beach Management.....266
Melanie Gingras, James C. Gibeaut, Michael Starek and Philippe Tissot*

Ecosystem response to freshwater inflow: determining a link between freshwater pumping regimes, salinity, and benthic macrofauna270
Elizabeth A. Del Rosario, Paul A. Montagna*

Resilience in the face of sea level rise: What do people value?273
David Yoskowitz and James Gibeaut

Using Radar Remote Sensing to Map Wetlands in the Chesapeake Bay For the Purpose of Understanding Carbon Cycling Processes275
A. Brian Lamb, B. Maria Tzortziou C. Kyle McDonald

Electrospun Chitosan and Cyclodextrin Nanofibers For Oil Absorption277
De'Marcus Robinson-

Long-term changes in seagrass distribution using a high-spatial resolution satellite image, historic aerial photography and field data279
Mariana C. León-Pérez, Roy A. Armstrong, and William J. Hernandez

Estimate CDOM and DOC in estuarine waters in the Chesapeake Bay and the Gulf of Mexico from ocean color281
Fang Cao, Maria Tzortziou*

Surface Modification of Polyethersulfone Membrane to Control Organic Fouling.....283
Efosa Igbiginun, Yaolin Liu, Ramamoorthy Malaiasamy, Kimberly Jones, and Vernon Morris**

Onsite Bioremediation of Hydrocarbons Using Anaerobic Processes.285
Brian Wartell and Michel Boufadel

THEME I

Climate Adaptation and Mitigation

An informed society anticipating and responding to climate and its impacts



Precipitation variations during the recent Sea Surface Temperature warming period in the Intra-Americas Region, 1982–2012

E. Glenn¹, M. Angeles², J. González² and T. Smith³

¹*The City College of New York, NOAA-CREST, eglenn00@citymail.cuny.edu*

²*The City College of New York, Department of Mechanical Engineering*

³*NOAA/STAR/SCSB and CICS/ESSIC, University of Maryland – College Park*

Abstract

A recent warming trend of sea surface temperatures (SST) has been detected in the Intra-Americas Region (IAR) for the past 30 years (1982-2012), which could have potential implications for precipitation variation within the Caribbean and the surrounding region. This study investigates precipitation trends for the same period to determine variations as a result of warming SSTs.

Introduction

The Intra-Americas Region (IAR), defined as the geographical region that includes the Caribbean, Mexico, Central America and parts of North and South America, is a region of distinct climatological activity. A recent warming trend of sea surface temperatures (SSTs) has been detected in the IAR for the past 30 years (1982-2012), with the warmest trends occurring during the latter half of the period [1]. Warming SSTs in the Caribbean and surrounding region can have potential implications for Tropical precipitation variation. Results show that SSTs are increasing annually for the region and slightly faster than the annual global rate of 0.011°C per year. The two characteristic Caribbean rainy seasons, the Early Rainfall Season (ERS) from April to June and the Late Rainfall Season (LRS) from August to November, also show an increase in SSTs for the 30-year period. Increases in SSTs during the LRS are of particular importance because temperatures during this season reach 26°C and above, which is the threshold for deep convection. Within this temperature range (26°C – 29°C), rainfall dependence on SSTs increases by a factor of 5 and the atmosphere becomes the principal modulator of thermal convection [2]. In this way, SSTs influence Tropical precipitation.

For this study, we investigated climatological precipitation trends within the IAR for the observed SST warming period from 1982-2012. To identify trends, statistical significance and related variations between SSTs and precipitation, the following statistical analysis methods were applied: linear regression, the modified Mann-Kendall trend test and joint Principal Component Analysis (PCA), also referred to as Empirical Orthogonal Function (EOF) analysis. The Global Precipitation Climatology Project (GPCP) precipitation dataset used for this research was provided by NOAA/OAR/ESRL/PSD from their website at <http://www.esrl.noaa.gov/psd/> [3]. The GPCP dataset combines observations and satellite precipitation data into 2.5°x2.5° global grids and provides mean monthly rainfall rates (in mm). The SST dataset was acquired from the NOAA National Centers for Environmental Information (NCEI), available at <http://www.ncdc.noaa.gov/sst>. This dataset is the Optimum Interpolation Sea Surface Temperature Product, referred herein as OISST, which uses Advanced Very High Resolution Radiometer (AVHRR) infrared satellite SST data from the Pathfinder satellite combined with buoy data, ship data, and sea ice data SST datasets [4]. The data has a spatial grid resolution of 0.25° and the temporal resolution is daily.

The precipitation analysis, using the GPCP monthly precipitation dataset, shows that the

Methodology and Conclusions

past 15 years (1997-2012) average precipitation for the LRS has been slightly above the climatology calculated from the years 1982 to 2012. Results suggest that the observed increases in SSTs may be connected to the changes in precipitation for the same period. SST daily anomalies reflect a warming trend over the past 15 years, which further suggests the significant influence that SSTs potentially have on precipitation. During the ERS, warming SSTs in the region North of South America and above the threshold for vertical convection were found to be highly cross-correlated (0.79) with precipitation. For the LRS, cross-correlation with precipitation and the SSTs near South America also show a high, positive cross-correlation (0.78), similar to ERS results.

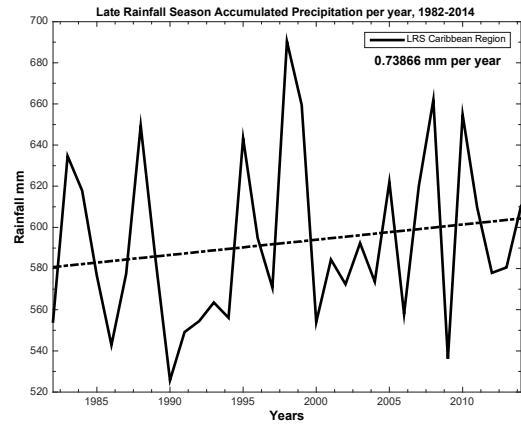
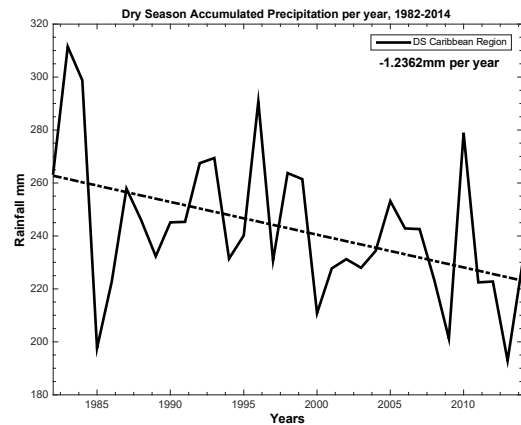
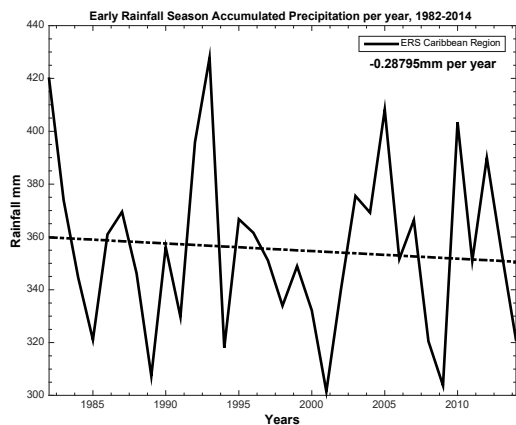
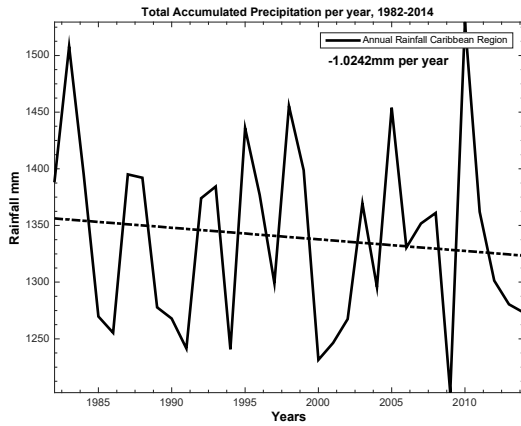


Figure 1. Summary of results for the regional (spatial) average trend for the years 1982-2014 – clockwise from top left: total accumulated rainfall per year, total accumulated Early Rainfall season rainfall per year, total accumulated Dry Season rainfall per year, total accumulated Late Rainfall Season rainfall per year.



Linear and nonlinear analyses of precipitation trends reveal that regionally averaged accumulated rainfall is decreasing for all seasons except the LRS, but were not determined to be statistically significant for the 30-year period. However, per-grid analyses show that accumulated rainfall per season has been increasing in the southern part of the region, with high statistical significance primarily for the LRS. Conversely, the Dry Season (DS), from December to March, reflects

the steepest decreasing trends associated with statistically significant p-values (Figure 1). Furthermore, the areas determined to be statistically significant are primarily over ocean versus trends observed over land. Additional biases were reflected in high-elevation land-masses indication of regional orographic rainfall.

References

- [1] E. Glenn, D. Comarazamy, J. González, and T. Smith, *Geophys. Res. Lett.*, **42** (2015) 6785–6792.
- [2] I. Folkins, C. Braun, *J. Climate*, **16** (2003) 1807-1820.
- [3] R. Adler, G. Huffman, A. Chang, R. Ferraro, P. Xie, J. Janowiak, B. Rudolf, U. Schneider, S. Curtis, D. Bolvin, A. Gruber, J. Susskind, P. Arkin, *J. Hydrometeor.* **4** (2003) 1147-1167
- [4] R. Reynolds, T. Smith, C. Liu, D. Chelton, K. Casey, M. Schlax, *J. Climate*, **20** (2007) 5473-5496.

Acknowledgement

This study was supported and monitored by National Oceanic and Atmospheric Administration (NOAA) under the Office of Education Partnership Program award NA11SEC4810004 and the Graduate Research Training and Scholarship Program. The statements contained within the manuscript/research article are not the opinions of the funding agency or the U.S. government, but reflect the author's opinions.

Mapping Field-Scale Soil Moisture Using Ground-Based L-band Passive Microwave Observations in Western Puerto Rico

Jonathan Nunez-Olivieri¹, Jonathan Munoz-Barreto¹, Rebecca Tirado-Corbala³, and Tarendra Lakhankar⁴

¹*Department of Civil Engineering and Surveying, University of Puerto Rico – Mayaguez, Puerto Rico*

³*Department of Agro-Environmental Sciences Agricultural Experiment Station (AES) – Mayaguez, University of Puerto Rico - Mayaguez*

⁴*NOAA-CREST, City University of New York, New York, NY*

Presenting Author: Jonathan Nunez-Olivieri

Email: jonathan.nunez1@upr.edu

Address: Fajardo Gardens Calle Cedro 375 Fajardo, PR 00738

Introduction

Ground-based L-band passive microwave observations are needed to test the accuracy in the measurements made by satellite-based radiometers such as the NASA's Soil Moisture Active Passive (SMAP) mission. Satellite-borne microwave radiometers have been providing products about atmospheric and oceanic parameters for several years [1].

This project will provide new information related to soil and vegetation parameters by performing ground measurements of soil moisture content from L-band passive microwave observations. These parameters influence the readings of the L-Band Microwave Radiometers Satellite and will be useful for the calibration and validation of the data provided by the NASA Soil Moisture Active Passive (SMAP) mission. Also, more accurate readings of soil moisture content in the western are of Puerto Rico are to be provided. These results will help the characterization and modeling of spatial characteristics of soil moisture over Puerto Rico soils, which are highly representative of the soils in the tropics.

The availability of accurate and representative soil moisture content data provides a significant amount of resources for important applications such as:

- Weather and Climate Forecasting. Accurate soil moisture data enhances the products of numerical weather prediction and

seasonal climate models, which will represent a good benefit for climate-sensitive activities [2].

- Droughts. Having a continuous monitoring system for soil moisture will enhance the models which are used to determine potential water shortage and drought events, which is strongly useful for agricultural development [2].

- Floods. The surface soil moisture state is highly related to the partitioning of precipitation into infiltration and runoff which are key variables for flood prediction modeling [2].

- Agricultural Productivity. Determination of accurate soil moisture data is an essential parameter for the application of best agricultural management practices. The availability of continuous updated dataset of spatio-temporal soil moisture measurements can be used to improve irrigation scheduling, enhancing water use and productivity of the crops and by reducing water costs of the agricultural activities.

The project is being coordinated by the Professor Jonathan Muñoz-Barreto, PhD, from the Department of Civil Engineering and Surveying at the University of Puerto Rico Mayagüez, the Professor Rebecca Tirado-Corbala from the Department of Crops and Agro-environmental Sciences of the University of Puerto Rico Mayagüez, the Research Professor Tarendra Lakhankar, PhD, from the

CUNY-CREST Institute at The City College of New York, graduate student Jonathan Nuñez-Olivieri from the Department of Civil Engineering and Surveying at the University of Puerto Rico Mayagüez, and the project is running in collaboration with NOAA-CREST and the USA Corps of Engineers.

Experiments and Conclusions

The CREST L-band (1.48 GHz) microwave radiometer (LBMR) observation unit was used in three temporal sites for soil moisture monitoring. The observations include spatiotemporal measurements of L-band brightness temperatures, surface temperature, and soil moisture. These observations are to be made on soils under variable conditions like bare soil and soil under a variation of crops. These sites, located in Mayagüez, Lajas, and Isabela, are all part of the Agricultural Experiment Stations (AES) program of the University of Puerto Rico.

Correlation between brightness temperature and in-situ soil moisture is to be studied to make preliminary inferences on the attenuation effect of the radiometric response due to the presence of different types of vegetation. This correlation is expected to tend to negative values, indicating that an increase in soil moisture leads to a decrease in brightness temperature. Another expected result is a potential attenuation on the radiometric response of the soil, which will confirm that different crops and vegetation conditions does reduce the sensitivity of the microwave sensor to the soil moisture.

Further studies will include the specific determination of the attenuation factor for each crop studied, the implementation of the microwave emission model Tau-Omega to determine the soil moisture content, and the validation of satellite-based radiometers.

References

- [1] F. T. Ulaby, R. K. Moore, and A. K. Fung, 1986. *Microwave Remote Sensing. Active and Passive*. Vol. 3
- [2] Entekhabi, D., Njoku, E. G., O'Neill, P. E., Kellogg, K. H., Crow, W. T., Edelstein, W. N., ... Van Zyl, J. (2010). The soil moisture active passive (SMAP) mission. *Proceedings of the IEEE*, 98(5), 704–716. doi:10.1109/JPROC.2010.2043918.

Acknowledgement

This study was sponsored by the Puerto Rico Water Resources and Environmental Research Institute and Hatch 202. Special thanks to all members of the Geospatial Research Lab at the University of Puerto Rico Mayaguez.

Development of a Mid-Infrared Sea and Lake Ice Index (MISI) using the GOES Imager

¹Peter Dorofy, ¹Rouzbeh Nazari, ²Peter Romanov, ³Jeffrey Key

¹Rowan University

²NOAA Cooperative Remote Sensing Science & Technology Center

³NOAA National Environmental Satellite, Data, and Information Service (NESDIS)

Abstract

An automated ice-mapping algorithm has been developed and evaluated using data from the GOES-13 imager. The approach used in the algorithm development includes cloud-clear image compositing as well as pixel-by-pixel image classification using spectral criteria. Data in available spectral channels (reflectance and infrared brightness temperature) have been tested and used to develop the algorithm. The algorithm uses an alternative to the Normalized Difference Snow Index (NDSI). The newly proposed Mid-Infrared Sea and Lake Ice Index (MISI) is the ratio of the VIS (0.62 μm) band and the reflective component of the mid-infrared, MIR (3.9 μm) band. Incorporating MISI into a sea or lake ice mapping algorithm allows mapping of thin or broken ice with no snow cover (nilas, frazil ice) and thicker ice with snow cover to a degree of confidence that is comparable to other ice mapping products.

Introduction

Ice on the Great Lakes region impacts society in various sectors; including, hydropower generation, commercial shipping, and the fishing industry. Changes in ice also effect navigation as heavy ice changes the water level. Scientists observe long-term changes in ice cover as a result of global warming. Studying ice coverage over the Great Lakes provides an opportunity for scientists to study regional climate patterns.

NDSI has been used in algorithms for snow and ice mapping products. NDSI is the normalized difference between the 0.6 μm visible band and the 1.6 μm shortwave infrared (SWIR) band. NOAA's Geostationary Operational Environmental Satellites (GOES) have been the backbone of geosynchronous environmental monitoring of the Americas since 1975. These satellites provide both the temporal resolution and regional coverage over the Great Lakes required for this particular study. The GOES 5-channel imager does not operate in the SWIR, necessary for NDSI; it does however operate in the MIR.

The basis of using MIR reflectance has been employed in previous studies in demonstrating snow/cloud discrimination from the ratio of VIS/MIR, used for automated snow mapping.

The focus of this study is to apply the ratio of VIS/MIR to sea and lake ice mapping. The goal of MISI is to distinguish between sea and lake ice pixels and ice-free water bodies. Furthermore, MISI considers the spectral property differences between thick ice and the relatively darker, grey ice; such as frazil or nilas in both the VIS and MIR.

The proposed index has been applied over the Great Lakes region and qualitatively compared against the Ice Mapping System (IMS), the National Ice Center ice concentration maps and MODIS snow cover products. The application of MISI may open additional possibilities in climate research and sea and lake ice studies using historical GOES imagery that did not operate in the SWIR. Furthermore, MISI may be used in addition to the current NDSI in ice identification for building more robust ice mapping algorithms or as a replacement to NDSI in the event of a sensor failure in the SWIR band in next generation GOES.

Experiments and Conclusions

The Great Lakes was selected as the study site. Data collected by the GOES-13 imager instrument was used in this study. The GOES imager is a 5-channel instrument (one visible,

four infrared). The approach used in the algorithm development includes pixel-by-pixel image classification. The classification is based on specific spectral criteria. Thick ice and snow will have relatively high reflectivities in the visible, but noticeably lower reflectivities in the mid-infrared. It is these specific differences in spectral signatures that is the basis for identifying and discerning between thin and or broken ice and thicker ice. Reflectances of GOES-13 channels 1 and 2, VIS (0.62 μm) and MIR (3.9 μm) are used in development of MISI. A decision tree routine has been employed on a pixel-by-pixel basis. The major criteria in discriminating between “thicker” ice from grey ice is based on the comparison in VIS reflectances ($\text{VIS}_{\text{thick ice}} > \text{VIS}_{\text{grey ice}}$) and the VIS/MIR ratio (MISI). Pixels with less than unity for MISI are classified as grey ice. Ice pixels greater than unity persist as thick ice. The model produces a daily composite lake ice map with four classes: water, grey ice, ice, and cloud.

Comparison of the final products with the Interactive Multisensor Snow and Ice Mapping System (IMS) maps show that the proposed model has high potential in lake ice mapping and shows better resolution with finer pixels. The MODIS snow product has higher resolution; however, the temporal resolution of GOES-13 allows for better cloud contamination resilience. The model also demonstrates a more comprehensive product; includes both grey ice and thick ice. One of the principle motivations of this project is to contribute to the ongoing GOES-R satellite research and preparation which is scheduled to launch in 2016. GOES-R will have both increased temporal and spatial resolution and operate not only in the 1.6 μm which is currently used in traditional NDSI snow mapping, but also in the 3.9 μm which has been the focus of this study for lake ice mapping. The proposed lake ice algorithm will produce the first comprehensive ice map from a U.S. optical geostationary satellite. The algorithm may open a new era in the capabilities of ice mapping systems and climate studies using historical GOES imagery data.

References

- [1] Allen Jr, R. C., Durkee, P. A., & Wash, C. H. (1990). Snow/cloud discrimination with multispectral satellite measurements. *Journal of Applied Meteorology*, 29(10), 994-1004.
- [2] Baum, B. A., & Trepte, Q. (1999). A grouped threshold approach for scene identification in AVHRR imagery. *Journal of Atmospheric and Oceanic Technology*, 16(6), 793-800.
- [3] Dozier, J. (1989). Spectral signature of alpine snow cover from the Landsat Thematic Mapper. *Remote sensing of environment*, 28, 9-22.
- [4] Hall, D. K., Riggs, G. A., & Salomonson, V. V. (1995). Development of methods for mapping global snow cover using moderate resolution imaging spectroradiometer data. *Remote sensing of Environment*, 54(2), 127-140.
- [5] Haq, M. A., Jain, K., & Menon, K. P. R. (2012). Development of new thermal ratio index for snow/ice identification. *Int. J. Soft Comput. Eng*, 1(6), 2231-2307.
- [6] Kyle, H. L., Curran, R. J., Barnes, W. L., & Escoe, D. (1978). A cloud physics radiometer. In *3rd Conference on Atmospheric Radiation* (pp. 107-109).
- [7] Lee J., Chung C., Ou M. (2015). Evaluation of the Geostationary Satellite Based Snow and Sea Ice Detection Algorithm. National Institute of Meteorological Research/Korea Meteorological Administration, Gisangcheong-gil 45, Seoul, Republic of Korea
- [8] Nazari, R. (2010). *Development of an advanced technique for mapping and monitoring sea and lake ice for the future GOES-R Advanced Baseline Imager (ABI)* (Doctoral dissertation, CITY UNIVERSITY OF NEW YORK).
- [9] Perovich, D. K. (1979). *The optical properties of young sea ice* (No. SCIENTIFIC-17). WASHINGTON UNIV SEATTLE DEPT OF ATMOSPHERIC SCIENCES.
- [10] Perovich, D. K. (1996). *The Optical Properties of Sea Ice* (No. MONO-96-1). COLD REGIONS RESEARCH AND ENGINEERING LAB HANOVER NH.

[11] Perovich, D. K., Roesler, C. S., & Pegau, W. S. (1998). Variability in Arctic sea ice optical properties. *Journal of Geophysical Research: Oceans*, 103(C1), 1193-1208.

[12] Riggs, G., & Hall, D. K. (2004, June). Snow mapping with the MODIS Aqua instrument. In *Proceedings of 61st Eastern Snow Conference* (pp. 9-11).

[13] Romanov, P., Gutman, G., & Csiszar, I. (2000). Automated monitoring of snow cover over North America with multispectral satellite data. *Journal of Applied Meteorology*, 39(11), 1866-1880.

[14] Salisbury, J. W., D'Aria, D. M., & Wald, A. (1994). Measurements of thermal infrared spectral reflectance. *Journal of Geophysical Research*, 99(B12), 24-235.

[15] Valovcin, F. R. (1976). *Snow/Cloud Discrimination* (No. AFGL-TR-76-0174). AIR FORCE GEOPHYSICS LAB HANSCOM AFB MASS.

[16] ZENG, Q., CAO, M., FENG, X., LIANG, F., CHEN, X., & SHENG, W. (1984). Study on spectral reflection characteristics of snow, ice and water of northwest China. *SCIENTIA SINICA SERIES B-CHEMICAL BIOLOGICAL AGRICULTURAL MEDICAL & EARTH SCIENCES*, 27(6), 647-656.

Acknowledgement: The research was funded by Rowan University

Drought Response Timescales from Thermal Emission versus Shortwave Remote Sensing

Erika Andujar¹, Nir Krakauer², Chuixiang Yi³, and Felix Kogan⁴

¹*The City College of New York, New York, NY, Eanduja00@citymail.cuny.edu*

²*The City College of New York, New York, NY, Nkrakauer@ccny.cuny.edu*

³*Queens College, Flushing, NY*

⁴*NOAA/NESDIS, College Park, MD*

Abstract

Several different approaches based on remote sensing have been used for monitoring drought impacts on ecosystems, but few large-scale comparisons of the response timescale to drought of different vegetation remote sensing products are available. Here, we computed correlations of two different NOAA vegetation health products derived from polar-orbiting radiometer observations with a meteorological drought indicator available at different timescales, the Standardized Precipitation Evapotranspiration Index (SPEI), to evaluate possible differences in ecosystem drought response timescales across latitudes and biomes. The remote sensing products are Vegetation Condition Index (VCI), which uses Normalized Difference Vegetation Index (NDVI) anomalies computed from visible and near-infrared reflectance to identify plant stress, and Temperature Condition Index (TCI), based on thermal infrared emission as a measure of land surface temperature.

Our results suggest that different vegetation remote sensing approaches tend to respond to different timescales of meteorological drought, and that thermal emission based approaches may be better suited for early drought detection than vegetation color based approaches.

Introduction

Drought can reduce access to water supplies, leading to malnutrition and famine as well as disturbances in ecosystems [1]. As a result of anthropogenic global warming, it is expected that the frequency and intensity of drought will increase in many areas of the world driven by reductions in precipitation along with increased evapotranspiration from higher temperatures [2]. One of the major concerns associated with drought effects include changes in ecosystem dynamics as a result of tree and other plant mortality [3] which can lead to alterations in plant community composition, species distributions and carbon and water cycling [4].

Remote sensing can be applied to drought monitoring by monitoring surface radiative properties related to vegetation stress or soil moisture status [5]. The goal of this study is to determine how long meteorological drought takes to manifest globally, and in croplands, grasslands and evergreen broadleaf forest ecosystems, in the remotely sensed Vegetation Condition Index (VCI) and

Temperature Condition Index (TCI) products. VCI is a reflective index that uses land surface color to assess vegetation stress, while TCI uses thermal emission to assess land surface temperature (LST). These vegetation health indices are derived from NOAA's Advanced Very High Resolution Radiometer (AVHRR) sensor data and available from the NOAA STAR Global Vegetation Health Products webpage [6] for most weeks since 1981. Based on the review of earlier studies, it is hypothesized that the response timescale to meteorological drought onset will be shorter for TCI than for VCI and that the response of remote sensing based indicators to drought will vary depending on ecosystem.

Experiments and Conclusions

Pearson correlation analysis between the meteorological drought indicator SPEI, and VCI and TCI was computed at different drought timescales (1-24 month SPEI) to determine the drought timescales for which VCI and TCI responded most globally and for cropland, grassland and evergreen broadleaf forest ecosystems. SPEI is based on anomalies

in monthly average precipitation (P) minus potential evapotranspiration (PET) [7]. SPEI products were accessed from the Global SPEI database. Ecosystem types were delineated from the MODIS 2009 MODIS land-cover data product (MCD12Q1) [8]. All rasters were resampled to have the same 0.5 x 0.5 degree resolution and extent before the correlation analysis was performed.

Globally, the best correlation for TCI was with the two-month timescale SPEI, while VCI correlated best with much longer timescale droughts (17 month timescale). Among specific land cover types, cropland, grassland and evergreen broadleaf forest showed a peak response time of two months for TCI, and about 10 months for VCI. Additionally, the magnitude of correlation of SPEI with TCI was generally higher than that of VCI, which can partly be a result of the common temperature component in SPEI and TCI. The later response time of VCI relative to TCI could be due to the biophysical changes necessary in vegetation before drought can be detected, as opposed to TCI which reflects the faster onset of heat and moisture limitation. Our findings suggest that thermal based emission approaches may be better suited than color based approaches for earlier drought detection.

References

- [1] IPCC, "Climate Change 2007: Working Group II: Impacts, Adaptation and Vulnerability," 2007. [Online]. Available: https://www.ipcc.ch/publications_and_data/ar4/wg2/en/ch3s3-4-3.html. [Accessed 22 June 2016].
- [2] J. Sheffield and E. F. Wood, "Projected changes in drought occurrence under future global warming from multi-model, multi-scenario, IPCC AR4 simulations," *Climate Dynamics*, vol. 31, pp. 79-105, 2008.
- [3] E. Pasho, J. J. Camarero, M. d. Luis and S. M. Vicente-Serrano, "Impacts of drought at different time scales on forest growth across a wide climatic gradient in north-eastern Spain," *Agricultural and Forest Meteorology*, pp. 1800-1811, 2011.
- [4] R. L. Scott, E. Hamerlynck, G. D. Jenerette, M. S. Moran and G. A. Barron-Gafford, "Carbon dioxide exchange in a semidesert grassland through drought-induced vegetation change," *Journal of Geophysical Research*, vol. G3, p. 115, 2010.
- [5] M. Choi, J. M. Jacobs, M. C. Anderson and D. D. Bosch, "Evaluation of drought indices via remotely sensed data with hydrological variables," *Journal of Hydrology*, vol. 471, pp. 265-273, 2013.
- [6] NOAA, "Vegetation Health Product: Algorithm Description," [Online]. Available: <http://www.ospo.noaa.gov/Products/land/vhp/algo.html>. [Accessed 2 May 2016].
- [7] S. Vicente-Serrano, S. Beguería and J. I. López-Moreno, "A Multiscalar Drought Index Sensitive to Global Warming: The Standardized Precipitation Evapotranspiration Index," *Journal of Climate*, vol. 23, pp. 1696-1718, 2008.
- [8] M. Friedl, D. McIver, J. Hodges, X. Zhang, D. Muchoney, A. Strahler, C. Woodcock, S. Gopal, A. Schneider, A. Cooper, A. Baccini, F. Gao and C. Schaaf, "Global land cover mapping from MODIS: algorithms and early results," *Remote Sensing of Environment*, vol. 83, no. 1-2, pp. 287-302, 2002.

Acknowledgement

This study was supported and monitored by National Oceanic and Atmospheric Administration (NOAA) under NOAA-CREST Grant # NA11SEC4810004 The statements contained within the manuscript/research article are not the opinions of the funding agency or the U.S. government, but reflect the author's opinions.

Absorption of Near UV Light by HNO₃/NO₃ on Sapphire SurfacesManuvesh Sangwan¹, William R. Stockwell², Devoun Stewart² and Lei Zhu³¹ *New York State Department of Health, Wadsworth Center, Albany, New York 12201, United States*² *Howard University, Department of Chemistry, Washington, D.C. 20059, United States*³ *SUNY-Albany, Department of Environmental Health Sciences, Albany, New York 12201, United States***Abstract**

Near UV light (290 – 350 nm) absorption by nitric acid was determined using Brewster angle cavity ring-down spectroscopy. Near monolayer HNO₃ surface absorption cross-section data have been obtained; they range between $(1.7 \pm 1.1) \times 10^{-19}$ and $(0.29 \pm 0.03) \times 10^{-19}$ cm²/molecule. This study suggests that a small percentage (<5%) of adsorbed HNO₃ formed by HNO₃ deposition on sapphire surfaces is dissociated into surface nitrate on the timescale of about 10-15 minutes. These values were used to model the photolysis rates of HNO₃/NO₃⁻ absorbed on aerosols surfaces and its relative importance in the atmosphere was determined.

Introduction

Each year mineral dust aerosols contribute significantly to the global aerosol load. Work done by Yu shows that from 2007 to 2013, 28 Tg a⁻¹ of dust were estimated to have been deposited into the Amazon Basin [1]. Gas phase HNO₃ can undergo physical and chemical interactions with various environmental surfaces including the surfaces of mineral dust aerosols and the ground [2]. It is believed that mineral dust aerosols may provide reactive sites for many tropospheric reactions to occur [3]. HNO₃/NO₃⁻ deposited on aerosol surfaces can undergo photolysis. Even though gas phase HNO₃ photolysis is slow, studies have shown that HNO₃/NO₃⁻ deposited on surfaces can undergo photolysis at a faster rate [2]. Zhou et al, reported that HNO₃ absorbed on environmental surfaces such as the ground and vegetation undergo photolysis 1-2 orders of magnitude faster than in the gas phase to form NO_x and HONO [4]. NO_x and HONO are two important precursors that lead to tropospheric Ozone formation.

In order to understand the reactivity of mineral dust, SiO₂ and Al₂O₃ surfaces are often used to mimic the reactivity of mineral dust surfaces [5] since they are the two most abundant oxides present in mineral dust. Studying the reactivity of mineral dust surfaces

will add to our understanding of the fate of many atmospheric gases. The objective of this paper is to determine the near UV absorption cross sections of HNO₃ deposited on sapphire and to calculate the photolysis rate constant of HNO₃/NO₃⁻ absorbed on aerosol.

Experiments and Conclusions

Near UV absorption by HNO₃ deposited on sapphire surfaces was measured by injecting a linearly polarized probe beam into the ring-down cavity containing a sapphire Brewster window [2]. More details on the experimental setup can be found elsewhere [1]. The photolysis rate coefficient was calculated using a radiative transfer model. The photolysis rate constant can be determined using the equation shown below.

$$J = \int \Phi(\lambda, T) \sigma(\lambda, T) \Phi(\theta, \lambda) d\lambda$$

E1

where Φ is the quantum yield, σ is the absorption cross-section, a function of wavelength, λ and temperature, T and $\Phi(\theta, \lambda)$ is the actinic flux. Literature solar flux data for best albedo was used with the assumption of clear sky. The quantum yields for surface HNO₃/NO₃⁻ was assumed to be unity. The photolysis rate constant was determined as a function of solar zenith angle between 0 and 90 degrees.

The near UV light (290-345 nm) absorption by HNO_3 deposited on sapphire surfaces was determined using Brewster angle cavity ringdown spectroscopy. The apparent monolayer surface absorption cross section values of HNO_3 was measured. The results obtained from this experiment shows evidence for the dissociative adsorption of HNO_3 on sapphire surfaces [1]. The near UV absorption cross sections of nitrate on solid surfaces were also reported in the 320-345 nm region [1].

The photolysis rates of $\text{HNO}_3/\text{NO}_3^-$ on urban grimes were also modeled. The results obtained suggest that the J values for surface absorbed HNO_3 is higher than that of surface absorbed NO_3^- in the 0-90 zenith angle range (figure 1). Our estimated photolysis rate constant for surface absorbed $\text{HNO}_3/\text{NO}_3^-$ were in agreement with field observed photolysis rate constants on urban grimes in Toronto Canada.

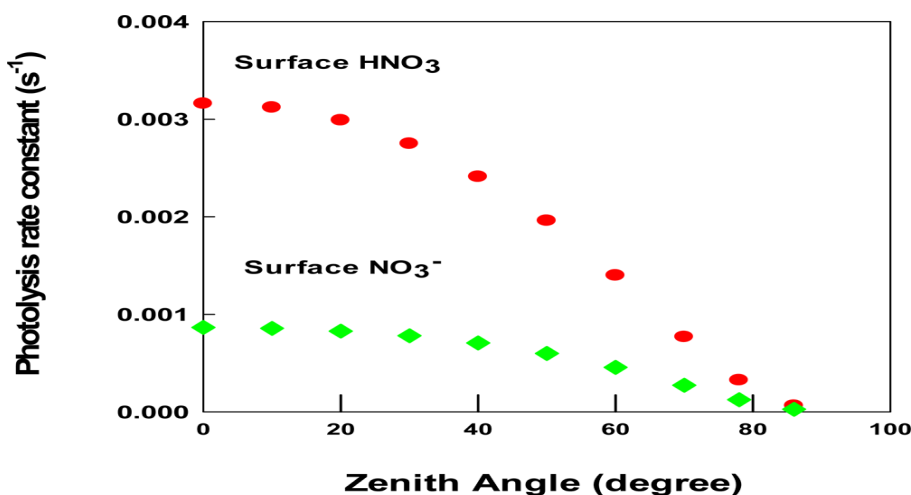


Figure 1: Modeled surface absorbed photolysis for $\text{HNO}_3/\text{NO}_3^-$ on sapphire surfaces [1].

This study was supported and monitored by the National Science Foundation under grant #AGS-1405610 and the National Oceanic and Atmospheric Administration (NOAA) under

References

- [1] H. Yu, M. Chin, T. Yuan, H. Bian, L. A. Remer, J. M. Prospero, A. Omar, D. Winker, Y. Yang, Y. Zhang, Z. Zhang, C. Zhao, *Geophys. Res. Lett.* **42** (2015) 1984-1991.
- [2] M. Sangwan, W.R. Stockwell, D. Stewart, L. Zhu, *J. Phy. Chem.* **120** (2016) 2877-2884.
- [3] C.R. Usher, A.E. Michel, V.H. Grassian, *Chem Rev.* **103** (2003) 4883-4940
- [4] X. Zhou, Y. He, G. Huang, H. Thornberry, T.D. Carroll, M.A. Bertman, *Geophys. Res. Lett.* **29** (2002) 26-1
- [5] M.N. Romanias, A. El zein, Y. Bedjanian, *J. Photochem. Photobiol. A. Chem.* **250** (2012) 50-57

Grant – NOAA Center for Atmospheric Sciences (NCAS) Grant # NA11SEC4810003.

The statements contained within the manuscript/research article are not the opinions of the funding agency or the U.S. government, but reflect the author's opinions.

Acknowledgement

The Structure and Evolution of the Urban Boundary Layer

D. Melecio-Vazquez, J.E. Gonzalez-Cruz, P. Ramamurthy, M. Arend

The City College of New York

Abstract

The boundary layer dynamics of urban microclimates has important effects on precipitation, cloud formation, and air quality and dispersion processes. It is thus important to understand the evolution of boundary layer dynamics. Despite this importance, urban effects on the distributions of key weather variables in the boundary layer are not well-understood. Herein, an extreme local convective event with a maximum lapse rate of 14.5 K/km was analyzed along with seasonal averages of vertical profiles. The non-heat event period considered experienced a maximum of about 6 K/km. Vertical distributions of the thermal and moisture variables, such as temperature and water vapor density, were measured from microwave radiometer measurements at the City College of New York. Traditional convective mixed layers usually exhibit a uniform distribution in the potential temperature and other conserved variables. These urban profiles however showed non-instantaneous mixing, with a very noticeable minimum in potential temperature at about ~250-500m into the mixed layer.

Introduction

Stratification, or the difference in density with height in the atmosphere, creates a layering of the atmosphere (i.e. mixing layers, residual layers, entrainment zones, stable boundary layer, etc.) in response to the complex exchange processes that occur in this near-surface region of the troposphere.

Microwave remote sensing, used to produce the vertical profiles in this paper, takes advantage of the Rayleigh-Jeans approximation that simplifies the radiative transfer problem by being able to neglect scattering (Petty 2006). Scattering only becomes important during precipitative events where raindrops, hail and snow, therefore microwave radiometers can maintain their usefulness even in non-precipitating cloudy conditions (Xu et al. 2015).

In an urban context, temperature profile data are not as prevalent as wind profiles (Barlow 2014), especially in the upper levels of the urban boundary layer. Some of the works on the temperature structure in urban areas were performed in the comparison of urban and rural profiles up to 600m such as in Khaikine et al. (2006). Datasets of temperature profiles, as presented here are, therefore, very valuable for bringing insights into the overall vertical

structure of the urban atmospheric boundary layer.

Instrument Locations and Data

The instrument used in this observational report is the Radiometrics Profiling Radiometer model MP-3000A (a microwave radiometer: MWR). The MWR is located at the roof of the engineering building at the City College of New York (40.821519°-73.948184°). The MWR is a passive instrument that provides estimates of the vertical profiles of the temperature, the relative humidity, water vapor density and the liquid water density. This is done by measuring the brightness temperatures at several bands and then using a neural network to estimate the vertical profiles (58 levels; non-uniform spacing, with finer resolution in the boundary layer). At every level, the virtual potential temperature is calculated, $\theta_v = \theta (1 + 0.61r_v - r_l)$ where θ , is the potential temperature, r_v is the water vapor mixing ratio, and r_l is the liquid water mixing ratio.

For this observational report, only the winter and summer seasons will be examined. The summer season spans the months of June, July, and August of 2015, while the winter months span December 2014, January 2015 and February 2015.

Virtual Potential Temperature Structure and Evolution

Figure 1 contains the vertical profiles of virtual potential temperature for the winter/summer daytime/nighttime (4 profiles in total). Each average is across 6 hours during the daytime and nighttime. The wintertime (daytime is an average between 10AM and 4PM; nighttime is an average between 10PM and 4AM) profiles are about 20 K cooler than the summertime profiles. The standard deviations of the wintertime and summertime profiles is ~10 K and ~5 K, respectively.

These vertical profiles allow us to estimate the approximate thermal planetary boundary layer height (TPBLH; or the height at which a raised parcel from the surface becomes neutrally buoyant) in order to track the vertical structure. The winter daytime and nighttime profiles exhibit smaller TPBLH due to the relative lack of upward buoyant motion present during the summer, with values ranging from 200-250m for the nighttime and 600m for the daytime. The summer daytime profile exhibits a much larger TPBLH, estimated at about 1200m. The summer nighttime profile however is very stable and does not have a noticeable TPBLH, as defined for the other profiles but the temperature increases with height which denotes a stable atmosphere.

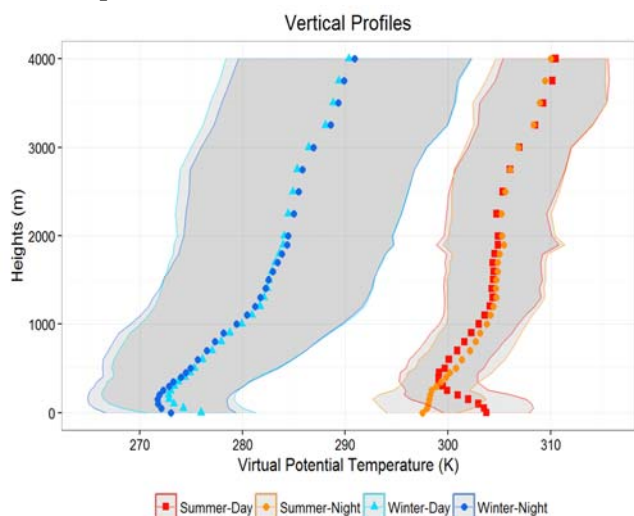


Figure 1: Seasonal averages of vertical profiles of the virtual potential temperature. Daytime averages are done between the hours of 10AM to 4PM. Nighttime averages are done between the hours of 10PM and 4AM.

Figure 2 tracks the time evolution of the virtual potential temperature under mean (left) and extreme heat event conditions (right). These two dates are compared against the summer diurnal average (shown in the black contour lines). The figure shows that both dates have a similar structure as the average diurnal profile with the majority of the changes being in the difference in magnitudes experienced in other layers. The nocturnal layer is much more diminished in both time and vertical extent during the heat event than before it.

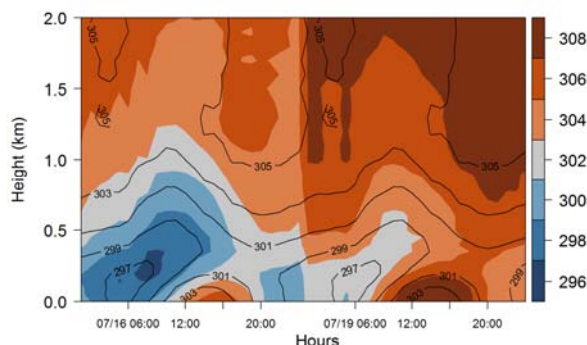


Figure 2: Time evolution of the vertical profile of virtual potential temperature for a heat event compared to the diurnal average of the summer. The filled contours represent two dates of a July 2013 heat event; the left 24hr period is on 07/16/2013 which is the day before the start of the heat event; the right 24hr period is the third (and final) day of the heat event.

Conclusions and Future Work

The work done in understanding the observations of the vertical structure of the urban atmospheric boundary layer is performed in order to yield insight into the underlying physics. Then the structure can then be parameterized into numerical weather

prediction models which can lead to better forecasts in urban centers.

References

- [1] Barlow, Janet F. 2014. *Urban Climate* 10 (December): 216–40. doi:10.1016/j.uclim.2014.03.011.
- [2] Khaikine, M. N., I. N. Kuznetsova, E. N. Kadygrov, and E. A. Miller. 2006. *Theor. Appl. Climatol.* **84** (1-3): 161–69. doi:10.1007/s00704-005-0154-z.
- [3] Petty, Grant W. 2006. 2nd ed. Madison, Wis: Sundog Pub.
- [4] Xu, Guirong, Baike Xi, Wengang Zhang, Chunguang Cui, Xiquan Dong, Yuanyuan Liu, and Guopao Yan. 2015. *J Geophys Res Atmos* **120** (19): 10,313–10,323. doi:10.1002/2015JD023438.

Acknowledgement

This study was supported and monitored by National Oceanic and Atmospheric Administration (NOAA) under Grant No: NA11SEC4810004.

Climatology analysis of cirrus cloud in Three different ARM sites

K.Olayinka¹, S.Li(Dr.)², E. Joseph(Dr.)³

¹Howard University 1, Ph.D student 1 Email: kafayat.olayinka@bison.howard.edu

²Howard University 1, Mentor 1 Email: siwei.li@howard.edu

³SUNY Albany 1, Advisor 1 Email: ejoseph@albany.edu

Abstract

Cirrus cloud play an important role in the atmospheric energy balance and hence in the earth's climate system. The properties of optically thin clouds can be determined from measurements of transmission of the direct solar beam. The accuracy of cloud optical properties determined in this way is compromised by contamination of the direct transmission by light that is scattered into the sensors field of view. With the forward scattering correction method developed by Min et al., (2004), the accuracy of thin cloud retrievals from MFRSR has been improved. In this study, we do statistics studies on cirrus clouds properties based on multi-years cirrus cloud measurements from MFRSR at ARM sites and HUBC site. The site locations include mid-latitude, tropics and North-pole regions. Through the statistic studies, temporal and spatial variations of cirrus clouds are investigated.

Introduction

Studies have shown about 20%-30% annual mean of cirrus cloud are present in the global atmosphere, which contributes in the net atmospheric radiation budget. Cirrus clouds are thin clouds in a form of ice crystals located at the upper altitude of the atmosphere. In the presence of cirrus "thin" clouds, both the reflection of incoming solar radiation and the outgoing infrared radiation emitted by earth surface has an impact in the warming of the earth surface. Although, cirrus radiative influence is mostly overlooked, it is important to investigate its microphysical properties. The retrieval of cirrus optical depth is possible by using both remotely sensed satellite data and ground base instruments like the Multi-Filter Rotating Shadowband Radiometer (MFRSR).

In this research, the variance and mean of over a decade data (1998-2012) of cirrus clouds is investigated in different ARM region (mid-latitude, tropics, and the polar).As well as the occurrence of thin clouds in these sites. And because the presence of cirrus cloud increases the effect of greenhouse gases, the retrieval the aerosol optical depth in all the cirrus cloud regions using a radiative transfer

model for atmospheric correction is implemented.

Experiments and Conclusions

With the in-situ instrument (Multi-Filter Rotating Shadowband Radiometer (MFRSR)), it is possible to retrieve daily atmospheric measurements within Southern Great Plain (SGP), Northern Slope of Alaska (NSA), and Tropical Western Pacific (TWP) sites. Also, in order to understand the climatology of cirrus "thin" clouds, it is of a great relevance to identify the range of cirrus clouds (altitude), the size properties, the optical depth distributions, and occurrences. The monthly mean of these sites shows the statistical estimator of cirrus to have quasi-stationary properties (i.e., its monthly variation does not change much). With a graphical representation of cirrus cloud distribution, the observation shows average of cirrus optical depth to be between 1 and 2(COD) in the 3-region's atmosphere. Calculating the total cirrus detection time over the total instrument measurement time gives us monthly occurrences of cirrus.

References

- [1] C.Hoareau et al.: Adecade cirrus clouds climatology. Atmos.Chem.Phys.,13,6951-6963,2013.
- [2] E.Joseph and W. Wang: Cirrus radiation parameterization for GCM. Jon. Of Geophys. Research,vol104,NO. D8,pg. 9501-9515,1999.
- [3] Steve Graham 1999. “the earth climate system constantly adjust.” clouds and radiation

Acknowledgement

Howard University NCAS (NOAA Center of Atmospheric Sciences) NA11SEC4810003

Observations of Saharan dust long-range transport and optical properties at the Caribbean area

Wilson Pena ^{1*}, Nathan Hosannah ¹, Jorge Gonzalez ¹, Yonghua Wu ¹, Fred Moshary ¹, R. Solis², H. Parsiani², M. Angeles², L. Aponte², R. Armstrong², B. Bornstein², E. Harmsen², L. Leon², D. Niyogi², P. Ramamurthy², M. Angeles², N. Ramirez².

¹ Electrical Engineering Department at the City College of New York, * Email: wpenalo000@citymail.cuny.edu

² University of Puerto Rico, Mayaguez (UPRM) Campus

Introduction: Long-range transport of Saharan Dust (SD) across the tropical Atlantic Ocean makes potential impacts on the Caribbean basin that are related to the variabilities of climate and ecosystem environment, particularly during the midsummer drought (MSD) in June and July (Prospero, et al., 2013). A field campaign measurement was made to investigate the effects of Saharan Dust (SD) on precipitation development at Puerto Rico between June 22 and July 12 of 2015 (a midsummer drought (MSD)) (Hosannah, et al., 2015). This study presents the observation-based SD optical properties, long-range transport and potential impacts on the air quality over UPRM. The data are collected from a three-channel Lidar, ceilometer (Vaisala CL-51), and multiple AERosol RObotic NETwork (AERONET) sunphotometers at La Parguera, Mayagüez, CAPE San Juan, and Guadeloupe. The trans-Atlantic transport pathways and spatial patterns of SD are evaluated with the satellites data (MODIS, CALIPSO, OMI) and NOAA-HYSPLIT model. The variations of surface PM10 and PM2.5 are analyzed during the SD intrusion periods.

As shown in Fig.1, the ground-based show that the SD layers are mainly located below 4.0 km altitude on June 24, 2015. The aerosol optical depths (AOD) increase up to 0.6 at 500-nm while the Angstrom exponents become smaller with the range of 0.1~0.3 at the wavelength pair of 440-870 nm (not shown here). Meanwhile, both high levels of MODIS-AOD and OMI-aerosol index (AI) clearly indicate the transport pattern or the

zone (5°N-25°N) of the SD across the Atlantic Ocean. The NOAA-HYSPLIT model indicates that the SD at 2-4 km levels travels for about 5-7 days from the Africa coast to the Caribbean area. On June 18, 2015, a dust storm episode was further verified in the latitude between 5° and 30° N over the African deserts from the CALIPSO measurements. The dust layers are generally below 6-km with the large depolarization ratio of 0.2~0.3 and color ratio. The surface PM10 data over the Puerto Rico show a relatively large value with the daily average concentration of 84 µg/m³.

Acknowledgements: This study was supported and monitored by National Oceanic and Atmospheric Administration (NOAA) under Grant No: NA11SEC4810004.

We also acknowledge the data from NASA MODIS, CALIPSO and NOAA-HYSPLIT.

References

- [1] Joseph M. Prospero and Olga L. Mayol-Bracero, Understanding the Transport and Impact of African Dust on the Caribbean Basin, *Bulletin of the American Meteorological Society*, 94:9, 1329-1337, 2013
- [2] Nathan Hosannah, H. Parsiani, J. E. González, N. D. Ramirez, D. V. Morris, R. A. Armstrong, A Field Campaign for Tropical Convective Precipitation During Saharan Dust Season, AMS annual meeting, January 04 - 08, 2015, Phoenix, AZ, USA.

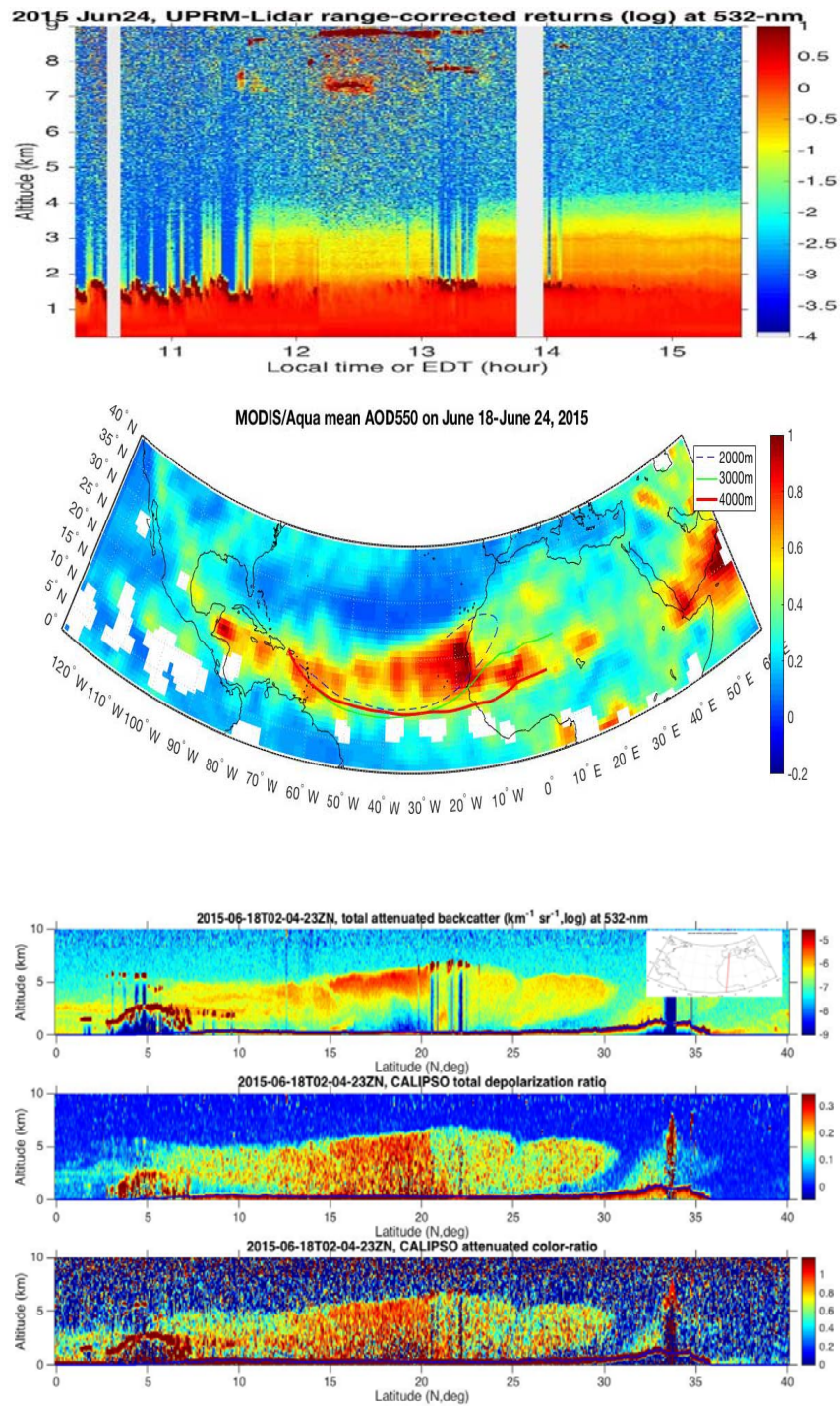


Figure 1 (top) Range-corrected lidar returns at UPRM on June 24, 2015, (middle) MODIS/Aqua AOD and HYSPLIT air backward trajectories at 2-4 km, (bottom) CALIPSO total attenuated backscatter, depolarization ratio and color ratio on June 18, 2015.

Atmospheric Ozone and Ultraviolet B Radiation Coupling Impact on Sensitive Crops Production, at Beltsville, Maryland

¹Lekealem Taku,²Ricardo Sakai,³Everette Joseph

¹Howard University, Ph. D student

²Howard University, Mentor

³SUNY Albany, Advisor

Abstract

Over the past decades, annual average background surface ozone concentration [O₃] and ultraviolet 'B' radiation have been identified as two major surface atmospheric factors that have been increasing annually, at different level based on location. But in most places, the O₃ increase with an average of 0.3 ppb per year due to anthropogenic and natural activities in the environment. This increase has led to environmental stresses such as phototoxicity and phytotoxicity in vegetation and human respectively. Due to the fact that both atmospheric factors have similar impacts on vegetation, lots of research studies carried have attributed the causes of vegetation damage to either one of these factor without clear distinction of the two. There is no research publication on UV-B and O₃ pairing impact on sensitive vegetation in the environment, causing necrosis and chlorosis. The objective here is to perform statistical analyses on the daily 8 hour O₃ concentration and UV-B daily mean values (integrated over time), NDVI, CO₂ and PAR from 2006 – 2015 during growing seasons in order to understanding which of the factors causes more stress to sensitive crops and the frequency of it during growing season that could be used for policy making. This would be helpful to farmers' decision making. The following corn and soybean's sensitivity threshold limit leading to damage acquired from experiments were used as a baseline for the trend analysis, such as for ozone 70 ppb; meanwhile for UV-B is 12 kJ/m²/d.

Introduction

Over the past decades, annual average background surface ozone concentration [O₃] and ultraviolet 'B'(UV-B) radiation have been two major tropospheric components impacting the environment with phototoxicity and phytotoxicity (Agrawal et al., 2006; WHO, 2016) on vegetation and human respectively. Based on the status quo of experimental studies, it was estimated that ambient O₃ exposure leads to national-level economic major crops yield loss approximately \$1 billion per year in the United States (EPA, 1996), and globally approximately \$14 to 26 billion per year for rice, soybean, maize and wheat combined (Royal Society, 2008). Crop damage by UV-B is estimated to increase up to 23.4 billion by the year 2075 (Lee, 1989).

The HYPOTHESE is that given the strong relationship between Ozone and UV-B and

their similar impacts on crops (causing necrosis and chlorosis), how could one differentiate crop yield loss cause by O₃ or UV-B or both while putting into consideration other major factors?

Understanding of the relationship between ozone, ultraviolet (UV-B) and their impact on the ecosystem and human environment is of great interest. From research findings, it is well understood that background surface ozone is a major atmospheric constituent whose interaction with UV-B radiation (a major solar radiation constituent) has drew the attention to many scientist as well as policy makers in the human environment. The mechanism for O₃ formation involves both natural source (stratospheric intrusions of O₃ from the upper atmosphere and lightning during thunderstorms) and anthropogenic source (photochemical reaction cycle, driven by UV from sunlight). The later formation consist of

the most important mechanism for the formation of O₃ at the earth surface (Krupa et al 2000). From the Scientific committees, 2007, the sun is the most common source of ultraviolet radiation (UV). The UV radiation leads to the formation of ozone from its precursors such as volatile hydrocarbons (VOCs) and the oxides of nitrogen, which are produced by both anthropogenic and natural biological processes (Krupa et al 2000).

The UV radiation is divided into three major bands of which UV-B (the medium-wavelength, 280–315 nm), is approximately 10% of the UV radiation that reaches the Earth's surface. From WHO, 2016, the UV-B (medium-wavelength) is very biologically.

High levels of both O₃ and UV-B lead to similar acute and chronic symptoms of foliar injury such as leaf bronze, glazing, necrosis and necrotic spots (Krupa et al 2000; Kakani et al, 2003). Ozone is the major constituent of photochemical smog (a combination of smoke and fog e.g., peroxy acetyl nitrate [PAN]), and the level changes because of the seasonal changes in the intensity of the sun, high O₃ concentrations occur during the plant-growing season. With regards to the global UV irradiance reaching the Earth's surface, the past decades estimated data from satellite reveals that there has been a significant rise in zonal average ultraviolet irradiance at all latitudes from the period of 1979 to 1989, with exception to the equatorial zone (Herman, 2010). During the summer period of July 18 to 23, 2011, there was a recorded high temperature (41.7°C) and poor air quality (with daily maximum 8-h average (MDA8) ozone of approximately 97.0 part per billion by volume (ppbv)), caused by a classic heat wave that hit the metropolitan Baltimore/Washington area (He et al., 2014).

Studies have been carried out in order to show that air pollution from ozone may have adverse impacts on crops production such as *Vigna radiata* L. (mung bean) plants grown from germination to maturity around peri-urban and rural areas, based on 6 -h daily mean O₃ concentrations varied from 9.7 to 58.5 ppb. It was found out that this levels of ozone cause phytotoxicity to plants that led to the reductions in biomass accumulation, low quality and poor

seed yields in highest ozone concentrations (Agrawal et al., 2006). Exposure to elevated O₃ concentration typically results in suppressed photosynthesis, accelerated senescence, decreased growth and lower yields. Various approaches used to evaluate O₃ effects generally agree that current yield losses vary from 5% to 15% among sensitive plants (Booker et al., 2009). O₃ damage to soybean crop was documented by Fishman et al., 2010.

Experiments and Conclusions

To better address these hypotheses, the corn and soybean's O₃ and UV-B sensitivity threshold limit acquired from experiments were used as a baseline for the trend analysis. Ozone was 70 ppb; and UV-B was 12 kJ/m²/d. This is due to the fact that the global terrestrial UV-B radiation levels range between 0 and 12 kJ/m²/day (Kakani, 2003) and also too based on the US, air quality guidelines for ozone, established in order to protect human health and vegetation, the current secondary ozone standard designed to protect human welfare and vegetation was proposed to be the maximal 8 hour average O₃ concentration of 75 ppbV that should not be exceeded more than 3 times per year, with the average fourth highest concentration over a 3-year period determining whether a location is out of compliance (Van Dingenen, 2009).

Data analysis involves seasonal, monthly, and weekly plots of UV-B, Ozone, NDVI (Normalized Differential Vegetation Index, 400-900nm), CO₂ and PAR at the surface level from 2006-2015. NDVI, tells of the vegetation greenness and health, and PAR (Photosynthetic Active Radiation, 600-800nm), tells of the amount of light received for photosynthesis and photomorphogenesis, because insufficient or excessive light levels can lead to excessive stress. In addition, data for weekly crop condition update is used to match results. Data for the annual yield of crop would be performed also.

In conclusion, O₃ and UV-B have do not have a strong relation during high pollution episodes of O₃ and UV-B turns to be more steady in all the years, meanwhile PAR is highly affected by cloud/aerosols and

atmospheric pollution especially, 2011, which intend affects the NDVI.

References

- [1] [1] U.S. Environmental Protection Agency. 1996. Air Quality Criteria for Ozone and Related Photochemical Oxidants, Volume I of Ill Document 1 of 1. Page 53.
- [2] [2] U.S. Environmental Protection Agency. 1996. Air Quality Criteria for Ozone and Related Photochemical Oxidants, Volume I of Ill Document 1 of 1. Page 53.
- [3] [3] Lee S.D G.J.R., Wolters L.D. Grant T. Schneider, 1989. Atmospheric Ozone Research and its Policy Implications. New York, NY Elsevier Science Publishers, table 1 on page 899. First Edition.

Acknowledgement

This study was supported and monitored by National Oceanic and Atmospheric Administration (NOAA) under Grant – Howard University NCAS (NOAA Center for Atmospheric Science) Grant # NA11SEC4810003. This study was also supported by Beltsville Center for Climate System Observation (BCCSO). I also want to thank, Dr. Joseph and Dr. Sakai for their relentless supports.

An Environmental Perspective on the Water Management Policies of the Upper Delaware River Basin

A. Arun Ravindranath¹, B. Naresh Devineni¹, and C. Peter Kolesar²

¹*City University of New York, City College, Department of Civil Engineering, Center for Water Resources and Environmental Research, NOAA-Cooperative Remote Sensing Science and Technology Center*

²*Columbia University, Columbia Business School, Columbia Water Center*

Abstract

Since 1954, the Delaware River has been managed under the framework of a Supreme Court decree and the subsequent concomitant intergovernmental collaboration between New York State, New Jersey, Pennsylvania, Delaware, New York City (NYC) and the US federal government. Taking an environmental perspective, we review the evolution of water release policies for three NYC reservoirs from the issuance of the 1954 decree through the implementation of the Flexible Flow Management Program (FFMP) of 2007–2015 and examine the policies' impact on the upper Delaware River. We describe governmental and institutional constraints on the development of Delaware water policy and show how modifications of release policies have enhanced aquatic habitat and ecological health in the upper Delaware while reliably delivering water to NYC and the Delaware's other principal stakeholders. We describe the development of the FFMP in 2006, its subsequent modification, and its augmentation by NYC's Operations Support Tool in 2012. Finally, we discuss the negative ecological consequences of the 2010–2016 stalemate on Delaware water policy resulting from conflicts between the decree parties about current and future water rights, and how the stalemate derives partially from the decision structure imposed by the 1954 decree and the Good Faith Agreement of 1983.

Introduction

The Delaware River, originating in the Catskill Mountains of New York State, is the longest undammed river in the United States east of the Mississippi [2]. It flows through the states of Pennsylvania, New Jersey, and Delaware, emptying into the Atlantic Ocean in the Delaware Bay after running 330 miles from the confluence of its east and west branches at Hancock, New York [2]. Consequently, all four states have claims to Delaware water. The Delaware River Basin (DRB) drains roughly 13,000 square miles and supplies more than 15 million people with water for drinking, agricultural and industrial use. The river is also an important recreational boating and fishing resource, and has tremendous economic value. The Delaware contributes to the water supplies of New York City and Philadelphia, and to parts of central New Jersey that are outside the basin. It provides aquatic habitats that are

crucial for wildlife throughout its reaches, ranging from the trout of the upper river to the oysters of Delaware Bay.

The river supports cold-water species in the upper river and migratory fish, including the American shad, blueback herring, alewife, sea lamprey, American eel and shortnose sturgeon [6]. It is home to aquatic invertebrate and freshwater mussel species including the federally endangered dwarf wedge mussel [8]. The trout of the upper Delaware, in particular, feed on various species of aquatic insects, the survival of which is highly dependent on sufficient water flows [4]. Moreover, the Delaware indirectly supports non-aquatic fauna, such as black bears, bald eagles, and ospreys [8]. Water storage reservoirs built by New York City on the headwaters upstream of these habitats divert water out of the basin, thereby modifying upper river flows and directly impacting the aquatic insects and cold-water

marine life, and potentially affecting other wildlife as well.

In the NYC metropolitan area, more than 9 million people are served by the City's upstate reservoirs in Westchester County, the Catskill Mountains and the Delaware drainage of the Catskills. Roughly 50% of the inflow to the City's three upper Delaware ("PCN") reservoirs is diverted out of the Delaware Basin to the City and these diversions constitute about 50% of the City's needs. Mandated releases into the river from the PCN reservoirs are intended to meet multiple downstream objectives, including notably protecting the water supply well downstream for Trenton, Philadelphia and much of central New Jersey, and supporting the cold-water fisheries below the dams. Since 1932, the primary water policy/water management issue on the Delaware has been and remains today, how to balance the diversion needs of New York City, the interests of down-basin stakeholders and the needs of the aquatic ecology downstream of the reservoirs.

We discuss the evolution of PCN reservoir release policies. Our analysis starts with the framework set out by the 1954 Supreme Court decree (347 U.S. 995 (1954)) that governs much of Delaware water policy and continues to the signing of the Interstate Delaware Compact of 1961, which established the Delaware River Basin Commission (DRBC) as a regulatory and supervisory body. We then move on to discuss the 'Good Faith Agreement' of 1983, a release policy modification that was motivated primarily by Delaware's 1960s drought of record. We discuss the development of Delaware's current Flexible Flow Management Program (FFMP), which incorporates the technology of New York City's recently developed computer-based Operations Support Tool (OST) algorithm. Amplifying previous work, and adding a broad policy context, our review goes back to examine the history of the Delaware release policies prior to the FFMP, and then extends the picture to include the modifications to the FFMP made since 2007, most notably the incorporation thereto of the City's OST algorithm in 2011 [7]. We statistically assess

the trends in the annual reservoir storage levels, releases, spills into the river, water diversions to New York City and a system risk metric, the number of 'drought days' for the PCN reservoir system, using the Mann-Kendall non-parametric trend test [4,5]. We also conducted a non-parametric rank sum test to verify whether the differences (before and after the FFMP) in the 7-day low flows (a measure of the ecological health of the river) below the dams are statistically significant.

Conclusions

Our quantitative analysis indicates both long-term and immediate-term patterns of improving water availability for the ecology of the upper Delaware. Both the narrative of the evolution of DRB water policy and the analysis suggest that to a considerable extent the stated goals of the FFMP, to revise the previous release policies, to better sustain the fisheries and aquatic habitat downstream of the dams and to mitigate potential flood impacts in the basin, without increasing the drought risk to the City have been achieved. Unfortunately, there remain policy stalemates among the Decree Parties on policy modifications to the FFMP since 2010. This is indicative of deep, unresolved problems that, so far, have left no clear path to a resolution.

References

- [1] Caucci, A. (1998). The Delaware's second season. Fly Fisherman Magazine, 23(4), 38–44, 74, 76.
- [2] Delaware River Basin Commission (2013). The Delaware River Basin Commission. Available at: <http://www.state.nj.us/drbc/> (accessed 10 January 2015).
- [3] Elliott, W. P. (1998). Delaware River Basin releases from a trout's perspective. Clearwaters Magazine 27(1), 37–42.
- [4] Helsel, D. R. & Hirsch, R. M. (2002). Statistical Methods in Water Resources Techniques of Water Resources Investigations. Book 4, chapter A3, 522 pages. U.S. Geological Survey. Available at: <https://pubs.usgs.gov/twri/twri4a3/>.

- [5] Mann, H. B. (1945). [Nonparametric tests against trend](#). *Econometrica* 13(3), 245–259.
- [6] Sheppard, D. & Karat, E. (1978). Water for the charmed circle. *The Conservationist* 44, 1–13.
- [7] New York City Department of Environmental Protection (2011). Water System Safe Yield Calculation – 2011. City of New York. Available at: http://www.nyc.gov/html/dep/pdf/ffmp/water_system_safe_yield_calculation_2011.pdf (accessed 12 January 2015).
- [8] US National Park Service, National Wild and Scenic Rivers System, US Department of the Interior (2012). Delaware River Basin: National Wildlife and Scenic River Values. National Park Service. Available at: http://www.nps.gov/dsc/ne/DelawareRiverBasin_Sept2012.pdf (accessed 12 January 2015).

Acknowledgments

This research was supported by:

- (a) National Science Foundation grant 1360446 (Water Sustainability and Climate, Category 3).
- (b) Professional Staff Congress – City University of New York award 67832-00 45.
- (c) City University of New York – Collaborative Incentive Research Grant award 80209-13 21.
- (d) National Oceanic and Atmospheric Administration – Cooperative Institute for Climate and Satellites – Maryland award 76514-05 01.

Development of a Demand Sensitive Drought Index and its Application for Agriculture over the Conterminous United States

E. Etienne¹, N. Devineni¹, R. Khanbilvardi¹, and U. Lall²

¹*CUNY – City College, NOAA-CREST*

²*Columbia University, Columbia Water Center*

Abstract

A new drought index is introduced that explicitly considers both water supply and demand. It can be applied to aggregate demand over a geographical region, or for disaggregated demand related to a specific crop or use. Consequently, it is more directly related than existing indices, to potential drought impacts on different segments of society, and is also suitable to use as an index for drought insurance programs targeted at farmers growing specific crops. An application of the index is presented for the drought characterization at the county level for the aggregate demand of eight major field crops in the conterminous United States. Two resiliency metrics are developed and applied with the drought index time series. In addition, a clustering algorithm is applied to the onset times and severity of the worst historical droughts in each county, to identify the spatial structure of drought, relative to the cropping patterns in each county. The geographic relationship of drought severity, drought recovery relative to duration, and resilience to drought is identified, and related to attributes of precipitation and also cropping intensity, thus distinguishing the relative importance of water supply and demand in determining potential drought outcomes.

Citation: Etienne, E., Devineni, N., Khanbilvardi, R. and Lall, U. (2016). Development of a Demand Sensitive Drought Index and its application for agriculture over the conterminous United States. *Journal of Hydrology*, 534, pp.219-229.

Introduction

Drought leads to high economic and social impacts. The diverse sectors affected by drought, its wide spatial and temporal distribution, and most importantly, the demand placed on water supply by human use systems makes it a complex phenomenon that needs systematic understanding [1]. While many global and national drought indicators exist none directly connect existing or projected water demand to the potential water deficit during the drought. They are essentially supply based. The standardized drought indices [2] consider only water supply but not water use by sector or in aggregate. Drought's impacts manifest as a supply - demand imbalance issue, and vary by location and by sector of use. If a location has low demands, drought as manifest in the usual indices does not really have the

same impact, as in a region where most water is appropriated or allocated. In this paper, we present a new Demand Sensitive Drought Index (DSDI) that is based on daily water demand for selected crops, and the daily precipitation over the continental United States. Two measures for drought resiliency that are based on the probability of transitioning to a satisfactory state from an unsatisfactory state are presented at the county level. Proposed changes in a crop mix, i.e., the distribution of area allocated to each crop, can be mapped to changes in the DSDI, and hence both the changes in the potential resilience and the drought severity and duration conditional on a crop mix can be evaluated. An application to the conterminous USA is developed and presented.

Methodology and Conclusions

We present a demand sensitive drought index, DSDI, which considers day-to-day rainfall variability as well as water demands to develop aggregate or disaggregated indices for water uses. The methodology is based on the sequent peak algorithm that is commonly used for the sizing of reservoirs [3]. Variants of this methodology have been presented earlier to measure current water risk in India [4] and the United States [5]. Applied to a time series of water supply and demand, the algorithm identifies the drought stress as the cumulative deficit over the period under consideration. DSDI can thus be represented considering daily resolution of time series of supply and demand for a geographic unit j (e.g. U.S. county) as follows:

$$deficit_{j,t} = \max(deficit_{j,t-1} + D_{j,t} - S_{j,t}, 0), \text{ where } deficit_{j,t} \text{ is the cumulative deficit at time } t \text{ for geographic unit } j.$$

$$DIC_j = \max_t (deficit_{j,t} | t = 1:n \times 365)$$

$deficit_{j,t}$ refers to the accumulated daily deficit, $D_{j,t}$ to total or sector wise daily water demand, $S_{j,t}$ to the total water daily supply volume, for geographical location j , and day t ; and n is the total number of years in the analysis.

The maximum accumulated deficit estimated over the n -year period without breaking it into sub-periods is defined as DIC_j (Drought Index Cumulated). This measures the potential impact of multiyear droughts per demand sector, or in aggregate. One can develop the corresponding normalized drought index as:

$$DSDI_j = DIC_j / AR_j$$

Where AR_j is the average annual rainfall volume (cropped area * average depth of precipitation) for the county j .

We also estimate the resiliency of a given region using two measures, the resiliency rate (i.e. the probability of recovery from a drought state) and the relative recovery (that indicates on an average basis whether the drought events recover faster than they last).

The drought index described above is developed and presented for the agricultural sector over the continental United States given that agricultural water demand is dominant over much of the country. For conciseness, we present the results for the total agricultural water demand but the index can be disaggregated into individual crop/demand indices. Furthermore, the index can be derived for or integrated with other water use sectors such as industrial and domestic uses.

In terms of assessing drought impacts, the indicator portrayed in this study has the advantage of breaking supply and demand down into their respective components, allowing us to better understand the causes of drought frequency, duration and severity from an impact perspective. As such, the index can contribute to developing more effective planning strategies for the regional managers to minimize drought impacts in the current or future/projected climate and demands. The daily integration feature of the index makes it possible to be examined at different levels of aggregation, e.g., seasonal, annual or over the period of record. The index directly informs storage requirements needed to meet the projected supply-demand imbalance at desired levels of reliability (explicit or implicit), and hence can be connected more directly to infrastructure, planning or water conservation needs, or the size of trans-basin diversions. The index also reveals the dependence of a county on external water source such as groundwater stores or inter-basin transfers. We found that most counties in the mid-west presented chronic stress and can be assumed to fall in this category. The derivation of resiliency measures makes it easy to understand the potential exposure by location, and is hence useful for siting decisions. Future climate scenarios or season ahead climate forecasts can be readily accommodated to provide projected risk per demand sector, and integrated with a drought monitoring plan that indicates the current level of accumulated deficit or stress. Potential impacts of climate change on supply and demand and hence drought impacts can also be explored along with whether conservation/efficiency improvement efforts or

different ways of caching surface and groundwater through infrastructure and water transfers are likely to be more effective to mitigate climate/drought impacts in a county/regional situation.

References

- [1] D. Wilhite, Drought: A Global Assessment **1** (2000) 3-18
- [2] T. McKee, N. Doesken, J. Kleist, American Meteorological Society *8th Conf.* (1993) 179-184
- [3] H. Thomas, R. Burden, Harvard Univ. Div. of Eng. and Appl. Phys. (1963)
- [4] N. Devineni, S. Perveen, U. Lall, Water Resour. Res. **49** (2013) 2135-2145
- [5] N. Devineni, U. Lall, E. Etienne, D. Shi, C. Xi, Geophysical Res. Lett. **42** (2015) 2285-2293

Acknowledgement

This study was supported and monitored by National Oceanic and Atmospheric Administration (NOAA) under Grant – NOAA-CREST Grant # NA11SEC4810004. The statements contained within the manuscript/research article are not the opinions of the funding agency or the U.S. government, but reflect the author’s opinions.

Remote Sensing of Snow Estimation: Satellites, Models and Field Experiment

Tarendra Lakhankar¹, Peter Romanov^{1,2}, Carlos Perez¹, and Reza Khanbilvardi¹

¹NOAA-CREST, City University of New York, New York, NY, USA

²Center for Satellite Applications and Research, NESDIS/NOAA, College Park, MD, USA

Abstract

Remote sensing provides local, regional and global observations of seasonal snow, providing key information on snowpack processes. The characterization of intra-seasonal variations of snow pack properties is critical for hydro- meteorological applications. In this presentation, capabilities of current and future satellite sensors, several methods of mapping snow-cover extent, snow albedo, snow grain size, snow water equivalent, melt detection and snow depth using remote sensing will be discussed. Also, we will provide a detailed description and lesson learned from remote sensing experiment (CREST-SAFE) that being carried out since 2011. The primary objective of observations is to monitor seasonal properties of the snow pack through the winter season and their changes with atmospheric conditions, support studies of physical and radiative transfer processes in the snow pack as well as to help validating and calibrating snow retrievals from satellite microwave sensors. The set of instruments installed at the station provides measurements of the snow pack emission at 10.65, 19, 37 and 89 GHz at both polarizations, snow depth, snow water equivalent, snow pack skin temperature, snow pack temperature profile as well as measurements of major meteorological parameters. Effects of changing snow pack properties on the observed microwave emission will be demonstrated and analyzed.

Introduction

The storage of water in snowpack affects runoff and soil moisture, and is therefore important at the regional scale for various hydrologic applications as flood prediction and water resource management. Rain on snow combined with warm air temperatures can lead to fast snowmelt. These conditions are responsible for the majority of spring floods in mid- and high latitude areas [1–3]. Satellite observations in the microwave spectral range have been used for the global monitoring of snow cover properties for more than three decades. Microwave emission from snowpack depends on the snow grain size, density, depth, snowpack and soil temperature, along with snow and soil wetness [4]. The evolution of snowpack temperature and soil temperature throughout the winter season as they affect microwave emission [5] are not well studied. As well, microwave emission of wet snow depends on the liquid water content in the snowpack. Therefore, the snow profile physical temperature can be critical to interpreting

microwave signals during the spring melting and refreezing period. In situ observations of the microwave emission of snow, coupled with other meteorological and snowpack measurements, are critical in the development and validation of algorithms to retrieve snow depth or SWE from remote sensing measurements in the microwave. Earlier snow field experiments [6–9]. have used microwave radiometers to study snowpack microwave emission properties. Conducting such experiments is important to improve understanding of the complex influence of different snow characteristics (grain size, density, snow temperature) on the microwave emission and on snow retrievals from microwave measurements.

This paper presents an overview of the CREST-Snow Analysis and Field Experiment (CREST-SAFE) and comparative preliminary analysis of snowpack observations during past winter seasons. The current experiment builds on earlier studies by extending over the full winter season instead of only one or a few days,

thus allowing processes of snowpack accumulation, metamorphism, and melting, and their impacts on microwave emissivity, to be observed sequentially at the same site. The objective of this long term field experiment was to characterize the behavior of snow-emitted microwave radiation throughout the winter season. In this experiment, ground microwave observations are collocated and synchronous with detailed observations of snowpack temperature. The effect of snowpack temperature (related to dry and wet snow conditions) on the microwave brightness temperature has been examined and interpreted.

Experiments

The CREST-SAFE has been carried out since January 2011 (its setup was done during February 2010) at the research site (Figure 1) of the National Weather Service office in Caribou, ME, USA (46°52'59" N, 68°01'07"W, 190m elevation). In this long term experiment, dual-polarized microwave (originally 37 and 89 GHz; 10.65 and 19 GHz were installed afterwards) observations are accompanied by detailed synchronous meteorological observations. The objective of this field experiment is to improve the understanding of the effect of changing snow characteristics (i.e., grain size, density, temperature) under various meteorological conditions on snow microwave emission to improve snow cover properties' retrievals from satellite observations [10].

Caribou has a humid continental climate and offers fitting conditions for snow studies. The cold season has an average daily high temperature below 0°C and lasts from mid-December to early March. Snow cover commonly withstands from mid-November to early April. Regular seasonal snowfall is approximately 116 inches (2.9 m). The record snowfall is 197.8 inches (5.02 m) and it happened in the winter of 2007-2008.

Results and Discussion

The CREST-SAFE field experiment, carried out during past four winter seasons and microwave and surface observations were collected to analyze the snowpack seasonal change and its impact on the passive

microwave emission of the snowpack. This type of long term field experiment helps to improve our understanding of microwave radiative transfer during melting-refreezing, snow metamorphism, and under various meteorological conditions.



Figure 1: Microwave Radiometers (10, 19, 37 and 89 GHz) at CREST-SAFE

All observations performed at the stations are collocated to within several meters. Therefore, when comparing measurements made with different sensors the effect of the spatial variations of the snowpack is minimized. All automated observations are performed continuously at the time interval of 30 sec. to 3 min. Thus we can capture and characterize the diurnal and seasonal changes of the snow pack properties as well as the snow pack response to shorter in time natural events as heat waves, snow falls and rainfalls. As part of the program we routinely acquire observations from satellite microwave sensors AMSR2 and SSMIS, match them with microwave emission measurements at the station and generate matched collocated satellite-in situ datasets.

The comparison of microwave brightness temperature in matched in situ and at satellite has revealed their strong correlation during the winter season. Correlation of most emission parameters (individual radiances, spectral and polarization differences) ranged within 0.6 to 0.8 indicating that seasonal and short-term changes in the snow pack emission properties observed in situ also affect satellite data. It should be noted however that the amplitude of temporal variations of all spectral features was much larger at the ground than at the satellite.

References

- [1] G.J. McCabe, L.E. Hay, M.P. Clark, Bull. Am. Meteorol. Soc. 88 (2007) 319–328.
- [2] F. Papa, C. Prigent, W.B. Rossow, J. Geophys. Res. 112 (2007) 1–11.
- [3] G. Singh, G. Venkataraman, Geocarto Int. 25 (2010) 187–212.
- [4] N. Grody, IEEE Trans. Geosci. Remote Sens. 26 (1988) 850–859.
- [5] L. Brucker, G. Picard, L. Arnaud, J. Barnola, M. Schneebeli, E. Lefebvre, M. Fily, J. Glaciol. 57 (2011) 171–182.
- [6] K. Elder, D. Cline, G.E. Liston, R. Armstrong, J. Hydrometeorol. 10 (2009) 320–329.
- [7] T.J. Hewison, S.J. English, IEEE Trans. Geosci. Remote Sens. 37 (1999) 1871–1879.
- [8] A. Langlois, D.G. Barber, B.J. Hwang, Remote Sens. Environ. 106 (2007) 75–88.
- [9] G. Macelloni, S. Paloscia, P. Pampaloni, M. Brogioni, R. Ranzi, A. Crepaz, IEEE Trans. Geosci. Remote Sens. 43 (2005) 2431–2442.
- [10] T.Y. Lakhankar, J. Muñoz, P. Romanov, A.M. Powell, N.Y. Krakauer, W.B. Rossow, R.M. Khanbilvardi, Hydrol. Earth Syst. Sci. 17 (2013) 783–793.

Acknowledgement

This study was supported and monitored by National Oceanic and Atmospheric Administration (NOAA) under Grant # NA11SEC4810004. The statements contained within the manuscript/research article are not the opinions of the funding agency or the U.S. government, but reflect the author’s opinions.

Characterizing Aerosol Impacts on the Distribution of Water in the Tropospheric Column During the Monsoon Season in the Philippines

Kar'retta Venable¹ and Vernon Morris²

¹Howard University Program in Atmospheric Sciences, NOAA Center for Atmospheric Sciences, Mailing Address: 6197 Trestlewood Drive Apt. C Columbus, GA 31909

²Howard University Department of Chemistry, NOAA Center for Atmospheric Sciences, Mailing Address: 1840 7th Street NW Suite 305 Washington, D.C. 20001

Introduction

The Philippines (RP) possesses a complex topography and extensive regional urban air pollution that may influence precipitation variability. Precipitation variability induces localized extremes in rainfall intensity creating pronounced floods and droughts. Cloud and precipitation formation depend upon the availability and physical properties of particulates suspended within the atmosphere and the distribution of water in the troposphere. The primary goal is to examine the impact of local and regional pollutants on the distribution of water in the

atmospheric column and precipitation variability within the archipelago. Second, it seeks to identify if specific satellite signatures of monsoonal precipitation can be identified with satellite retrievals of hydrologic related cloud optical properties. Additionally, identify any significant trends which exist within observed precipitation extremes of the past decade. This dissertation investigates how aerosols impact the spatial and temporal distribution of tropospheric water and hydraulic cloud optical properties during the monsoon season.

Experiments and Conclusion

The data obtained in this study is taken from the decade 2001 to 2010 (during the Western North Pacific Summer Monsoon (WNPSM)). Monthly averaged Level-3 MODIS Terra global data retrievals and TRMM V7 3B-43 precipitation data during June through December are employed. 10 MODIS hydrologic cloud retrievals and aerosol properties are examined. Baseline comparisons between the decadal rainfall patterns during the monsoon season and the 50 year climatology are presented.

Results revealed seasonal differences in regions exist between precipitation, hydrologic cloud optical properties, and aerosols loading from the satellite retrievals in the last decade where a dominant southeasterly (northwesterly) latitudinal gradient exist during JAS (OND) is apparent within most assessed variables. Decadal rainfall on average has decreased by 54% in comparison to the baseline. Principal Component Analysis on 9 of the 11 variables conducted indicated, most variability is

accounted between precipitation (48% - 66%), aerosol optical depth (AOD), and angstrom exponents (AE). Highest AOD (0.2 - 0.4) loading is associated with urban/industrial aerosols during JAS in the advent of higher rainfall events with smaller particles where AEs exceed 1. Furthermore, extreme decadal rainfall occurs along the western and eastern coasts of the RP which are influenced by marine and urban/industrial aerosols.

References

- [1] I. Akasaka, International Journal of Clim. **30** (2009) 1301
- [2] Y. Ding, Journal of the Met. **85B** (2007) 21
- [3] A. Hazra, B. Goswami, J. Chen, Journal of the AMS. **70** (2013) 2073

Acknowledgments

This material is based upon [work] supported by the National Oceanic and Atmospheric Administration, Educational Partnership Program, U.S. Department of Commerce, under Agreement #. NA11SEC4810003.

Biophysical Impacts of Sea Level Rise Coastal Policies in Galveston Bay, Texas

¹Rachel Edwards*, ¹James Gibeaut, ¹Marissa Dotson, ¹Mukesh Subedee, and ¹Richard McLaughlin
¹Harte Research Institute at Texas A&M University- Corpus Christi

Primary Author Contact:
Rachel.Edwards@TAMUCC.edu
6300 Ocean Drive Unit 5869
Corpus Christi, TX 78412

Abstract

The Galveston Bay region in Texas is at particular risk of sea level rise (SLR) induced hazards because of its unique geography and geology, including relatively high subsidence rates due to mineral and groundwater extractions. SLR is an exceptionally difficult public policy problem because shorelines have a dynamic nature while laws are static. This study examines the effects that various development policies could have on community resilience. Using the Sea Level Affecting Marshes Model (SLAMM), the possible effects of SLR under four development policy scenarios are examined in four regional subsites that each represents a different natural and built environment. The policy scenarios are “no dikes” which serves as a control and employs no shoreline protection, business as usual which models the current situation regarding development and armoring, green infrastructure which shows what may happen if living shorelines were used instead of dikes, and shoreline armoring which describes the armoring of the entire coastline. Coastal habitats and their ecosystem services are hypothesized to be most reduced under the armoring and business as usual scenarios due to coastal squeeze. Initial results indicate that over 700 hectares of developed land just in the Surfside Beach, TX subsite would be inundated under 1.8m of SLR by 2100 in a business as usual policy scenario. Action should be taken immediately to develop policies that foster resiliency and avoid the worst outcomes for both human and non-human communities in Galveston Bay. This work is part of a larger study on living with sea level rise along the Texas coast.

Introduction

Galveston Bay, TX is a very important region both from an ecologic and anthropogenic perspective. It has the second largest fisheries production of any estuary in the United States and is a hub for birdwatchers. Galveston Bay is also home to one of the largest petrochemical complexes in the world as well as the Greater Houston metropolitan area, three international ports, and the Houston Ship Channel. The region is extremely vulnerable to sea level rise (SLR) largely due to human-induced changes.

Galveston Bay has one of the highest vulnerabilities to large storms and sea level rise in the country due to its high population pressures, costly infrastructure, and natural properties [1]. Presently, the predominant protection paradigm emphasizes shoreline

hardening as the primary mode to combat SLR. In recent years, however, there has been recognition of the benefits that natural shorelines offer [2]. This has resulted in a push towards utilizing a green infrastructure approach called living shorelines. There are many benefits of protecting the connectivity of land and sea in such a way.

Additional study is necessary to gain a broader understanding of SLR impacts including the long-term effects of community response strategies that may be enacted. A greater recognition of the complexity and far-reaching effects of resiliency strategies will be a first step in providing the necessary research to communities so that they can construct policies that target their individual priorities. As an initial step towards considering the long-

term effects of SLR-mitigation strategies, this study focuses on a desktop analysis that quantifies the areal extent of SLR-triggered biophysical change. Using the Sea Level Affecting Marshes Model (SLAMM), the impacts of four different response strategies were modeled to the year 2100 at three SLR scenarios at four subsites. Emphasis is placed on modeling wetland responses to SLR with particular emphasis on marshes and developable dry land. The response strategies incorporated are: 1) do nothing, i.e. no adaptive measures taken, 2) business as usual which represents the armoring situation in 2007 which is when the data was collected, 3) the hardening of all shorelines, and 4) the installation of living shorelines. Three SLR scenarios were selected in order to show the differences caused from low levels of SLR compared to high levels: 0.2m, 0.74m, and 1.8m SLR by 2100. By looking at how far inland water inundated under the no dikes scenario, a setback distance can be tailored to each subsite as well. This work is part of a larger project on living with SLR on the Texas coast.

Experiments and Conclusions

For this study, the Sea Level Affecting Marshes Model (SLAMM) was used to calculate the areal extent of biophysical changes accompanied with different policies and SLR scenarios at the four subsites around Galveston Bay. SLAMM is a rule based model that is used to project changes on coastal wetlands in response to SLR and other “dominant processes [3]. The data inputs were created as part of earlier work done on the project and include the following: a Bare Earth DEM in meters above NAVD88, created from LIDAR data; a National Wetlands Inventory (NWI) wetland type layer; slope in degrees calculated from the DEM; subsidence which specifies vertical land movement for the study site in cm/year, calculated from data compiled around Galveston Bay; percent impervious which classifies how developed or undeveloped an area is; and VDATUM which converts NAVD88 to mean tide level as required by SLAMM.

All the inputs were at 1m resolution; data that was originally at higher resolutions was converted to 1m resolution. SLAMM is generally used at lower resolutions than 1m, so other changes had to be made such as turning off the Soil Saturation module to limit streaking. Site and model parameters including sedimentation, accretion and erosion rates as well as scenario and execution options were specified to each subsite as part of the work done previously on the project by Dotson.

Initial simulations have been completed for the Anahuac subsite located at the northeastern corner of Galveston Bay. SLR is expected to cause a loss of 4 percent of Anahuac’s developed uplands from 2007 to 2100 under the no dike policy scenario. Anahuac’s marshes are best preserved under the living shoreline scenario; 60 percent more marshes are preserved by 2100 under the living shoreline scenario than the business as usual scenario. Lastly, estuarine beaches tend to be negatively impacted the most under the shoreline armoring scenario.

The four subsites in this study have very different community structures and economic goals. They also have very different built environments. Because of this, different SLR protection strategies are appropriate for each. There are many factors to consider when determining what type of shoreline protection is best for a given community; priorities of the region and what is valued by its people are two of them. As such, shoreline armoring may be the best option for some situations despite the fact that wetland habitats are lost due to coastal squeeze. Sea level is rising, and coastal counties are vulnerable. Due to its history of subsidence from groundwater and petrochemical extractions and its heavily populated coastal areas, Galveston Bay is at particular risk. It is important that considerations are taken at present to plan for these hazards. Reactive strategies generally ignore the issue until a natural disaster strikes and extreme measures must be taken to minimize human harm and suffering. By researching the issues and the related benefits and constraints of potential proactive actions, human suffering can be minimized and the

associated costs can be far less than those of a reactive strategy. As Benjamin Franklin famously stated, an ounce of prevention is worth a pound of cure. The four subsites in this study can be used as examples for similar communities on and around Galveston Bay.

References

- [1] Arkema, K. K., Guannel, G., Verutes, G., Wood, S. A., Guerry, A., Ruckelshaus, M., Kareiva, P., Lacayo, M., Silver, J. (2013). Coastal habitats shield people and property from sea-level rise and storms. *Nature Climate Change*, 3(10), 913–918.
- [2] Caldwell, M., & Segall, C. H. (2007). No day at the beach: sea level rise, ecosystem loss, and public access along the California coast. *Ecology LQ*, 34, 533.
- [3] Clough, J.S., Park, R. A., and Fuller, R. (2008). SLAMM 5.0. 2 Technical Documentation.

Acknowledgement

This study was supported and monitored by National Oceanic and Atmospheric Administration (NOAA) under Texas A&M University at Corpus Christi Grant # NA11SEC4810001. Partial funding was also provided by the Houston Endowment. The statements contained within the manuscript/research article are not the opinions of the funding agency or the U.S. government, but reflect the author's opinions.

**Examining the Energetic Importance of Two Gulf Coast Barrier Islands for Transient Birds
During Spring Migration**

Melanie L. Mancuso, Alan H. Kneidel, Armando A. Aispuro, Lori A. Lester, Christopher M. Heckscher

*Delaware State University
Department of Agriculture and Natural Resources
1200 N. Dupont Highway
Dover, DE 19901
NOAA Environmental Cooperative Science Center
mancuso.melanie@gmail.com*

Introduction

Coastal ecosystems on the north coast of the Gulf of Mexico are under significant threats due to human disturbance and development, climate change, and sea-level rise. Barrier islands along this coastline provide many benefits to the wetlands and coastal communities that they protect by functioning as a first line of defense against strong winds and waves. However, these dynamic islands are expected to experience drastic alterations and land loss in the future as a result of rising sea levels, a deficit of sediment, and frequent intense storms [1]. While coastal communities depend on these barrier islands for protection, they are also important for a wide variety of wildlife by providing habitat for many breeding and migratory species, including migratory songbirds. Many of these songbirds are already facing population declines, [2] and stressors experienced during migration account for a large percentage of those mortalities [3]. With human development, climate change, and rising sea levels, several of these stressors may become more severe, particularly for species that travel across the Gulf of Mexico. For many of these birds, barrier islands on the north coast of the Gulf of Mexico are critical stopover habitats, providing them with a place to rest and refuel before continuing on to their breeding grounds [4].

My study examines the energetic importance of two very different barrier islands, St. George and St. Vincent, as it relates to Neotropical-Nearctic migratory songbirds. Both of these islands are located within the boundaries of the Apalachicola National Estuarine Research Reserve, but they differ in

size and shape, habitat types, human disturbances, and management strategies.

Experiments and Conclusions

Since 2013, our lab has been investigating the use of these barrier islands by migratory songbirds. During the peak of spring migration each year, our team captured migratory birds on these two islands using mist-nets. After receiving a unique numeric identification band, each bird was physically assessed, taking note of fat and muscle scores, wing chord, and mass. Additionally, Gray Catbirds (*Dumetella carolinensis*) were studied to determine their refueling rate during their stopover. A small sample of blood was taken from Gray Catbirds and used to measure plasma triglyceride concentrations, a measure of refueling rate in birds.

St. George Island had more migrant species and individuals captured as compared to St. Vincent Island. When adjusting for unequal mist-netting effort between islands, St. George Island had significantly higher birds per net hour than St. Vincent Island. However, comparing metrics of physiological condition of migrants between islands resulted in similar values.

This study emphasizes the importance of the Apalachicola Bay for migratory songbirds. Understanding the ecosystem functioning of these islands as it relates to migrant songbirds will allow conservationists to better manage these vulnerable lands for the wildlife that depend on them, especially as barrier island ecosystems are altered due to climate change and sea-level rise.

References

- [1] R.A. Morton. J. Coastal Res. 24(6) (2008) 1587-1600.
- [2] G. Ballard, G.R. Geupel, N. Nur, T. Gardali. Condor. 105 (2003) 737-755.
- [3] T.S. Sillett, R.T. Holmes. J. Anim. Ecol. 71 (2002) 296-308.
- [4] D.W. Mehlman, S.E. Mabey, D.N. Ewert, C. Duncan, B. Abel, et al. Auk. 122(4) (2005) 1281-1290

Acknowledgements

Funding and support for this study was provided by the National Oceanic and Atmospheric Administration Environmental Cooperative Science Center Award # NA11SEC4810001.

Global Trends in Mean and Extreme Runoff and Streamflow Simulations Based on Observations and Climate Models

Behzad Asadieh^{1*}, Nir Y. Krakauer², Balazs M. Fekete³

^{1,2,3} *Civil Engineering Department and NOAA-CREST, The City College of New York, the City University of New York, New York, USA*

** Correspondence: Behzad Asadieh (basadie00@citymail.cuny.edu)*

Abstract

To understand changes in global mean and extreme streamflow volumes over recent decades, we statistically analyzed runoff and streamflow simulated by the WBM-plus hydrological model using either observational-based meteorological inputs from WATCH Forcing Data (WFD), or bias-corrected inputs from five global climate models (GCMs) provided by the Inter-Sectoral Impact Model Intercomparison Project (ISI-MIP). Results show that the bias-corrected GCM inputs yield very good agreement with the observation-based inputs in average magnitude of runoff and streamflow. On global average, the observation-based simulated mean runoff and streamflow both decreased about 5.7% from 1971 to 2001. However, GCM-based simulations yield increasing trends over that period, with an inter-model global average of 4.4% for mean runoff and 3.9% for mean streamflow. In the GCM-based simulations, relative changes in extreme runoff and extreme streamflow (annual maximum daily values and annual-maximum seven-day streamflow) are slightly greater than those of mean runoff and streamflow, in terms of global and continental averages. Observation-based simulations show increasing trend in mean runoff and streamflow for about one-half of the land areas and decreasing trend for the other half. However, mean and extreme runoff and streamflow based on the GCMs show increasing trend for approximately two-thirds of the global land area and decreasing trend for the other one-third. Further work is needed to understand why GCM simulations appear to indicate trends in streamflow that are more positive than those suggested by climate observations, even where, as in ISI-MIP, bias correction has been applied so that their streamflow climatology is realistic.

Introduction

Anthropogenic changes in global climate and alteration of Earth's hydrological cycle have resulted in increased heavy precipitation with consequent increased surface runoff and flooding risk, which is likely to worsen in the future. Climate change is expected to change the pattern, frequency and intensity of precipitation and result in increased intensity and frequency of floods and droughts, with damaging effects on environment and society [1, 2]. Increased risk of flooding due to anthropogenic climate change has been stressed often in the literature. However, there are few studies of trends in flooding at global or continental scales [3, 4], as most studies have been limited to basin or country scales. A study

of global runoff projections from three GCMs for the last decades of the 21st century shows, with large variation among the models, strong increase at high latitudes and significant decrease at some mid-latitude regions [5]. Analysis of future projections of runoff from 23 GCMs from the Fourth Assessment Report (AR4) of IPCC also revealed projected increases in northern regions and decreases in some parts of the mid-latitudes [6].

In the present study, runoff and streamflow generated by the WBM-plus global hydrological model, based on the observation-based meteorological inputs from WATCH Forcing Data (WFD) are statistically analyzed at global and continental scales, for the time period of 1971–2001. Runoff and streamflow

generated by the WBM model based on bias-corrected outputs of GCMs, provided by the ISI-MIP, are also analyzed to compare the modeled and observational meteorology based trends in runoff and streamflow for the time period of 1971–2001, at global and continental scales. The WFD datasets are used in ISI-MIP project for bias correction of GCMs [7] and provide a fair basis for comparison of GCMs with observation-based simulations. We study changes in mean and extreme runoff and streamflow. Mean runoff is defined as the annual-mean daily runoff, which is the annual average of daily runoff values. Extreme runoff is defined as the annual-maximum daily runoff, in which the maximum daily runoff is selected for each year. Similar to runoff, mean streamflow is defined as the annual-mean daily streamflow, in which the daily flow rates are averaged for each year. Extreme streamflow is defined as the annual-maximum daily streamflow, in which the maximum daily flow rate value is selected for each year. Annual-maximum 7-day streamflow is also calculated, for which average flow rate is calculated for each consecutive 7-day period (moving average) and then the maximum value is selected for each year.

ISI-MIP presents bias-corrected daily meteorological fields, at a uniform 0.5-degree spatial resolution, from 5 selected GCMs from the fifth phase of the Coupled Model Intercomparison Project (CMIP5), which provides the opportunity to investigate the impacts of climate change from a range of GCMs on water resource system design after bias correction. The first fast-track phase of the ISI-MIP project presents outputs from the following 5 GCMs: GFDL-ESM2M, HadGEM2-ES, IPSL-CM5A-LR, MIROC-ESM-CHEM and NorESM1-M [4]. ISI-MIP also provides runoff and streamflow simulations, which have been simulated by various global hydrological models based on bias-corrected outputs of the 5 CMIP5 global climate models. For the purposes of the present study, the runoff and streamflow simulations of the WBM hydrological model based on bias-corrected GCM inputs are obtained from the ISI-MIP.

The trend slope (b) obtained from the linear regression method, which assumes that the data variability follows a normal distribution, is utilized for parametric trend strength analysis and comparison of the datasets. The relative change in runoff and streamflow is also defined as the trend slope divided by the average value of the grid cell. The Z-score (Z) obtained from the Mann-Kendall test and Qmed from the Sen's slope estimator are also applied in order to confirm the results of linear regression using non-parametric trend detection approaches.

Results and Conclusions

Linear regression indicates that 43.4% of the grid cells show positive trend in streamflow, including 5.3% that are statistically significant at 95% confidence level. The remaining 56.6% of the grid cells show negative trend, including 8.3% that are statistically significant at 95% confidence level. GCMs on average show increasing trend in mean streamflow for 62.4% of the grid cells and decreasing trend for the other 37.6%. Similar to mean streamflow, extreme (annual maximum 1-day) streamflow shows increasing trend for 64.8% and decreasing trend for 35.2% of the grid cells. An assessment of the trend in annual-maximum 7-day streamflow also resulted in similar numbers (63.2% increase and 36.8% decrease). This finding is in line with the earlier study that shows increases in the 30-yr return level of 5-d average peak flows (Q30) over approximately two-thirds of the global land area, in data provided by ISI-MIP from 1971 to 2000 [8].

On global average, the mean runoff simulated based on meteorological observation-based data (WFD) has decreased from 1971 to 2001. GCMs show very good agreement with observation-based estimates in case of average magnitude of mean runoff, which is expected given the bias correction procedure applied on the GCM outputs. The GCMs on average show increasing trend in mean runoff between 1971 and 2001, with an inter-model global average of 4.4% over that 31-year period, despite the 5.9% decrease seen in observation-based simulations. The observation-based mean streamflow has decreased by an average of 5.7% from 1971 to 2001. The GCM average shows a global

averaged increase of 3.9%. In fact, each of the 5 GCMs considered yields larger global average trend for mean runoff and streamflow, compared to observation-based estimates. Results show that values of relative change in mean streamflow for GCMs are very similar to those of runoff, on global and continental scale, which means that changes in runoff have been well translated to corresponding changes in streamflow.

Relative changes in extreme runoff (and streamflow) are very similar to those of mean runoff (and streamflow), in terms of global and continental averages. However, extreme runoff (and streamflow) show relatively faster rate of change compared to mean runoff (and streamflow). Relative change in annual-maximum 7-day streamflow for the GCMs is also very similar to those of annual-maximum 1-day streamflow (extreme streamflow) and of mean streamflow. Observation-based estimates show increasing trend in mean runoff and streamflow for about one-half of the land areas and decreasing trend for the other half (Only a minority of these gridcell-level trends are statistically significant at 95% confidence level). However, on average, mean and extreme runoff and streamflow based on GCMs show increasing trend for approximately two-thirds of the global land area and decreasing trend for the other one-third.

Results show that despite the bias-correction procedure applied on the GCM outputs in ISI-MIP, streamflow simulated based on corrected GCM outputs shows different trends compared to observation-based simulations. These differences in streamflow trends simulated over recent decades, depending on whether

observation-based or bias-corrected GCM-based climate forcing is used to drive a hydrological model, deserve further investigation to understand the main contributing factors and to refine predictions for changes in water resource availability and flood hazards over the coming decades.

References

- [1] I. M. Held, B. J. Soden, *J. Clim.* **19**, 5686–5699 (2006).
- [2] F. J. Wentz, L. Ricciardulli, K. Hilburn, C. Mears, *Science (80-.)*. **317**, 233–235 (2007).
- [3] Y. Hirabayashi, S. Kanae, S. Emori, T. Oki, M. Kimoto, *Hydrol. Sci. J.* **53**, 754–772 (2008).
- [4] L. Warszawski *et al.*, *Proc. Natl. Acad. Sci.* **111**, 1–5 (2013).
- [5] S. Hagemann *et al.*, *Earth Syst. Dyn.* **4**, 129–144 (2013).
- [6] Q. Tang, D. P. Lettenmaier., *Geophys. Res. Lett.* **39** (2012), doi:10.1029/2011GL050834.
- [7] S. Hempel, K. Frieler, L. Warszawski, J. Schewe, F. Piontek, *Earth Syst. Dyn.* **4**, 219–236 (2013).
- [8] R. Dankers *et al.*, *Proc. Natl. Acad. Sci.* **111**, 3257–3261 (2013).

Acknowledgement

The authors gratefully acknowledge support from NOAA under grants NA11SEC4810004, NA12OAR4310084, NA15OAR4310080, and from PSC-CUNY Award # 68346-00 46. All statements made are the views of the authors and not the opinions of the funding agency or the U.S. government.

Toxic Tides (or A Fatal Coupling of Climate Change & Legacy Pollution)

Lemir Teron

Florida A&M University

NOAA Environmental Cooperative Science Center

School of the Environment, 201 Beggs Av, Orlando FL 32801

Lemir.Teron@famu.edu

Abstract

Introduction

With the projected advance of climate change and associated extreme weather events, including intensified storm surges and elevated tide levels, coastal communities are expected to face significant challenges over the next century. A largely unexamined threat related to these developments includes the mobilization of legacy pollutants as sediment based toxins are dispersed by storm related activity. This research examines the related human dimensions impacts using GIS and climate modeling tools. Though the analysis is based along Florida's Gulf Coast, considering the scope of the nation's coastal populations – nearly 40% of all Americans live in shoreline counties -- the research's concentration is relevant to the entire nation.

The analysis is advanced by its assessment of individual communities' vulnerability via the *toxics mobilization index* (TMI). The TMI allows for a programmatic way to prioritize legacy pollution sites that acutely considers the concerns of areas prone to hurricanes, flooding and other features related to extreme storms, while simultaneously considering local human conditions and the capacity for resilience. This study has the capacity to: i) inform actions on behalf of policy makers to promote the true identification of toxic sites, ii) allow for the ordering of priority list sites that goes beyond examining the chemical and geological profile of an area by additionally considering the vulnerability that human communities face from hotspots in the context of extreme weather and iii) act as an

impetus for emergency response officials to recognize unforeseen threats and to design response mobilization which more thoroughly considers the challenges of emergency management and response coordination.

Experiments and Conclusions

After identifying NOAA classified coastal counties along Florida's Gulf Coast, GIS was used to plot National Priorities List sites. The TMI, using an assortment of variables (including storm surge potential, storm frequency, storm intensity, chemical profile of toxins, freshwater input and socioeconomic data) was developed to determine the vulnerability of locales. The analysis shows that marginalized communities have a heightened vulnerability to toxics mobilization and thus are at higher risk from extreme storms. A range of parties including policy makers, planners and coastal managers along with disaster management and emergency response officials should work in concert to remediate legacy pollution sites and to protect coastal communities and ecologies from disaster.

Acknowledgement

This study was supported and monitored by National Oceanic and Atmospheric Administration (NOAA) under Grant – Environmental Cooperative Science Center Grant #NA11SEC4810001. The statements contained within the manuscript/research article are not the opinions of the funding agency or the U.S. government, but reflect the author's opinions.

The Relationship between Global Crop Yield and Climatic Trends and Technology Enhancement

Ehsan Najafi, Naresh Devineni, Reza Khanbilvardi

Civil Engineering Department and NOAA-CREST, The City College of New York

Abstract

Attempts to predict food availability in the future around the world can be partly understood from the impact of changes to date. Although yields are only one part of food system, changes in the global crop yield is one of the important drivers of food security. Here, using multiple linear regression (MLR), the relationship between the crop yield data of most of the global countries and some major climatic indicators including ENSO, drought, geopotential height (GPH) and annual average CO₂ has been examined. The Palmer Drought Severity Index (PDSI) is applied to quantify the severity of droughts. In order to investigate the impact of technology enhancement, time-trend as a relatively reliable approximation of technology measurement is implemented. Some countries showed no relationship to these variables, however, results demonstrated that historical yield data of most of them can be explained by these indicators.

Introduction

To date, numerous studies have dealt historical crops trend and climatic and non-climatic drivers which influence on it, including climate change, drought and water availability, fertilizer, deforestation, biofuels, technology improvement, etc. Global food security threatened by climate change is one of the most important challenges in the 21st century (Rosegrant, 2003), however effects are already being felt and will have adverse impacts on supply chains, market prices, livelihood and human health (FAO, 2008). Because agriculture is more susceptible to global climate change, the impact of climate change on agriculture has attracted numerous of empirical studies (Chen et al., 2013). Jaggard et al. (2010) concluded that by 2050 CO₂ increment probably will increase yields of most crops. Climate change impacts on farmers will vary by region which depends on their use of technology (Brown & Funk, 2008). Crop yields affected by climate change are projected to be different in various areas, in some areas crop yields will increase, and for other areas it will decrease based on their latitude and irrigation application. (Kang, Khan, & Ma, 2009). Rosenzweig and Parry (1994) used different scenarios to assess the impact of climate change on world food supply. Their results show that doubling of the concentration of atmospheric carbon dioxide will decrease global crop production and developing countries are likely to get harmed more. Another study shows that climate change is likely to reduce agricultural production to 2030, thus reducing food availability (Lobell et al., 2008). In addition it has been observed that many extreme droughts were caused by anomaly of atmospheric dynamics caused by climate change (Hayes & Decker, 1998). Relationship between drought and agriculture was a classical topic for many of scientific studies, which most of them focused on drought monitoring and production estimation using remote sensing, ecosystem modelling, and statistical analysis (Hayes & Decker, 1998). Seasonal temperature and precipitation in many regions are influenced by ENSO (Ropelewski & Halpert, 1987), which in turn can impact crop yields. The global-mean yields of some major crops like wheat, rice, maize, soybean during La Niña years tend to be below normal and generally the overall impacts of ENSO on global yields are uncertain (Iizumi et al., 2014).

Experiments and Conclusions

Indeed, projecting crop yields is full of uncertainty. (Fischer, Byerlee, & Edmeades, 2014). Attempts to predict food availability in the future around the world can be partly understood from the impact of changes to date. In this study we used multiple linear regression using to evaluate the

impact of technology and climate trends including ENSO, drought, geopotential height and CO₂ on average of crop yields at the country scale. Using regression analysis, we can understand how the dependent variable's value changes when any of the predictors is varied, while the other predictors are held fixed. In this study, Time trend (as indicator Results indicate that the technology coefficient in 85 countries (out of 157 countries) are significant. During El Niño episodes, normal patterns of tropical

$$\ln(\text{Yield}) = \beta_0 + \beta_1 \cdot \text{Year} + \beta_2 \cdot \text{ENSO} + \beta_3 \cdot \text{PDSI} + \beta_4 \cdot \text{GPH} + \beta_5 \cdot \text{CO}_2$$

precipitation and atmospheric circulation are disrupted, causing extreme climate events around the globe. While drought is the main threat to food production, El Niño can also cause heavy rains, floods or extremely cold or hot weather. Crops yield of 26 countries which most of them are small countries, like Guatemala and Sri Lanka were influenced by ENSO. Based on results, PDSI coefficients of 26 countries are significant. High PDSI shows wet conditions and more favorable situation for crops. The positive PDSI coefficients of countries with upward historical crops yield show that higher PDSI positively contributed on crops yield which is reasonable. Floods can impose some degree of damage to the crops and regions where experience floods are associated with high PDSI. So it can be one explanation for countries that their crops yield decreased with higher PDSI. Coefficient of GPH for 41 countries in MLR model were found significant. In addition, results show the impact of CO₂ on crops yield in 106 countries is significant. The carbon dioxide-mediated yield increase results from an increase in the efficiency of photosynthesis, one of the known correlates is that plants become more efficient with regard to their consumption of water as carbon dioxide increases.

References

[1] Brown, M., & Funk, C. (2008). Food Security Under Climate Change. *Science*, 319(February), 580–582.

of technology enhancement), ENSO index, PDSI, GPH and annual average of CO₂ at Mauna Loa as predictors from 1961 to 2007 are chosen to explain crops yield data of global countries. In this study the following equation shows the mathematic expression of relationship between predictors and dependent variables.

<http://doi.org/10.1126/science.1154102>

- [2] Cane, M. a, Eshel, G., & Buckland, R. W. (1994). Forecasting Zimbabwean Maize Yield Using Eastern Equatorial Pacific Sea-Surface Temperature. *Nature*. <http://doi.org/Doi10.1038/370204a0>
- [3] Chen, Y., Wu, Z., Okamoto, K., Han, X., Ma, G., Chien, H., & Zhao, J. (2013). The impacts of climate change on crops in China: A Ricardian analysis. *Global and Planetary Change*, 104, 61–74. <http://doi.org/10.1016/j.gloplacha.2013.01.005>
- [4] Falcon, W. P., Naylor, R. L., & Asia, S. (2008). Needs for Food Security in 2030 Region. *Science*, 319(February), 607–610.
- [5] FAO. (2008). Climate change and food security: A framework document. *Food and Agriculture Organization of the United Nations*, 93. Retrieved from <http://rstb.royalsocietypublishing.org/content/360/1463/2139.short>
- [6] Fischer, T., Byerlee, D., & Edmeades, G. (2014). Crop yields and global food security. *Australian Centre for International Agricultural Research*, 660.
- [7] Hayes, M. J., & Decker, W. L. (1998). Using satellite and real-time weather data to predict maize production. *International Journal of Biometeorology*, 42, 10–15. <http://doi.org/10.1007/s004840050077>
- [8] Iizumi, T., Luo, J.-J., Challinor, A. J., Sakurai, G., Yokozawa, M., Sakuma, H., ... Yamagata, T. (2014). Impacts of El Niño Southern Oscillation on the global yields of major crops. *Nature Communications*, 5(May), 3712. <http://doi.org/10.1038/ncomms4712>
- [9] Jaggard, K. W., Qi, A., & Ober, E. S.

- (2010). Possible changes to arable crop yields by 2050. *Philosophical Transactions of the Royal Society of London. Series B, Biological Sciences*, 365(1554), 2835–51. <http://doi.org/10.1098/rstb.2010.0153>
- [10] Kang, Y., Khan, S., & Ma, X. (2009). Climate change impacts on crop yield, crop water productivity and food security - A review. *Progress in Natural Science*, 19(12), 1665–1674. <http://doi.org/10.1016/j.pnsc.2009.08.001>
- [11] Ropelewski, C. F., & Halpert, M. S. (1987). Global and Regional Scale Precipitation Patterns Associated with the El Niño/Southern Oscillation. *Monthly Weather Review*. [http://doi.org/10.1175/1520-0493\(1987\)115<1606:GARSPP>2.0.CO;2](http://doi.org/10.1175/1520-0493(1987)115<1606:GARSPP>2.0.CO;2)
- [12] Rosegrant, M. W. and S. A. C. (2003). Global food security: Challenges and policies. *Science*, 302, 1917–1919.
- [13] Rosenzweig, C. (1994). Potential impact of climate change on world food supply. *Nature*, 367, 133–138. <http://doi.org/10.1038/367133a0>

Acknowledgement

This study was supported and monitored by National Oceanic and Atmospheric Administration (NOAA) under Grant NOAA-CREST – Cooperative Agreement # NA11SEC4810004. The statements contained within the manuscript/research article are not the opinions of the funding agency or the U.S. government, but reflect the author’s opinions.

Hydro-climatological Assessment of New York City Water Supply Management: Towards a Sustainable Seasonal Inflow Forecast Based on Climate Indices and Water Releases and Storages

Nasser Najibi¹ and Naresh Devineni²

^{1,2}*Department of Civil Engineering, Center for Water Resources and Environmental Research (City Water Center), NOAA-Cooperative Remote Sensing Science and Technology Center (NOAA-CREST), City University of New York (City College), New York, NY 10031, USA*

Emails: nnajibi@ccny.cuny.edu; ndeiveneni@ccny.cuny.edu

Website: <http://crest.cuny.edu/water/>

Abstract

New York City (NYC) water supply and management is an important issue for the city residents, governments and scientists as well as the environment. The climate-based streamflow forecasting combined with adaptive reservoir operation policy can potentially improve those decisions made by the water suppliers and watershed stakeholders in the city which are often straying too far from their current management practices. This study presents a multi decisions framework for utilizing streamflow forecasts that can be applied to the works within the existing management structure and climate indices. To do this, the climate predictors are employed to develop the seasonal inflow forecasts behind the dam for the major NYC's water supply reservoirs including the Cannonsville, Neversink and Pepacton dams. Also, those physically plausible climate-based reservoir inflow forecasts corresponding to March, April and May are developed and presented in details. Moreover, multivariate regression model and physical prediction approaches are employed to statistically build a sustainable framework for release/storage procedures based on the existing climate indices variations to specify the operating rules. This can help ultimately to have a more sustainable water supply strategy for the current NYC water supply management and systems.

Introduction

New York City (NYC) as the most populous city (8.5 million people) in the U.S. is extended to 1214 km² area [1]. In order to provide the drinkable water for this extremely large urban area and its surrounding, the upstate watersheds of Catskill/Delaware and Croton watersheds (i.e. Ashokan, Rondout, Neversink, Pepacton, and Cannonsville reservoirs) are allocated to supply water demands for NYC [1].

Although the aforementioned NYC's water supply systems and resources are employed based on a range of interconnections and strategies in order to enhance the flexibilities through water exchange from one reservoir to another one, but recent increase in both the water demands as well as frequency of

extreme climatic events (e.g. sea surface temperature variation, drought, flood, storm, etc.) can provoke destructive changes into the stability of current water supply management's potentials and designs [2,3,4]. For example, an extensive drought over entire Northeast of U.S. can destroy the existing interconnections among each component of NYC's water supply system that were initially built to mitigate the localized drought by getting the excess water from any of other watersheds.

In addition to this, abrupt increase in water demands can endanger the current NYC's water supply policies [5, 6, 7]. For instance, development of highly water-demanded crops in NYC upstate will consume a large portion of water and thus the existing NYC's water

supply system stability will inevitably change [8, 9]. Therefore, it is necessary to assess the vulnerability of current NYC’s water supply system policies under rapidly increase in water-demanded issues and climate change phenomena.

Objectives

There are three main questions that we are trying to address in this study as follows:

- How is the effect of large scale atmospheric teleconnections in particular, the sea surface temperature (SST) on NYC water supply resources and reservoirs (here as Cannonsville reservoir)?
- How can we employ the climate indices which are here the concurrent (March, April and May) and precursor (December, January and February) indicators related to Atlantic SST and Pineapple Express (PE) indices, respectively as inflow predictors for forecasting of inflow and storage volume consequences in Cannonsville reservoir?
- Can we predict the sustainable storage

- volume on May 31 for each year by considering the climate indices, predicted inflow and reservoir mass balance including the release rates, reservoir-lake evapotranspiration, annual drought curves and Cannonsville reservoir’s conservative storage?

Recent changes in climate patterns and societal stabilities [6] motivate us to focus on NYC’s water supply system vulnerability and prediction in order to mitigate upcoming severities, excesses and interruptions in providing required water for the most populous city in the U.S. and its upstate water-related consumptions. This will result in a better understanding of current situation in order to be used for forecasting and preparing necessary strategies for water supply management in the mega cities like NYC.

Methodology and Approaches

The majority of data analysis and data assimilation will be performed based on multivariate regression and nonparametric regression methods (i.e. LOWESS and thin-

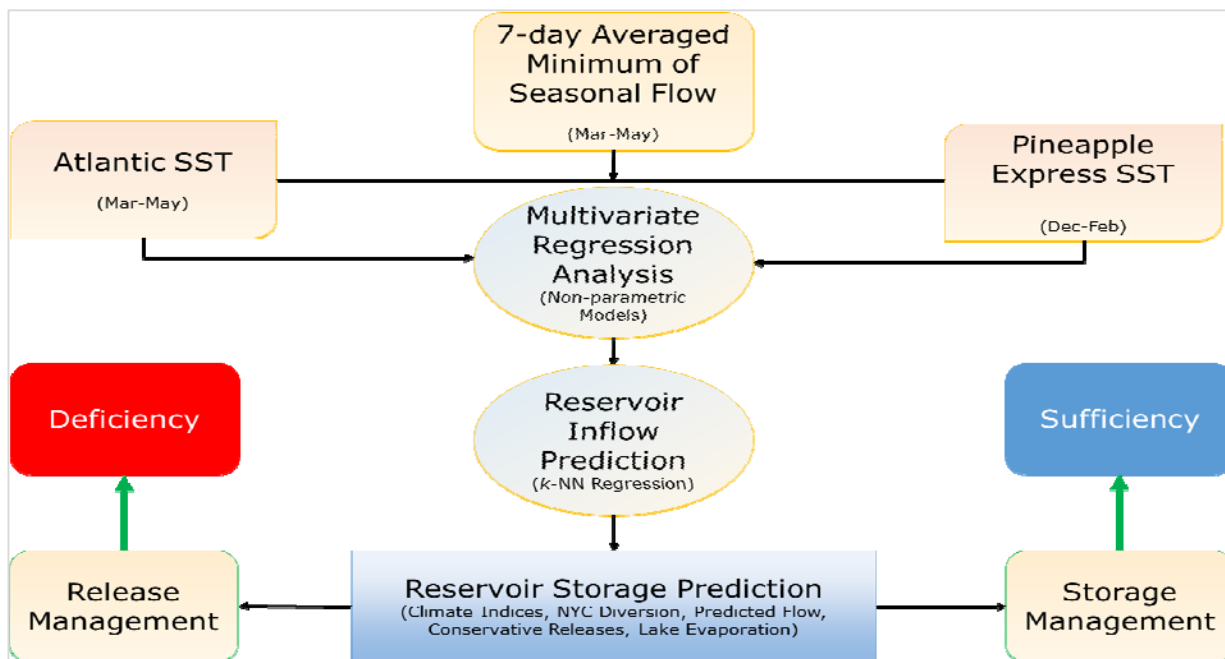


Fig. 1: Proposed methodology to optimally manage the reservoirs release/storage procedures based on preceding and concurrent climate indices

plate spline models) as well as k-Nearest

Neighbors (k-NN) algorithm regression. Next, the reservoir mass balance (reservoir storage formulation framework) will be presented to assess the predicted inflow rates subjected to target factors (i.e. target storage, target

release) [5]. Figure 1 presents the overall approach, proposed steps and expected results in this study.

References

[1] UN-WWAP, www.unesco.org/water/wwap.
 [2] J. Ganoulis (1996). Springer, 479 pages.
 [3] New York City Drinking Water Supply and Quality Report, 2005, 11373-5108.
 [4] K. Golembesky, A. Sankarasubramanian, & N. Devineni (2009). Journal of Water Resources Planning and Management, (June), 188–197.
 [5] W.S. Cleveland (1979). J. Amer. Statist. Assoc. **74** (368): 829–836.
 [6] N. Devineni, A. Sankarasubramanian & S. Ghosh (2008). Water Resources Research, **44** (9), W09404. doi:10.1029/2006WR005855.
 [7] A. Sankarasubramanian, U. Lall, N. Devineni, & S. Espinueva (2009). J. App. Meteo. Climat. **48** (7), 1464–1482.
 [8] R.E. Steuer (1986). New York, John Wiley.
 [9] USEPA (1996), <http://water.epa.gov/type/watersheds/nycityfi.cfm>.

Acknowledgment

This research is supported by NOAA-CREST–Cooperative Agreement NA11SEC4810004, National Science Foundation, Paleo Perspective on Climate Change (P2C2) program– award number: 1401698, National Science Foundation, Water Sustainability and Climate (WSC) program– award number: 1360446 and Ralph E Powe Junior Faculty Award year 2015-2016. The statements contained within the manuscript/research article are not the opinions of the funding agency or the U.S. government, but reflect the author’s opinions.

Legal and Policy Aspects of Adapting to Sea-Level Rise Along the Texas Coast

Richard J. McLaughlin
Harte Research Institute for Gulf of Mexico Studies
Texas A&M University-Corpus Christi
6300 Ocean Drive, Unit 5869
Corpus Christi, TX 78412-5869
richard.mclaughlin@tamucc.edu

The Harte Research Institute at Texas A&M University – Corpus Christi has received funding from the Houston Endowment for a multi-year project that will provide an assessment of the impacts of sea-level rise (SLR) on the greater Houston area and upper Texas coast with the goal of providing the knowledge to mitigate and adapt to higher sea level during the next 50-100 years. The assessment will involve projecting the geographic changes that SLR is expected to cause, the economic impact on the natural and built environments, and an analysis of current policies and laws for coastal zone management that may create barriers or opportunities in respect to adapting to SLR.

I propose to present findings on the progress to date of the portion of this study addressing how current policies and laws affect potential options available to the State of Texas and local communities in adapting to climate change. I will describe innovative measures that other states and nations are employing to deal with the problem and describe the legal and policy implications of several projected SLR scenarios. The presentation will compare and contrast the likely impacts of SLR on private and public property located on Gulf of Mexico-facing coastal areas compared to bay-facing coastal property. It will also describe how these impacts may be mitigated or exacerbated by potential adjustments in state or local legal and regulatory regimes.

The increased vulnerability partially caused by climate change-induced eroding shorelines and stronger storms leave humans and infrastructure along the coast at a greater

risk for SLR-related hazards. In bay-facing areas engineered solutions such as seawalls, bulkheads, groins, levees, or jetties may be a necessary response to the threat of SLR. However, most experts in the field believe that these hard structure approaches should be reserved for only those areas that are particularly well suited and defensible. An alternative approach known as “living shorelines” is gaining increasing acceptance by the coastal scientific and policy communities. The concept uses plants, including salt marsh grasses, mangroves, as well as structural materials such as oyster shells, earthen material, or riprap to protect property from erosion. The friction from marsh vegetation dissipates wave energy which reduces the risk of inundation of inland areas. This, in turn, can protect coastal development from SLR-related hazards and can lead to higher property values, more economically efficient coastal infrastructure investment, lower insurance rates, and improved local economies.

From a legal and policy perspective, there are few impediments in Texas to prevent bay-facing property owners from using engineered solutions such as seawalls and bulkheads as long as they do so on private property. Texas law provides the General Land Office, which manages state submerged lands, only with jurisdiction over public lands that are below the mean high tide line (MHTL). If a rising sea is triggering erosion, the land owner must only get the land surveyed. Armoring may then be employed as long as it is just above the MHTL and thus not on public lands, regardless of whether coastal squeeze will cause the loss of wetland habitats and their beneficial

ecosystem services. The only protection bay-facing wetlands and beaches have in Texas are standard, federal laws such as the Clean Water Act Section 404 which protects coastal wetlands or any incorporated city ordinances.

Incentives for more environmentally benign approaches such as living shorelines or organized retreat through long-term land planning are not generally provided at this time. Texas state agencies are beginning to examine methods of altering the existing system to educate the public regarding the benefits of non-hardened approaches and to encourage living shoreline projects when feasible. However, armored solutions to SLR-related shoreline retreat are still the norm along the state's bays and non-Gulf-facing beaches.

In contrast to the bay-facing areas, for decades, Texas has had some of the most progressive laws of any state in the United States when it comes to protecting Gulf of Mexico-facing beaches. The innovative Texas Open Beaches Act (TOBA) and Dune Protection Act ensure that Texas' Gulf-facing beaches are controlled by the state and that the public has unrestricted access to them, and that the dune systems are not damaged by coastal construction. An important feature of TOBA is the creation of what has come to be known as the "rolling easement doctrine." This doctrine has been interpreted by courts to prevent private land owners from locating structures on the state's beaches seaward of the vegetation line as it migrates due to natural forces. Consequently, the rolling easement doctrine has

been seen as a potentially effective tool to address SLR along some portions of the Gulf-facing Texas coast. Their use in more rural, undeveloped coastal areas may be especially valuable. Unlike urban areas where ecological losses are lower and replacement costs higher, imposing rolling easements in undeveloped areas will allow nature to take its course so that dune areas and coastal wetlands may migrate inland with the rising seas.

Examining how current laws and policies affect potential options to adapt to climate-related SLR will make it easier to be proactive rather than reactive to potential risks. Communities can either invest in protective and adaptive measures immediately, or invest much greater amounts in the future responding to severely eroding shorelines and natural disasters such as hurricanes and floods.

Acknowledgement

This study was supported by a grant from the Houston Endowment and by the National Oceanic and Atmospheric Administration, Educational Partnership Program, U.S. Department of Commerce, under Agreement #NA11SEC4810001.

Understanding the Risk to Recreational Fishers and Harvesters in Lee County, Florida from Exposure to Red Tides

Krystal Pree^a, Dr. Elijah Johnson^a, Theresa Goedeke^b, Larry Robinson^a, Richard Gragg^a, and Torhonda Lee^c

^a*School of the Environment, Florida Agricultural and Mechanical University, 1515 S. MLK BLVD, Tallahassee, FL 32307*

^b*Center for Coastal Monitoring and Assessment, National Ocean Service, National Oceanic and Atmospheric Administration, Building SSMC4, Rm 9326, 1305 East-West Highway, Silver Spring, MD 20910*

^c*Institute of Public Health, College of Pharmacy and Pharmaceutical Sciences, Florida Agricultural and Mechanical University, 1415 S. MLK BLVD, Tallahassee, FL 32307*

Presenter: Krystal Pree^a, krystal1.pree@famu.edu

Abstract

Florida red tides, predominately the photosynthetic dinoflagellate, *Karenia brevis*, produces compounds called brevetoxins that can cause illnesses and mortalities in fish, marine mammals and other marine life. Humans can be exposed to the effects of brevetoxins by inhalation of marine aerosols and ingestion of brevetoxin-contaminated shellfish, which may cause neurotoxic shellfish poisoning (NSP). NSP typically consists of gastrointestinal symptoms of nausea, diarrhea, abdominal pain and neurologic symptoms. As such, there is a cause for concern due to coastal communities depending on natural resources for food, health, economic security, cultural and spiritual benefits, and recreation.

Through online and paper surveys, this study seeks to understand the risk of exposure to licensed, recreational fin-fishers and shellfish harvesters from red tides as it relates to various variables (i.e., awareness, knowledge, beliefs, experiences, and characteristics). We expect to: 1) identify possible sub-groups that may be at more risk of exposure to red tides and what factors (i.e., purpose/beliefs) drive their decisions to engage in activities that expose them to red tides during a bloom; 2) identify possible sub-groups and quantity of licensed, saltwater fishing residents involved in shell-fishing as well as the quantity of those who have not reported symptoms of NSP; 3) determine the extent of compliance during shellfish bed closures; and 4) make recommendations for management based on research findings. In essence, it is important to identify ways to manage threats to public health from consuming brevetoxin-contaminated shellfish.

Introduction

Historically, the eastern waters of the Gulf of Mexico, namely Florida, have observed Harmful Algal Blooms (HABs) more regularly and is considered as one area of the United States that is a particular hotspot [1,2]. HABs are an algae made up of nonvascular aquatic plants that proliferates and are considered harmful and a nuisance, which adversely impacts natural resources or humans [1]. Specifically, the red tide,

Karenia brevis (*K. brevis*), is one of the most serious and highest ranking HAB in Florida due to several reasons. For instance, public health can be affected when exposed to HABs, where people can become ill via human respiratory irritations and the consumption of toxin-contaminated shellfish via the production of the toxic substance, called brevetoxin, causing neurotoxic shellfish poisoning (NSP) [1]. As stated by

Landsberg et al (2009) [3], brevetoxins are potent ichthyotoxins that are commonly responsible for fish kills and affects hundreds of species. Brevetoxins are intracellular toxins within *K. brevis* cells and are more widely available in the environment after *K. brevis* cells lyse or die [3]. Brevetoxin compounds that are released from the breaking of *K. brevis* cells by wind and wave action can become part of the marine aerosol or sea spray, which can cause respiratory irritation in people who inhale it [4].

NSP illnesses are poisonings from bivalve consumption that can cause gastrointestinal and neurological distress with symptoms, such as feeling hot or cold, extreme tingling sensations, nausea, respiratory irritation and diarrhea [1]. The extent to which these types of health effects interrupt the well-being of individuals may influence how people perceive Florida red tides as well as the need to mitigate blooms and control techniques [5]. *K. brevis* cell concentrations that are greater than 5×10^3 cells l^{-1} can close shellfish beds due to their NSP potential, while fish kills and manatee mortalities can occur at cell concentrations greater than 1×10^5 l^{-1} [1,6]. Reported cases of NSP, investigated by the Florida Department of Health, have occurred during illegal recreational shellfish harvesting [7], yet can occur if harvesters are unaware of shellfish bed closures or, theoretically, through ingestion of commercially harvested shellfish. However, state monitoring programs have been actively using actions of early closures of commercial, aquacultured, and recreational shellfish beds when there are increased concentrations of *K. brevis* cells [8]. Many NSP cases go undocumented if the contaminated person does not seek medical care or result in unrecognized and untreated cases of NSP [8,5]. Additionally, many health care providers may not be cognizant that NSP is a reportable disease in Florida [9,7] causing a number of cases to go under-reported even while treatment takes place in a health care environment [8].

Thus, the assessment of public perceptions regarding HAB toxins in contaminated recreational waters along with the extent of

public support for increased monitoring will inform water quality monitoring and short-term response strategies (Bauer et al., 2006). This research would provide coastal managers, planners, public health officials and other local and state decision-makers with critical information related to HABs and personal-use harvest activities. The overarching goal of this study is to clearly understand the knowledge, values, perceptions, behaviors, and activities of HABs and seafood safety held by local recreational fishers in Lee County, FL. This would also give rise to any sub-groups of the population that are at more risk of exposure to NSP, and if so, answer what factors drive their decisions to engage in behaviors that may expose themselves, their family, or friends to risk.

Experiments and Conclusions

To confirm the site selection of Lee County, FL, this study utilized a combination of a report by Bricker et al (2007) [10] regarding environmental conditions pertaining to the Caloosahatchee River region (located within Lee County, FL) and the National Oceanic and Atmospheric Administration (NOAA) "Harmful Algal BloomS Observing System (HABSOS) database, which combines cell counts and environmental information on an ArcGIS-powered map, resulting in the most accurate depiction of HAB location and quantity.

Moreover, this investigation uses a mixed-method analysis, where the qualitative component consisted of in-depth interviews with nine key members of the Local and State Government. The purpose of the interviews (30 min – 2 hrs) were to assist in developing the survey instrument. Interviews were recorded and transcribed verbatim, then coded and analyzed to identify significant themes emerging from across the data using the qualitative data analysis software package, Atlas.ti. A directory of licensed saltwater fishes were obtained from the Florida Fish and Wildlife Conservation Commission and a random sample was drawn. Modified methods by Dillman et al (2014) [11] were

used to develop and distribute surveys. This component of the study is currently underway and is being pretested before carrying out further data collection. Cover letters with a unique Universal Resource Locator (URL) link (with a drawing for a monetary incentive upon survey completion) is sent to fishers' email addresses explaining the background of this study and need for their participation. Reminder letters will follow for non-respondents. Surveys will be completed online using the survey software tool, Qualtrics.

The qualitative component (interviews) revealed that red tides are one of the most frequent environmental stressors. One of the main potential social impacts of red tides on fishers is the disruption of leisure time with family/friends; a potential cultural impact is a language barrier among managers and public; and a potential health impact is that some harvesters do not comply with shellfish bed closures (whether knowingly or not).

In conclusion, this research will allow officials (i.e., coastal managers, planners, public health officials, etc.) to: direct their financial resources properly; establish better lines of communication between managers and the public; stimulate public educational activities (workshops, revised messages and cater to sub-groups); stimulate changes in public behaviors and activities. Overall, we seek to provide critical information needed to meet public needs, protect public health and interests, manage actual blooms, correct misinformation, and allay fears.

References

- [1] Steidinger, K.A., Landsberg, J.H., Tomas, C.R., Burns, J.W. Harmful Algal Blooms Task Force Technical Advisory Group (1999).
- [2] Capper, A., Flewelling, L.J., Arthur, K. Harmful Algae **28**:1-9 (2013).
- [3] Landsberg, J.H., Flewelling, L.J., Naar, J. Harmful Algae **8**:598–607 (2008).
- [4] Kirkpatrick, B., Currier, R., Nierenberg, K., Reich, A., Backer, L.C., Stumpf, R., Fleming, L., Kirkpatrick, G. Science of the Total Environment **402**:1–8 (2008).
- [5] Kuhar, S.E., Kirkpatrick, B., Tobin, G.A. Public perceptions of Florida red tide risks. Risk Analysis **29**(7):96–969 (2009).
- [6] Tester, P., Stumpf, R., Steidinger, K. A. p.149–150. In Eighth International Conference on Harmful Algae. Reguera, B., Blanco, J., Fernández, M. L. and Wyatt, T. [eds.], Xunta de Galicia and IOC (1998).
- [7] Watkins, S.M., Reich, A., Fleming, L.E., Hammond, R. Mar. Drugs **6**:431-455 (2008).
- [8] Neirenberg, K., Byrne, M.M., Fleming, L.E., Stephan, W., Reich, A., Backer, L.C., Tanga, E., Dalpra, D.R., Kirkpatrick, B. Harmful Algae **9**:600–606 (2010).
- [9] Hopkins, R.S., Heber, S., Hammond, R. Fla. Med. J. **84**:441–445 (1997).
- [10] Bricker, S., Longstaff, B., Dennison, W., Jones, A., Boicourt, K., Wicks, C., Woerner, J. NOAA Coastal Ocean Program Decision Analysis Series No. 26. National Centers for Coastal Ocean Science, Silver Spring, MD. 322 pp. (2007).
- [11] Dillman, D. A., Smyth, J.D., Christian, L.M. Fourth Edition, Hoboken, NJ: John Wiley and Sons, Inc. (2014).

Acknowledgement

This study was supported and monitored by National Oceanic and Atmospheric Administration (NOAA) under Grant – Florida Agricultural and Mechanical University's Environmental Cooperative Science Center, Grant # NA11SEC4810001 for funding this project. The statements contained within the manuscript/research article are not the opinions of the funding agency or the U.S. government, but reflect the author's opinions.

Satellite-based microwave global land emissivity estimation and its application for freeze/thaw detection

Satya Prakash¹, Hamid Norouzi¹, and Christian Campo²

¹New York City College of Technology, CUNY, Brooklyn, NY

²The City College of New York, CUNY, New York, NY

Presenting author's email address: sprakash@citytech.cuny.edu

Abstract

Reliable land surface emissivity estimates play key role in retrieval of several atmospheric variables associated with land surface processes, and in numerical weather prediction data assimilation for weather/climate process studies. Remote sensing of land emissivity from microwave satellite sensors are proven to be reliable and cost-effective in the last three decades. A long-term record of satellite-based land emissivity estimate using a common algorithm is crucial to study its variability at different scales and applications towards land surface processes. Freeze and thaw process is one of most important phenomena in the high-latitude regions, which is sensitive to surface temperature, land cover types and soil moisture. The use of passive microwave emissivity in freeze/thaw states detection is supposed to be more promising, because emissivity is free from atmospheric effects and can be used as real representative of the surface state change. Instantaneous land surface emissivity has been estimated from the AMSR-E and AMSR2 sensors for late 2002 to 2015 using near-simultaneous ancillary data sets and employing a robust algorithm. The potential of estimated land emissivity in freeze/thaw states detection is also investigated.

Introduction

Accurate estimates of land surface emissivity are very important for the monitoring of vegetation phenology and land surface properties, and for data assimilation in the numerical models. The *in situ* observations of land emissivity are inconsistent and sparse at the global scale. The remote sensing satellites provide an alternative solution to obtain a comprehensive global map of land emissivity. However, the retrieval of land surface emissivity from satellite measurements is challenging due to large variability of emissivity, and its sensitivity to soil moisture, land cover type, surface roughness, etc. Passive microwave (PMW) sensors are supposed to be advantageous for land emissivity retrieval due to its rather high revisit time and having several frequency channels. In the last three decades, several algorithms are developed so far to retrieve land surface emissivity from passive microwave sensors. But, there is a great need

of long-term multi-satellite land emissivity estimates using a common robust algorithm for a wide range of applications.

A significant portion of the global land areas exhibits seasonal freezing and thawing, which has paramount impacts on carbon cycle, terrestrial water cycle and surface energy budget. The freeze-thaw (FT) process is sensitive to land cover types, soil temperature, soil moisture, etc. The ground observations of FT states are rather sparse over the high-latitude regions, which are more prone to FT cycle. PMW remote sensing has great potential for the reliable detection of FT states. The available PMW-based FT detection algorithms use the brightness temperature (TB) data, which includes atmospheric effects. However, the land emissivity derived from PMW sensors are free from atmospheric effects and supposed to better representative of the surface state and dielectric constant change. Therefore, the use of PMW-based land emissivity

estimates rather than TBs appears to be promising for FT states detection.

The objective of this study is to develop a consistent instantaneous cloud-free land surface emissivity data set from the combined use of AMSR-E and AMSR2 sensors employing a common robust algorithm. Near-simultaneous ancillary data sets from MODIS and AIRS sensors onboard the Aqua satellite are used to mitigate the atmospheric effects from the PMW observations. The potential of the present land emissivity estimates in the high-latitude FT states detection over the Northern Hemisphere is also investigated.

Results and Conclusion

In order to retrieve the cloud-free instantaneous land emissivity from AMSR-E and AMSR2 TBs at 0.25° equal-area grid, the

ancillary data sets are re-projected at the same grid. The land emissivity is computed for all the frequencies at both horizontal and vertical polarizations using the procedure described by Norouzi *et al.* [1]. Moreover, to mitigate the discrepancy between penetration depths of PMW-based TBs and infrared skin temperatures [2], a simplified correction factor is applied to the land emissivity estimates, primarily over the arid regions. A detailed description of the development of this land emissivity estimate is recently highlighted by Prakash *et al.* [3]. This estimate is available since late 2002 to December 2015 with a data gap between late 2011 and mid-2012, due to non-availability of AMSR-E/AMSR2 sensor. The present estimate is capable to capture all the well-known features of global land emissivity.

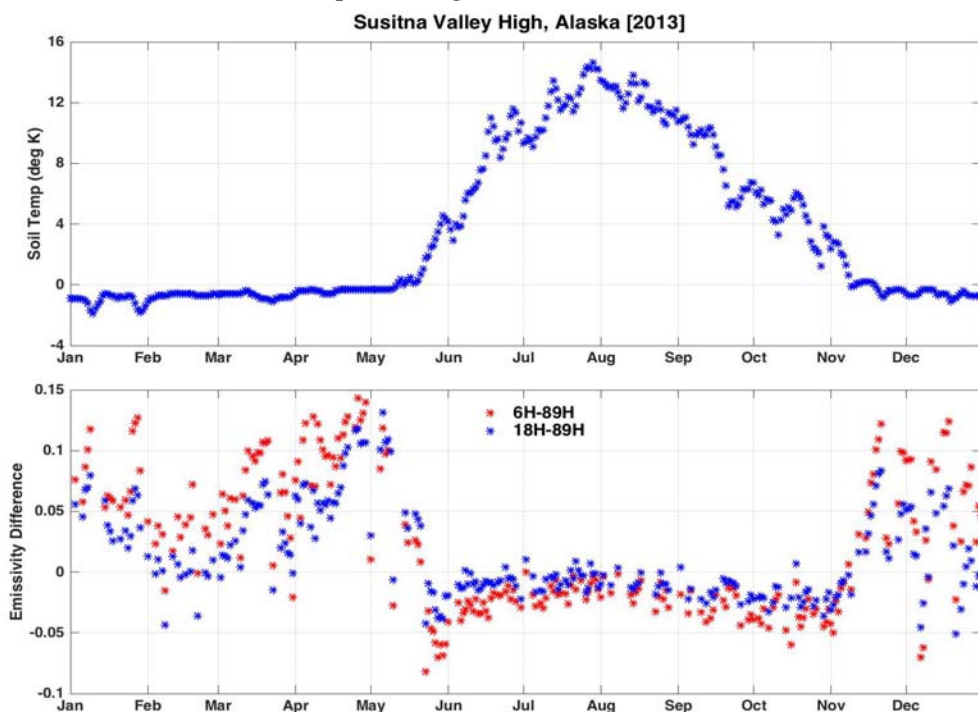


Figure: Time-series of daily nighttime (upper panel) 5 cm soil temperature from ground observations and (lower panel) AMSR2-derived emissivity difference at horizontal polarization for 2013 over a SNOTEL site of Alaska.

The available FT detection algorithms use PMW-based TBs and ground-based air temperature data sets [4]. To study the soil states using ground observations, soil temperature is supposed to be better indicator of FT states than air temperature. Furthermore, land emissivity is free from atmospheric effects; its use for FT detection is more promising than the direct use of TBs. To

demonstrate the potential of land emissivity in FT states detection, time-series of nighttime AMSR2-derived emissivity difference between lower and higher frequency channels along with *in situ* soil temperature is shown.

References

- [1] H. Norouzi *et al.*, Hydrol. Earth Syst. Sci. **15** (2011) 3577-3589, DOI:10.5194/hess-15-3577-2011.
- [2] H. Norouzi *et al.*, Remote Sens. Environ. **123** (2012) 470-482, DOI:10.1016/j.rse.2012.04.015.
- [3] S. Prakash *et al.*, IEEE Geosci. Remote Sens. Lett. (2016) DOI:10.1109/LGRS.2016.2581140.
- [4] Y. Kim *et al.*, IEEE Trans. Geosci. Remote Sens. **49** (2011) 949-960.

Acknowledgement

This study was supported by the Department of Defense – Army Research Office (ARO) under grant W911NF-15-1-0070. The statements contained within the manuscript/research article are not the opinions of the funding agency or the U.S. government, but reflect the authors’ opinions.

The 2016 CREST Undergraduate Research Experience (CURE) at Hampton University

Baseemah Rucker, Maurice Roots, Kamali Lowe, Millan Robinson and John Anderson
Department of Atmospheric and Planetary Science
Hampton University
Hampton, VA 23669
JOHN.ANDERSON@hamptonu.edu

Abstract

Six undergraduate students are participating in the CREST Undergraduate Research Experience (CURE) program during the 2016 summer at Hampton University. The program covers 8 weeks between May 27 and July 22. A total of 4 students are fully supported by CREST while the other 2 students will be supported from the NASA AIM program. During the program, each student is matched up with a faculty member and chooses a NOAA CREST related focused research project, including Social Science, under the guidance of their mentor. The students will write AMS style extended abstracts documenting their research and give final oral presentations on their respective projects. As part of the program, weekly scientific seminars are given by Department of Atmospheric and Planetary Science (APS) faculty. APS graduate students assist the undergraduate participants by answering research questions, helping in their code development and in various social activities during the duration of the program. Science-Enrichment activities included field trips to the NOAA Science-on-a-Sphere display at the Nauticus museum, Norfolk, VA, the NWS Wakefield VA Forecasting Office, the Virginia Air and Space museum, the NASA Langley Research Center, and the Thomas Jefferson National Accelerator Facility. We will present a summary of the research activities involved during the 2016 summer program.

Ozone Mapping and Profiler Suite Aerosol Analysis

The first research project consisted of analyzing data that the Ozone Mapping and Profiler Suite (OMPS) Limb Profiler instrument produced in 2014. The OMPS LP is a remote sensing joint NOAA-NASA satellite instrument designed to measure high quality vertical profiles of ozone and different aerosols in the stratosphere. One of the techniques it uses is the Limb Scattering technique which allows the limb profiling instrument to make measurements that are uniformly spread over the whole sunlit portion of the earth. The reflectivity and retrieval extinctions were compared between areas with light background and areas with dark backgrounds. The results from this research project will provide NOAA with a better understanding of the relationships between aerosols in the stratosphere and remote sensing technologies.

Weather Station Refurbishment

A second research project consisted of upgrading and refurbishing a weather station that has been inactive and discontinued on site at Hampton University for what appears to be over ten years. The goals of this project are to test, measure, and calibrate all of the instruments and electronics of the weather station. When the station becomes operational and responsive, the goal is to integrate a Raspberry Pi 3B into the control module and have the Raspberry pi periodically distribute data to a personal computer and website. The weather station will bring accurate weather data in real time to a website and be distributed to the Hampton University campus population for common knowledge and research elements. In addition, we will explore data distribution to the Weather Underground.

Fort McMurray Wild Fire

The third project consists of utilizing various remote sensing satellite data to determine the

environmental effects of the Fort McMurray, Canada, fire of May 2016. The Giovanni database offers images of chemical levels in the atmosphere as well as aerosol optical depth. The capacity to determine how much aerosol was released due to the Fort McMurray fire can be ascertained through Calypso data as well as Modis and Viirs (on Suomi NPP). In addition, the use of the Hysplit Trajectory Model will help glean information on the dispersion of the fire's smoke.

Weather Literacy and Preparedness in the Hampton Roads Area

The final project involved gauging weather literacy and preparedness of the Hampton Roads, Virginia populace. This project attempts to gauge how effective NOAA has been in reaching the general population of the given area in understanding weather terminology and their own determination of preparedness for extreme weather situations. To collect data, a survey was distributed through physical and

electronic means utilizing popular social media platforms in order to reach the largest pool of people. The anonymous survey consists of many categories of questions concerning demographics, prior weather related knowledge, and common emergency weather threats facing the area. The results of this project could provide NOAA with greater insight into the challenges and shortcomings of helping the people of the Hampton Roads area in regards to weather literacy and preparedness. This information could be used to reverse negative weather literacy trends in the area and maintain an informed populace.

Acknowledgements: This study was supported by a grant the National Oceanic and Atmospheric Administration, Educational Partnership Program, U.S. Department of Commerce, under Agreement #. NA11SEC4810004.

Mapping Building Energy Consumption in New York City

Yoribaldis Olivo, Prathap Ramamurthy, and Gehovanny Baez

¹NOAA-CREST

²The City College of New York

Presenting Author's Email: Yoribaldis@gmail.com

Abstract

In the United States, nearly 40% of energy is spent on heating and cooling building spaces. However, building energy use data for large dense cities is not available at the required spatial scales. This building energy use significantly influences the local climate and this impact has not yet been integrated into regional or local scale weather models. The primary objective of this research is to understand and map building energy consumption to quantify its impact on local climate. The project involves a detailed classification of residential and commercial buildings in the city and the estimation of building energy consumption through computer simulations and approximations. The outcome of this study is two fold. First, a spatial representation of building energy use using physics based model. Secondly, the numerical scheme gives us the flexibility to test various mitigation strategies to reduce building energy consumption. For example, a higher roof albedo, increased insulation thickness, and building orientation. Mapping energy use patterns of urban areas is one of the highest uncertainties in urban weather prediction and forecasting. Thus, addressing this issue will give a platform to determine and estimate climate changes in urban environments.

Introduction

The increase in Carbon Dioxide (CO₂) and environmental changes has augmented the importance of reducing building energy consumption. Over the last three decades the use of energy consumption has increased by approximately 50% while the amount CO₂ released into the environment increased by 43% in that same period [1]. An even more worrisome prediction according to the United States Energy Information Administration, is that energy consumption is projected to increase by 56% by 2040 [2]. Thus, is necessary that measures are taken to reduce energy consumption. However, to progress towards environmental and energy sustainability we need to improve our understanding of the climate energy nexus. In order to close this gap, this research focuses on implanting a bottom-up approach utilizing singles building energy models to patternalize building energy consumption in NYC. Thus, *how is energy consumption and energy use varying spatially and temporally in a dense, mega city environment? Can single building*

energy models be used to scale up total energy consumption? With the use of single building energy models, the energy consumption and heat rejected can be quantified for different building categories in NYC to in a near future understand the climate energy nexus.

Experiments and Conclusions

Utilizing publicly available NYC building database PLUTO, a classification scheme was developed to fit the city. With the categories developed different building models were created in the building energy modeling software eQuest. Simulations yielded energy-end use values, on hourly and yearly time scale, for the different building models developed, which were then used to scale it up to the whole city with the classification scheme at hand. Overall the results obtained provide the general picture of energy use patterns in NYC for the different building categories and areas. Predominantly commercial areas are seen as the high consuming sectors in the city when compared to communities composed mainly of residential housing. On the other hand, the heat rejected by each of the

respective categories did not differ much in magnitude, which results in an approximately similar values for the heat rejected by each category. With the developed scheme, the input is flexible and controlled by the user. The more variables known for a respective area, the more accurate the results obtained from the model at an hourly scale.

With the results obtained, the heat rejected can be mapped as with the energy consumption, to obtain a visual representation and idea of what areas would be optimal for buildings, providing urban planners the most promising areas in the city. For future analysis and studies, the numerical scheme gives us the flexibility to test various mitigation strategies to reduce building energy consumption like a higher roof albedo, increased insulation thickness, and building orientation. For further analysis, one can couple the output of these building models with environmental models to understand how the building energy consumption affects the environment.

References

- [1] Pérez-Lombard, Luis, José Ortiz, and Christine Pout. "A Review on Buildings Energy Consumption Information." *Energy and Buildings* 40.3 (2008): 394-98.
- [2] "U.S. Energy Information Administration - EIA - Independent Statistics and Analysis." *EIA Projects World Energy Consumption Will Increase 56% by 2040*. N.p., n.d. Web. 17 July 2016.
- [3] "Climate Change Science Overview." *Science*. N.p., n.d. Web. 17 July 2016. Horton 2005. Environment Agency.

[4] Howard, B., L. Parshall, J. Thompson, S. Hammer, J. Dickinson, and V. Modi. "Spatial Distribution of Urban Building Energy Consumption by End Use." *Energy and Buildings* 45 (2012): 141-51.

[5] Heiple, Shem, and David J. Sailor. "Using Building Energy Simulation and Geospatial Modeling Techniques to Determine High Resolution Building Sector Energy Consumption Profiles." *Energy and Buildings* 40.8 (2008): 1426-436.

Acknowledgement

This study was supported and monitored by National Oceanic and Atmospheric Administration (NOAA) under Grant – (name of your center) Grant # NA11SEC4810004. The statements contained within the manuscript/research article are not the opinions of the funding agency or the U.S. government, but reflect the author's opinions.

A Delayed-Action Oscillator Model for El Niño

Nour Hadjih^{1,2} Hassebo¹, and Frank Wang¹

(nhaduk0001@gmail.com presenter and corresponding author), Ahmed Yassebo², Yasser

¹*LaGuardia Community College of the City University of New York, Long Island City, NY*

²*The City College of the City University of New York, New York, NY*

Introduction

This research involves data correction, Fourier analysis, and mathematical modeling through studying the El Niño events in the equatorial Pacific. The El Niño Southern Oscillation (ENSO) is the most prominent signal of interannual climate variability; it is driven by the interaction between tropical Pacific Ocean and the atmosphere. Since 1899 there have been 29 recorded El Niño events, an average period of 3.7 years. There is evidence to suggest that El Niño events are becoming stronger and more frequent: there have been 6 events in the last 20 years, (given an average period of 3.3 years), two of which were the strongest of the 20th century [2].

Methodology

El Niño events are characterized by positive sea surface temperature (SST) anomalies. Historically, scientists have classified the intensity of El Niño based on the 3-month running mean of the SST anomalies exceeding 0.5° C for five consecutive months in a certain region of the equatorial Pacific [3]. The most commonly used region is the Niño 3.4 region, which extends from longitude 120° West to 170° West, and latitude 5° North to 5° South. The ENSO data are available at the National Oceanic and Atmospheric Administration (NOAA) website [3]. After obtaining the Niño 3.4 anomalies monthly data from 1950 January to 2016 June, we perform a Fast Fourier Transform (FFT) using the `fft` command of MATLAB [4]. The periodogram reveals multiple peaks centered around a period of 3.69 years, and this pattern indicates the quasi-periodic nature of the ENSO.

To ascertain the reliability of MATLAB's `fft` function, we test it using simulated and actual data with known frequencies. One of our test data is the weekly

Mauna Loa *in situ* CO₂ data obtained from the Scripps Institute of Oceanography. We reproduced the well-known Keeling Curve, the time series of CO₂ concentration since 1958. After removing the upward trend using a polynomial fit of degree 3, we perform an FFT. The periodogram has a sharp peak corresponding to a period of 52 weeks, which is the expected annual cycle. However, we also discover a weak but statistically significant peak corresponding to a period of 3.6 years. While this peak requires a further investigation, a connection between ENSO and CO₂ concentration in the atmosphere seems possible.

To gain a deeper sense of the SST, we download the Earth Surface Temperature dataset from NASA. The data are provided as text files: each file contains a 3-hour mean temperature of squares forming an earth grid of 72×144 . The records contain occasional outliers, and through a 5-stage process to manage these outliers we obtain the corrected contour maps. The results of our own data correction for the set from 2000 to 2005 are in good agreement with the SST published in the NOAA website.

The Delayed-Action Oscillator

To study the ENSO phenomenon quantitatively, we consider a delayed-action oscillator proposed by Max J. Suarez and Paul S. Schopf [1], and its extension by Ian Boutle, Richard H. S. Taylor, and Rudolf A. Römer [2]. This is a one-dimensional, nonlinear ordinary differential equation with a delay term. The time rate of change of the SST depends on the existence of a strong positive feedback in the coupled ocean-atmosphere system, and on a nonlinear mechanism that

limits the growth of unstable perturbations. A key element in this model is the inclusion of the effects of equatorially trapped oceanic waves (Kelvin and Rossby waves) propagating in a closed basin through a time delayed term. Using the values of 1.4 m/s for a Kelvin wave and 0.47 m/s for the Rossby wave, we calculate a total delay of 349 days. Employing MATLAB's `dde23` command, we solve the delay differential equation numerically, and the delayed-action model indeed produces self-sustained oscillations. By varying the time delay, we discover that the oscillatory period increases as the delay decreases. When the delay drops to a threshold of 203 days, the oscillations cease. (Mathematically, this is called bifurcation—drastic qualitative changes in the solution curves.) We add a constant term to the equation, representing the effect of global warming of 5° C per century, and there is little change in the behavior of the original equation. Yet when we increase the global warming rate to 63° C per century (quite impossible in reality), the oscillations cease—another bifurcation point.

Random variation plays an important part in the irregularity of El Niño events, and for this reason we include a stochastic term to the delay differential equation. We also add a sinusoidal term that models the periodic heating and cooling of the equator during the annual cycle. With all the effects, we produce some very realistic solution curves that look similar to the observed data. Notably, the regularity of the original oscillations is broken and sometimes a complete El Niño event has vanished.

Conclusions

Our bifurcation analysis shows that a minimum delay is needed for SST oscillations to occur in a basin. This property offers a plausible explanation of the lack of El Niño in smaller water bodies such as the Atlantic and Indian Oceans.

References

- [1] I. Boulte, R. H. S. Taylor, and R. A. Römer, *Am. J. Phys.* **75** (2007) 15.
- [2] M. J. Suarez and P. S. Schopf, *J. Atmos. Sci.* **45** (1988) 3283.
- [3] NOAA National Centers for Environmental Information, <https://www.ncdc.noaa.gov/teleconnections/enso/indicators/sst.php>, accessed Aug 13, 2016.
- [4] F. Wang, *Introduction to Fourier Analysis*, <http://ciles.cuny.edu/>, accessed Aug 13, 2016.

Acknowledgement

This paper has grown from a research project conducted during the 2016 NASA Goddard Institute for Space Studies Summer Internship Program. The research is funded partially by the NASA New York Space Grant: Community College Partnership Program and the Alliances for Continuous Learning Environments in STEM (CILES) funded by the U. S. Department of Education Title V Grant No. P031C110158 at LaGuardia Community College.

THEME II

Weather Ready Nation

Society is prepared for and responds to weather-related events

The Impact of Lightning on Intensity Forecasts Using the HWRf Model

Keren Rosado¹, Vijay Tallapragada², Gregory Jenkins³

*Corresponding author address: Keren Rosado,
5830 University Research CT Cubicle 2783 College Park,
MD 20740; e-mail: keren.rosado@noaa.gov*

¹*Howard University NOAA/EPP/GRTSP Fellow*

²*NOAA/NWS/EMC/GCWMB*

³*The Pennsylvania State University*

Abstract

The National Oceanic and Atmospheric Administration (NOAA) created the Hurricane Forecast Improvement Project (HFIP) in 2010 with the ten-year goal of improving tropical cyclone intensity and track forecasts by 50% for days one through five. Part of this goal is to improve forecasts of the tropical cyclone intensification. In order to contribute to this goal, I investigated the role of lightning during the life cycle of a tropical cyclone using the Hurricane Weather Research and Forecast (HWRf) 2015 operational model. In this study, we tested a scheme that we implemented into the HWRf operational model under the NOAA EPP GRTSP award in 2015. A 126 hours cycle simulation of hurricane Earl and tropical storm Fiona, was conducted to evaluate the evolution of the spatial distribution of lightning location and density. HWRf model output with lightning parameterization model was analyzed and compared observations. Results from these experiments shown that the relationship between lightning and intensity changes exist. Furthermore results shown that a peak in lightning occurred hours before intensity peak.

Introduction

Due to the low confidence when forecasting intensity and trajectory of tropical cyclones The National Oceanic and Atmospheric Administration (NOAA) created the Hurricane Forecast Improvement Project (HFIP) in 2010 with the ten-year goal of improving tropical cyclone intensity and track forecasts by 50% for days one through five. Part of this goal is to improve forecast of the tropical cyclone rapid intensification. In order to contribute to this goal, we have investigated the role of lightning during the life cycle of a tropical cyclone using the Hurricane Weather Research and Forecast (HWRf) hurricane model.

Previous researches show that there is a correlation between lightning and intensity changes in tropical cyclones [1, 2, 3, 4, 5, 6]. The association between lightning and intensity changes allows us to use lightning as a proxy to calculate tropical cyclone intensity changes. Some of the microphysics associated with lightning and tropical cyclones are graupel and hail located in the “charging zone”. When graupel and hail increase in a tropical cyclones the refractivity values increase as well the more probability for lightning to occur [7, 8].

This study will evaluate the implementation of a lightning parameterization called Lightning Potential

Index (LPI) into Hurricane Weather Research and Forecast (HWRF) operational. The case study that will be analyzed and evaluated is hurricane Earl and tropical storm Fiona. The two leading questions that will be addressed are “How well does the HWRF model forecast lightning spatial distributions before, during, or after tropical cyclone intensification?” and “What is the functional relationship between atmospheric moisture content, lightning, and intensity in the HWRF model?” The hypothesis is that an improvement in the forecast of lightning may lead to corresponding reductions in the HWRF hurricane model intensity bias.

2. Methodology

2.1 Hurricane WRF

HWRF operational computer model is atmospheric – ocean model non-hydrostatic fully compressible with 61 atmospheric vertical levels and model top 2hPa [9,]. The HWRF model provides high-resolution real time tropical cyclone forecasts for the Atlantic, Eastern Pacific and West Pacific Oceans. This model was designed based on the Weather Research and Forecast system (WRF) [9] and the Geophysical Fluids Dynamics Laboratory (GFDL) hurricane model. HWRF is composed of one outer domain $80^\circ \times 80^\circ$ (18km) with grid spacing of 0.135° with two-way movable nested grids that follow tropical cyclones i.e. intermediate domain $12^\circ \times 12^\circ$ (6km) with a grid spacing of 0.045° and cloud resolving domain $7.1^\circ \times 7.1^\circ$ (2km) with a grid spacing of 0.015° .

2.2 Lightning Parameterization

The LPI is the measurement of the potential for charge generation and separation that leads to lightning flashes in a convective thunderstorm between 0°C and -20°C , where the charge separation is driven by collisions of ice and graupel particles in the presence of supercooled water that is most effective [10, 11]. The LPI is calculated by using simulated

grid-scale vertical velocity and simulated hydrometeor mass mixing ratios of liquid water, cloud ice, snow, and graupel.

2.3 Case Study: Earl and Fiona

Hurricane Earl when into a rapid intensification period on August 29 at 1200 UTC. This period of rapid intensification lasted until August 30 1200 UTC. Earl reached its maximum wind speed on September 2, around 0600 UTC [12]. During the life cycle of Earl the WWLLN data recorded more than 48,000 lightnings making it good case study [13].

Tropical storm Fiona was a strong tropical storm short-lived (five days) that never reached the hurricane classification but it was noticed that system had significant amount of lightning. Fiona was always under the influence of the shear produced by hurricane Earl preventing its intensification.

3. Experimental Design

A 126-hour simulation for each of the tropical cyclones e.g. Earl and Fiona with lightning parameterization has been conducted to evaluate the evolution of the spatial distribution of lightning location and density.

4. Results and Conclusions

Output from the HWRF simulations has been analyzed and compared to observations. The observations were retrieved from The National Hurricane Center (NHC) and the lightning data was acquired from the World Wide Lightning Location Network (WWLLN). Results from this investigation shown: a correlation between lightning and intensity changes exist; the potential for lightning increases to its maximum peak hours prior to the tropical cyclone reaching its maximum intensity. Results from this investigation will improve our knowledge of the mechanism behind lightning as a proxy for tropical cyclone

steady state intensification and tropical cyclone rapid intensification forecast, consequently, moving a step closer to achieving NOAA's goal of reducing the intensity error by 50% for days one through five.

References

- [1] C. Price, M. Asfur, Y. Yair, *Nature Geoscience*. **2** (2009) 329.
- [4] J. N. Thomas, N. N. Solorzano, S. A. Cummer, R. H. Holzworth, *J. Geophys. Res.* **115** (2010) A00E15.
- [5] M. DeMaria, R.T. DeMaria., J.A. Knaff., D. Molenaar, *Mon. Wea. Rev.* **140** (2012) 1828.
- [6] A. O. Fierro, E.R. Mansell, C. L. Ziegler, D. R. MacGorman, *J. Atmos. Sci.*, **72** (2015) 4167.
- [7] D. R. MacGorman, D. W. Burgess, V. Mazur, W. D. Rust, W. L. Taylor, and B. C. Johnson, *J. Atmos. Sci.*, **46** (1989) 221.
- [8] MacGorman, D. R., and W. D. Rust, Oxford University Press. (1998) 422.
- [9] V. Tallapragada, L. Bernardet, M. K. Biswas, I. Ginis, Y. Kwon, Q. Liu, T. Marchok, D. Sheinin, B. Thomas, M. Tong, S. Trahan, W. Wang, R. Yablonsky, X. Zhang, 2015 Scientific Documentation. (2015) 113.
- [10] C. P. R Souder, *Space Sci. Rev.* **137** (2008) 335.
- [11] Y. Yair, B. Lynn, C. Price, V. Kotroni, K. Lagouvardos, E. Morin, A. Mugnai, M.d.C. Llasat, *J. Geophys. Res.* **115** (2010) D04205.
- [12] J. P. Cangialosi, *Tropical Cyclone Report Hurricane Earl (AL072010)*. National Hurricane Center (2011).
- [13] S. N. Stevenson, K.L. Corbosiero., J. Molinari, *Mon. Wea. Rev.* **142** (2014) 4364.

Acknowledgement

This study was supported and monitored by National Oceanic and Atmospheric Administration (NOAA) under Grant – (NOAA Center for Atmospheric Science) Grant No NA11SEC4810003. The statements contained within the manuscript/research article are not the opinions of the funding agency or the U.S. government, but reflect the author's opinions

The Validation of Suomi NPP OMPS Limb Profiler Ozone Measurements

S. Buckner^{1,2}, L. Flynn², and D. Barnes¹

¹*Department of Atmospheric and Planetary Sciences, NOAA-CREST, Hampton University*

²*Center for Weather and Climate Prediction, National Oceanic and Atmospheric Administration*

Abstract

The Ozone Mapping and Profiler Suite (OMPS) Limb Profiler makes measurements of limb-scattered solar radiances over Ultraviolet and Visible wavelengths. These measurements are used in retrieval algorithms to create high vertical resolution ozone profiles to help to monitor the evolution of the atmospheric ozone layer. NOAA is in the process of implementing these algorithms to make near-real-time versions of these products. The main objective of this project was to generate estimates of the accuracy and precision of the OMPS Limb products by analysis of matchup comparisons with similar products from the International Space Station Stratospheric Aerosol and Gas Experiment (ISS SAGE III) and Earth Observing System Microwave Limb Sounder (EOS Aura MLS). The studies investigated the sources of errors; classified them with respect to height, geographic location, and atmospheric and observation conditions; and worked with the algorithm developers to attempt to develop corrections and adjustments for them.

Introduction

The Ozone Mapping and Profiler Suite Limb Profiler (OMPS-LP) instrument on the Suomi-National Polar-Orbiting Partnership (SNPP) satellite measures limb-scattered radiances over visible and ultraviolet wavelengths. In an effort to further calibrate and validate OMPS-LP measurements, comparisons were made with measurements from the Microwave Limb Sounder (MLS) instrument on Aura. In some respects, MLS measurements can be thought of as the standard for current ozone measurements, because of the length of time that it has been taking measurements. This project examined the differences, bias, and errors between the two instruments. Ozone measurements for individual days were examined and compared, and the process was automated in order to make comparisons for the entire lifespan of OMPS.

Process

Daily data files for both instruments were downloaded, dating from the start of 2012 and running through the present (June, 2016). This date range was chosen in order to give the maximum amount of data, as the beginning of 2012 is when the OMPS instrument began to take consistent measurements, almost every day. From here, the files were compared to find all of the matching dates. Once this had been established, the ozone volume mixing ratio (VMR) data, along with other necessary data (including geolocation data and ancillary data), could be extracted from both files for each daily pair. With the data extracted, processing could then take place, to get each dataset to the point that it could be compared to the other.

The data processing involved trimming both datasets and making their sizes compatible, so that they could be compared one to one. First, the data was averaged longitudinally, combining each individual

orbit from each day. This resulted in a dataset that could be plotted as a function of latitude and pressure. From here, in order to better accommodate the MLS data, the data was averaged into 2 degree latitude bins. The data was then trimmed to show from 60°S to 60°N, as this was the area that had the most consistent coverage from OMPS. OMPS itself can take measurements poleward of 80°, but various factors, such as polar night and differences in solar zenith angle, can restrict the data to the point that good measurements can sometimes only reach as far as about 60°. Each dataset was also trimmed to pressure levels between 100mb and 1mb, to emphasize the stratosphere. Due to the difference in resolution, the OMPS and MLs datasets had different numbers of pressure levels between 100mb and 1mb. To account for this, a spline was taken of the OMPS data to reduce its resolution to that of MLS. It was done in this direction since MLS is being assumed to be the standard for these measurements. Plots for the OMPS spline data and the final MLS data for April 18, 2016 can be seen in figures 1 and 2 respectively.

Preliminary Results

After the spline was taken, the OMPS and MLS datasets were of the same size, and comparisons could then be made. Three different types of comparisons were made on this data: residuals (simply subtracting the OMPS data from the MLS data), percent bias, and percent difference. An example of each of these, for April 18, 2016, can be seen in figures 3, 4, and 5, respectively. The residual map shown in figure 3 is fairly typical of most days. Generally, the equatorial and tropical region around 10mb has a distinct split, with an area of higher OMPS values between 10mb and 1mb, while there are areas of higher MLS values between about 10mb and 30mb. In most other areas of the plot, the difference values are closer to

0, but generally lean towards a slight MLS higher bias. The percent bias map, showing the same data as the residual map but scaled differently, shows again that a small MLS bias exists over most of the map, with the exception of the equatorial and tropical regions between 10mb and 1mb. As noted before, this general structure can be seen in a majority of the days plotted.

The percent difference maps generally have more variation to them than the residual maps and percent bias maps. Though, that being said, the largest differences usually occur right around 100mb in the equatorial region. This could be due to different factors, but likely comes as a result of the very small VMR values that exist in this region. This is part of the reason that the data was trimmed to only show the general area of the stratosphere, even though both instruments can observe a much, much greater vertical scale. Beyond that difference, the same general structure can be seen throughout the map that was consistent with the percent bias and residual maps, though the magnitude of these features is dwarfed by that of the low altitude feature. Most percent difference maps show a general trend of less than 30% difference outside of the low altitude levels.

Once the differences have been classified more, there is the possibility of working with NOAA scientists to change the OMPS-LP retrieval algorithm to better reflect the biases. These comparisons will also be invaluable in the calibration and validation process of the Stratospheric Aerosol and Gas Experiment on the International Space Station (SAGE III ISS) when it launches in the fall of 2016

Continued Project

As a part of a NOAA Student Scholarship Internship Opportunity funded through NOAA CREST, this project was extended during the summer of 2016. Under the guidance of Dr Lawrence Flynn at the NOAA

Center for Weather and Climate Prediction, OMPS-LP data will be used to enhance the NOAA Unique CrIS/ATMS Processing System (NUCAPS). NUCAPS products are combinations of the Cross-track Infrared Sounder instrument and Advanced Technology Microwave Sounder instrument, both on SNPP. NUCAPS has several products, one of which is globally gridded ozone mixing ratio. This ozone mixing ratio

product requires an a-priori ozone input. It is thought that the product can be improved by changing the a-priori to be a daily ozone measurement made by OMPS-LP. Doing this would make the a-priori more robust and would bring it more up to date and be more comprehensive. It has yet to be seen what effect this will have on the end product, but one can assume that the accuracy will increase.

Figures

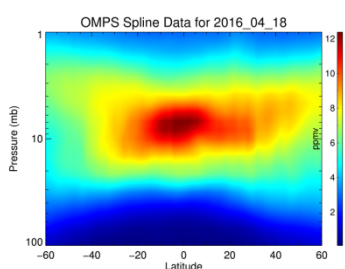


Figure 1: OMPS Spline Data

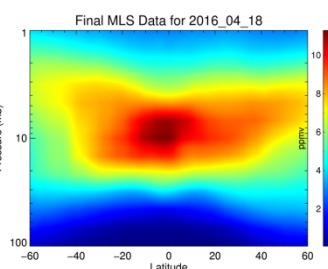


Figure 2: MLS Data

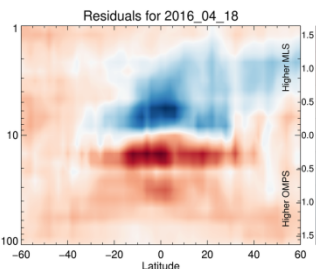


Figure 3: Residual Measurements

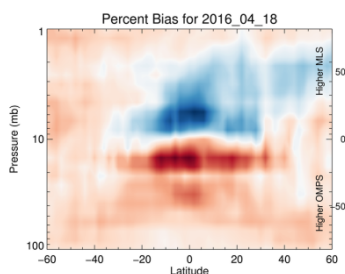


Figure 4: Percent Bias

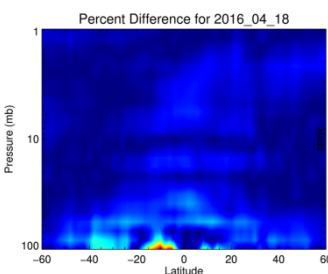


Figure 5: Percent Difference

Acknowledgement

This study was supported and monitored by National Oceanic and Atmospheric Administration (NOAA) under Grant NA11SEC481004. The statements contained within the manuscript/research article are not the opinions of the funding agency or the

U.S government but reflect the author’s opinions.

Presenting and Corresponding Author:

Steven Buckner, PhD Candidate, Department of Atmospheric and Planetary Sciences, Hampton University
Email: stevenb1@umbc.edu

Towards a unified representation of the planetary boundary layer and shallow cumulus convection in numerical climate models

David A. New¹

¹Department of Atmospheric and Oceanic Science, University of Maryland, College Park
Corresponding Author: David A. New (dnew1@umd.edu)

Introduction

Shallow cumulus (SCu) clouds are simply the saturated tops of convective thermals or jets originating in the planetary boundary layer (PBL). As such, SCu clouds can be viewed as local extensions of the PBL into the free atmosphere. However, typical numerical climate models account for PBL turbulence/convection and SCu convection in separate computational modules or parameterizations, which may only communicate with each other through the resolved model state or minimal empirical closures. This separate representation of dry and moist convection is problematic and has long been identified as a critical roadblock for the advancement of numerical climate modeling [1].

We present a unified PBL-SCu parameterization based on a combined mass flux-statistical approach. Under this framework, a model column is orthogonally decomposed into an updraft/convective component and a complementary environmental component. The properties of the updraft component are determined using a mass flux approach, whereby a steady-state updraft model diagnoses the vertical transport of atmospheric properties due to convection. The properties of the environmental component are determined using a statistical approach, whereby up to the second-order statistical moments of atmospheric properties within the environment are determined via prognostic equations.

The key innovation contributed by our approach is the inclusion of a PDF-based statistical updraft model. While typical

updraft models utilized in mass flux schemes diagnose only up to the first-order moments of convective properties, our updraft model diagnoses up to the second-order moments and assumes a joint probability distribution function of those properties. This formulation lends itself to an elegant and physically appealing closure for estimation of convective detrainment.

Experiments and Conclusions

As a proof-of-concept for the proposed parameterization, we present a dry PBL-only version of our scheme in a single-column model (SCM) and test it against day 33 of the Wangara experiment [2], a field project carried out to collect data on convective boundary layers. Day 33 was selected because of its clear skies, lack of large-scale forcing, and its popular use in previous studies. We compare our SCM results directly to the Wangara data as well as to a large-eddy simulation (LES) driven from initial conditions and forcings derived from the Wangara test case.

We compare the PBL height, top entrainment, and turbulence kinetic energy/buoyancy flux profiles between the SCM and LES results to determine the fidelity of our prediction. Our combined mass-flux approach proves to be promising. Technical/computational/numerical issues are discussed, and the extension of our scheme to shallow cumulus-topped PBLs is outlined.

References

- [1] A. Arakawa, J. Climate **17** (2004) 2494-2525
- [2] R. Clarke, A. Dyer, R. Brook, D. Reid, A. Troup, Tech. Paper 19, Div. Met. Phys. CSIRO Aus. (1971)

Acknowledgement

This study was supported by the National Aeronautic and Space Administration

(NASA) Earth and Space Sciences Fellowship (NESSF) and by National Oceanic and Atmospheric Administration (NOAA) Center for Atmospheric Science (NCAS) – NOAA EPP/MSI Grant # NA11SEC4810003. The statements contained within the article are not the opinions of the funding agency or the U.S. government, but reflect the author’s opinions.

Urban Impacts on New York City Weather During a Heat Wave

Luis E. Ortiz¹, Jorge E. Gonzalez¹, Wei Wu², Robert Bornstein³, Martin Schoonen², and Jeffrey Tongue⁴

¹*Department of Mechanical Engineering, NOAA CREST Center
The City College of New York, New York, NY 10031*

²*Biological, Environmental & Climate Sciences Department, Brookhaven National
Laboratory*

³*Department of Meteorology and Climate Science, San Jose State University, San Jose, CA
95192*

⁴*National Weather Service New York Office, Upton, NY 11973*

Abstract

Extreme heat events are projected to increase in magnitude and frequency throughout the 21st century, which combined with the urban heat island effect will present challenges to urban policy and infrastructure. This study presents an application of the factor separation method to assess the contributions of the impervious land cover, the representation of the urban environment, and large scale heat wave conditions to temperatures over New York City. Results of a simulation study found that while the synoptic heat wave conditions had the largest contribution to the temperature field, the surface factors could match it in magnitude in locations where wind flows encounter the urban barrier, such as along eastern Manhattan and along the southern coasts of the city where the tallest buildings are located. The overall effect of the land cover and urban representation held a higher relative contribution at nighttime and early morning, when calmer land breeze conditions result in a marked urban heat island effect. The contribution of the interaction between all three factors is positive during morning and night, which results in a magnification of the urban heat island during a heat wave. A vertical cross-section across part of the city where the urban canopy is densest show effects near the surface that follow the patterns observed in the 2 m air temperature field.

Introduction

Extreme heat events are one of the most damaging weather phenomena, impacting human health, infrastructure, and the environment. Heat waves, typically defined as a series of days with higher than usual maximum temperatures, were the leading cause of weather related fatalities in the United States for the period between 2005 to 2014 ((National Weather Service 2015)). With heat waves projected to increase in magnitude, duration, and frequency in the United States (G. A. Meehl and C. Tebaldi 2004), it is important to understand the interactions of the urban heat island and their surroundings during these potentially catastrophic events. New York City is divided into five boroughs covering 788.9

km², with a greater metropolitan area of 17,405 km². This heavily urbanized region has been the focus of several studies with the aim of characterizing its UHI and its impacts. The NYC UHI signal is strongest during nighttime, with a summertime of 4 °C, with the highest values occurring when surface wind speed was less than 5 kts (2.572 m/s) (Gedzelman et al. 2003). Gedzelman et al. also showed that sea breeze plays an important role in the development of the UHI, with the daytime easterly easterly breeze cooling the coastal and inner city area. In the case of a nighttime easterly or south easterly breeze, the UHI development was delayed, but was not reduced considerably in magnitude. Bornstein (1968) described the vertical structure of the UHI based on a set of

airborne observations during the morning, finding that the temperature increase due to the city extended from the surface to up 300-500 m, with elevated weak inversion layers that starting at almost the same height of the UHI warm layer. It was shown by Gaffin et al. (2008) that due to the complex nature of the urban morphology and their interaction with seasonal wind patterns, the UHI exhibited both spatial and temporal changes, with temperatures varying by as much as 2 °C between inner-city sites. These spatial differences have been shown to be in part due to the heterogeneity of the urban environment, with differences in building and street geometry affecting the intensity of the UHI (Oke 1988). This has been corroborated in more recent studies via use of Computational Fluid Dynamics (CFD) techniques by (Schrijvers et al. 2015; Santiago et al. 2013), showing how wind flow and surface flux patterns change for different height and width configurations. This study focuses on an analysis of the interactions between the urban environment and synoptic conditions, along with their relative impacts to the temperature and wind fields.

Experiments and Conclusions

In order to study the impacts of urbanization to temperature and winds, a factor separation analysis experiment has been carried out, following the methodology of Stein and Alpert (1993). A set of simulations using the Weather Research and Forecast model (WRF) version 3.5.1 were design using as the factors the impervious urban land cover, the representation of the urban morphology, and the synoptic heat-wave conditions. To quantify the contributions of each factor (and their interactions), horizontal temperature field over the NYC Metropolitan Area, as well as a vertical cross-section through Midtown Manhattan. The analysis presented shows an application of the factor separation method to

assess the contribution of the impervious land cover, the representation of the urban canopy, and large scale heat wave conditions, along with the effect of the interactions between them over New York City. The simulation results and analysis showed that both the contributions from individual factors as well as their interactions are significant. Under heat wave conditions, the UHI effect intensifies during the early morning, with the land cover and the interaction between all three factors working to increase the magnitude of the temperature field. At both times studied the temperature field is mostly dominated by the synoptic conditions, with the impervious surfaces-urban representation being of comparable magnitude along hot spots near the western bank of the Hudson River and southern, coasts of Staten Island and Long Island. Surprisingly, however, the interaction between all three factors is negative in magnitude along much of the city itself. Results from the vertical structure show that the effects of the urban land cover and three-dimensional representation, as well as their interactions, follow similar patterns as the horizontal distributions. In general, urban land surface and urban representation lessen with height, while the heat wave conditions are higher aloft. During the afternoon, the urban canopy, with its complex three-dimensional geometry and energy exchanges, appears to determine the vertical wind circulations. Meanwhile under minimum temperature conditions, the wind pattern is dominated by the large scale circulations and are enhanced by the effect of the land cover. The impervious land cover and the urban morphology contributions are higher during the afternoon, with the heat wave taking a more prominent role in the lower temperature part of the diurnal cycle.

While this work focuses on a single heat-wave event, the conditions that led to it are typical of heat waves in the northeast United States, with a high pressure system stagnating

over the eastern sea board (or in some cases, just off the coast). Future works will focus on separating the aspects of the urban representation in order to better understand how these factors interact under extreme heat events, and in applications for future projections of extreme heat events.

References

- [1] Bornstein, R. D., 1968: Observations of the Urban Heat Island Effect in New York City. *J. Appl. Meteorol.*, **7**, 575–582, doi:10.1175/1520-0450(1968)007<0575:OOTUHI>2.0.CO;2.
- [2] Gaffin, S. R., and Coauthors, 2008: Variations in New York city’s urban heat island strength over time and space. *Theor. Appl. Climatol.*, **94**, 1–11, doi:10.1007/s00704-007-0368-3.
- [3] Gedzelman, S. D., S. Austin, R. Cermak, N. Stefano, S. Partridge, S. Quesenberry, and D. A. Robinson, 2003: Mesoscale aspects of the Urban Heat Island around New York City. *Theor. Appl. Climatol.*, **75**, 29–42, doi:10.1007/s00704-002-0724-2.
- [4] National Weather Service, 2015: *NWS Weather Fatal. Inj. Damage Stat.*, <http://www.nws.noaa.gov/om/hazstats.shtml> (Accessed November 20, 2015).
- [5] Santiago, J. L., O. Coceal, and A. Martilli, 2013: How to Parametrize Urban-Canopy Drag to Reproduce Wind-Direction Effects Within the Canopy. *Bound.-Layer Meteorol.*, **149**, 43–63, doi:10.1007/s10546-013-9833-y.
- [6] Schrijvers, P. J. C., H. J. J. Jonker, S. Kenjereš, and S. R. de Roode, 2015: Breakdown of the night time urban heat island energy budget. *Build. Environ.*, **83**, 50–64, doi:10.1016/j.buildenv.2014.08.012.
- [7] Stein, U., and P. Alpert, 1993: Factor Separation in Numerical Simulations. *J. Atmospheric Sci.*, **50**, 2107–2115, doi:10.1175/1520-0469(1993)050<2107:FSINS>2.0.CO;2.

Acknowledgement

This study was supported and monitored by National Oceanic and Atmospheric Administration (NOAA) under Grant # NA11SEC4810004. The statements contained within the manuscript/research article are not the opinions of the funding agency or the U.S. government, but reflect the author’s opinions.

Remote Sensing Monitoring of Canadian Wildfire Smoke and its Impact on Baltimore Air Quality

Shelbi Tippet^{1,2}, Ruben Delgado¹

¹*Joint Center for Earth Systems Technology, UMBC, 1000 Hilltop Cir, Baltimore, MD 21250*

²*Department of Mechanical Engineering, UMBC, 1000 Hilltop Cir, Baltimore, MD 21250*

Introduction

High spatial and temporal resolution Elastic *light detection and ranging* (lidar) measurements allows to monitor long-range transport of particulates, such as dust and smoke, that impact local and regional air quality. These lidar measurements enhance current knowledge and understanding on how vertical layering and long range transport of natural and anthropogenic particle pollution may alter the relationship between column aerosol optical depth and surface particle pollution concentrations.

We analyze the impact and frequency of the transportation of Canadian wildfire smoke to the Mid-Atlantic. We will present a statistical analysis of data from ground based air quality monitors and remote sensing instrumentation which yield the chemical, physical, and optical properties of particle pollution during these events.

Analysis and Conclusions

During the months of June-September, for the years 2009-2015, there have been approximately 30 instances (one or consecutive days) when Canadian smoke has effected Baltimore. This observation includes both cases of layers aloft and mixing within the Planetary Boundary Layer (PBL). When particle pollution is present over Baltimore, the UMBC Elastic Lidar Facility can detect its presence. The lidar profiles can show where in the atmosphere and how much aerosols are present. If aerosols are observed, steps are taken to determine the type and origin of the particulates.

By looking at data from ground based sources such as Particulate Matter (PM) 2.5 monitoring stations, we are able to identify when smoke events occur. A burning biomass will produce smoke comprised of particulates that are small in size, therefore a peak in PM 2.5 values will occur if smoke is present. These particles are particularly dangerous because they are easily inhaled which can have a harmful effect on people's health. During the Canadian smoke events in Baltimore, elevated PM 2.5 values, averaged from multiple Maryland stations, ranged from approximately 15 to 34 $\mu\text{g}/\text{m}^3$. It has also been observed, from the retrievals of our monitor, that there is typically a corresponding peak in extinction during these events due to the increased absorption. There is also a correlation between the presence of wildfire smoke and increased ozone formation. Fires release nitrogen oxides and hydrocarbons; when combined with warm, stagnant summer conditions, ozone can become very high. Canadian wildfire smoke has been shown to elevate Baltimore ozone levels to a maximum of 94 parts per billion over the past 9 years.

Another method for monitoring smoke is to analyze sun photometer data. We look at multiple inversions of data from the AERONET system including size distribution, single scattering albedo, and extinction vs. absorption exponents used for a cluster analysis. A size distribution for Baltimore during a Canadian smoke event could consist of a peak in both fine and coarse mode depending on the aging and coagulation of the particles. Single scattering

albedo (SSA) values typically coincide with the amount of black carbon (BC) present in the aerosol. A larger BC to organic matter ratio in smoke could be suggested by a negative slope in an SSA plot [2]. Forest fires tend to have less absorptive properties because most of the combustion occurs during the smoldering phase which yields higher SSA values [1]. Performing a cluster analysis of daily extinction and absorption averages for months with smoke events reveal that smoke is present on days that typically have an Absorption Ångström Exponent above the value of 1 [2].

We can also compare ground based sources to satellite imagery in order to further verify the nature and origin of particle pollution. A back trajectory analysis of winds can be modeled to show that smoke is carried from Canada to the Mid-Atlantic. MODIS true color images are used to detect and track the presence of smoke, which can be indicated by gray hazy regions. Moderately dense plumes have been visible over Baltimore during these wildfire smoke events. Lastly, the Aerosol Optical Depth (AOD) can identify regions of heavy aerosol loading which would be the condition observed for Baltimore when smoke is aloft. One case, in June 2015, yielded a 245% increase in AOD when compared to the average mean, over ten years, for the month of June.

By researching past smoke events, we are able to identify conditions that enable the long range transport of these particles which

could assist with air quality forecasts. Improving these forecasts could help citizens by providing them with more accurate warnings for poor air quality days. It is also important to differentiate between particles generated by local sources and those of long range transport to ensure that the state is in compliance with national air quality standards. Hopefully, understanding the impact of these particles can help determine what actions should be taken to prevent high amounts of exposure to these emissions.

References

- [1] Oleg Dubovik, Brent Holben, Thomas F. Eck, Alexander Smirnov, Yoram J. Kaufman, Michael D. King, Didier Tanré, and Ilya Slutsker, 2002: Variability of absorption and optical properties of key aerosol types observed in worldwide locations, *J. Atmos. Sci.*, **59**, 3, 590-608.
- [2] P.B. Russell, R. W. Bergstrom, Y. Shinozuka, A. D. Clarke, P. F. DeCarlo, J. L. Jimenez, J. M. Livingston, J. Redemann, O. Dubovik, and A. Strawa, 2010: Absorption Angstrom Exponent in AERONET and related data as an indicator of aerosol composition. *Atmospheric Chemistry and Physics*, 10: 1155-1164.

Acknowledgements

This research is supported by NOAA-CREST, Grant-NA11SEC481004. the Joint Center for Earth Systems Technology, and NOAA Office of Education Educational Partnership Program.

Remote sensing of river ice and ice jams using an automated algorithm with local cloud mask for MODIS and VIIRS: Application over the Lower Susquehanna River (2001-2016)

S. Kraatz^{1,2,*}, P. Romanov¹, and R. Khanbilvardi^{1,2}

¹*NOAA-CREST Institute, The City College of New York (CUNY), NY, NY*

²*Dept. of Civil Engineering, The City College of New York (CUNY), NY, NY*

*Corresponding author: skraatz00@citymail.cuny.edu

The City College of New York (CUNY), 160 Convent Avenue, ST-513, NY, NY 10031

Introduction

Ice jams are accumulations of smaller ice fragments and frazil which may partially obstruct the natural flow of the river when present. Ice jams are natural occurrences during the winter seasons, in particular during the freeze-up and break-up periods during which ice tends to be mobile and have a higher likelihood of forming ice dams. In severe cases, ice dams may cause the river stage to rapidly increase over a short period of time [1]. Hence, ice jams are difficult to model and predict and potentially severe and unexpected floods may occur over a short period of time. Satellite observations may be used to observe the river surface for indicators of ice jams. Daily river ice maps are being generated based on the CREST River Ice Observing System (CRIOS) using the Moderate Resolution Imaging Spectroradiometer (MODIS) [2]. CRIOS relies on the global cloud product (unobstructed FOV flags from MOD35 [3]) to inform on where river ice may be observed. However due to the global nature of the cloud products errors may occur locally such as false cloud detections [4]. The cloud products may also correctly identify semitransparent clouds. In both cases it may still be possible to correctly ascertain whether ice is present or not, potentially resulting more ice observations. For this purpose we developed the semi-transparent cloud algorithm (STC) which was thoroughly

tested and validated with MODIS on Aqua data [5].

Experiments and Conclusions

In this experiment the methodology within STC was applied to both MODIS instruments as well as VIIRS and applied to twelve winter seasons within the 2001-2016 time period. Overall results indicate that this scheme is most effective when applied to MODIS-Aqua data, because the cloud mask (unobstructed field of view flags) incorporated within its atmospherically corrected reflectance product (MOD09GA) appears to have a significant bias toward cloud detection when snow and ice is present. Irrespective of to which platform the STC method was applied, it is shown that at any given time 23%, 45% and 10% more grid cells are found as reasonably cloud free with respect to the global cloud masks, for Terra, Aqua and VIIRS, respectively. With respect to river ice extent and amount, STC also provides consistent ice cover results between platforms with overall correlation of 95% on same day observations, while mean absolute differences in ice extent and amount are small (near 5%). Reflectance difference maps were also found to be useful in identifying ice jam events (as opposed to ice cover), locations and extent. Between the platforms, the probability of detection (POD) for ice is 87-91% proportion correct (PC) is

91-94% and false ice detection (FD) and non-detections of 4-7% and 0-2%, respectively.

References

- [1] S. Beltaos. Cold Regions Science and Technology, **51**(1):2–19 (2008).
- [2] N. Chaouch et al. Hydrological Processes, **28**(1), 62-73 (2012)
- [3] S.A. Ackerman et al. Journal of Geophysical Research: Atmospheres, **103**(D24), 32141-32157 (1998)
- [4] D.K. Hall, G.A. Riggs. Hydrological Processes, **21**(12), 1534–1547 (2007).
- [5] S. Kraatz, R. Khanbilvrdi, P. Romanov. Accepted at Cold Regions Science and Technology (2016).

Acknowledgement

The authors would like to thank Dr. Bill Rossow (CCNY) for his insights and useful suggestions with respect to the algorithm and the reviewers for their helpful comments. This work is supported by the National Oceanic and Atmospheric Administration (NOAA) under CREST grant #NA11SEC4810004. The views, opinions and findings contained in this report are those of the authors and should not be construed as an official NOAA or U.S. Government position, policy or decision.

A Complete Picture of Boundary Layer Events in the Plains Elevated Convection at Night (PECAN) Campaign Including Low-level Jet Vertical Winds

Brian Carroll^{1*}, Belay Demoz¹, Ruben Delgado¹, Bruce Gentry²

¹University of Maryland, Baltimore County

²NASA Goddard Space Flight Center

*Presenting author, *brian25@umbc.edu*, 12706 North Cliff Rd, Bowie, MD, 20720

Abstract

The Plains Elevated Convection at Night (PECAN) field campaign was a large cooperative experiment performed during summer 2015 in the Southern Great Plains region of the United States. PECAN featured intensive observation of nocturnal convection and related events. Nighttime heavy rainfall and thunderstorms are common in the region and crucial to the local agriculture and everyday life. Despite this, predicting such weather events remains very challenging. The preliminary results of two case studies (a LLJ and a bore) presented here will advance the understanding of these phenomena. These studies focus on Doppler lidar wind measurements supplemented by a suite of other instruments.

Introduction

Continuous measurement of tropospheric wind profiles is a vital component to advancing understanding of weather phenomena. Winds reflect dynamic processes in the atmosphere such as transport of heat, moisture, and aerosols which in turn impact cloud diagnostics and pollution. The research to be presented focuses on Doppler lidar wind measurements of mesoscale events supplemented by other instruments retrieving temperature, relative humidity, and more during the Plains Elevated Convection at Night (PECAN) field campaign.

PECAN was a large cooperative experiment performed during the period of June 1st to July 15th in the Southern Great Plains region of the central United States. The multi-agency project included instrumentation and personnel from the NSF, NASA, NOAA, DOE, and universities. PECAN operations focused on intensive observation of convective rain and related atmospheric events, particularly nocturnal convection with a stable boundary layer, nocturnal low-level jets (LLJs), and the largest convectively

available potential energy (CAPE) located above the boundary layer. Nighttime heavy rainfall and thunderstorms are common in the region and crucial to the local agricultural economy and lifestyle. Nocturnal LLJs have been linked with these rainstorms, the quantitative forecasting of which is crucial and very difficult [1].

Data and Research Approach

Two case studies of particular interest will be discussed: a LLJ transporting moisture and a gust front undular bore related to mesoscale convective system (MCS) generation. These events will be studied primarily with data taken at PECAN Fixed Site 2 (FP2) in south central Kansas, near the center of the campaign domain. Two Doppler lidars were stationed at FP2: one 1.54 micron coherent aerosol detection system and one 355nm molecular double-edge direct detection system. These systems are well suited to profile winds and aerosol backscatter with 50m resolution in the first few kilometers of the atmosphere (aerosol-detection system) and provide winds up to

30km altitude with 100m resolution (molecular-detection system) [2]. FP2 also hosted a diverse multitude of other instruments including radiosonde launches, a microwave radiometer, tethered sonde, Atmospheric Emitted Radiance Interferometer (AERI), micropulse lidar, water vapor lidar, K-band radar, and surface instruments to capture a wide range of atmospheric parameters. These provide wind retrieval validation as well as profiling of other key variables like temperature and water vapor to reveal the full dynamic and thermodynamic evolution of the phenomena.

This presentation will also show preliminary results of a study addressing vertical winds during PECAN LLJs. LLJs are identified by a strong, persistent wind maximum within the planetary boundary layer. They are important to the convective systems in the region and also transport heat and mass, affecting other atmospheric dynamics and air quality. There is no discussion in literature concerning vertical winds during LLJs, despite the important implications that vertical air motions would have in understanding and modeling the phenomenon. This study will analyze vertical and horizontal wind speeds over a multitude of spatial and temporal scales to reveal any net vertical motion during LLJs, as well as any correlations between vertical winds, LLJ evolution, and other key atmospheric variables.

Conclusions

Nocturnal convection is a common and crucial aspect of weather in the Great Plains that impacts agriculture and everyday life, and yet quantitative prediction of strong events is very difficult with current knowledge. PECAN provided opportunities to collect extensive data on such events as well as precursor and resulting phenomena. This LLJ case study is a valuable detailed look at moisture transport feeding an MCS. The undular bore is an important feature of MCS outflows. Characterizing the behavior and impact of these dynamic events will advance understanding and hence allow for better modeling and weather prediction in the future.

References

- [1] T. Weckwerth, D. Parsons, S. Koch, S. Moore, M. LeMone, B. Demoz, C. Flamant, B. Geerts, J. Wang, W. Feltz, Bull. Amer. Meteor. Soc. **85** (1986) 253-277.
- [2] C. Flesia, C. Korb, Appl. Opt. **38** (1999) 432-440.

Acknowledgement

This study was supported by NOAA-CREST Grant NA11SEC481004.3. The statements contained within the manuscript are not the opinions of the funding agency or the U.S. government, but reflect the author's opinions.

Weather: An Exploration of Public Engagement and Understanding of Science through NOAA'S Twitter

L. Williams

Howard University, NOAA Center for Atmospheric Sciences
leticia.williams@bison.howard.edu
525 Bryant St. NW
Washington, D.C. 20059

Introduction

Scholars have defined science communication as communication from experts or professional communicators (i.e. scientists, journalists, and public information officers) to the public and non-experts (Treise & Weigold, 2002). This communication most commonly occurs through newspapers, television, magazines, the Internet (Besley & Tanner, 2011), and recently social media. However, there is scant research about the social media as an effective channel for science communication (Gastrow, 2015; Lee & VanDyke, 2015), and these studies merely quantify how scientists use communication technologies to engage in public communication (see Dudo, 2012). Hence, there is a need for science communication scholars to examine science discourse via social media such as Twitter.

The purpose of this research study is to explore whether Twitter can increase public engagement and understanding of science. Since *science* is a broad term that encompasses many different areas of study and disciplines, this study focused on tweets posted by the National Oceanic and Atmospheric Administration (NOAA) about severe weather. This federal science agency was selected because it has been examined in previous studies (see Lee & VanDyke, 2015; Spence et al., 2015), which yielded

contradictory findings about whether NOAA was able to use Twitter effectively.

Experiments and Conclusions

This study was designed as a qualitative thematic analysis of NOAA's Twitter to provide an in-depth analysis of the meaning, themes, and patterns in tweets. Data were collected using purposeful sampling to limit the tweets to messages posted by NOAA, which included their primary Twitter handle (@NOAA) and additional Twitter accounts (i.e. NOAA Climate, NOAA Satellites). The unit of analysis was each individual tweet. Tweets were coded into the following categories: definition/content knowledge, feedback, additional information, behavior, and other. Definition/content knowledge provides information about scientific content or terminology. Feedback engages Twitter users in communication through questions, comments, or responses. Additional information presents more information by asking Twitter users to "click" for more information, "read" a link for more information, or "bookmark" information for later review. Behavior provides specific actions for Twitter users engage in offline (i.e. emergency preparation). Other includes tweets that could not be categorized as definition/content knowledge, feedback, additional information, or behavior.

Preliminary analysis of tweets demonstrated that NOAA used Twitter to share information about severe weather, but minimally engaged the public in communication about science and preparedness for severe weather. This is consistent with previous research, which found that providing information was the most used social media strategy by federal government science agencies (Lee & VanDyke, 2015). Hence, NOAA primarily engaged in one-way communication with limited use of the dialogic loop that occurs during feedback when a science agency starts a dialogue with the general public on Twitter,

and continues when the agency responds or acknowledges that specific user's question, comment, or response. In terms of their feedback, NOAA did not explicitly ask users for feedback, but did engage in the dialogic loop by responding to user's replies and comments. These findings not only contribute to the understanding of science communication, but also offer guidelines for the effective use of social media to ultimately benefit both scientists and society with the opportunity to share information and engage the public through social media.

References

- [1] Besley, J. C., & Tanner, A. H. (2011). What science communication scholars think about training scientists to communicate. *Science Communication*, 33(2), 239-263.
- [2] Dudo, A. (2012). Toward a model of scientists' public communication activity: The case of biomedical researchers. *Science Communication*, 35(4), 476-501.
- [3] Gastrow, M. (2015). Science and the social media in an African context: The case of the Square Kilometer Array telescope. *Science Communication*, 37(6), 703-722.

- [4] Lee, N. M., & Van Dyke, M. S. (2015). Set it and forget it: The one-way use of social media by government agencies communicating science. *Science Communication*, 37(4), 533-541.
- [5] Spence, P. R., Lachlan, K. A., Lin, X., & Del Greco, M. (2015). Variability in Twitter content across the stages of a natural disaster: Implications for crisis communication. *Communication Quarterly*, 63(2), 171-186.
- [6] Treise, D., & Weigold, M. F. (2002). Advancing science communication: A survey of science communicators. *Science Communication*, 23(3), 310-322.

Acknowledgement

This study was supported and monitored by National Oceanic and Atmospheric Administration (NOAA) under Grant – NOAA Center for Atmospheric Sciences

Grant #NA11SEC4810003. The statements contained within the manuscript/research article are not the opinions of the funding agency or the U.S. government, but reflect the author's opinions.

Use of LIDARs in Atmospheric Sciences

Richard Medina¹

¹Howard University, Program in Atmospheric Sciences, Post-Doctoral Fellow
richard.medinacalde@howard.edu

Abstract

The analysis of data and relevance of using Light Detection and Ranging (LIDAR) in Atmospheric Sciences are described. Calculation of aerosol backscattering profiles from Raman LIDAR data and comparison with the CL25K Ceilometer and the Cloud-Aerosol Lidar and Infrared Pathfinder Satellite Observation (CALIPSO) are also presented.

Introduction

In-situ measurements of atmospheric composition as well as optical parameters provide valuable information for climate and atmospheric radiation processes. Remote sensing instrumentation play a significant role in the detection of these parameters and today the use of lasers for particle detection and ranging has become obligatory in almost all atmospheric research centers in the world. In this sense, LIDARs (Light Detection and Ranging), for example, are pulsed laser transmission and receiving systems that were created for long range detection and to show their products in both spatial and temporal dimensions.

The LIDARs operating in the NOAA Center for Atmospheric Sciences (NCAS) at Howard University, Beltsville Campus, Maryland are in-situ instruments that provide a variety of measurements, including, but not limited to aerosol backscattering coefficients, water vapor mixing ratios, nitrogen concentrations and cloud heights. These products are compared with Satellite information for specific days providing a full detail of the atmospheric composition of aerosols and water vapor for the region.

In this presentation, the uses and benefits of the VAISALA CL31 [1], CL51 [2] and CT25K [3] Ceilometers, the Howard

University Raman Lidar (HURL) and the Cloud-Aerosol Lidar and Infrared Pathfinder Satellite Observation (CALIPSO) satellite [4] are described. Also, aerosol backscattering coefficients are compared with these instruments and presented for two specific days.

Experiments and Conclusions

The HURL Lidar makes daytime and nighttime measurements by using three detection channels and a narrow-field-of-view. The products measured are Rayleigh-Mie and pure rotational Raman scattered photons at 354.7 nm, Raman scattered photons from nitrogen molecules at 386.7 nm, and Raman scattered photons from water vapor molecules at 407.5 nm. These measurements are made over temporal and vertical dimensions with resolution of 7.5 m in the vertical range and from 10 s in time resolution. The aerosol backscatter coefficients $\beta_{\pi}^{aer}(\lambda, r)$, are obtained from the molecular backscattering coefficients $\beta_{\pi}^{mol}(\lambda, r)$, and from the HURL aerosol scattering ratio (ASR). The ASR is defined as the ratio of total scattering coefficients (molecular plus aerosol) to molecular scattering coefficients, i.e.,

$$ASR(\lambda, r) = [\beta_{\pi}^{mol}(\lambda, r) + \beta_{\pi}^{aer}(\lambda, r)] / \beta_{\pi}^{mol}(\lambda, r)$$

at wavelength λ and range r [5].

The Ceilometers installed at Howard University Beltsville Campus consists of VAISALA models CL31, CL51 and CT25K. On site data collection for the CL51 started on May, 2013. CL31 data are available from February, 2013 and it was removed from site on October, 2014. The data from the CT25K are available from February, 2006 until March, 2013. Data from ceilometers come in different formats and differ in range and both spatial and temporal resolution. The CL51, for example, provides a spatial resolution of 10 meters from ground level to 15000 meters (~ 50000 feet). The return signal is sampled every 67 ns from 0 to 100 μ s. Cloud detection from this ceilometer is reported up to 13000 meters. The CL31 has shorter detection range than the CL51. It provides a spatial resolution of 5 to 10 meters from ground to a distance of 7620 meters (~ 25000 feet). It digitally samples the return signal every 33 or 67 ns from 0 to 50 μ s. Information about fog, precipitation, and cloud base is possible from the return signal for this ceilometer for the specified height range. On the other hand, the CT25k ceilometer provides a spatial resolution of 15.24 meters (~ 50 feet) from ground to 7620 meters (~ 25000 feet). The CT52K digitally samples the signal every 100 ns from 0 to 50 μ s. From this return signal, information about fog and precipitation, as well as clouds can be derived.

The Cloud-Aerosol Lidar and Infrared Pathfinder Satellite Observation (CALIPSO) satellite - Level 2 Clouds and Aerosol Data Products v3.01 are obtained from the Atmospheric Science Data Center for specific days and compared with ground base measurements from the LIDARs at Howard University Beltsville Campus (HUBC) site.

Data from CALIPSO are organized by latitude and longitude as well as vertical and temporal resolution. Description of the scientific data set can be found at https://eosweb.larc.nasa.gov/project/calipso/calipso_table.

In conclusion, the comparison and validation of backscattering coefficient profiles obtained from both ground and sky LIDARs will allow a better understanding of the aerosol composition of the atmosphere and other optical parameters derived from LIDARs like cloud optical depths and water vapor mixing ratio. Furthermore, LIDARs data can be combined with radiative transfer models to evaluate the radiative forcing that occurs in the region.

References

- [1] Vaisala Oyj, Vaisala Ceilometer CL31 User's Guide, Finland, 2004.
- [2] Vaisala Oyj, Vaisala Ceilometer CL51 User's Guide, Finland, 2010.
- [3] Vaisala Oyj, Vaisala Ceilometer CT25K User's Guide, Finland, 1999.
- [4] Calipso Quality Statements: Lidar Level 2 Cloud and Aerosol Profile Products v3.01, Atmospheric Science Data Center, <http://eosweb.larc.nasa.gov>.
- [5] D. N. Whiteman, Appl. Opt. **42** (2003) 2593.

Acknowledgement

This study was supported and monitored by National Oceanic and Atmospheric Administration (NOAA), Educational Partnership Program, U.S. Department of Commerce, under Grant # NA11SEC4810003. The statements contained within the manuscript/research article are not the opinions of the funding agency or the U.S. government, but reflect the author's opinions.

The Continuing Convection, Aerosol, and Synoptic-Effects in the Tropics (CAST) Field Experiment

Nathan Hosannah¹, Jorge González¹, Rafael Rodriguez-Solis², Hamed Parsiani², Fred Moshary¹, Luis Aponte², Roy Armstrong², Eric Harmsen², Prathap Ramamurthy¹, Moises Angeles¹, Leyda León², Robert Bornstein³, Nazaro Ramirez², Robert Davis¹, Wilson Peña¹, Chris Lunger¹, and Dev Niyogi⁴

¹*NOAA CREST and Department of Mechanical Engineering, The City College of New York*

²*Department of Electrical and Computer Engineering, The University of Puerto Rico at Mayaguez*

³*Department of Meteorology, San Jose State University*

⁴*Department of Agronomy- Crop, Soil and Environmental Sciences, and Department of Earth and Atmospheric Sciences, Purdue University*

Corresponding Author: Nathan Hosannah, Presenter Email: nhosannah@gmail.com

Abstract

The Convection, Aerosol, and Synoptic-Effects in the Tropics (CAST) experiment. Is a continuing atmospheric monitoring experiment based in Puerto Rico. CAST instruments include remote and ground-based sensors including a three-channel LIDAR system, a ceilometer, multiple sunphotometers in the Aerosol Robotic Network (AERONET), soil moisture sensors, radiosondes, a disdrometer, high resolution Tropinet radar, and an air sampler. CAST provided an opportunity to study the large, local, and micro-scale processes important for Caribbean rain production. CAST Phase I (22 June 2016 – 10 July 2016) kicked off during the summer of 2015-one of the driest summers in recent history. Investigation of large scale datasets and local CAST data during Phase I showed that the presence of a strong El Niño, moderate vertical wind shear (VWS), reduced sea surface temperature (SSTs) and high concentrations of Saharan dust led to drier conditions over the Caribbean. CAST Phase II was conducted during a low dust dry season that produced multiple intense rain events (6 – 22 February 2016). Analysis of the low dust Phase II rainfall events suggest that local wind direction, soil moisture, and topography are vital for storm production. Phase III (25 April 2016 – 6 May 2016) showed that synoptic systems and predominately southeasterly winds led to intense island wide rainfall. Lastly, phase IV (27 June 2016 – 12 July 2016) showed that moisture advection and converging trade-winds and sea-breezes overcame dust to produce localized afternoon storms.

Introduction

The Caribbean is a highly complex region in which understanding the factors affecting water availability and the related rainfall production are important for the survival of millions of people. Precipitation in the Caribbean is characterized as bimodal

[1], with peaks in the early (ERS, from April to July) and late (LRS, from August to November) rainfall seasons. The midsummer drought (MSD) occurring in June through July is a drier period within the early rainfall season with reduced rainfall [2]. Saharan dust peaks during the MSD and

has large-scale through micro-scale effects on local weather and climate as it can create a drier atmosphere in the region, promote warming in the dust layer, and suppresses cloud droplet growth via an increase in hydrophobic cloud particle concentrations.

Although large scale systems steer climatological and day-to-day Caribbean precipitation, much of the Caribbean's island-scale rainfall is fueled by local convective processes impacted by topography, land type variations, and site proximity to the coastal waters [3,4]. For example, Puerto Rico has the Cordillera Central, a large mountain range along its center with several peaks above 1 km, the highest of which is Cerro de Punta (18.17 N, 66.59 W) at 1.34 km. The El Yunque natural rain forest is located at the highest peak on the eastern side of the island (18.32 N, 65.78 W) at 1.07 km. These high elevations aid in the production of orographic precipitation when moist air is forced upwards to flow over them. Another location dependent process occurs when the easterly trade-winds converge with the westerly sea-breeze at the western edge of the island; inducing intense afternoon convective storms in the northwest quadrant.

The work herein involves the observational monitoring of the local environment of Puerto Rico to see if evidence of the aforementioned interactions could be attained. The island of Puerto Rico is home to over a hundred surface weather stations, soil moisture sensors, a next generation radar (NEXRAD) system, multiple aerosol robotic network (AERONET) sunphotometers, and National Weather Service (NWS) conducted radiosonde launches. Since a large portion of these instruments are on the east side of the island, more ground-based and in-situ sensors were necessary to supplement the existing network and properly monitor the convective dynamics on the west side of the

island. This led to the inception of the Convection, Aerosol, and Synoptic-Effects in the Tropics (CAST) campaign.

With CAST we ask: Can we prove via a focused surface-atmospheric multi-sensor measurement campaign that large-scale conditions interact with local scale processes to modulate seasonal rainfall? We answer this via the analysis of regional variables including SST, precipitable water, aerosol optical thickness (AOT), and vertical wind shear (VWS) in addition to local multi-sensor data from CAST.

Experiments and Conclusions

CAST was conducted by a team of researchers from multiple institutions including The University of Puerto Rico at Mayaguez (UPRM), The City College of New York (CCNY), the NWS (San Juan), Purdue University (PU), and San Jose State University (SJSU). We scheduled the CAST phases to monitor western Puerto Rico during the MSD (22 June 2015 – 10 July 2015), the DS (6 – 22 February 2016), and the ERS (25 April 2016 – 6 May 2016).

The supplemental CAST instrumentation included up to two radiosonde launches per day, cooperative operation of three high resolution radars, a ceilometer, a disdrometer, a set of soil moisture sensors, and an aerosol speciation sampler, all on the west side of the island. UPRM was the main site, with a CL51 ceilometer (Vaisala), a CIMEL Electronique 318A spectral radiometer (AERONET), and nearby Echo EC-5 soil moisture sensors set at multiple depths between the surface 100 cm. Meteomodem M10 radiosondes were launched from the roof of one of the UPRM buildings. The La Parguera site had an AERONET radiometer in addition to an air sampler for speciation measurements. The Tropinet radar network consists of three

short range dual polarized X-band Doppler radars.

To ensure optimal launch times and ensure that a series of atmospheric conditions were met, radiosondes were launched after thorough analysis of weather maps, NWS forecasts, and AOT forecasts from the NASA GEOS-5 model. The disdrometer, soil moisture sensors, and the ceilometer ran continuously. We made an effort to launch radiosondes within a half hour before the start of rain events and just after the completion of afternoon/evening showers during the DS, ERS, and MSD 2016 phases. CAST results show evidence of local modification of atmospheric dynamics, producing different weather conditions across the island. These local effects interact with large scale processes such as ENSO and Saharan dust. CAST is our first step in understanding the interconnectedness of multi-scale precipitation drivers in over Puerto Rico. The overall long-term goal is to improve our understanding of the atmospheric conditions in the sensitive and complex Caribbean region.

References

- [1] [1] M. E. Angeles, J. E. González, N. D. Ramírez-Beltrán, C. A. Tepley, and D. E., Comarazamy, Origins of
- [2] the Caribbean rainfall bimodal behavior., *J. Geophys. Res.*, **115** (2010), D11106,
- [3] doi:10.1029/2009JD012990.
- [4] [2] D.W. Gamble and S. Curtis, Caribbean precipitation: Review, model, and prospect., *Prog. Phys. Geog.*,
- [5] **32** (2008), 265–276.
- [6] [3] M. R. Jury, S. Chiao, and E. W. Harmsen, Mesoscale structure of trade wind convection over Puerto Rico:
- [7] Composite observations and numerical simulation., *Boundary-Layer Meteor.*, **132** (2009), 289-314.
- [8] [4] N. Hosannah, H. Parsiani, and J.E. González, 2015: The Role of Aerosols in Convective
- [9] Processes during the Midsummer Drought in the Caribbean, *Adv. in Meteor.*, **2015**,
- [10] doi:10.1155/2015/261239.

Acknowledgement

This study was supported and monitored by the NSF Atmospheric and Geospace Sciences Postdoctoral Research Fellowship (AGS-1433430), and National Oceanic and Atmospheric Administration (NOAA) under Grant – NOAA-CREST Grant #NA11SEC4810003. The statements contained within the manuscript/research article are not the opinions of the funding agency or the U.S. government, but reflect the author’s opinions.

Evaluation of MODIS land surface temperature with in situ snow surface temperature from CREST-SAFE

Carlos Perez¹, Tarendra Lakhankar¹, Peter Romanov^{1,2}, Jonathan Muñoz³, Reza Khanbilvardi¹, and Yunyue Yu²

¹*NOAA-CREST, City University of New York, New York, NY, USA*

²*Center for Satellite Applications and Research, NESDIS/NOAA, College Park, MD, USA*

³*Universidad de Puerto Rico, Recinto de Mayagüez, Recinto Universitario de Mayagüez, Universidad de Puerto Rico, Departamento de Ingeniería Civil y Agrimensura, Mayagüez, PR*

Abstract

This paper presents the procedure and results of a temperature-based validation approach for the Moderate Resolution Imaging Spectroradiometer (MODIS) Land Surface Temperature (LST) product provided by the National Aeronautics and Space Administration (NASA) Terra and Aqua Earth Observing System satellites using in situ LST observations recorded at the Cooperative Remote Sensing Science and Technology Center - Snow Analysis and Field Experiment (CREST-SAFE) during the years of 2013 (January-April) and 2014 (February-April). A total of 314 day and night clear-sky thermal images, acquired by the Terra and Aqua satellites, were processed and compared to ground-truth data from CREST-SAFE with a frequency of one measurement every 3 min. Additionally, this investigation incorporated supplementary analyses using meteorological CREST-SAFE in situ variables (i.e. wind speed, cloud cover, incoming solar radiation) to study their effects on in situ snow surface temperature (T-skin) and T-air. This paper also attempts to answer the question of whether a single pixel (1km²) or several spatially averaged pixels should be used for satellite LST validation by increasing the MODIS window size to 5x5, 9x9, and 25x25 windows.

Several trends in the MODIS LST data were observed, including the underestimation of daytime values and night-time values. Results indicate that, although all the data sets (Terra and Aqua, diurnal and nocturnal) showed high correlation with ground measurements, day values yielded slightly higher accuracy (~1°C), both suggesting that MODIS LST retrievals are reliable for similar land cover classes and atmospheric conditions. Results from the CREST-SAFE in situ variables' analyses indicate that T-air is commonly higher than T-skin, and that a lack of cloud cover results in: lower T-skin and higher T-air minus T-skin difference (T-diff). Additionally, the study revealed that T-diff is inversely proportional to cloud cover, wind speed, and incoming solar radiation. Increasing the MODIS window size showed an overestimation of in situ LST and some improvement in the daytime Terra and nighttime Aqua biases, with the highest accuracy achieved with the 5x5 window. A comparison between MODIS emissivity from bands 31, 32, and in situ emissivity showed that emissivity errors (Relative error = -.003) were insignificant.

Introduction

Land surface temperature (LST) is an important parameter for hydrological, meteorological, climatological, and environmental studies because it integrates the products of all surface-atmosphere interactions and energy fluxes [1]. Knowledge of the LST and its fluctuations provide information on the temporal and spatial variations of the surface equilibrium state [2]. Generally, LST is observed through infrared emission. However, due to the limitation that ground stations (i.e. lack of stations in some regions of the World, point-based observations, physical inaccessibility to sites, and digital inaccessibility to the data) present to provide global LST readings, satellite remote sensing (RS) has been the adopted method for LST retrievals over large areas, with the aid of in situ stations [3–5].

The Moderate Resolution Imaging Spectroradiometer (MODIS) is a 36-channel (ranging in wavelength from 0.4 μm to 14.4 μm) visible to thermal-infrared sensor onboard the Terra (1999) and Aqua (2002) satellites launched by the flagship of the National Aeronautics and Space Administration's (NASA) Earth Observing System (EOS) program. MODIS collects visible and infrared imagery and radiometric measurements of the land, atmosphere, cryosphere, and oceans. MODIS daily LST products provide radiometric LST values over land and larger inland waters in swath and grid format. However, it is necessary to assess the accuracy and precision of the retrievals to provide potential LST users with reliable information on the quality of the data. Hence, MODIS LST validation is required to identify possible deficiencies and subsequently introduce improvements in the algorithms. Two methods are commonly applied to validate the LST products generated from RS data: the temperature-based method (T-based) and the radiance-based method (R-based). The

T-based method involves direct comparison with ground measurements performed at the thermally homogenous sites concurrent with the satellite overpass. The R-based method does not require ground measured LST values but does require atmospheric temperature and water vapor profiles, and the surface emissivity over the validation site at the time of satellite overpass [1]. This study focuses on using the T-based method for the T-based validation of the MODIS MOD11A1 (Terra) and MYD11A1 (Aqua) LST products. The T-based method was applied using automated and continuous in situ LST data from a snow-covered suburban site in the sub-Arctic Caribou, Maine, USA. The results will aid the existing MODIS LST literature by providing another T-based validation for a snow-covered site. In addition, it will include the results of supplementary analyses using other meteorological variables (i.e. wind speed, percentage of cloud cover, and incoming solar radiation) recorded at the site to study their effects on in situ snow surface temperature (T-skin) and near-surface air temperature (T-air), and it will study the effects of different MODIS window sizes on in situ LST estimations.

Experiment

The Cooperative Remote Sensing Science and Technology Center - Snow Analysis and Field Experiment (CREST-SAFE) is a ground station located within the premises of the National Weather Service (NWS) office in Caribou, ME, USA (46°52'59"N, 68°01'07"W, 190 m elevation) that has been operational since January 2011. The objective of this field experiment/ground station is to improve the understanding of the effect of varying snow characteristics (*i.e.*, grain size, density, depth, snowpack temperature, T-skin, snow water equivalent (SWE), volumetric water content) on snow microwave emission [6]. Manual and automated observations on snow properties

and meteorological conditions at the site are conducted and recorded all-year round. The station site is mostly comprised of residential houses, grasslands, and the Caribou Municipal Airport. The MODIS 1km² grid cell for the station contains mostly snow, grassland, and some forest cover. Cloud cover is not frequent throughout the year in Caribou.

Results and Discussion

Remotely-sensed LST validation results for daytime observations were better than those during nighttime, indicating higher confidence in the MODIS cloud mask during the day. Furthermore, all biases displayed a MODIS LST underestimation of in situ LST. This is indicative of needed improvements in the MODIS cloud mask for nighttime observations to yield more reliable LST. In general, all biases were low (~1-2°C) and indicative of good agreement between the MODIS LST product and in situ LST. Therefore, MODIS LST readings are reliable for estimating in situ T-skin in areas nearby the station, extending all the way to 25km, as demonstrated by increasing the window size. Additionally, the validation results of pixels with different land covers from the one surrounding the site indicate that CREST-SAFE might be representative of similar surfaces under similar atmospheric conditions.

References

- [1] H. Li, D. Sun, Y. Yu, H. Wang, Y. Liu, Q. Liu, Y. Du, H. Wang, B. Cao, *Remote Sens. Environ.* 142 (2014) 111–121.
- [2] Z.-L. Li, B.-H. Tang, H. Wu, H. Ren, G. Yan, Z. Wan, I.F. Trigo, J.A. Sobrino, *Remote Sens. Environ.* 131 (2013) 14–37.
- [3] Z. Xia, Lang, Mao, Kebiao, Ma, Ying, Zhao, Fen, Jiang, Lipeng, Shen, Xinyi, Qin, *Sensors* 14 (2014) 21385–21408.
- [4] S.M. Robeson, *Clim. Change* 29 (1995) 213–229.
- [5] M. Jin, R.E. Dickinson, *Environ. Res. Lett.* 5 (2010) 044004.
- [6] R. Lakhankar, T.Y., Muñoz, J., Romanov, P., Powell, A.M., Krakauer, N.Y., Rossow, W.B., and Khanbilvardi, *Hydrol. Earth Syst. Sci. Discuss.* 17 (2013) 783–793.

Acknowledgement

This study was supported and monitored by National Oceanic and Atmospheric Administration (NOAA) under Grant #NA11SEC4810003. The statements contained within the manuscript/research article are not the opinions of the funding agency or the U.S. government, but reflect the author's opinions.

A multilevel Poisson regression model to detect trends in frequency of extreme rainfall events

Saman Armal¹, Naresh Devineni², Reza Khanbilvardi²

¹Department of Civil Engineering, City University of New York (City College), 160 Convent Ave, New York, NY 10031, United States

²Department of Civil Engineering, NOAA – Cooperative Remote Sensing Science and Technology Center, City University of New York (City College), 160 Convent Ave, New York, NY 10031, United States,

Abstract

This study presents a new approach to understand the time-space structure of extreme rainfall events and predict their frequency. A multilevel model is developed to consistently account for the temporal trends and variation, using climate estimators. Model coefficients are extracted with respect to the observed local parameters. The model is then validated using a 10-out cross validation approach. The results of Multilevel model were then examined using PCA/Wavelet analysis.

Introduction

The impact of climate variability can increase frequency of heavy precipitation events, particularly in the high latitudes and tropical regions, and in winter in the northern mid-latitudes[1]. In recent years, several studies investigated this interaction by evaluation of the extreme precipitation trends, over global [2] and national scale [3] [4] or at a regional scale [5] [6]. The indicators that trend analysis have been relied on are commonly random variables such as annual maximum daily rainfall, the number of the days above a given threshold or Rainfall intensity-duration-frequency (*IDF*) curves. There is now a growing effort to develop methods and models to understand complex data in a space-time structure.

The common method has been adopted by many authors, is a type of fitting regression, developed based on well-known probabilistic models including Log-Normal distribution, Gumbel [7], Gamma distribution[8] [9], Generalized Pareto [10][11] Generalized Logistic [12] or more frequently, Generalized Extreme Value[13] [14] [15]. One

complication arises from the difference in time-length and duration of datasets. To overcome this problem, Kamruzzaman et al. [16] applied a linear mixed effects to encapsulate the effect of spatial and temporal correlation between different monitoring stations for seasonal rainfall maxima.

For some studies, the objective of rainfall extreme evaluation is to find whether there is a significant positive or negative trends in each monitoring station [13][17]. They might be accurate in temporal trend estimation, but they are not able to capture the consistency between stations, over the region of interest. To resolve this problem, some studies applied Statistical Field Significance techniques[18]. This approach successfully indicates significant trends and spatial consistency but still, it's not applicable in a formally quantitative approach. Recent studies [19][20] [21],[22][23], particularize the power of hierarchical Bayesian approach in frequency analysis and forecasting. The main advantage of these models is to chronicle the data of different sites together with their regional coherence. As the name

suggests, the hierarchical Bayesian models are basically applied in hierarchical (Multi-level) form of different units [24][19] and the role of Bayes theorem is to integrate them; while the within-unit's analysis can describe the respond of individual predictors, across-units process will define the heterogeneity and diversity of the units. The simultaneous inference of variables allows the interaction of estimation errors at different levels and leads to more precise predictive uncertainty. With increase of computational speed and recent numerical advances, *MCMC* methods has been recognized suitable in compatibility with hierarchical models [25]. In the context of Hydrology studies, we can take advantage of this feature and take into account the non-climate variables as well as climate parameters [23].

The model developed in this study, presents a Bayesian Hierarchical model to understand the time-space structure of extreme rainfall events at a national scale. The index applied in the model is the number of days with rainfall more than 95-percentile of the whole period of record (hereinafter, Count Analysis).

Methods and Conclusion

The current Multilevel Model was constructed based on a matrix of 1252 columns and 115 rows, for which each value indicates in a given year of specified station, how many days have been recorded with a total precipitation above 95-percentile (95% count analysis). As well as count analysis values, the geographic information of each station, including longitude, latitude and elevation was incorporated into the model. The climate index considered in the model is *ENSO* (Nino3.4). Since the model is driven by count data, we consider a Poisson distribution in a non-stationary form [26][27]. To confirm the model performance, the leave-m-out cross-validation method was used. The procedure is carried out by leaving out *m* randomly selected data points from the observational dataset for validation, and the model is

developed using the remaining $(n - m)$ observations[28]. Additionally, to understand the spatial correlation of count analysis in different stations, *PCA* analysis was performed on 95% count analysis results. The map projection of *PCA* leading components allow the detection of major climate influences (In this case, *ENSO*). Moreover, to detect the nonstationary trend of extreme rainfall, wavelet analysis was carried out on time series of the first three major *PCs* [29] [30]. Also, to explore the coherence of *PCs* with *ENSO*, the Cross-Wavelet analysis was carried out. With comparison of peak cycle in Cross-Wavelet spectrum, the consistency of *ENSO* effects can be accordingly evaluated [18].

As a result of *PCA* analysis, three major regions with different climate influences, are recognized across the United States. The identified regions are visually consistent with the model findings with respect to the stations' temporal trend. It is obvious that along the line of east coast, and in north eastern/western part of united states there is an increasing trend in the number of extreme events. In the central regions, far from main coast lines, the trends are reversing and the number of extreme events decreases. Furthermore, the model spatial variability on *ENSO* parameters suggest that the location of sites with high corresponding responds is comparable with active area of pacific jet streams storm track [31]. For this reason, the southern stations are showing stronger correlation with *ENSO* variation.

The results of cross wavelet analysis confirm that the *PC3* is more considerably modulated by *ENSO* effects. According to cross wavelet spectrum analysis, *PC3* presents the strongest power level among the leading *PCs*. Based on the results, similar to Wavelet analysis of *ENSO*, the peak cycle of *PC3* can last up to 8 yrs.

The comparison between model parameters and *PCA* results reveals that the spatial

coherence of extreme trends, is more significant in central and north-eastern regions of united states. In other words, negative trend sites hold for higher portion of variability among the data. The comparability of clustering effect in *ENSO* coefficient and *PC3*, suggests that other climate variables rather than *ENSO*, may be more dominant in extreme trends.

References

- [1] IPCC, Managing the risks of extreme events and disasters to advance climate change adaptation, 2012. doi:10.1596/978-0-8213-8845-7.
- [2] B. Asadieh, N.Y. Krakauer, Global trends in extreme precipitation: Climate models versus observations, *Hydrol. Earth Syst. Sci.* 19 (2015) 877–891. doi:10.5194/hess-19-877-2015.
- [3] J. Toggweiler, R. Key, Ocean circulation: Thermohaline circulation, *Encycl. Atmos. Sci.* 4 (2001) 1549–1555. doi:10.1002/joc.
- [4] J. Zhu, Impact of Climate Change on Extreme Rainfall across the United States, *J. Hydrol. Eng.* 18 (2013) 1301–1309. doi:10.1061/(ASCE)HE.1943-5584.0000725.
- [5] G. Villarini, J.A. Smith, M.L. Baeck, R. Vitolo, D.B. Stephenson, W.F. Krajewski, On the frequency of heavy rainfall for the Midwest of the United States, *J. Hydrol.* 400 (2011) 103–120. doi:10.1016/j.jhydrol.2011.01.027.
- [6] D. Parr, G. Wang, K.F. Ahmed, Hydrological changes in the U.S. Northeast using the Connecticut River Basin as a case study: Part 2. Projections of the future, *Glob. Planet. Change.* 133 (2015) 167–175. doi:10.1016/j.gloplacha.2015.08.011.
- [7] S.A. AlHassoun, Developing an empirical formulae to estimate rainfall intensity in Riyadh region, *J. King Saud Univ. - Eng. Sci.* 23 (2011) 81–88. doi:10.1016/j.jksues.2011.03.003.
- [8] L.S. Hanson, R. Vogel, The Probability Distribution of Daily Rainfall in the United States, *World Environ. Water Resour. Congr.* 2008. (2008) 1–10. doi:10.1061/40976(316)585.
- [9] B. Scian, J. Pierini, Variability and trends of extreme dry and wet seasonal precipitation in Argentina. A retrospective analysis, *Atmosfera.* 26 (2013) 3–26. doi:10.1016/S0187-6236(13)71059-2.
- [10] A.A.C. Davison, R.L. Smith, S. Journal, R. Statistical, S. Series, Models for Exceedances over High Thresholds Published by: Wiley for the Royal Statistical Society, 52 (1990) 393–442.
- [11] F. Nippgen, B. McGlynn, R. Emanuel, J. Vose, Water Resources Research, *Water Resour. Res.* (2016) 1–20. doi:10.1002/2014WR015716.
- [12] M.M. Rahman, S. Sarkar, M.R. Najafi, R.K. Rai, Regional extreme rainfall mapping for Bangladesh using L-moment technique, *J. Hydrol. Eng.* 18 (2013) 604–615. doi:10.1061/(ASCE)HE.1943-5584.0000663.
- [13] S.M. Papalexiou, D. Koutsoyiannis, Battle of extreme value distributions: A global survey on extreme daily rainfall, *Water Resour. Res.* 49 (2013) 187–201. doi:10.1029/2012WR012557.
- [14] H. Kuswanto, S. Andari, E.O. Permatasari, Identification of extreme events in climate data from multiple sites, *Procedia Eng.* 125 (2015) 304–310. doi:10.1016/j.proeng.2015.11.067.
- [15] S. Beskow, T.L. Caldeira, C.R. de Mello, L.C. Faria, H.A.S. Guedes, Multiparameter probability distributions for heavy rainfall modeling in extreme southern Brazil, *J. Hydrol. Reg. Stud.* 4 (2015) 123–133. doi:10.1016/j.ejrh.2015.06.007.
- [16] M. Kamruzzaman, S. Beecham, A. V. Metcalfe, Estimation of trends in rainfall extremes with mixed effects models, *Atmos. Res.* 168 (2016) 24–32. doi:10.1016/j.atmosres.2015.08.018.

- [17] L. Bocheva, T. Marinova, P. Simeonov, I. Gospodinov, Variability and trends of extreme precipitation events over Bulgaria (1961-2005), *Atmos. Res.* 93 (2009) 490–497. doi:10.1016/j.atmosres.2008.10.025.
- [18] F. Cioffi, U. Lall, E. Rus, C.K.B. Krishnamurthy, Space-time structure of extreme precipitation in Europe over the last century, *Int. J. Climatol.* 35 (2015) 1749–1760. doi:10.1002/joc.4116.
- [19] B. Renard, A Bayesian hierarchical approach to regional frequency analysis, *Water Resour. Res.* 47 (2011) 1–21. doi:10.1029/2010WR010089.
- [20] X. Chen, Z. Hao, N. Devineni, U. Lall, Climate information based streamflow and rainfall forecasts for Huai River basin using hierarchical Bayesian modeling, *Hydrol. Earth Syst. Sci.* 18 (2014) 1539–1548. doi:10.5194/hess-18-1539-2014.
- [21] X. Sun, M. Thyer, B. Renard, M. Lang, A general regional frequency analysis framework for quantifying local-scale climate effects: A case study of ENSO effects on Southeast Queensland rainfall, *J. Hydrol.* 512 (2014) 53–68. doi:10.1016/j.jhydrol.2014.02.025.
- [22] X. Sun, U. Lall, Spatially coherent trends of annual maximum daily precipitation in the United States, *Geophys. Res. Lett.* 42 (2015) 9781–9789. doi:10.1002/2015GL066483.
- [23] M.R. Tye, D. Cooley, A spatial model to examine rainfall extremes in Colorado's Front Range, *J. Hydrol.* 530 (2015) 15–23. doi:10.1016/j.jhydrol.2015.09.023.
- [24] G.M. Allenby, P.E. Rossi, Hierarchical Bayes Models, *Handb. Mark. Res. Uses, Misuses, Futur. Adv.* (2006) 1–59. doi:10.1111/j.1749-6632.2009.05310.x.
- [25] C.K. Wikle, L.M. Berliner, N. Cressie, Hierarchical Bayesian space-time models, *Environ. Ecol. Stat.* 5 (1998) 117–154. doi:10.1023/A:1009662704779.
- [26] J.H. Andrew Gelman, *Data Analysis Using Regression and Multilevel/Hierarchical Models*, Cambridge University Press, 2007, 2007.
- [27] C.V.-F. Richard M. Feldman, Non-Stationary Poisson Processes, in: *Appl. Probab. Stoch. Process.*, Springer Science & Business Media, 2009, 2009: pp. 114–140.
- [28] N. Devineni, U. Lall, N. Pederson, E. Cook, A tree-ring-based reconstruction of delaware river basin streamflow using hierarchical Bayesian regression, *J. Clim.* 26 (2013) 4357–4374. doi:10.1175/JCLI-D-11-00675.1.
- [29] L.A. Barford, R.S. Fazzino, D.R. Smith, An introduction to wavelets, Hewlett-Packard Labs, Bristol, UK, Tech. Rep. HPL-92-124. 2 (1992) 1–29. <https://www.hpl.hp.com/techreports/92/HPL-92-124.pdf> <http://www.hpl.hp.com/techreports/92/HPL-92-124.pdf>.
- [30] C. Torrence, G.P. Compo, A Practical Guide to Wavelet Analysis, *Bull. Am. Meteorol. Soc.* 79 (1998) 61–78. doi:10.1175/1520-0477(1998)079<0061:APGTWA>2.0.C;20
- [31] Mike Halpert, United States El Niño Impacts, (2014). <https://www.climate.gov/news-features/blogs/enso/united-states-el-ni%C3%B1o-impacts-0>.

Classifying Vertical Wind Speed Profiles for Offshore Wind Resource and Power Assessment

Alexandra St.Pé^{1*}, Shelbi Tippet¹, Scott Rabenhorst², Ruben Delgado³

¹NOAA CREST Center, University of Maryland, Baltimore County, Baltimore, MD 21250, USA,

*Email: astpe@umbc.edu

²Naval Research Laboratory, Washington D.C., 20375, USA

³Joint Center for Earth Systems Technology, Baltimore, MD, 21250, USA

Abstract

To justify the economic viability of a potential offshore wind energy project, an accurate assessment of the site-specific wind resource, thus expected energy yield, is required prior to wind farm construction. Unfortunately, uncertainties during this assessment exist, due in-part to limited offshore wind measurements throughout a turbine's rotor-layer (~40-200m) and related uncertainties predicting a turbine's available power. To better understand these uncertainties in the Mid-Atlantic USA, Doppler wind lidar and other met-ocean measurements were collected offshore within Maryland's Wind Energy Area from July-August 2013. Given the diversity of vertical wind speed profile (VWP) observations, VWPs are classified based on the goodness-of-fit to several mathematical expressions. Results demonstrate VWP variability is related to prevailing wind direction (i.e. offshore fetch), as more unexpected VWP are found during wind regimes blowing from land to sea. In terms of potential impact on a wind turbine's available power, unexpected VWP types are associated with greater variability in critical superimposed meteorological features known to impact turbine performance, therefore the importance of predicting such variability cannot be understated. Finally, the sensitivity of several techniques used to estimate a turbine's available power are demonstrated, elucidating how both an overestimate and underestimate in available power may occur given distinct VWP type and the technique employed, representing a possible concern for the offshore wind energy industry in the Mid-Atlantic USA.

Introduction

It is well known that a turbine's operational power performance (i.e. power curve) may deviate significantly from *expected*, prior to wind farm construction. This is a critical offshore wind industry challenge to overcome given its impact on the accuracy of a proposed project's economic viability (i.e. Annual Energy Production (AEP)). In part, expected energy yield uncertainties are related to limitations in the current industry standard approach for estimating turbine power, which relies on hub-height wind speed values only, as it is assumed to be representative of the wind speed throughout the turbine's entire rotor-layer (~40m-200m), thus the shape of the Vertical Wind speed

Profile (VWP) is logarithmic-like. Using high spatial and temporal wind measurements the validity of this assumption was questioned, and it is now known that VWPs can deviate significantly from logarithmic-like behavior, thus similar hub-height wind speed with varying VWP shape may not produce identical turbine power [1]. To overcome this power assessment challenge, a new Rotor-Equivalent Wind (REW) term was introduced to account for the influence of wind speed shear and turbulence throughout a turbine's rotor-layer on performance, yielding a reduction in power estimate uncertainties compared to techniques using hub-height wind speed values only [1].

However, although REW techniques may reduce power assessment uncertainty, uncertainties introduced when *characterizing a site-specific wind resource* can limit the applicability of REW power assessment. Given a severe lack of offshore met-ocean measurements throughout a potential turbine's rotor layer, during a wind resource assessment, the industry relies on a power law technique to extrapolate surface wind data and estimate variability in the offshore VWP shape. As a result, the limitations inherent in standard power assessment also transpire in standard wind resource assessment, as the VWP is often assumed to be logarithmic-like. This is a salient challenge within a coastal environment, as research suggests VWPs often deviate from theoretical, logarithmic-like shape, due to land-sea discontinuities and the presence of internal boundary layers that propagate from land to sea [2, 3].

As trends towards larger offshore turbine rotor-swept areas continue, measurement and prediction of unexpected VWP shapes (i.e. non-conformity to logarithmic-like shape) driving differences between hub-height wind speed and REW power assessment techniques is also needed to reduce uncertainties in a project's expected energy yield. In this study, we classify the variability of offshore VWPs during the summer season across the offshore Mid-Atlantic's environment using goodness-of-fit to mathematical expressions. Once VWP types are classified, additional met-ocean data are investigated to test relationships with local meteorological regimes and understand the predictability of such VWP variability. Finally, to relate varying offshore VWP shapes to potential uncertainty in turbine performance, the sensitivity of turbine available power estimate techniques to each VWP type is demonstrated.

Experiment and Conclusions

The University of Maryland Baltimore County (UMBC) deployed Doppler wind lidar technology and other in-situ instruments within Maryland's offshore Wind Energy Area (WEA) during the State's sponsored geophysical survey (July-August 2013). Commercial Doppler wind and Elastic lidars (Windcube V2 and ALS-450) collected vertical profiles of aerosols and wind (speed and direction) on board the *Scarlet Isabella*. To understand variability in VWP shape, 10-minute mean VWPs (40m-220m) were classified based on goodness-of-fit to several mathematical expressions. Results suggest a low-level wind maximum as the most frequent VWP *type* (~37%), while only ~17% resembled industry-standard logarithmic-like, power law wind profiles. In addition, a strong dependence between VWP type and wind direction are found, with power-law profiles persisting during northeasterly hub-height (100m) wind flow, while more *unexpected* VWP types occur during southwesterly. Using data from the nearest buoy, relationships between local met-ocean conditions and offshore VWP types are also explored; suggesting slightly cooler air temperature and unstable atmospheric conditions during power-law VWPs compared to unexpected VWP types.

Rotor-Equivalent Wind (REW) turbine available power estimation techniques, which account for the superposition of several wind parameters throughout a turbine's rotor layer, are found to improve estimates of turbine available power compared to the industry-standard hub-height wind speed only technique. To elucidate the potential impact of VWP variability on turbine available power estimates, several modifications of REWs with industry standard techniques are compared. On average, REW estimates demonstrate less available power than the industry-standard *measured* hub-height wind

speed approach. However, REW available power estimates are greater on average when compared to the wind resource assessment standard approach of extrapolating offshore surface wind data to estimate hub-height wind speed and power, assuming a power law relationship between wind speed and height (i.e. VWP shape). Therefore, results demonstrate that while measured hub-height wind data may overestimate available power, extrapolation of surface wind data to estimate hub-height values for available power estimates may underestimate the wind resource potential. This trend is consistent when comparing available power estimates for each VWP type, except for linear and low-level wind minimum VWP types, which yield REW available power estimates greater than the measured hub-height wind power approach. Although the true impact of VWP type on a turbine's available power is unconfirmed without actual turbine power data, the results elucidate how both an overestimate and underestimate in turbine available power may occur given distinct VWP type variability and the available power estimate technique employed.

References

- [1] Wagner, Rozenn, et al. "The influence of the wind speed profile on wind turbine performance measurements." *Wind Energy* 12.4 (2009): 348-362.
- [2] Kettle, Anthony J. "Unexpected vertical wind speed profiles in the boundary layer over the southern North Sea." *Journal of Wind Engineering and Industrial Aerodynamics* 134 (2014): 149-162.
- [3] Mahrt, L., Dean Vickers, and Edgar L. Andreas. "Low-level wind maxima and structure of the stably stratified boundary layer in the coastal zone." *Journal of Applied Meteorology and Climatology* 53.2 (2014): 363-376.

Acknowledgement

This study was supported and monitored by National Oceanic and Atmospheric Administration (NOAA) under (CREST) Grant # NA11SEC481004. The statements contained within the manuscript/research article are not the opinions of the funding agency or the U.S. government, but reflect the author's opinions.

Determination of Planetary Boundary Layer Heights from Doppler Wind Lidar Measurements

Benjamin Tucker^{1,2}, Ruben Delgado¹, Brian Carroll¹, Belay Demoz¹, Thomas Rieutord³, Alan Brewer⁴, Aditya Choukulkar⁵, Timothy Bonin⁵

¹*Joint Center for Earth Systems Technology, UMBC 1000 Hilltop Circle, Baltimore MD 21250*

²*Department of Mechanical Engineering, UMBC 1000 Hilltop Circle, Baltimore MD 21250*

³*Météo-France*

⁴*NOAA Earth System Research Laboratory*

⁵*Cooperative Institute for Research in Environmental Sciences, Boulder, CO*

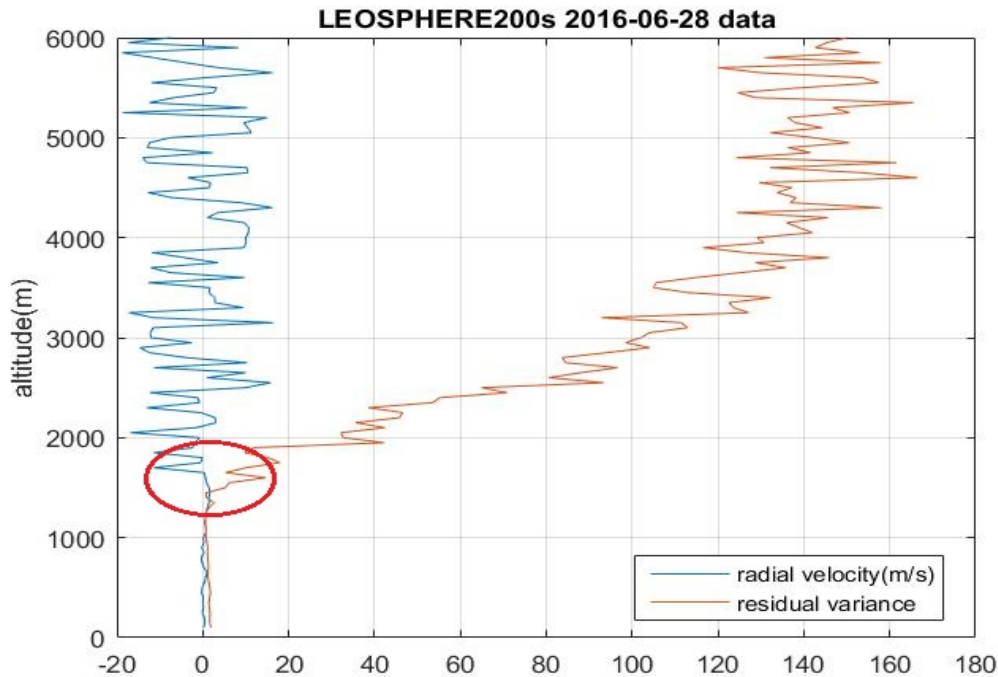
Abstract

The purpose of this study is to determine the planetary boundary layer height (PBL) measurements from Doppler wind lidar measurements. Three numerical analysis methods will be tested on the collected Lidar data. First, the peak detection method based on Haar wavelet transform will be directly applied to the range-corrected intensity profiles to detect the peak of wavelet covariance transform as the boundary layer height estimate. The second method, peak-based thresholding method, defines the highest point within the threshold connected to the ground as the boundary layer height from the velocity variance profiles. The third method is called the classic Cluster Analysis, which automatically selects different types of scans for each specific time period of the day based on the range change of the boundary layer height. This algorithm helps improve the accuracy of the boundary layer height measurement. The three numerical analysis methods will be applied to data collected during the Plains Elevated Convection at Night (PECAN) campaign. The results will be compared to PBL heights determined by aerosol elastic lidars, radiosondes and microwave radiometers.

Introduction

Aerosol particles tend to congregate within the planetary boundary layer (PBL), this makes accurate measurements of the PBL height a valuable tool in air pollution forecasting, and air pollution dynamics. Another result of this congregation, is sharp gradients in aerosol concentration occurring at the top of the PBL, making it measurable by observing the carrier to noise ratio (CNR). Although, aerosol concentration is not the only factor that experiences this sharp gradient, it is seen with wind velocity as well. By making a line of best fit for the radial velocity and subtracting each velocity value from the corresponding point in the fit, a residual value for each velocity in the dataset can be found. The vector formed by taking

the variance of the residuals at each altitude experiences the same gradient at the end of the boundary layer as aerosol concentration and wind speed. This is shown below by a random velocity profile in a dataset and the residual variance vector for that set. The location of the sharp gradient is observed to be almost the same, it is circled in red.



The simplest way to find the PBL height is by observation, but this would be close to impossible when working with very large datasets. Applying the covariance wavelet transform (CWT) to CNR or velocity profiles has proved effective, but it often picks up smaller gradients that do not correspond to the top of the PBL. Because of this, a great deal of filtering and re-application of the CWT is necessary to obtain reasonable results. In an attempt to improve this method, the CWT will be applied to the residual variance and the Cramer-Rao lower bound minimum variance, in hopes that these profiles experience less sharp gradients within the PBL than CNR or radial velocity. That way the CWT will only pick up gradients at the very top of the boundary layer.

Measurements and Algorithms

The data used for testing was taken by UMBC's Leopshere 200s Doppler Wind Lidar on June 28, 2015. It was observed that the most accurate PBL heights were found using 45° PPI scans. MATLAB code was

written to determine wind velocity residual variance and Cramer-Rao lower bound variance. Again, using MATLAB, the CWT was applied to these profiles, local minimum values were found for each transform and the lowest local minimum corresponds to the edge of the boundary layer. With this, a series of PBL heights was determined. Once a PBL height was found values. It first makes sure the height is above 500m, then, it ensures that at each height, its two adjacent heights are within 500m of it, if they are not, the wavelet is rerun until it is. Once the entire set of heights is ran through, a continuous, accurate PBL height remains.

Conclusion

The planetary boundary layer height is a useful parameter in wind forecasting, air pollution forecasting and air pollution dynamics. An accurate measurement of it using only data from ground based wind LIDARs is an extremely helpful tool, and would greatly benefit the scientific community.

References

- [1] Jaime C. Compton, Ruben Delgado, Timothy A. Berkof, Raymond M. Hoff, Determination of Planetary Boundary Layer Height on Short Spatial and Temporal Scales: A Demonstration of the Covariance Wavelet Transform in Ground-Based Wind Profiler and Lidar Measurements
- [2] Thomas Rieutord, Automatic detection of the boundary layer using Doppler LIDAR measurements

Acknowledgement

This study was supported and monitored by National Oceanic and Atmospheric Administration (NOAA) under Grant – (Joint Center for Earth Systems Technology) Grant #NA11SEC4810004. The statements contained within the manuscript/research article are not the opinions of the funding agency or the U.S. government, but reflect the author’s opinions.

Investigating the Effects of Saharan Dust on Tropical Deep Convection using Spectral Bin Microphysics

Matthew Gibbons¹, Qilong Min¹, and Jiwen Fan²

¹ *Atmospheric Science Research Center, State University of New York, Albany NY 12203, USA*

² *Earth Systems Analysis & Modeling, Pacific Northwest National Laboratory*

Presenting Author: Matthew Gibbons, Matthew.Gibbons@albany.edu

Abstract

To better understand the impacts of dust aerosols on the macrophysical and microphysical properties of deep convective cloud (DCC) systems, a case study in the tropical eastern Atlantic was investigated using the Weather Research and Forecasting (WRF) model coupled with a Spectral Bin Microphysics (SBM) model.

Introduction

Deep convective clouds, such as those found within mesoscale convective systems (MCS), have a large impact on regional cloud cover, radiative transfer, and atmospheric circulations. They are also significant sources of precipitation especially in the tropics ([1]; [2]). Quantifying the effects of dust and other aerosols on deep convective clouds (DCC) is difficult due to the complex coupling between microphysical, dynamical and radiative processes involved, especially regarding ice and mixed phase processes ([3]; [4]; [5]). Dust aerosols have been observed at significant concentrations even in remote locations far from their expected source regions [6] and have been established to act as effective ice nuclei (IN; [7]). The action of dust as IN is particularly important since the majority of precipitation formation occurs in the ice phase. Case study observations have reported that dust aerosols have strong microphysical impacts on MCSs for similar dynamical conditions ([8]; [9]; [10]; [11]) which may alter precipitation vertical structures, shift the precipitation size distribution from heavy to light precipitation, and even suppress precipitation entirely. These changes in precipitation vertical structure can have a profound impact on the latent heat profiles of the atmosphere and

subsequently regional and global circulations ([12]; [13]).

Experiments and Conclusions

To improve the understanding of dust aerosol-DCC interactions, we have subjected the case study first proposed by [8], and later expanded by [9], [10], and [11], to a detailed numerical simulation using the WRF with a Spectral Bin Microphysics (SBM; [14]) model. A MCS developing in the tropical eastern Atlantic was simulated under pristine and dusty conditions. Dust cases added a layer of IN between 1km and 3km, featuring number concentrations of: 0.12 cm^{-3} (case D.12), 1.2 cm^{-3} (case D1.2a), and 12 cm^{-3} (case D12), respectively. In addition, two sensitivity studies were undertaken, based on the D1.2a case, to test the effects of removing ice formation by deposition (D1.2b) or immersion (D1.2c) freezing on the resulting cloud and precipitation properties.

We found that the greater heterogeneous ice formation in the dust cases resulted in stronger midlevel ice growth and increased vertical motion due to greater latent heat release. When IN number was increased, initial ice formation in the dust cases shifted from homogenous to heterogeneous freezing. This change in the heterogeneous and homogeneous ice partition lowered cloud top height in the dust cases, by up to 3.29 km in

the D12 case, despite the stronger vertical motion present. This is consistent with the findings of [9], and is due to a greater percentage of large particles at the cloud top and stronger internal circulations.

The formation of small heterogeneous ice reduces riming efficiency, leading to smaller graupel sizes, and increases the formation of snow by ice particle aggregation. Competition for available resources limits the growth of individual particles near the freezing level and delays precipitation formation to higher altitudes. The increased formation of large snow in the dust cases results in larger reflectivity values above the freezing level. Smaller particles forming near the freezing level and transported down melt and reduce reflectivity values near the surface, consistent with observations.

Total surface precipitation accumulation is reduced proportionally as IN concentration is increased, due to less efficient graupel formation reducing convective rain rates. Stratiform precipitation accumulation is increased due to more active snow formation, but does not counteract the reduced convective accumulation. In addition, two dust cases with identical IN concentrations were simulated to test the contributions of immersion and deposition freezing on the resulting hydrometeor profiles. Removal of deposition freezing results in a deeper liquid layer and enhanced total surface precipitation, while removal of immersion freezing reduces surface precipitation between that of the D1.2a and D12 cases.

References

- [1] Arakawa, A. (2004). *Journal of Climate*, 17(13), 2493-2525.
- [2] Solomon, S., Qin, D., Manning, M., ... & Wratt, D. (2007). Technical summary.
- [3] Tao, W. K., Chen, J. P., Li, Z., Wang, C., & Zhang, C. (2012). *Reviews of Geophysics*, 50(2).
- [4] Boucher, O., Randall, D., ... & Zhang, X. Y. (2013). ... *fifth assessment report of the intergovernmental panel on climate change* (pp. 571-657). Cambridge University Press.
- [5] Gibbons, M., Min, Q., and Fan, J. (2016). *Atmos. Chem. Phys. Discuss.*, doi:10.5194/acp-2016-368
- [6] Prospero, J. M. (1999). *J. of Geophys. Res.: Atmospheres* (1984–2012), 104(D13), 15917-15927.
- [7] Pruppacher, H. R., & Klett, J. D. (1997). *Microphysics of Clouds and Precipitation ...*, 954pp.
- [8] Min, Q. L., Li, R., ... & Chang, F. (2009). *Atmos. Chem. and Phys.*, 9(9), 3223-3231.
- [9] Min, Q., & Li, R. (2010). *Atmos. Chem. and Phys.*, 10(16), 7753-7761.
- [10] Li, R., & Min, Q. L. (2010). *J. of Geophys. Res.: Atmospheres* (1984–2012), 115(D9).
- [11] Min, Q. L., Li, R., ... & Wang, S. (2014). *Atmospheric Research*, 143, 64-72.
- [12] Tao, W. K., Smith, E. A., Adler, R. F., & Haddad, Z. S. (2006). *Bul. Am. Met. So.* 87(11), 1555.
- [13] Wei-Kuo, T., Houze Jr, R., & Smith, E. A. (2007). *Bul. Am. Met. So.* 88(8), 1255.

Acknowledgement

This work was supported by the NSF under contract AGS-1138495, by US DOE's Atmospheric System Research program (Office of Science, OBER) under contract DE-FG02-03ER63531, and by the NOAA Educational Partnership Program with Minority Serving Institutions (EPP/MSI) under cooperative agreements NA11SEC4810004 and NA17AE1623. J. Fan is supported by the U.S. Department of Energy (DOE) Atmospheric System Research (ASR) Program. The Pacific Northwest National Laboratory (PNNL) is operated for the DOE by Battelle Memorial Institute under contract DE-AC06-76RLO1830. The statements contained within the manuscript/research

article are not the opinions of the funding agency or the U.S. government, but reflect

the author's opinions

.

Determining Planetary Boundary Layer Heights from NWS ASOS Ceilometer Network

Kweku Mills-Robertson, Ruben Delgado¹, Kevin Vermeesch¹, Ricardo Sakai², Dennis Atkinson³, Michael Hicks³, Belay Demoz¹

University of Maryland, Baltimore County

Co-authors affiliation: ¹University of Maryland Baltimore County, ²Howard University, ³NOAA National Weather Service

Abstract

The National Research Council identified lower tropospheric profiling of trace gases, aerosol and thermodynamic quantities as a cross-cutting need for air quality, weather, climate, energy and other national priority economic areas. The planetary boundary layer (PBL) height is an important meteorological parameter that affects near-surface atmospheric pollutant concentrations since it determines the volume of air into which pollutants and their precursors are emitted. This height is also important in determining the relationship between column measures of gases and aerosols, the concentration measured at the surface, since pollutants are frequently created and contained within the PBL, and serves as a diagnostic to improve air quality forecasting and dispersion models. This presentation will explore the application of the Covariance Wavelet Technique (CWT) to ceilometer data from the National Weather Service Automatic Surface Observing System's (ASOS) to examine the possibility of accurate and continuous PBL height measurements.

Introduction

The planetary boundary layer (PBL) is the lowest part of the of the atmosphere and it is directly influenced by contact with the planetary surface. In this section of the atmosphere (troposphere), PBL continuously changes and is affected by wind speed and thickness of the air as a function of temperature [Haby 2016]. Thus during the day and especially in the warmer seasons, PBL levels tend to have a higher thickness with increased temperature. While the summer days are getting warmer, there is a mixture of aerosols in the air, causing the PBL to expand and become denser throughout the day.

The lowest two kilometers of the atmosphere are only probed infrequently in time and sparsely in the United States. In particular, the 00Z and 12Z launches of radiosondes are particularly ill-posed to obtain planetary boundary layer height (PBLH), mixing, and depth at the peak of the

heating cycle in the daytime. Potential for continuous monitoring of PBL heights with ceilometer is examined. The top of the convective mixed layer can be retrieved from ceilometer returns, using aerosols as a tracer, and analytically using the covariance wavelet technique (CWT) [Brooks, 2003]. Accurate determination of the PBL height using the CWT will allow improved weather and air quality identification.

Method

A ceilometer is a LIDAR (Light Detection and Ranging) device that uses scattering of photons (laser) to determine the PBL and its corresponding heights. This device allows us to measure backscattering phenomenon by using short pulses of light that from the transmitter on the ceilometer to the atmosphere, then back to the receiver to compute the signal of backscattering light. This is employed using the Covariance Wavelet Transform (CWT) function on

Matlab, and we can measure the PBL and planetary boundary layer heights (PBLHs).

The CWT function analyzes every backscatter profile using the Haar function:

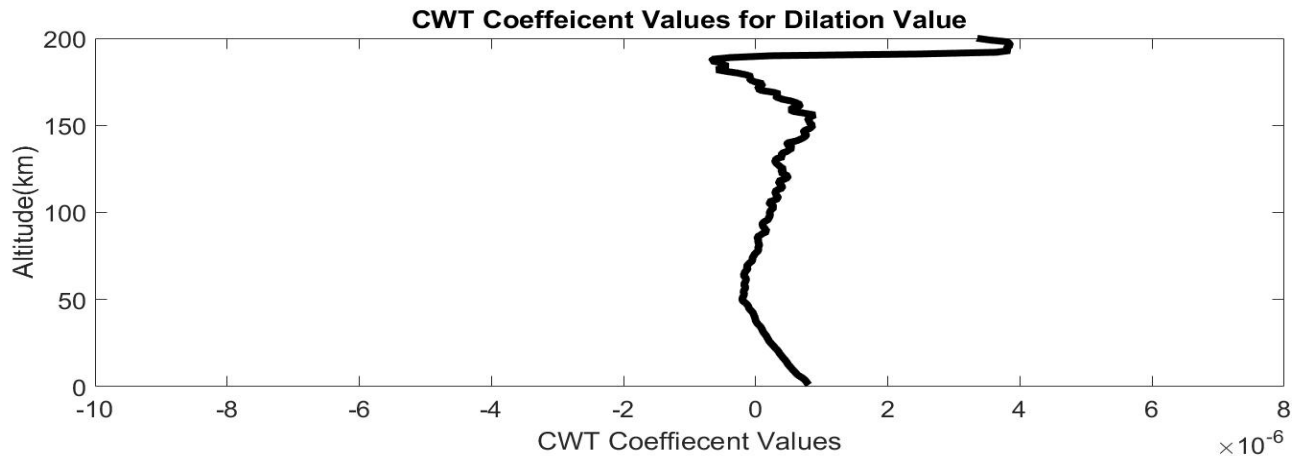
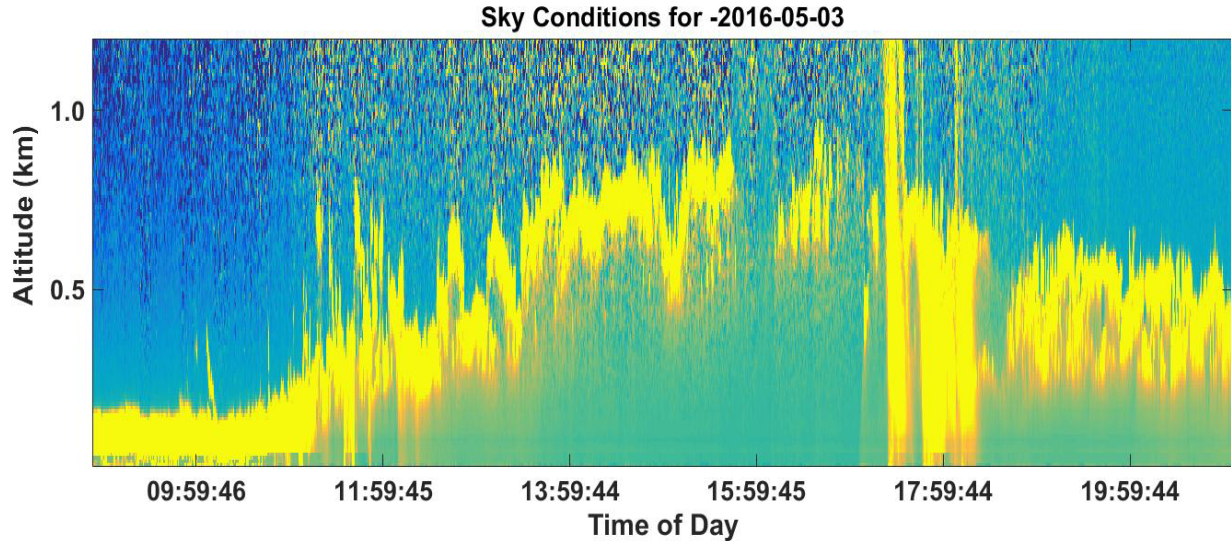
$$h\left(\frac{z-b}{a}\right) = \begin{cases} -1: & b - \frac{a}{2} \leq z \leq b \\ +1: & b \leq z \leq b + \frac{a}{2} \\ 0: & \text{elsewhere} \end{cases} \quad (1)$$

where 'h' is the vertical distance, 'b' is the center of the Haar function, and 'a' is the

dilation number. The CWT of the Haar function in turn is defined by the Gamage and Hagelberg by this equation:

$$W_f(a,b) = \frac{1}{a} \int_{z_1}^{z_2} f(z) h\left(\frac{z-b}{a}\right) dz \quad (2)$$

where $\frac{1}{a}$ is the normalization factor and f(z) is the signal being analyzed as a function of the altitude.



Here is a figure of the planetary boundary layer based on the CWT function. It is a time-height image obtained on May 3rd. This is a false color contour representation of the relative backscatter from aerosols in the PBL. It is evident that as the progresses

towards 4PM, PBL growth continues to approach a maximum, and then begins to decrease towards the night. This was a very dense aerosol day due to the heavy boundary layer produced. A dilation value of 200 was used to obtain the boundary layer in the first figure due to the day being very hazy. The

bottom picture shows how a dilation value produces local minimums at PBLH of all the gradients. Thus larger gradient will be located at the top. The CWT function can correctly identify PBLH but this is still undergoing modifications to improve its detection.

References

[1] Haby, Jeff. n.d. "The Planetary Boundary Layer." theweatherprediction.com. Accessed June 2016.
<http://www.theweatherprediction.com/basic/pbl/>.

[2] Brooks, I.M., 2003: Finding the boundary layer top: application of a wavelet covariance transform to lidar backscatter profiles. *J. Atmos. Oceanic Technol.*, 20: 1092-1105.

[3] NRC. 2009. *Observing Weather and Climate from the Ground Up: A Nationwide Network of Networks*. Washington, DC. National Academy Press.

Acknowledgement

NOAA CREST CCNY Grant –
NA11SEC4810004, NOAA Office of
Education.

Study of Photolysis Rate Coefficients to Improve Air Quality Models

Suhail Mahmud¹, Pema Wangchuk¹, Rosa Fitzgerald², Dr. William Stockwell³, Dr. Duanjun Lu⁴

¹University of Texas at El Paso, Computational Science Department

²University of Texas at El Paso, Physics Department

³Howard University, Chemistry Department

⁴Jackson State University, Physics and Meteorology Department

Abstract

The main objective of this work is to measure hemi-spherically integrated spectrally resolved solar photon flux between the wavelengths of 300 and 700 nm (actinic flux), and use the measured actinic flux to improve air quality simulations. Photolysis is the main driver of ozone production and this factor defines the significance of this research work. The actinic flux has been measured during the summer of 2015 in the El Paso-Juarez Airshed, at the UTEP campus location to calculate photolysis rate coefficients for nitrogen dioxide (NO₂), ozone (O₃) and formaldehyde (HCHO). The improved photolysis rate coefficients have been integrated into a photochemical air quality model (CAMx), and simulations for a selected modeling summer 2015 ozone episode have been performed in the El Paso-Juarez Airshed in an attempt to improve on air quality forecasting. Although this methodology is applied in the El Paso-Juarez Airshed, it can be used in any US region.

Introduction

Photolysis rate coefficients are known as “j-values” or photolysis frequencies. A j-value, is determined by the product of the spherically integrated photon flux, $I(\lambda)$, the compound’s absorption cross sections, $\sigma(\lambda)$, and its quantum yields, $\phi(\lambda)$, all integrated over the range of available wavelengths.

$$J = \int I(\lambda) \times \sigma(\lambda) \times \phi(\lambda) d\lambda \quad (1)$$

A j-value is a frequency because its dimension is (time)⁻¹. A photolysis rate is the product of the j-value and the photolyzed species concentration. The differences between modeled photolysis rate coefficients and those based on measured actinic flux may be very different. These differences have a strong effect on air quality simulations of ozone and these are discussed in Stockwell and Goliff (2004).

Experiments and Conclusions

A spectrally resolved radiometer (spectrometer) was used to measure actinic flux, subsequently the photolysis frequencies were obtained. The actinic flux spectrometer is located on the roof of the Physical Sciences Building at the University of Texas, located in the city of El Paso. Due to the lack of the presence of clouds, two days were selected for the simulations, July 1 and 2. Using the improved photolysis frequencies the air quality simulations were performed using the CAMx model for the El Paso-Juarez Airshed (Stockwell, Fitzgerald, Lu, Perea, 2013).

Three cases were selected for simulation for the selected days: “Base case” (with j-values calculated according to standard modeling methods), “P10” (increasing the j-values for all species by 10% from the base case) and “ozone column” (matching the instrument’s

measured and modeled surface ozone j-values by adjusting the ozone column used to calculate all j-values.

Figure 1 shows the time series inter-comparison of all 3 cases against TCEQ data for July 1, 2 for the TCEQ monitoring station, CAMS12, located in the UTEP campus. The Base case and the ozone column case are superimposed on each other and appear as a single line in the scale shown.

studies and to develop a multi-variate methodology that optimizes the photolysis rate coefficients not only for ozone, but also for NO₂ and formaldehyde. This will result in an improved methodology and more accurate forecasting.

4. For the July 2 analysis, Hysplit analysis was used to study the transport of air masses from west Texas towards western states, causing the July 1 ozone episode disturbance based in the

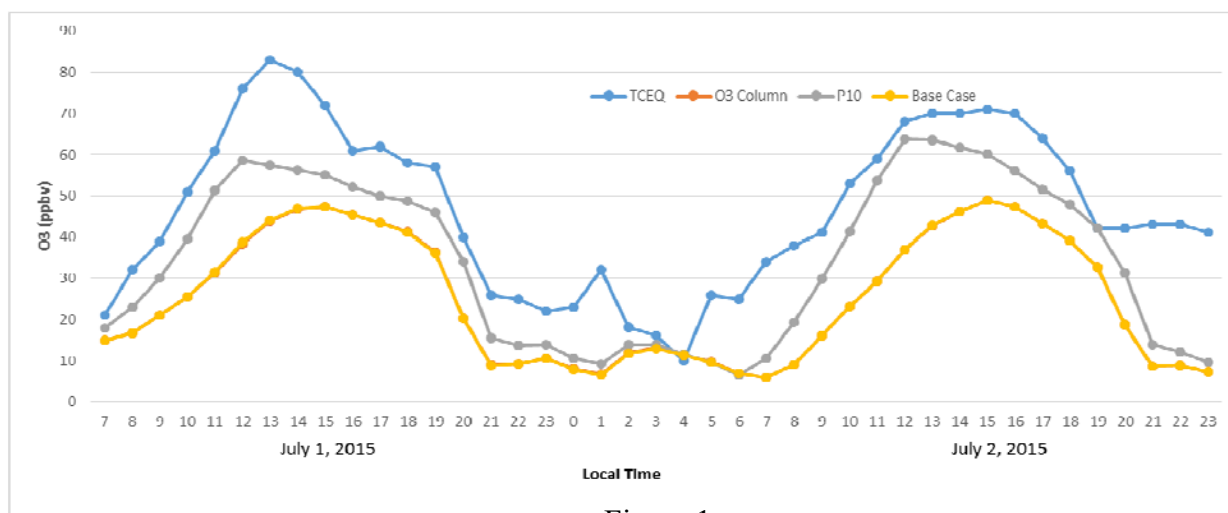


Figure 1

It is concluded:

1. The model simulation for the Base case under-predicts ozone but all cases follow faithfully the overall trend of the experimental ozone results.
2. The case that performed best was the P10 case, as observed in Figure 1. It is concluded that as the photolysis rate coefficients for all the species are raised by 10% the NO₂ concentration decreases, and it appears that the NO decreases even faster, causing the

Ozone to increase its concentration, in closer agreement to the experimental values.

3. The ‘ozone column case’ shows a slight increase in surface ozone, which is not visible in the scale chosen for the graph, which was selected to exhibit all cases. It is evident that it would be necessary to perform further

El Paso-Juarez region, to move towards the west.

References

[1] W. Stockwell and W.S. Goliff, Atmos. Environ., 38, 5169-5177, 2004.
 [2] W. Stockwell, R. Fitzgerald, D. Lu, R.Perea, Journal of Atmospheric Chemistry, 70, 91-104, 2013.

Acknowledgement

This study was supported and monitored by National Oceanic and Atmospheric Administration (NOAA) under Grant (NCAS), Grant # NA11SEC4810003. The statements contained within the manuscript/research article are not the opinions of the funding agency or the U.S. government, but reflect the author’s opinions.

Risk Analysis of New York City Extreme Rainfalls Applying Nonparametric Simulation on Radar Rainfall Data

Ali Hamidi, Naresh Devineni, Reza Khanbilvardi

NOAA-CREST Institute, The City College of New York, CUNY

Abstract

The goal of this study is to apply simulation based approach to reproduce spatially dependent storm data and use it to quantify the risk of extremes in New York City and to compare with the current design criteria.

Introduction

Flood response in an urban area is basically the product of interactions of spatially and temporally varying rainfall (e.g., [1]), and infrastructures (e.g., [2]). An improved representation of the critical forcing of urban hydrologic systems by meteorological and climatic processes is an essential aspect of predicting their function. Today, much of the stormwater in New York City (NYC) flows over impervious surfaces into roof drains or catch basins in the streets and from there into the sewers that can pose challenges to the City in the form of flooding and combined sewer overflows (CSOs). Stormwater management systems must be sized to detain a required volume while achieving the release rate consistent with DEP's stormwater performance standard. Scenarios that properly represent likely storm tracks through the city and the associated space-time patterns of rainfall can help improve the operation of these systems and the assessment of system performance. Knowing the rainfall pattern in order to select the simulation method is an essential step. Hamidi et al. (2016) [3] recently demonstrated that there is a distinct spatial clustering of extreme rainfall events in NYC for the summer and winter time and thus there is a spatial structure in radar rainfall data set suggesting a potential for joint or discrete occurrence of extreme rainfall events. The goal of this study is to apply simulation based approach to generate spatially dependent

storm field data and use it to quantify the risk of extremes in NYC and to compare with the current DEP design criteria. We follow a multivariate simulation method described by Lall et al (2015) [4] using nonparametric copula approach together with a sampling strategy which the desired multivariate dependence and spatial structure is simulated by appropriately reordering the simulations from each individual site's probability distribution. Using copula concept, an arbitrary multivariate distribution function is decomposed into marginal distribution functions, which can be independently different for each variable, and a copula function describing the dependence part of the distribution. In this study, radar data stage IV from 2002-2015 is employed to determine extreme rainfall events and examine the spatial consistency between them in NYC. In the simulation step, 100 random simulations are developed from the current storm fields.

Methodology and Conclusions

We used 14 years of daily stage IV radar data from 2002 – 2015. The data provides spatial resolution of 4km×4km, archived by NCEP and are available in Earth Observing Laboratory (EOL), (<http://data.eol.ucar.edu>). The 95th percentile, of the rainfall was identified at each grid box and then we look through all 5112 days in the 14 years record and process the daily rainfall data to identify the rainfall in a grid box that exceeds the estimated 95th percentile for that grid box in

that day. This resulted in a total of 598 extreme event days. This data set is imported to the simulation model.

The notion of copula is very useful to implement efficient algorithms for simulating joint distributions in a realistic way where the dependence structure is modeled independently of the margin distributions [5]. Let F be a joint distribution of multiple random variable and F_i is the marginal distribution function for x_i $i=1:m$. Copula is introduced as a distribution function that links the joint distribution F to its univariate marginal F_i . Sklar (1959)[5] proved that for every multivariate distribution F there exists a copula such that:

$$F(x_1, x_2, \dots, x_m) = C(F_1(x_1), F_2(x_2), \dots, F_m(x_m)) \quad (1)$$

where $F_i \sim U[0,1]$. When the margins are continuous we can write Eq-1 based on density function:

$$f(x) = f_1(x_1)f_2(x_2)\dots f_m(x_m)c(u_1, u_2, \dots, u_m) \quad (2)$$

where u_i are uniformly distributed random variables. Then we should fit an appropriate probability density, $f_i(x_i)$, to the data for the i^{th} variable, and an appropriate copula function across all variables based on following steps :

1- log-spline density estimation is fitted to each $i=1:102$ grids including $j=1:598$ i.e.d rainfall extreme events. From each fitted $f_i(x_i)$, a random sample (x'_{ij}) and corresponding rank (R'_{ij}) with the length $n=598$ event are drawn. This step is repeated 100 times (no. of simulation). Keeping the record of rank of each sample is to remain the spatial dependency through the simulation.

2- For the copula part $c(u_1, u_2, \dots, u_{102})$, empirical (pseudo) copula is considered. In this case, copula function is applied on the empirical distribution functions of historical data set x_j , $j=1:598$ where basically provides vector r_j ($j=1:598$), corresponding to x_j . Under this approach, empirical copula $C_{emp}\{z_j, j=1:598\}$ is constructed where z_j is a rank matrix. From rank matrix z_j , 598 sample are

drawn with replacement (bootstrap) and recorded as z'_j , $j=1:598$. This step is also repeated 100 times (no. of simulations).

3- Finally, having the rank matrix from marginal distribution, R'_{ij} , as well as rank matrix from empirical copula, z'_{ij} , the new variable is defined as: $w_{ij} = x'_{ij} \delta(z'_{ij} - R'_{ij})$ where δ is delta function, equals to 1 if the argument is 0 and 0 else.

Results of simulation indicates the pattern of correlation remains the same as observation verifying the simulation approach. NYC design rainfall intensity (e.g., 98%ile of time history data) is taken from observational station at Central Park and the exceedance map for the City is provided employing the median rainfall from simulated data. Results indicate that Manhattan and Staten Island Boroughs experience more exceedance comparing to Queens, Brooklyn and Bronx. We can see imaginary line between upper west and lower east part of NYC. Also, using NYC land-use, composite runoff coefficient (C) is developed for each sub-watershed. Subsequently, using rational method and having the area (A) and intensity (I) of simulated data, discharge $Q=CIA$ of each sub-watershed of NYC is determined and mapped.

In this study, we used simulated data to generate extreme rainfall field for NYC. Usually, in the city scale we need high resolution data to better understand the pattern of rainfall. However, these data sets suffer of limited time history. In traditional method of generating design storm, neighbor grids or stations data is used to substitute of space for time. In this study, however, we generated a simulation of extreme rainfall field with the corresponding uncertainty for each grid to resolve the problem of limited time history and in this case the discharge maps and exceedance maps are more realistic.

References

- [1] Arnoud, P., C. Bouvier, L. Cisneros, and R. Dominguez (2002), Influence of rainfall spatial variability on flood prediction, *J. Hydrol.*, 260(1–4), 216–230, doi:10.1016/S0022-1694(01)00611-4.
- [2] Smith, J. A., M. L. Baeck, J. E. Morrison, P. Sturdevant-Rees, D. F. Turner-Gillespie, and P. D. Bates (2002), The regional hydrology of extreme floods in an urbanizing drainage basin, *J. Hydrometeorol.*, 3(3), 267–282.
- [3] Hamidi A., N. Devineni, J.F. Booth, A. Hosten, R.R. Ferraro, and R. Khanbilvardi, (2016), Classifying Intensity and Area of Extreme Rainfall in Greater New York Area using Weather Radar Data, Submitted to *Journal of Hydrometeorology*.
- [4] Lall, U., N. Devineni, and Y. Kaheil, (2015). An Empirical, Nonparametric Simulator for Multivariate Random Variables with Differing Marginal Densities and Nonlinear Dependence with Hydroclimatic Applications. *Risk Analysis*.
- [5] Sklar A. Fonctions de repartition à n dimensions et leurs marges. *Publications de l'Institut de statistique de l'Université de Paris*, 1959; 8:229–231.

Acknowledgement

This study was supported and monitored by NOAA-CREST – Cooperative agreement NA11SEC4810004.

Tracking Volcanic Aerosols Using CALIPSO and HYSPLIT

Sean Leavor¹ and Michael Hill¹

¹*Hampton University*

893 Charlotte Drive, Newport News, VA 23601 | leavorsr@gmail.com

23 Tyler Street, Hampton, VA 23668 | michael.hill@hamptonu.edu

Introduction

Volcanic aerosols with a high stratospheric aerosol loading can have a significant impact on the atmosphere. These aerosols have an effect on stratospheric and surface temperature and are linked to the destruction of ozone. Volcanic eruptions can release sulfur dioxide (SO₂) into the atmosphere, which can later be converted into sulfuric acid (H₂SO₄). These aerosols can absorb radiation from the Earth's surface, which warms the stratosphere, and they reflect radiation from the sun, cooling the surface. Sulfuric acid provides a surface area for nitrogen compounds (NO_x) to react and form nitric acid (HNO₃). The nitrogen compounds, which react with ozone destroying chlorine compounds to form inert compounds, are removed from the atmosphere, leading to an increase in the destruction of ozone.

The Kelud volcano, located in East Java, erupted on February 13, 2014 at 15:50 UTC with another large explosion following at 16:30 UTC, and the ash plume from the volcano reached up to 25 km. The eruption was observed by multiple satellite instruments, such as the VIIRS (Visible Infrared Imaging Radiometer Suite) instrument on the Suomi NPP satellite, and the CALIPSO (Cloud Aerosol Lidar and Infrared Pathfinder Satellite Observations) satellite passed over the ash plume at 18:13 UTC.

The CALIPSO satellite was launched on April 28, 2006 as a part of the A-train satellite constellation, which is composed of the OCO-2, GCOM-W1, Aqua, CALIPSO, CloudSat, and Aura satellites, with the purpose of studying climate change in the Earth's atmosphere. In particular, CALIPSO

studies the effects of aerosols and clouds on the climate. The satellite orbits the Earth about 14 times per day. The instruments onboard the satellite are the lidar, CALIOP (Cloud Aerosol Lidar with Orthogonal Polarization), the Infrared Imaging Radiometer, and the Wide Field Camera, with the main focus being on the lidar. The lidar can produce laser pulses at 532 nm and 1064 nm at a frequency of 20.25 Hz. Backscatter is taken in by a telescope, and the beams pass through interference filters to reduce noise, with the 532 nm beam passing through a beam splitter to polarize the beam into its perpendicular and parallel components.

The HYSPLIT (Hybrid Single-Particle Lagrangian Integrated Trajectory) trajectory model, managed by the Air Resources Laboratory of NOAA, is useful in tracking the aerosols from volcanic eruptions. By inputting the latitude, longitude, altitude, and time where an aerosol layer is located, HYSPLIT can create a forward or backwards trajectory for the aerosol layer. A new point is calculated for each hour of the trajectory, and the output from HYSPLIT is a text file of these points and a plot of the trajectory. Other information can be included in the trajectory, such as the terrain height.

Methodology

To create a trajectory for the Kelud eruption, the first step is looking through the online CALIPSO images produced by NASA to locate a high stratospheric aerosol loading. Then, the CALIPSO data is read to pinpoint the latitude, longitude, and altitude of regions of high backscatter, which can then be used with HYSPLIT to make an initial trajectory.

Because CALIPSO reports altitude above mean sea level and HYSPLIT outputs the altitude above terrain, the terrain height is added to the trajectory measurements to be consistent with CALIPSO. After the trajectory is made, it is compared with later CALIPSO measurements to find coincidences, points along the trajectory where CALIPSO also measures aerosols. Coincidences are found within 50 km and 24 hours of a HYSPLIT measurement. The reason for this is that the average distance between HYSPLIT measurements is about 50 km. The 24 hour time difference is used because the stratosphere is stable, and aerosols can stay in a region for long periods of time. Coincidences are only created using measurements from nighttime CALIPSO orbits to eliminate the solar noise of daytime orbits. Once a coincidence is found, it is entered into HYSPLIT as a means of refreshing the trajectory, as trajectories become less accurate after about 10 days. Then, the coincidences and trajectory are plotted together on latitude vs longitude and time vs altitude plots for a complete visualization of the trajectory.

Results and Future Work

From the CALIPSO browse images, there are three regions of high backscatter near the eruption between 18 and 19 km, between 22 and 23 km, and at 25 km. Three points were used to create a trajectory. The first point is at 7.533 S, 111.901 E, and 18539.6 m with a backscatter value of 0.08001. The second point is at 7.802 S, 111.843 E, and 18958.7 m with a backscatter of 0.01876, and the third point is at 7.668 S, 111.872 E, and 18359.9 m with a backscatter of 0.03307. A 10 day trajectory created with these points shows the aerosol layer moving southwest over the Indian Ocean for the first three days, with the layer moving mostly westward towards Africa afterwards. The trajectory for each point is similar until the last two days, where the

second point at 18.9 km is shown to have traveled 10 degrees longitude further to the west than the other points, passing over the northern tip of Madagascar. On February 14, each point rises in altitude by 0.5 km before dropping by the same amount a few hours afterwards, and the aerosols stay within 1 km of their starting altitude over the course of the trajectory. Because the trajectories for each point are similar, many of the reported coincidences are from aerosol layers that are shared between the points. There are other points within these coincident aerosol layers that can be tracked backwards with HYSPLIT to the Kelud eruption.

The next step in using the trajectory is to characterize the aerosols to help in determining their impact on the atmosphere. This can be done using depolarization ratio and color ratio measurements from CALIPSO. The depolarization ratio can be used to determine the shape of aerosols, and the color ratio can be used to determine the size of the aerosols. Other satellite instruments are also useful in characterizing the aerosols. For example, the MLS (Microwave Limb Sounder) instrument onboard the Aura satellite can provide measurements of SO₂ in a region. The Aura satellite is part of the same satellite constellation as CALIPSO, and the two satellites pass over the same region within 15 minutes of each other, which makes MLS particularly useful for characterizing the aerosols.

Acknowledgement

This study was supported and monitored by National Oceanic and Atmospheric Administration (NOAA) under Grant – (NOAA CREST) Grant # NA11SEC4810004. The statements contained within the manuscript/research article are not the opinions of the funding agency or the U.S. government, but reflect the author's opinions. This research is also supported by the data sets provided by the CALIPSO and MLS teams.

Modeling Regional & Global Atmospheric Chemistry Mechanisms: Observing Adverse Respiratory Health Effects due to Air Pollution from Modeling Output Data

A. Saunders, Emily M. & B. Stockwell, William R.
Howard University, NCAS (NOAA Center for Atmospheric Sciences)

Abstract

Atmospheric chemistry models are used for air quality forecasting and these require chemical reaction mechanisms to simulate the production of air pollution. Chemical boundary conditions are another necessity for the simulations. Global models may be used to provide boundary conditions to regional models. NOAA/NCEP uses the Community Multi-scale Air Quality Model (CMAQ) for air quality forecasting and one of its standard chemical mechanisms is the Regional Atmospheric Chemistry Mechanism, Version 2 (RACM2). The goal of this project is to develop the Global Atmospheric Chemistry Mechanism (GACM), a global version of RACM2. GACM is intended for use in global scale atmospheric chemistry models to provide chemical boundary conditions for regional scale simulations by models such as CMAQ. GACM includes additional chemistry for marine environments while reducing its treatment of the chemistry needed for highly polluted urban regions. This keeps GACM's size small enough to allow it to be used efficiently in global models. GACM's chemistry of volatile organic compounds (VOC) is highly compatible with the VOC chemistry in RACM2 allowing a global model with GACM to provide VOC boundary conditions to a regional scale model with RACM2 with reduced error. The GACM-RACM2 system of mechanisms should yield more accurate forecasts by regional air quality models such as CMAQ.

Introduction

Air Pollution occurs when gaseous and particulate contaminants are present within the earth's atmosphere. Some of the gaseous pollutants that are found within the atmosphere are nitric oxides (NO_x), ozone, and volatile organic compounds. Pollutants that are pumped into the atmosphere and directly pollute the air are called primary pollutants. Further air pollution can be produced if the primary pollutants in the atmosphere undergo chemical reactions and the resulting compounds that are called secondary pollutants. This research focuses on the production of tropospheric ozone (O₃) within the lower atmosphere, which is caused when NO_x and volatile organic compounds (VOCs) are mixed and irradiated by sunlight. According to EPA, ozone is a powerful air pollutant that can irritate the airways causing coughing, a burning sensations, wheezing and shortness of breathe. These symptoms can

contribute complications to asthma and other lung diseases such as bronchitis and chronic obstructive pulmonary disease. The main goal of this research project is to help people located in highly polluted regional and global cities understand how air pollution affects their health.

The main objectives of this project are to develop GACM and to compare model simulations made with GACM to those made with RACM2. Simulations will be made with chemical box models that focus on atmospheric chemistry in the absence of meteorology and also with meteorological transport – transformation models such as CMAQ and the 3-D Weather Research & Forecasting Model coupled with chemistry (WRF-Chem). Finally the air quality model simulations will be analyzed with the EPA's Environmental Benefits Mapping & Analysis Program – Community Edition (BenMAP-

CE) to estimate the human health impact and economic value of air quality changes.

Experiments and Conclusions

Chemical box models coupled with the regional and global atmospheric chemistry mechanisms (RACM2 & GACM) will be used to make simulations of the amount of tropospheric ozone, nitric oxides, and volatile organic compounds that are produced in regional and global communities. RACM2 was designed to simulate remote polluted conditions from the earth's surface to upper troposphere (Goliff, et al., 2013). The simulations focus on the Los Angeles' South Coast Air Basin (SoCAB) where the Pacific Ocean meets a highly polluted urban area.

These two mechanisms will be compared on the basis of simulated ozone concentrations over this marine-urban region. Simulations made with the more established RACM2 will be compared with simulations made with the newer GACM. In addition WRF-Chem will be used to simulate how RACM2 will produce regional simulations of tropospheric ozone and NO_x, which can be further, analyzed for air quality impacts. WRF-Chem allows the impact of gas-phase mechanisms on chemical predictions and the coupling between chemistry and meteorological processes to be assessed. There is a need for an accurate representation of such feedbacks through various atmospheric processes in the model (Zhang, et al., 2012). Both the regional and global model (coupled with climatological data from

measurement data) in WRF-Chem will be used to predict how the concentrations of ozone and nitrogen oxides change over land and ocean.

The air quality model simulation results will be applied to the BenMAP-CE, which estimates the human health impact and economic value of air quality changes. After the atmospheric chemistry model simulations the results will be analyzed through creating time series for O₃, NO_x, & VOC and creating two-dimensional isopleths. The air quality simulation results will be analyzed with the BenMAP-CE program to understand how air pollution affects human respiratory health in highly polluted regional and global regions.

References

- [1] Goliff, W., Stockwell, W. R., & Lawson, C. V. (2012). The Regional Atmospheric Chemistry Mechanism, Version 2, *Science Direct, Volume 68*, Pages 174-185.
- [2] Zhang, Y., Chen, Y. C., Sarwar, G., & Schere, K. (2012). Impact of gas-phase mechanisms on WRF/Chem predictions: mechanism implementation and comparative evaluation. *J. Geophys. Res.*, 117, D01301.

Acknowledgement

This study was supported and monitored by the National Oceanic and Atmospheric Administration, Office of Education Educational Partnership Program award NA11SEC4810003. Its contents are solely the responsibility of the award recipient and do not necessarily represent the official views of the U.S. Department of Commerce, National Oceanic and Atmospheric Administration.

Episodic Rainfall and Saharan Dust Events Analysis Using Ceilometers CL31 and CL51, Satellite and Surface Measurements

M.J. Santiago¹, R.A. Armstrong¹, and N. Hosannah³

¹University of Puerto Rico, Mayaguez, NCAS

³City University of New York, CREST

Abstract

The presence of clouds as well as suspended aerosols from Saharan dust events have a significant impact by means of reduction and/or dispersion in the amount of solar radiation that reaches the Earth's surface. This work involves analysis of the cloud features and backscatter properties over the tropical environment of Puerto Rico during different weather scenarios, and investigation of the Saharan dust impacts on cloud formation. The Vaisala CL31 ceilometer located at the Aerosol and Radiation Network (AERADNET) station in La Parguera, Puerto Rico and CL 51 at the University of Puerto Rico detects low and mid-cloud base heights (CBH), cloud intensity, and backscatter properties. Satellite sensors such as the Moderate Resolution Imaging Spectroradiometer (MODIS) can accurately detect clouds at high altitudes. The CL-View/BL-View software is used for ceilometer data visualization and analysis purposes. Satellite imagery provides high-level cloud detection for the selected episodic events. Additional surface measurements of precipitation, at-surface solar radiation, temperature, and other weather related data are measured using a Davis Weather Station Vantage Pro 2 located at AERADNET station in La Parguera.

Introduction

Aerosol particles are one of the main constituents that seeds cloud formation. Some of the most common aerosols particles monitored are dust, smoke and sulfates as its presence pose a threat to human health [1]. Ceilometers can be used to quantify the presence of low-level aerosols using backscattering measurements [2]. Rosenfeld and contributors (2001) indicated that mineral dust suppresses precipitation due to the small size range of cloud condensation nuclei (CCN) leading to clouds with small droplets (non-precipitation clouds) [3]. On the contrary, Khain and collaborators stated that cloud formation is only delayed due to a large number of small droplets with a low collision rate and decreased falling speeds which prevents a decrease in vertical velocity leading to increased latent heat and higher level convective clouds [4]. Sharma et al.,

(2015) indicated that the ceilometer provides low to mid cloud data that can be useful to determine cloud type and cloud cover along with other vertical properties, while satellite sensors like MODIS are better suited for the detection of high level clouds [5].

This work involves the analysis of cloud features and backscatter properties over the tropical environment of Puerto Rico with particular emphasis in the western region during different weather scenarios, and the assessment of Saharan dust impacts on cloud formation. The study required ground-based, satellite and modeled data in order to identify weather phenomena such as rainy or Saharan dust events.

Experiments and Conclusions

Ground-base data were obtained from the NCAS Aerosol and Radiation Network (AERADNET) station in La Parguera and

CREST research station at University of Puerto Rico at Mayaguez. Cloud depth, intensity and backscattering data were retrieved from the Vaisala CL31 ceilometer located in La Parguera and the CL51 ceilometer in Mayagüez. Weather conditions were obtained using a Davis Weather Station Vantage Pro 2 located at AERADNET and the Doppler RADAR archive from the NWS-San Juan. Other instrumentation included the Aerosol and Radiation Network (AERONET) in each of the stations to examine aerosol optical depth (AOD) in order to identify Saharan Dust events. Satellite-derived images from MODIS were useful to identify cloud features at high altitude, particularly for episodic rainfall events. The Navy Aerosol Analysis and Prediction System (NAAPS) model from the NRL Monterrey Aerosol website supported evidence of the type of aerosols over the study region and the NOAA Hybrid Single Lagrangian Integrated Trajectory Model (HYSPLIT) provided backward trajectories to identify its source. Finally, the Cloud-Aerosol Lidar and Infrared Pathfinder Satellite observation (CALIPSO) offered additional information on the vertical structure of clouds as well as aerosol properties at a larger scale. Preliminary findings suggest that convective clouds can

develop during moderate Saharan dust events over Puerto Rico.

References

- [1] J. Liu, D. L. Mauzerall, L. W. Horowitz, *Atmos. Environ.* **43** (2009) 4339.
- [2] A. M. Sundström, T. Nousiainen, T. Petäjä, *J. Atmos. Ocean. Technol.* **26** (2009) 2340
- [3] D. Rosenfeld, Y. Rudich, R. Lahav, *Proc. Natl. Acad. Sci.* **98** (2001) 5975
- [4] A. P. Khain, D. Rosenfeld, A. Pokrovsky, *Quart. J. Roy. Meteor. Soc.*, **131** (2005) 2639
- [5] S. Sharma, R. Vaishnav, M. V. Shukla, P. Kumar, P. K. Thapliyal, S. Lal, Y. B. Acharya, *Atmos. Meas. Tech. Discuss.* **8** (2015) 11729

Acknowledgement

This study was supported and monitored by National Oceanic and Atmospheric Administration (NOAA) under Grant – (NCAS) Grant # NA11SEC4810003 and Grant – (NOAA-CREST) Grant # NA11SEC4810004. The statements contained within the manuscript/research article are not the opinions of the funding agency or the U.S. government, but reflect the author’s opinions.

Tracking and Characterizing Stratospheric Aerosols from the Nabro Volcanic Eruption of 2011

Ariana Atwell

Hampton University

Coauthors: M. Patrick McCormick, Michael Hill

ariana_reese@yahoo.com

The Nabro volcanic eruption in Eritrea, Africa in June 2011 injected aerosols into the stratosphere, which were transported globally over the next several weeks. These aerosols can influence both surface and stratospheric temperatures in addition to facilitating stratospheric ozone depletion through heterogeneous reactions. Air mass trajectories from the Hybrid Single Particle Lagrangian Integrated Trajectory (HYSPPLIT) model are used in conjunction with backscatter and depolarization measurements from the Cloud-Aerosol Lidar with Orthogonal Polarization (CALIOP) instrument on the Cloud-Aerosol Lidar and Infrared Pathfinder Satellite Observation (CALIPSO) platform to track and characterize these aerosols. Results show initial upper-level transport through the region of the Asian monsoon and subsequent longer transport westward across the Atlantic Ocean to the United States several weeks later. Ground-based local measurements from the Hampton University lidar in Virginia show a stratospheric aerosol layer in late July that can be traced back to Nabro in late June.

Explosive volcanic eruptions produce dangerous conditions for surrounding communities as they spew hot ash and gases, referred to as a volcanic plume, into the local atmosphere. Immediate safety hazards include: hot magma flow, local ash fallout, and dangerous flying conditions (Marzano, 2013). A powerful enough eruption can inject gaseous sulfur dioxide (SO₂), one of the main components of a volcanic plume, from the volcano directly into the stratosphere where it can remain in the form of sulphuric acid (H₂SO₄) for months to years (1/e cleansing time of approx. 1 year). The stratospheric

aerosol load resulting from a volcanic eruption, especially originating in the tropics, is circulated through the stratosphere to higher latitudes until globally dispersed, and can eventually perturb the radiative balance of the global atmosphere (McCormick et al., 1995).

Volcanic aerosols have been known to affect the earth's radiative balance as far back as the infamous eruption at Krakatau, Indonesia in 1883. The eruption produced about 50 Tg of total aerosol mass into the atmosphere (McCormick et al., 1995), and injected a thick layer of volcanic aerosol into the stable stratosphere. As a result, the stratospheric layer dispersed globally and eventually lowered the global temperature by 1.2 Celsius (Simkin et al., 1984)

Volcanic ash and smoke plumes can also halt local air traffic. For instance, the eruption of Eyjafjallajökull in Iceland in April 2010 severely disrupted all forms of air traffic in the days following the eruption. A strong northwesterly wind over Iceland carried fine volcanic ash from the eruption into crowded airspace in the United Kingdom and continental Europe (Petersen et al., 2010). This caused the biggest aerial shutdown in Europe since World War II, affecting approximately 10 million passengers (Gertisser et al., 2010) and the revenue loss for airlines was estimated at 1.7 billion US dollars (as a conservative estimate) (Mazzochi et al., 2010).

Nabro Eruption

Nabro caldera, located on the northeast coast of Africa in the State of Eritrea (13.37°N,

41.70°E), erupted for the first time ever on June 13, 2011 between 0300 - 0500 EAT (00 UTC) due to a sequence of earthquakes on June 12, 2011 UTC (Universal Coordinated Time (Sawamura et al., 2012). Nabro eruption was a significant stratospheric aerosol event as seen by multiple ground-based lidars (Uchino et al., 2012), and space-borne lidars such as CALIOP (Cloud-Aerosol Lidar with Orthogonal Polarization) onboard CALIPSO.

CALIPSO observed Nabro's highest volcanic aerosol layer between 15 and 19 km, reaching the stratosphere within the first ten days (Fairlie et al., 2014). Hampton University's lidar similarly observed an enhanced stratospheric aerosol layer between 15.3 and 18.8 km over Hampton, VA (37.02°N, 76.33°W) on July 14, 2011, one month after the eruption (Boyounk et al., 2012). This study will use CALIOP nighttime observations of Nabro's stratospheric aerosol layer paired with a HYSPLIT backtrajectory to validate NOAA ARL's HYSPLIT model, and confirm the circulation of stratospheric aerosol over Hampton University's lidar.

In A. E. Bourassa's 2012 article about Nabro's aerosol load, he and his team concluded that both deep convection and the asian monsoon circulation (an anticyclonic system that centers around central India) were responsible for transporting Nabro's aerosol into the stratosphere. Bourassa et al. used a limb-scanning instrument, Optical Spectrograph and Infra-Red Imaging System (OSIRIS), to investigate the aerosol, and found that Nabro's injection heights only reached 14 km (Bourassa et al., 2012). Published comments arose in result of Bourassa's findings as other atmospheric scientists observed a direct stratospheric injection pathway for the eruption instead (Fromm et al., 2013) (Fairlie et al., 2013). M. Fromm and his research team later identified the error of the OSIRIS instrument, which was an underestimation of aerosol height

by OSIRIS when the 750 nm aerosol extinction exceeded a certain threshold ($\sim 0.0025 \text{ km}^{-1}$) (Fromm et al., 2014).

Nabro was a moderate eruption, but affected the global stratosphere, and produced a discussion about the effect of the summer asian monsoon on the lofting aerosol into the stratosphere. Several of the aforementioned scientists, who responded to Bourassa's findings, utilized HYSPLIT trajectory model to demonstrate the dispersion of Nabro's aerosol; therefore, the validation of HYSPLIT model, using a reliable and high-resolution instrument like CALIOP, will further validate the use of this model in aerosol spatial evolution.

NASA's CALIOP, onboard CALIPSO, is a space-borne lidar launched April 28, 2006 flying in the A-Train constellation that observed Nabro's presence and evolution. CALIPSO's observations begin 3 days after the eruption due to an instrument issue from June 12 - June 15. CALIOP was used for determining the presence and optical properties of Nabro-produced volcanic aerosol, and the HYSPLIT model by NOAA ARL was used with CALIOP's aerosol backscatter data to validate the predicted transport of the volcanic aerosol globally. A 2011 study on the influence of tropical volcanic eruptions on the stratospheric aerosol layer suggests that there has been a 4 - 7 percent increase in the stratospheric aerosol load from 2000-2009 (Vernier et al., 2011). The secondary focus of this study was to explore the spatial and temporal evolution of the volcanic aerosol layer specifically produced by the 2011 eruption of Nabro caldera, and in turn determine the altitude levels, global dispersion, and optical trend of the layer using aerosol backscatter and optical depth.

References

- [1] ARL, N., 2013: A complete modeling system for simulating dispersion of harmful atmospheric material. Air Resources Laboratory.
- [2] Bourassa, A. E., A. Robock, W. J. Randel, T. Deshler, L. A. Rieger, N. D. Lloyd, E. J. Llewellyn, and D. A. Degenstein, 2013: Response to comments on "large volcanic aerosol load in the stratosphere linked to asian monsoon transport". *Science*, 339 (6120), 647, doi:10.1126/science.1227961, URL <http://www.sciencemag.org/content/339/6120/647.5.abstract>, <http://www.sciencemag.org/content/339/6120/647.5.full.pdf>.
- [3] Bourassa, A. E., A. Robock, W. J. Randel, T. Deshler, L. A. Rieger, N. D. Lloyd, E. J. T. Llewellyn, and D. A. Degenstein, 2012: Large volcanic aerosol load in the stratosphere linked to asian monsoon transport. *Science*, 337 (6090), 78–81, doi:10.1126/science.1219371.
- [4] Boyouk, N., M. T. Hill, K. Leavor, and P. McCormick, 2012: 2011 observations of stratospheric aerosol over hampton, va related to the nabro volcanic eruption in africa.
- [5] Fairlie, T. D., J.-P. Vernier, M. Natarajan, and K. M. Bedka, 2013: Dispersion of the nabro volcanic plume and its relation to the asian summer monsoon. *Atmospheric Chemistry and Physics Discussions*, 13 (12), 33 177–33 205, doi:10.5194/acpd-13-33177-2013, URL <http://www.atmos-chem-phys-discuss.net/13/33177/2013/>.
- [6] Fairlie, T. D., J.-P. Vernier, M. Natarajan, and K. M. Bedka, 2014: Dispersion of the nabro volcanic plume and its relation to the asian summer monsoon. *Atmospheric Chemistry and Physics*, 14 (13), 7045–7057, doi:10.5194/acp-14-7045-2014, URL <http://www.atmos-chem-phys.net/14/7045/2014/>.
- [7] Fromm, M., G. Kablick, G. Nedoluha, E. Carboni, R. Grainger, J. Campbell, and J. Lewis, 2014: Correcting the record of volcanic stratospheric aerosol impact: Nabro and sarychev peak. *Journal of Geophysical Research: Atmospheres*, 119 (17), 10,343–10,364, doi:10.1002/2014JD021507, URL <http://dx.doi.org/10.1002/2014JD021507>.
- [8] Fromm, M., G. Nedoluha, and Z. Charvt, 2013: Comment on "large volcanic aerosol load in the stratosphere linked to asian monsoon transport". *Science*, 339 (6120), 647, doi:10.1126/science.1228605.
- [9] Gertisser, R., 2010: Eyjafjallajkull volcano causes widespread disruption to european air traffic. *Geology Today*, 26 (3), 94–95, doi:10.1111/j.1365-2451.2010.00757.x, URL <http://dx.doi.org/10.1111/j.1365-2451.2010.00757.x>.

- [35] Griessbach, S., L. Hoffmann, R. Spang, M. von Hobe, R. Müller, and M. Riese, 2013:
- [36] Detection of volcanic sulfate aerosol with envisat mipas shown for the kasatochi,
- [37] sarychev, and nabro eruptions. 15, 3504.
- [38] Marzano, F. S., E. Picciotti, M. Montopoli, and G. Vulpiani, 2013: Inside volcanic
- [39] clouds: Remote sensing of ash plumes using microwave weather radars. Bull. Amer.
- [40] Meteor. Soc., 94 (10), 1567–1586.
- [41] Mazzocchi, M., F. Hansstein, M. Ragona, et al., 2010: The 2010 volcanic ash cloud
- [42] and its financial impact on the european airline industry. CESifo Forum, Ifo Institute
- [43] for Economic Research at the University of Munich, Vol. 11, 92–100.
- [44] McCormick, M. P., L. W. Thomason, and C. R. Trepte, 1995: Atmospheric effects of
- [45] the mt. pinatubo eruption. 373, 399–404.
- [46] Sawamura, P., et al., 2012: Stratospheric aod after the 2011 eruption of nabro volcano
- [47] measured by lidars over the northern hemisphere. Environmental Research Letters,
- [48] 7 (3), 034 013.
- [49] Seinfeld, J. H. and S. N. Pandis, 2006: Atmospheric Chemistry and Physics -
- [50] From Air Pollution to Climate Change (2nd Edition). John Wiley and Sons,
- [51] isbn:9780471720188.
- [52] Simkin, T. and R. Fiske, 1984: Krakatau 1883, The Volcanic Eruption and Its Effects.
- [53] Smithsonian.
- [54] Thomason, L. W. and M. C. Pitts, 2008: Calipso observations of volcanic aerosol in
- [55] the stratosphere. 71 5300–71 5300–8, doi:10.1117/12.804090.
- [56] Thomason, L. W., M. C. Pitts, and D. M. Winker, 2007: Calipso observations
- [57] of stratospheric aerosols: a preliminary assessment. Atmospheric Chemistry and
- [58] Physics, 7 (20), 5283–5290.
- [59] Uchino, O., et al., 2012: On recent (2008-2012) stratospheric aerosols observed by
- [60] lidar over japan. Atmospheric Chemistry and Physics, 12 (24), 11 975–11 984.
- [61] Vernier, J., J. Pommereau, D. Thomason, L. and Winker, and C. Trepte, 2010: Volcanic
- [62] contribution to the permanent stratospheric aerosol layer. SPIE Newsroom,
- [63] Remote Sensing, doi:10.1117/2.1201010.003218.
- [64] Vernier, J.-P., et al., 2011: Major influence of tropical volcanic eruptions
- [65] on the stratospheric aerosol layer during the last decade. Geophys-
- [66] ical Research Letters, 38 (12), n/a–n/a, doi:10.1029/2011GL047563, URL
- [67] <http://dx.doi.org/10.1029/2011GL047563>.

Applying The Deep Atmospheric Concept to The NCEP Mesoscale Spectrum Model. The First Part: Implementation of The Generalized Hybrid Coordinate

Jia-Fong Fan¹, Hann-Ming Henry² Juang and Tsann-Wang Yu¹

¹Howard University, Washington DC

²NOAA Environmental Modeling Center, NCEP, College Park, MD

Abstract

In this study, we are applying the deep atmospheric concept to the NCEP Mesoscale Spectral Model (MSM) (Juang, 2000) in an attempt to understand the impacts of the deep atmospheric model on weather forecast. The deep-atmospheric system includes the complete governing equations without approximations and it has multiple conservation properties. Theoretically, the use of the more complete equations is leading to the more accurate prediction and recently it is a trend for model development.

The MSM has been an operational model for weather forecast in the United States until 2011 and now it is an open-source model for worldwide community research and academic uses. The current MSM is a nonhydrostatic system in sigma (terrain-following) coordinates. The first part of this research is to re-derive the governing equations in generalized coordinates and the following is to implement the system into the model.

The generalized hybrid coordinates are combination of sigma and pressure coordinates, which use sigma surfaces near the ground surface and transit to the pressure surfaces near the top. The benefit to use the generalized vertical coordinate is that we can generate the deep-atmospheric equations from the shallow-atmospheric equations by modifying the existing terrain-following vertical coordinate, without the need to change substantially the scientific and computing infrastructure in the model. This presentation is to present some of the preliminary results of the implementation, and to discuss the future work.

Introduction

For the numerical weather and climate prediction models, there are four combinations of hydrostatic/nonhydrostatic and shallow/deep approximations: (1)non-approximated Euler equations(deep-nonhydrostatic); (2)the nondydrostatic primitive equations(shallow-nonhydrostatic); (3)the quasi-hydrostatic equations (deep-hydrostatic), and (4)the hydrostatic primitive equations(shallow-hydrostatic). The recent trend is to use less approximation and more complete equation set. The deep atmospheric system is the complete equation set (momentum equations, continuity equation and thermodynamic equation) without any

approximation. Most of weather prediction models employed shallowness approximation. Under shallowness approximation, the cosine terms of Coriolis force, curvature terms of vertical components are absent in order to satisfy the angular momentum conservation and the height effect is ignored. The deep atmospheric system remains the full Coriolis terms and also considers the height effect, which can cause the the inaccuracy to the weatehr forecast. Developing a multiple approximations model as a tool to investigate the impacts on the weather prediction is the final goal. This study will focus on the first step of implementing the generalized coordinate in the selected model.

Mesoscale Spectral Model(MSM) is chosen to be the tool to conduct this study. MSM used to serve as one of operational weather prediction model members in the United States until 2011. Presently, MSM becomes open-source and is now used for academic research. Our plan is to work on incremental changes on the top of the current model. The model will be developed of multiple options of different approximations under the same structure. Therefore, this model can be a handy tool to evaluate the performances between different approximations.

In this study, we demonstrated the coordinate transformation from the model's current terrain-following vertical coordinate to the combination of pressure and terrain-following coordinates and the its implementation to the model based on the model's structure as the first step toward to the deep atmospheric system.

Coordinate Transformation to the Generalized Coordinate

The hydrostatic relation used for the coordinate transformation is given by $\partial \bar{p} / \partial z = -\rho g$, where ρ satisfied the equation of state as $\bar{p} = \rho R \bar{T}$; where $\rho, \bar{p}, \bar{T}, p$ density, pressure, and temperature in the hydrostatic system respectively; g is gravitational constant; R is the gas constant for dry air; and z is the physical height. Here, we define the vertical coordinate as $\hat{p} = \hat{A} + \hat{B} \hat{p}_s$, where A and B are the constant coefficients which define pressure and sigma vertical distribution. The hydrostatic relation can be rewritten to represent the relation between the proposed vertical coordinate, p , and the physical height, z , as $\partial \bar{p} / \partial z = -\rho g = -\bar{p} / R \bar{T} \partial / \partial \bar{p}$.

Using the above definition for the coordinate, the vertical coordinate transformation can be given as

$$\frac{\partial}{\partial z} = \frac{\partial \bar{p}}{\partial \bar{p}} \frac{\partial \bar{p}}{\partial z} = \frac{\partial}{\partial \bar{p}} \left(-\frac{\bar{p}}{R \bar{T}} g \right) = \frac{-g \bar{p}}{R \bar{T}} \frac{\partial}{\partial \bar{p}},$$

and the transformation for others is

$$\frac{\partial}{\partial s} \Big|_t = \frac{\partial}{\partial s} \Big|_{\bar{p}} + \frac{\bar{p}}{R \bar{T}} \frac{\partial}{\partial \bar{p}} \frac{\partial \phi}{\partial s} \Big|_{\bar{p}},$$

where s can be x, y for spacial derivative or t for temporal derivitave and ϕ is geopotential height. The fully compressible nonhydrostatic system in MSM can be transformed to the generalized coordinates written as

$$\begin{aligned} \frac{du^*}{dt} &= f v^* - E \frac{\partial m^2}{\partial x} - RT \frac{\partial Q}{\partial x} - \frac{T}{\bar{T}} \frac{\partial Q}{\partial \ln \bar{p}} \frac{\partial \bar{\phi}}{\partial x} + F_u \\ \frac{dv^*}{dt} &= -f u^* - E \frac{\partial m^2}{\partial y} - RT \frac{\partial Q}{\partial y} - \frac{T}{\bar{T}} \frac{\partial Q}{\partial \ln \bar{p}} \frac{\partial \bar{\phi}}{\partial y} + F_v \\ \frac{dw}{dt} &= -g + g \frac{T}{\bar{T}} \frac{\partial Q}{\partial \ln \bar{p}} + F_w \\ \frac{dQ}{dt} &= -\gamma \nabla_3 \cdot V + \frac{\gamma F_T}{T} \\ \frac{dT}{dt} &= \kappa T \frac{dQ}{dt} + F_T \\ \frac{dq}{dt} &= F_q \\ \frac{d}{dt} &= \frac{\partial}{\partial t} + m^2 \left[u^* \frac{\partial}{\partial x} + v^* \frac{\partial}{\partial y} \right] + \dot{\zeta} \frac{\partial}{\partial \zeta} = \frac{\partial}{\partial t} + m^2 \left[u^* \frac{\partial}{\partial x} + v^* \frac{\partial}{\partial y} \right] + \dot{\zeta} \frac{\partial \bar{p}}{\partial \zeta} \frac{\partial}{\partial \bar{p}} \\ \dot{\zeta} \frac{\partial \bar{p}}{\partial \zeta} &= -\frac{\bar{p}}{RT} \left[g w - \left(\frac{\partial \phi}{\partial t} + m^2 u^* \frac{\partial \phi}{\partial x} + m^2 v^* \frac{\partial \phi}{\partial y} \right) \right] \\ \nabla_3 \cdot V &= m^2 \left[\frac{\partial u^*}{\partial x} + \frac{\partial v^*}{\partial y} + \frac{\bar{p}}{RT} \left(\frac{\partial u^* \partial \bar{\phi}}{\partial \bar{p} \partial x} + \frac{\partial v^* \partial \bar{\phi}}{\partial \bar{p} \partial y} \right) \right] = \frac{g \bar{p}}{RT} \frac{\partial w}{\partial \bar{p}} \\ \bar{\phi}_k &= \bar{\phi}_s + \int_{p_s}^p \frac{RT}{\bar{p}} d\bar{p} \\ \gamma &= C_p / C_v, \kappa = R / C_p \\ Q &= \ln(p) \\ E &= 0.5(u^{*2} + v^{*2}) \end{aligned}$$

where u^*, v^*, w^* are the wind speeds in the x, y , and z directions; Q is the logarithm of pressure; T is virtual temperature and q is specific humidity; m is the mapping factor; f is the Coriolis parameter, and $\dot{\zeta} \partial \bar{p} / \partial \zeta$ is the vertical flux(motion) related to the generalized coordinate.

The conservation of density in z coordinate is

$$\frac{d \ln \rho}{dt} = -m^2 \left(\frac{\partial u^*}{\partial x} + \frac{\partial v^*}{\partial x} \right) - \frac{\partial w}{\partial z},$$

with the coordinate transformation, the above equation can be rewritten in the generalized coordinate as

$$\frac{\partial \bar{p}_k}{\partial t} = m^2 \int_{\zeta_k}^{\infty} \left[\frac{\partial u \left(\frac{\partial \bar{p}}{\partial \zeta} \right)}{\partial x} + \frac{\partial v \left(\frac{\partial \bar{p}}{\partial \zeta} \right)}{\partial y} \right] d\zeta - \left(\dot{\zeta} \frac{\partial \bar{p}}{\partial \zeta} \right)_k$$

which presents the internally evolved hydrostatic pressure, and it can be written in another form by integrating the entire atmosphere, as

$$\frac{\partial \bar{Q}_s}{\partial t} = \frac{m^2}{\bar{p}_s} \int_{\text{surface}} \left[\frac{\partial u (\frac{\partial \bar{p}}{\partial \zeta})}{\partial x} + \frac{\partial v (\frac{\partial \bar{p}}{\partial \zeta})}{\partial y} \right] d\zeta.$$

The thermodynamic equation with the coordinate transformation for hydrostatic temperature can be written into

$$\frac{\partial \bar{T}}{\partial t} = -m^2 \left(u \frac{\partial \bar{T}}{\partial x} + v \frac{\partial \bar{T}}{\partial y} \right) - \zeta \frac{\partial \bar{T}}{\partial \zeta} + \kappa \bar{T} \left[\frac{B \bar{p}_s}{\bar{p}} \left(\frac{\partial \bar{Q}_s}{\partial t} + m^2 u \frac{\partial \bar{Q}_s}{\partial x} + m^2 v \frac{\partial \bar{Q}_s}{\partial y} \right) \right] + F_T$$

The six prognostic equations from the governing equations and the above two prognostic equations make this revised system. The details of the discretization and new derived perturbation equations, the semi-implicit methods and experiment results will be presented in the presentation.

Summary

This study illustrated the implementation of generalized coordinate to the MSM. The coordinate transformation is the incremental change on the top of the current model for the further goal, deep atmospheric system. The model is developed on the path to the multiple approximations dynamical cores and the goal is to understand the impacts of the

different dynamic cores on numerical weather prediction.

References

- [1] Hann-Ming Henry Juang, The NCEP mesoscale spectral model: a revised version of the nonhydrostatic regional spectral model. *Mon. Wea. Rev.*, **128**(2000), 2329-2362.
- [2] Hann-Ming Henry Juang, A multiconserving discretization with enthalpy as a thermodynamic prognostic variable in generalized hybrid vertical coordinates for the NCEP Global Forecast System. *Mon. Wea. Rev.*, **139**(2011), 1583-1607.

Acknowledgement

This study was supported and monitored by National Oceanic and Atmospheric Administration (NOAA) under Grant – NOAA Center for Atmospheric Sciences #NA11SEC4810003. The statements contained within the manuscript/research article are not the opinions of the funding agency or the U.S. government, but reflect the author’s opinions.

Aerosols and trace gases modeling in the tropical Atlantic during the summer of 2009

A. Jose M Tirado¹, B. Vernon R Morris²

¹Howard university, Program in Atmospheric Sciences
2212 Phelps Rd. apt. 110 Hyattsville, MD 20783
tirado.jose@gmail.com

²Howard University, Department of Chemistry

Abstract

Air quality simulations using the chemistry transport model Weather Research and Forecast Chemistry (WRF-CHEM) were performed to study the behavior of aerosol and chemical trace constituents on the tropical Atlantic during the month of July 2009. Aerosols have been shown to be at its peak during the month of July in the tropical Atlantic due in part to mineral aerosols (Saharan dust) that travel across the Atlantic to the Caribbean basin and portions of South and North America primarily during the boreal summer. The aim of this project was to observe how dust aerosols affected the tropospheric chemistry of key trace constituents like ozone during its journey to the Caribbean basin. Results from the simulations were compared with trace gases and aerosols data collected on the NOAA ship Ronald H. Brown during the AEROSE 2009 field campaign and data from air quality stations on the island of Puerto Rico. Sensitivity studies were performed to elucidate the contribution of different processes to the chemistry of the area.

Introduction

The study of atmospheric aerosols is of vital importance due to their complex roles in the earth climate system and human health. Aerosols represent one of the major uncertainties in climate prediction due to the competing effects they have on the climate system [1]. Aerosols also play a critical role in atmospheric chemistry by providing reactive surfaces on which heterogeneous and multiphase reactions can occur [2].

The Saharan desert has been recognized as the largest source of mineral aerosols into the atmosphere [3]. Dust from the Saharan desert reaches the Caribbean islands [4] and Puerto Rico [5] every year predominantly during the northern hemisphere summer. Dust have been shown to decrease the concentration of PM_{2.5} over polluted areas downwind of the source region [6], and is known to affect the tropospheric concentrations of ozone, odd nitrogen (NO_y), the hydroxide and hydro

peroxide radicals, sulfur dioxide and many organic species [7].

In this project I aim to identify the major effects Saharan dust has on anthropogenic pollutants (specifically fine particulates and ozone) in the tropical Atlantic and how they evolve by comparing chemistry transport simulations with data collected during the AEROSOL and Ocean Science Expedition (AEROSE 2009) and air quality sampling stations in the San Juan metropolitan area of the island of Puerto Rico.

Experiments and Conclusions

Version 3.5 of the chemistry transport model Weather Research and Forecast with chemistry (WRF-chem) was used to perform the simulations. The chemistry portion is fully coupled with the meteorology (online) and have the same transport scheme, grid, physics and time step [8]. The model uses the mass coordinate version of WRF called Advance Research WRF (ARW) which have

an Eulerian mass solver as a dynamic core. The domain has a grid distance of 101.8 kilometers centered at latitude 23.162° north and longitude -19.838° west. The domain includes the tropical Atlantic, the Saharan desert as the source region for the dust outflows, the island of Puerto Rico and a portion of the eastern Caribbean. Meteorological fields were calculated from the NCEP/NCAR final analysis data sets. The Carbon Bond Z (CBM-Z) chemical mechanism was used to drive the gas phase chemistry. Seven test simulations were performed during July 2009.

In terms of ozone the simulations show good agreement overall with the observations. The model over or under predictions were generally around 3 ppb along the cruise track. Calculations of the gross error and the bias indicate that the model performs well in predicting ozone and only slightly overestimate it in average. Our gross error value is 0.076 and the bias is 0.04. In terms of particulates, a comparison between the measured PM 2.5 collected with the QCM on the Ronald Brown and simulated PM 2.5 over the boat position show that the model over predicted PM 2.5 significantly along the cruise track with QCM daily average values between 5.81 and 61.14 μg per cubic meters compared to average values for the simulation in between 383.53 and 875.78 μg per cubic meters. Despite over prediction the model depict the behavior of the dust storm showing highs and lows on the same days of the observations. PM 10 exhibit the same over predicting behavior when compared to values on the island of Puerto Rico. Our results from the simulations indicate that the concentration of ozone decrease when particulate concentrations are elevated. The computed Pearson correlation coefficient r is -0.69 indicating an anti correlation between dust and ozone. An increase in ozone of up to 4 ppb is predicted by the model when the dust

option is turned off on the simulation. Comparing ozone and PM 10 in the Atlantic closer to the dust source also show a decrease in the concentration of ozone when the concentration of the particulates was elevated, the Pearson correlation coefficient is -0.35. In terms of particulates, PM 10 and PM 2.5 were found to increase on Puerto Rico during dust events. The average increase is around 30 $\mu\text{g}/\text{m}^3$ for PM 10 and around 20 $\mu\text{g}/\text{m}^3$ for PM 2.5.

References

- [1] P. Forster, V. Ramaswamy, P. Artaxo, D. C. Lowe, and G. Raga, "Changes in atmospheric constituents and in radiative forcing. In: Climate change 2007: The Physical science basis. Contribution of working group 1 to the fourth assesment report of the intergovernmental panel on climate change," Cambridge, United Kingdom, 2007.
- [2] C. R. Usher, A. E. Michel, and V. H. Grassian, "Reactions on mineral dust," *Chem. Rev.*, vol. 103, no. 12, pp. 4883–940, Dec. 2003.
- [3] A. T. Evan, G. R. Foltz, D. Zhang, and D. J. Vimont, "Influence of African dust on ocean–atmosphere variability in the tropical Atlantic," *Nat. Geosci.*, vol. 4, no. 10, pp. 1–4, Oct. 2011.
- [4] J. M. Prospero and P. J. Lamb, "African droughts and dust transport to the Caribbean: climate change implications.," *Science (80-.)*, vol. 302, no. 5647, pp. 1024–7, Nov. 2003.
- [5] E. A. Reid, J. S. Reid, M. L. Meier, M. R. Dunlap, S. S. Cliff, A. Broumas, K. Perry, and H. B. Maring, "Characterization of African dust transported to Puerto Rico by individual particle and size segregated bulk analysis," *J. Geophys. Res.*, vol. 108, no. D19, p. 8591, 2003.
- [6] K. Wang, Y. Zhang, a. Nenes, and C. Fountoukis, "Implementation of dust

emission and chemistry into the Community Multiscale Air Quality modeling system and initial application to an Asian dust storm episode,” *Atmos. Chem. Phys.*, vol. 12, no. 21, pp. 10209–10237, Nov. 2012.

- [7] C. E. Kolb, R. A. Cox, J. P. D. Abbatt, M. Ammann, E. J. Davis, D. J. Donaldson, B. C. Garrett, C. George, P. T. Griffiths, D. R. Hanson, M. Kulmala, G. McFiggans, U. Pöschl, I. Riipinen, M. J. Rossi, Y. Rudich, P. E. Wagner, P. M. Winkler, D. R. Worsnop, and C. D. O’Dowd, “An overview of current issues in the uptake of atmospheric trace gases by aerosols and clouds,” *Atmos. Chem. Phys.*, vol. 10, no. 21, pp. 10561–10605, Nov. 2010.

- [8] G. a. Grell, S. E. Peckham, R. Schmitz, S. a. McKeen, G. Frost, W. C. Skamarock, and B. Eder, “Fully coupled ‘online’ chemistry within the WRF model,” *Atmos. Environ.*, vol. 39, no. 37, pp. 6957–6975, Dec. 2005.

Acknowledgement

This study was supported by the National Oceanic and Atmospheric Administration (NOAA) thru the NOAA Center for Atmospheric Sciences (NCAS) program at Howard University under Grant# NA11SEC4810003 The statements contained within the manuscript/research article are not the opinions of the funding agency or the U.S. government, but reflect the author’s opinions.

NCAS-CAREERS Puerto Rico Weather Camp: a decade of achievements, challenges, and opportunities to foster diversity in STEM fields

Y. Detrés¹ and R. Armstrong²

1University of Puerto Rico at Mayagüez, NOAA Center for Atmospheric Sciences 2Institution 2, Affiliation

Presenter: yasmin.detres@upr.edu

Abstract

The University of Puerto Rico at Mayaguez, a Minority Serving Institution part of the NOAA EPP sponsored NOAA Center for Atmospheric Sciences (NCAS), hosted the NCAS-CAREERS Puerto Rico Weather Camp (PRWC), an immersive summer experience for high school students, from 2007 to 2016. During this decade the PRWC provided underrepresented students with tools for exploration of diverse STEM fields and careers and promoted educational experiences that increased student engagement and achievement in these disciplines. Out of a total of 160 participants, 98% were from the Hispanic/Latino ethnic group, 66% were women and approximately 80% of our alumni enrolled in undergraduate programs are pursuing careers in STEM. This successful initiative has been focused on an effective recruitment program, hands-on and inquiry-based learning activities and access to mentors, speakers and role models in the STEM fields. A summary of the most relevant achievements and opportunities identified during this decade of the PRWC will be presented.

Introduction

Motivated by the desire to broaden and increase exposure of underrepresented minorities (URM) in STEM fields, the NOAA Center for Atmospheric Sciences (NCAS) at the University of Puerto Rico at Mayaguez (a Minority Serving Institution part of the NOAA EPP), has hosted the NCAS-CAREERS Puerto Rico Weather Camp (PRWC) since 2007. Similar NCAS camps were also conducted annually at Howard University in Washington D.C., Jackson State University in Jackson, MS, and the University of Texas at El Paso 9 (Morris, et al., 2012). The PRWC immersive summer experience has been offered continuously from 2007 to 2016 and is one of the several weather camps that operated under the name CARRERS (Channeling Atmospheric Research into Educational Experiences) supported by NOAA, NSF, and other governmental

agencies, numerous private sector companies and individuals.

Experiments and Conclusions

In this residential camp highly motivated students from public and private high schools from Puerto Rico, the continental USA and US Virgin Islands, explored diverse STEM fields and careers in meteorology, atmospheric sciences, and oceanography. The camp provided a comprehensive educational experience that included site visits to NOAA facilities such as National Weather Service, Caribbean Tsunami Warning Program, Caribbean Integrated Ocean Observing System (CariCOOS) and local TV stations, training-at-sea onboard research vessels, trips to the NOAA Pacific Marine Environmental Laboratory CO2 and ICON-CREWS buoys, interactive workshops and field trips to tropical ecosystems. Participants also interacted with scientists and experts from the academic, private and federal sectors

including the NOAA offices of NESDIS, NCEP, Hurricane Research Division, and National Ice Center. Students learned about relevant topics in the atmospheric and oceanographic research and about the complex tropical weather and climate phenomena, the atmosphere-ocean connections, climate change impact in the Caribbean, ocean observing tools, climate and ecology and emergent research topics in these areas.

During this decade the PRWC has provided underrepresented students with unique educational experiences, thereby promoting an increment in the number of URM degree holders and professionals in STEM fields. Out of a total of 169 students who have participated in this residential camp, 98% were from the Hispanic/Latino ethnic group and 66% were women. Approximately 80% of our alumni enrolled in undergraduate programs are pursuing careers in STEM. The

success of this initiative is the result of an effective recruitment program, a hands-on and inquiry-based learning activities and access to mentors, speakers and role models in a wide variety of fields. In summary, the NCAS-CAREERS PRWC has made a significant contribution to improve the diversity of minority students in NOAA-related fields.

References

[1] V. Morris, H. Moguil, T. Yu. EOS 93 (15) (2012)

Acknowledgement

This study was supported and monitored by National Oceanic and Atmospheric Administration (NOAA) under Grant – (NCAS) Grant # NA11SEC4810003. The statements contained within the manuscript/research article are not the opinions of the funding agency or the U.S. government, but reflect the author's opinions.

Active standoff detection of CH₄ and N₂O leaks using hard-target backscattered light using an open-path quantum cascade laser sensor

A. Diaz¹, B. Thomas¹, P. Castillo², B. Gross¹ and F. Moshary¹
 Corresponding author: Adrian Diaz adiaz001@citymail.cuny.edu

¹The City College of New York, New York, NY, 10031

²Brookhaven National Lab, New York, NY, 11973

Introduction

Fugitive gas emissions from agricultural or industrial plants or natural gas pipeline infrastructure are an important environmental concern as they contribute to the global increase of greenhouse gas concentrations and global warming [1]. Moreover, they are also a security and safety concern because of possible risk of fire/explosion or toxicity. For these reasons, optical methods to detect fugitive emission of greenhouse or hazardous gases over large areas have been developed [2–5]. Most of these measurement techniques are either point samplers that deploy some sort of multi-pass cell or cavity, or fence-line systems that deploy a retro-reflector. The latter systems are not ideal for mobile or multidirectional measurements since the direction of the beam is defined by the system layout and has to be realigned when the system is moved, while point samplers cannot do remote detection of fugitive gas emissions. Remote leak detection systems require fast measurement cycle (>10 Hz), portability and sufficient range to scan large areas in short time [6].

We present in this study a potential system for remote gas leak detection using the backscattered light off a hard target. Our novel approach allows for simultaneously high spectral and temporal resolution gas spectroscopy and precise measurements of the target range using time resolved observations. These measurements are obtained with short measurement cycle and at sufficient range that fulfill the requirement for fast, mobile, or multidirectional gas leak monitoring.

Measurements were performed on methane (CH₄) and nitrous oxide (N₂O), respectively, the second and third most potent anthropogenic greenhouse gases [1]. In addition, methane is also a highly explosive gas when its concentration is >5 % in the ambient air, making it urgent to remotely and quickly detect methane leaks [7, 8].

Experiments and Conclusions

The system is based on active differential optical absorption spectroscopy (DOAS) [9]. A quantum cascade laser (QCL) emits a laser pulse towards a scattering target. A receiver system based on a Newtonian telescope, coaxial with the laser, and a mid-infrared detector are used to collect and detect the backscattered light from the target. During propagation from the laser to the target and then back to the detector, the laser light undergoes optical extinction due to the presence of gas molecules.

A remarkable feature of this system is that its laser source is not actively scanned, nor does it use a spectrally resolved detector. In order to measure an absorption spectrum, it uses the intra-pulse frequency chirp of a pulsed distributed feedback (DFB) QCL. As the laser is emitting the pulse, the substrate temperature varies causing a change in its refractive index. As a consequence, within the pulse duration, the frequency of the DFB-QCL is shifted from high to low with a given chirp rate (1 cm⁻¹ in ~200 ns in our case), in a stable and repeatable manner [10]. Therefore, the time-resolved intensity measurement can be converted to a spectrally resolved intensity

using the experimentally determined chirp rate of the QCL.

Path-averaged gas concentrations are retrieved using least-squares fitting technique that considers contributions from methane, nitrous oxide, and water vapor gas species; where either methane or nitrous oxide leaks are introduced and the two other gases are interfering species (at their respective ambient levels).

The infrared source used is a pulsed DFB-QCL operating with a pulse length of 200 ns and at 20 kHz repetition rate. The average power is 0.31 mW. The laser beam is then expanded by a 4× beam expander to decrease the divergence. The scattering target used is a near-Lambertian high diffuse reflectance in the near and middle infrared (larger than 94 %). The target is placed ~40 m away from the sensor. The backscattered light is collected by a coaxial F/3.7 Newtonian telescope with an 8" primary mirror diameter and focused on a thermo-electrically cooled infrared detector with a 1mm² effective optical area. The detector output is digitized at a 200 MSamples/s sampling rate. Its onboard FPGA

averages 1024 acquired waveforms at high repetition rate and then transfers this averaged waveform to the computer.

Gas puffs are obtained using a controlled leak of either pure CH₄ or pure N₂O. A valve is used to control when the gas is released at approximately one-meter range from the optical path. In the case of methane, the leak has a flux of approximately 50 mL/s ($\approx 2 \times 10^{-3}$ mol/s, or ≈ 30 mg/s). The valve was open for 5 s to release a total of 150 mg of CH₄. For N₂O, the leak flux was 2 mL/s ($\approx 10^{-4}$ mol/s, or ≈ 4 mg/s), and the valve is only open for 0.5 s, releasing 2 mg of N₂O. Gas dispersion in the air once released was not controlled.

Figure 1 shows the detection of a CH₄ leak. Instants before the CH₄ gas is released, the initial concentration oscillates around the ambient level (1.8 ppm). At t=8s, the CH₄ gas is released and the retrieved concentration rapidly rises while the gas puff occurs. Then, as the gas dissipates, the retrieved concentration decreases until reaching ambient levels once again.

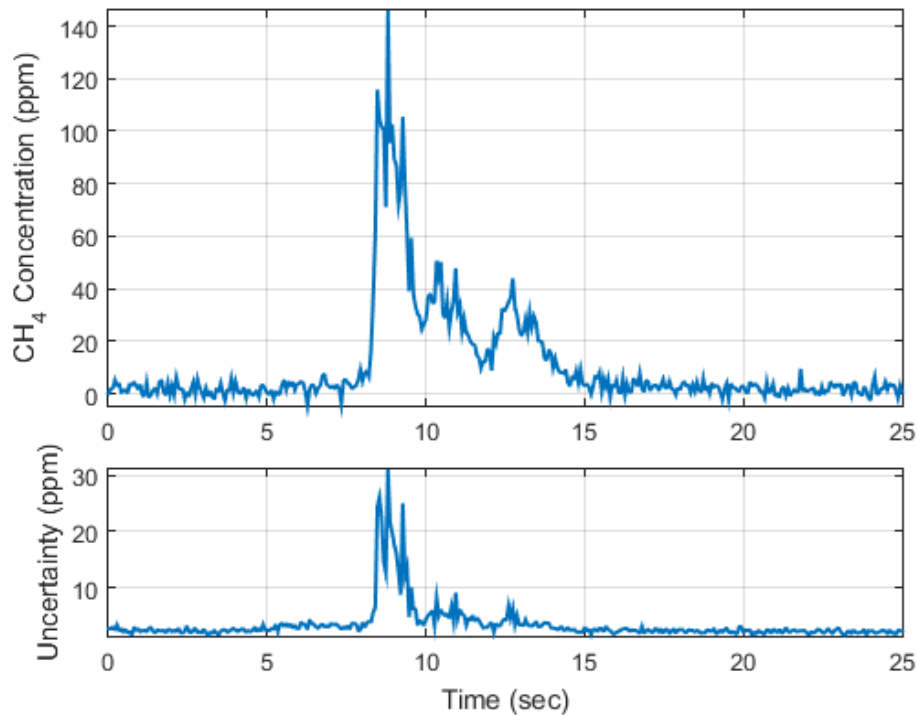


Figure 1. Time evolution of path-averaged concentration of CH₄ and its associated uncertainty.

The resulting detection limits for CH₄ and N₂O are respectively 117 and 12.8 ppm.m with a 15 Hz (~68 ms) measurement cycle, which correspond to 30 ppm.m Hz^{-1/2} for CH₄ and 3.3 ppm.m Hz^{-1/2} for N₂O. It is also important to note that the range to the scattering target is simultaneously retrieved from time resolved measurements for the relatively short pulses deployed and incorporated in the path-averaged concentration retrievals. A full spectrum is recorded for every pulse. Due to the relatively small frequency window used (~1 cm⁻¹) and the spectral stability of the QCL, the gas concentration revivals are not sensitive to the laser intensity fluctuations or the frequency dependence/variation in the backscatter coefficient of various hard (topographic) targets. Given these characteristics, this system is promising for

mobile or multidirectional search and remote detection of gas leaks.

References

- [1] T.F. Stocker, D. Qin, G.K. Plattner, M. Tignor, S.K. Allen, J. Boschung, B.M. Midgley: IPCC, 2013: Climate Change 2013: The Physical Science Basis. Contribution of Working Group I to the Fifth Assessment Report.
- [2] W. Demtröder, Laser Spectroscopy 2. Experimental Techniques (Springer, Berlin, 2008)
- [3] C. Weitkamp, Lidar, Range-Resolved Optical Remote Sensing of the Atmosphere (Springer, Berlin, 2005)
- [4] T. Fujii, T. Fukuchi, Laser Remote Sensing (CRC Press, Boca Raton, 2005)
- [5] J. Hodgkinson, R.P. Tatam, Meas. Sci. Technol. 24, 012004 (2013)
- [6] M.B. Frish, R.T. Wainner, M.C. Laderer, B.D. Green, M.G. Allen, IEEE Sens. J. 10, 639 (2010).
- [7] C.L. Yaws, Chemical Properties Handbook (McGraw-Hill, New York, 1999)

- [8] M.G. Zabetakis, Flammability characteristics of gases and vapors. Bureau Mines Bull. 627, 24 (1965)
- [9] U. Platt, J. Stutz, Differential Optical Absorption Spectroscopy (Springer, Berlin, 2008)
- [10] G. Duxbury, N. Langford, M.T. McCulloch, S. Wright, Chem. Soc. Rev. 34, 921 (2005)

Acknowledgement

This study was supported and monitored by National Oceanic and Atmospheric Administration (NOAA) under Grant – NOAA CREST Award # NA11SEC4810004. The statements contained within the manuscript/research article are not the opinions of the funding agency or the U.S. government, but reflect the author’s opinions.

Perceptions of Safety and its Gendered Differences: An Exploratory Analysis of Severe Weather Reactions

A. Shadya Sanders¹, B. Terri Adams-Fuller², and C. Everette Joseph³

¹*Howard University*

²*Howard University, Department of Sociology*

³*University at Albany, SUNY Department of Atmospheric Sciences*

Abstract

Residents of the United States are likely to see a wide variety of weather hazards throughout the year, and each weather phenomenon comes with its own warning method, and subsequent protective action, if any. In the previous five years alone, nearly 3,000 residents have lost their lives in a weather related situation. Many of these fatalities could have been prevented, and millions of dollars in lost productivity and property damages saved. While technology has advanced and forecasting becomes increasingly accurate, the understanding of the publics' reactions to and understanding of weather information has not yet reached its potential. The goals and wishes of the publics varies greatly and is consistently changing, so it is necessary to explore what these differences are in order to understand the direction meteorological forecasting needs to take. Residents of the United States are incredibly diverse, and gender is just a single point of differences residents across the country hold. Previous research has shown differences in fatality rates during hurricanes and tornadoes, as well as the likelihood of taking protective action. This study further investigates the differences seen, by gender, to severe weather warnings as well as differences in hypothesized actions once a warning is received. These are considered through a variety of severe weather phenomena potentially experienced in the United States.

Introduction:

Government and private agencies within the United States and around the world are making large investments in protecting their communities from the potential destruction for severe weather events. Along with large investments in mechanical technology and advanced measurement systems to better predict these events, research has shown that the human factor is incredibly important. The influence of social and human behavioral sciences is a crucial component that could greatly increase the effectiveness of expensive technologies in reducing the loss of life and property around the world. By

better understanding the people one is protecting more effective outcomes result.

Following an exploratory analysis of the Tuscaloosa-Birmingham long track tornado directly responsible for at least 62 fatalities in Alabama, a large discrepancy in fatalities by gender is seen. Based on statistical data, for the United States before 2010, it is most common to see a fatality breakdown of 51% to 49% male to female, respectively. In this particular track the fatality breakdown is 31% to 69% male to female, respectively. While widespread tornado outbreaks are incredibly devastating to the local communities affected, they are still relatively small based on the size of the nation. It does, however,

lead a researcher to investigate the potential gaps between scientific knowledge and public response to this information. An investigation on the general perceptions of tornado watches and warnings will be compared by gender as well as hypothetical reactions to different levels of warnings. This is done to investigate if gendered messaging is a factor that needs to be considered further in forecast messaging.

Experiments and Conclusions

While a combination of quantitative and qualitative data can give a much more robust view of information to a situation, in this case quantitative data is used via a nationwide online survey. Participants were asked to answer questions about where they go for weather information, their perception of different types of weather phenomena and how it might affect their communities. Participants were also asked about their hypothetical reactions to severe weather warnings from the National Weather Service. To administer the survey Qualtrics technologies were used and was intentionally oversampled for Black/African American and Hispanic/Latino communities.

While gender can play a large role in shaping perceptions and affect protective actions and survivability, the differences seen based on regional location are also crucial for understanding the challenges social scientists face in providing useful information to the public. Quantitative research alone cannot provide a robust enough view of this

issue. This web survey proved the need for additional qualitative research about perceptions of safety and protective actions, and how they differ based on gender.

References

- [1] H. Simmons, Kevin M., and Daniel Sutter. *Economic and Societal Impacts of Tornadoes*. Boston: American Meteorological Society, (2011).
- [2] Perry, Ronald W., and Michael K. Lindell. "The Effects of Ethnicity on Evacuation Decision-Making." *International Journal of Mass Emergencies and Disasters* 9.1 **47-68** (1991).
- [3] Neumayer, Eric, and Thomas Plümper. "The Gendered Nature Of Natural Disasters: The Impact Of Catastrophic Events On The Gender Gap In Life Expectancy, 1981-2002." *Annals of the Association of American Geographers* 97.3 (2007): **551-66**.

Acknowledgement

This material is based upon research supported by the National Oceanic and Atmospheric Administration, Educational Partnership Program, U.S. Department of Commerce, under Agreement #NA11SEC4810003. The statements contained within the manuscript/research article are not the opinions of the funding agency or the U.S. government, but reflect the author's opinions.

Inter-annual Variability in Urban Heat Island Intensity Over 10 Major Cities in The United States

Prathap Ramamurthy and Michael Sangobanwo

Department of Mechanical Engineering, the City College of New York, New York, NOAA-CREST

Abstract

Urban heat island intensity (UHI) has become a cross-cutting quotient to characterize the thermal environment of urban areas. In this study, we use publicly available weather data from ten metropolitan centers located in US to characterize the hourly, seasonal and yearly variability in air temperature based UHI. Our results revealed that while there are phenomenological similarities on UHI causes and trends, their order of influence in different cities is however distinct. Of cities compared here the coastal and arid cities exhibited high diurnal variability during the summer months. During the cold season, except for New York City, other cities had a flatter profile. Our analysis also shows that during extreme heat days in the warm season, the UHI is amplified in most cities. The UHI of cities located along the coast were highly sensitive to sea breeze and in general experience more extreme heat days than the inland cities.

Introduction

UHI is a measure of the impact of urbanization on the local thermal environment and is a quintessential factor that dictates weather patterns (Oke 1995) and several ecosystem functions that affect the local energy and the hydrological cycles (Arnfield 2003). The large scale anthropogenic modification of the land cover in urban areas have led to surfaces that are efficient in storing heat (C. S. B. Grimmond & Oke 1999) as opposed to moisture, and a geometry that assists in radiative trapping (Masson et al. 2002; Lemonsu et al. 2004; Kusaka et al. 2001). In addition, combustion from vehicles and waste heat (Gutierrez et al. 2015) from buildings contribute to creating a thermally aggravated environment. This modification directly impacts energy-use and human health (C. S. B. Grimmond et al. 2010). UHI, for the most part has been used as an indicator by physical and health scientists to quantify the amplified thermal state of the urban environment, lately even urban planners, architects (Shishegar 2014) and industry stakeholders alike are invested in understanding the influence of UHI to abet

smart and sustainable design. The convergence of various fields has expanded the applicability of the UHI quotient across various socio-economic and scientific dimensions. Hence it is crucial to adequately account for UHI and its variability across multiple spatial and temporal domains.

Experiments and Conclusion

The analysis relied on publicly available data from the National Weather Service's ASOS and AWS networks. Table 1 in the appendix describes the stations that were used for this analysis. The table also details the GPS coordinates and the land cover surrounding the station. Ten years of continuous air temperature data, spanning from 2005-2014 was used for this analysis. Multiple stations were used for every city and were averaged based on their time stamps. Due to discrepancy in the retrieval times at each site, data from each station were binned hourly. Rural reference stations were picked to calculate the UHI. These rural stations were meticulously picked in such a way that they were influenced by the same climatology as urban stations and were also approximately located at the same altitude.

The results obtained have showed the need for localized analysis, as the daily variability is related to local processes and dynamics. In most cities the hourly variability is inherently tied to its geophysical characteristics and hence any strategy to moderate the effects of UHI has to be based on local analysis that takes in to account the interplay between various factors. The analysis has also highlighted the crucial role played by sea breeze or coastal winds. Unfortunately, this area is insufficiently researched and more work is necessary to comprehend the impact of the coast on cities.

References

Akbari, H. et al., 1992. *Cooling our Communities. A Guidebook on Tree Planting and Light-Colored*, US Environmental Protection Agency, Climate Change Division.

Akbari, H., Konopacki, S. & Pomerantz, M., 1999. Cooling energy savings potential of reflective roofs for residential and commercial buildings in the United States. *Energy* 24(5), pp.391–407.

Anderson, B.G. & Bell, M.L., 2009. Weather-related mortality: how heat, cold,

and heat waves affect mortality in the United States. *Epidemiology (Cambridge, Mass.)*, 20(2), pp.205–213.

Angevine, W.M. et al., 2003. Urban–rural contrasts in mixing height and cloudiness over Nashville in 1999. *Journal of Geophysical Research: Atmospheres* (1984–2012), 108(D3), pp.4092.

Arnfield, A.J., 2003. Two decades of urban climate research: a review of turbulence, exchanges of energy and water, and the urban heat island. *International Journal of Climatology*, 23(1), pp.1–26.

Acknowledgement

This study was supported by the National Oceanic and Atmospheric Administration (NOAA) thru the NOAA Remote Sensing Science and Technology Program at City College of New York under Grant# NA11SEC4810004. The statements contained within the manuscript/research article are not the opinions of the funding agency or the U.S. government, but reflect the author’s opinions.

Guidance Index for Shallow Landslide Hazard Analysis

C Avalon Cullen^{1,2,3}, Rafa Al-Suhili², and R. Khanbilvardi^{2,3}

¹The Graduate Center, NOAA-CREST, ccullen@gc.cuny.edu

²City College of New York, ³NOAA-CREST

Abstract

Rainfall-induced landslides are one of the most frequent hazards on slanted terrains. They lead to considerable economic losses and fatalities worldwide. Intense storms with high-intensity and long-duration rainfall have high potential to trigger rapidly moving soil masses due to changes in pore water pressure and seepage forces. Nevertheless, regardless of the intensity-duration of the rainfall, shallow landslides are influenced by antecedent soil moisture conditions. To the present day, no system exists that dynamically interrelates these two factors.

This work establishes a relationship between antecedent soil moisture and rainfall expressed in the form of a Shallow Landslide Index (SLI) at 1km² resolution for the United States. The proposed mathematical model is based on a logistic regression-learning algorithm that systematically adapts from previous landslide events listed in a comprehensive landslide inventory. The logistic regression model is carried over to ArcGIS where all static variables are processed based on their corresponding coefficients. A regional slope susceptibility map for the continental United States is developed and analyzed against the available landslide records and their spatial distributions.

Consequently, a mathematical algorithm is proposed to determine landslide probability as a function of static and dynamic factors employing accumulated water volume. As rainfall thresholds alone do not provide information about the soil wetness profile

with depth, the Shallow Landslide Index (SLI) is intended to be an indicator of antecedent root soil moisture and rainfall accumulation over a 1km² pixel area. Experimentally, root-soil moisture retrieved from AMSR-E and rainfall retrieved from TRMM are used as proxies to develop such index. Static and dynamic conditions leading to each landslide event are examined over 60-days, 30-days, 10-days and 7-days. The input dataset is randomly divided into training and verification sets where validation results indicate that the best-fit model predicts the highest number of cases correctly at 93.2% accuracy. The resulting equation is then incorporated in a python subroutine that calculates the SLI for each of the 900,000-pixel points. For each pixel, the algorithm incrementally tries values from 0 to the value that makes the event probability equal to 1.

Since AMSR-E and TRMM stopped working in October 2011 and April 2015 respectively, a solution that works for the future is presented. Root-soil moisture retrieved from SMAP and rainfall retrieved from GPM are used to develop models that calculate the SLI for the continental United States for 10-days, 7-days, and 3-days. The resulting models indicated a strong relationship (93.4%, 93.8%, and 93.7% respectively) between the predictors and the prediction value. Nevertheless, as of the writing of this work, the SMAP root soil moisture product has a mean latency of 7-days hence the SLI is functional for 10 or 7 days. It is expected that as SMAP's latency is reduced, the SLI functionally can also be brought to a shorter period. The resulting SLI map can potentially

be used as an indicator of the total amount of rainfall needed for a given duration of time to trigger a shallow landslide in a susceptible area.

Findings

This work proposes a system that interrelates static and dynamic factors for the analysis of rainfall-triggered landslides at large extents. However, considerable discrepancies arise when monitoring landslides at large spatial resolutions over a vast domain. Therefore, the first step is to overcome this challenge by reducing uncertainties. This is achieved by utilizing buffer and threshold techniques to minimize uncertainty at the local scale so further analysis can be done on a larger scale. Various threshold percentages corresponding to 230 shallow landslides in the continental United States are tested in a logistic regression analysis. Findings are as follows:

- a. The AMSR-E model predicts the highest number of cases correctly at 92.7% accuracy.
- b. The RMSE between the resulting SLI and the actual events is 0.83 in a scale from 1-13.
- c. The resulting index map is useful to have an understanding of hazardous areas as precedent soil moisture conditions and rainfall are taken into consideration. Nevertheless, as AMSR-E is not longer functional, current and future guidance is not possible.

AMSR-E and TRMM are used in this work to learn and explore the feasibility of a system that can serve as a guide for antecedent moisture and rainfall triggers of shallow landslides. Nevertheless, as AMSR-E and TRMM stopped working on October 2011 and April 2015 respectively, a solution that works for the future is presented. New functional satellites SMAP and GPM are used to retrieve daily-modeled root soil moisture and rainfall respectively. The SLI is modeled for three time intervals 10-day, 7-day and 3-day and results are as follows:

- a. Variable relevance in the 3 models is the same. Slope is the variable with most influence followed by soil moisture content and rainfall in the form of SLI, soil type and land cover are subsequently in importance.
- b. The pseudo R^2 , the Nagelkerke R^2 fit for a logistic regression model for each model, 10-day, 7-day, 3-day, indicate a strong relationship (93.2%, 93.5% and 93.7% respectively) between the predictors and the prediction.

Acknowledgement

This study was supported and monitored by National Oceanic and Atmospheric Administration (NOAA) under (NOAA_CREST) Grant # NA11SEC4810004. The statements contained within the manuscript/research article are not the opinions of the funding agency or the U.S. government, but reflect the author's opinions.

Aerosol modeling of volatile organic compounds and sulfur dioxide during particle growth events at Beltsville, MD

Megan K. Payne¹, Everette Joseph^{1,2}, William R. Stockwell¹, and Fangqun Yu²

¹Howard University, NOAA Center for Atmospheric Sciences (NCAS)

²University of Albany, Atmospheric Sciences Research Center (ASRC)

Abstract

Introduction

Atmospheric aerosol properties are a challenging and complex problem to solve in the observational and modeling communities. Specifically, particle growth of new secondary organic aerosols present in the atmosphere are of concern because the of the large uncertainties aerosol properties have on climate (e.g. clouds), radiation (e.g. light scattering and absorption), and air quality. During July 2011 particle growth events were observed in Beltsville, MD along the interstate 95 corridor between the metropolitan areas of Washington DC and Baltimore, MD. An in depth analysis of the synoptic and meso-scale meteorological conditions relevant to the particle growth events and how differing air masses with different biogenic and anthropogenic sources showed that particle growth events occurred in cooler and drier air masses, shortly after significant cold air advection and precipitation [1]. Similar to other studies, more seasonal weather obtained after cold air advection supported a low pollutant and high organic-rich environment for new particles to grow into larger sizes with a maximum diameter of 100 nm. However, during a few events there moderate-high mixing ratios of sulfur dioxide were observed, likely coming from localized sources since the air masses recently changed to a cleaner trajectory. The main goal of this research was to determine what organic compounds were needed for the growth of new secondary aerosols at the research site, where the aerosols were coming from, and what the significance was of anthropogenic versus organic sources to

particle growth at the site. The study needed the support of atmospheric transport and chemical models to help answer the aerosol composition questions about the role of the organics on the growth of new aerosols and to what extent the gas-phased sulfur dioxide had on these events.

Experiments and Conclusions

For this study, two atmospheric models were used to test the role of organics on the growth of new aerosols as well as determine to what extent sulfur dioxide has on these events. First, a regional chemical mechanism model known as the Regional Atmospheric Chemical Mechanism, version 2 (RACM2) was used to weight and sort the significant organic sources during each case study, such as isoprene. The second model used was the NASA Goddard Earth Observing System Chemical (GEOS-Chem) model with Advanced Particle Microphysics (APM) model to validate the site observations and to help answer some questions about the dominant chemical sources of particle growth events that were not able to be concluded from just the observations. Given that GEOS-Chem/APM is a global model with a large grid domain, the model is successful at simulating particle growth events on the days that the site observed particle growth meaning that the model accurate accounts for the particle chemical and physical mechanisms needed to grow. The focus of this presentation is to discuss the key findings between the two models, the observational dataset, and relate how these findings are significant to the atmospheric science community as a whole.

References

[1] Payne, M.K., Joseph, E., Fuentes, J.D., Sakai, R., Stockwell, W.R., J. Atmos. Chem., **72** (2015), 423.

Acknowledgement

This study was partially supported by the National Atmospheric and Space Administration (NASA) Research

Cooperative Agreement # NNX08BA42A and the National Oceanic and Atmospheric Administration (NOAA) under NOAA Center for Atmospheric Sciences Grant # NA11SEC4810003. The statements contained within the manuscript/research article are not the opinions of the funding agency or the U.S. government, but reflect the author's opinions.

On the Creation of an Urban Boundary Layer Product Using the Radar Wind Profiler of the New York City Meteorological Network

Mark J. Dempsey^{1,2,3}, James F. Booth^{1,2,3}, Mark Arend^{2,3} and David Melecio-Vazquez^{2,3}

¹*The Graduate Center, CUNY*

²*The City College Of New York, CUNY*

³*NOAA CREST, City College of New York, CUNY,
New York, NY.*

Abstract

Introduction

The radar wind profiler (RWP) located on the Liberty Science Center in Jersey City, NJ is a part of the New York City Meteorological Network (NYCMetNet). An automatic algorithm based on those by Angevine [1] and Molod [2] is expanded upon and implemented to take RWP signal to noise ratio data and create an urban boundary layer (UBL) height product. Time series of the RWP UBL heights from clear and cloudy days are examined and compared to UBL height time series calculated from thermal data obtained from a NYCMetNet radiometer located on the roof of the Grove School of Engineering at The City College of New York. UBL data from the RWP are also compared to the MERRA (Modern Era Retrospective Analysis for Research and Applications) planetary boundary layer height time series product. A limited seasonal climatology is created from the available RWP data for clear and cloudy days and then compared to a limited seasonal climatology produced from boundary layer data obtained from MERRA and boundary layer data calculated from the CCNY radiometer. As with wind profilers in the NOAA wind profiler network, the signal return to the lowest range gates is not always the result of turbulent scattering, but from scattering from other targets such as the building itself, birds and insects. The algorithm attempts to address this during the daytime, when strong signal returns at the lowest range gates mask

the SNR maxima above which are representative of the actual UBL height. Detecting the collapse and fall of the boundary layer meets with limited success, also, from the hours of 2:30pm to 5:00pm. Upper and lower range gates from the wind profiler limit observation of the nighttime boundary layer for heights falling below the lowest range gate and daytime convective boundary layer maxima rising above the highest.

Preliminary results and conclusions

The average seasonal mean boundary layer height is plotted. The greatest fluctuations in boundary layer height occur between 4pm and 7pm. Summer and fall, both have a period of several hours where the boundary layer climbs higher after dark. Box plots of a seasonal range of daily maximum boundary layer heights demonstrate that fall shows the greatest range in daily maximum RWP UBL heights (~800m) as opposed to the winter, spring and summer (~500m, ~300m, ~350m respectively). Climatologically, the boundary layer heights obtained from the wind profiler are compared to the boundary layer heights obtained from both MERRA and the radiometer. Summertime RWP boundary layer heights compare less well to the radiometer, coming in lower during mid-afternoon. Boundary layer height evolution for all three, compare extremely well in the fall and the winter on clear days. During cloudy days in the winter, RWP boundary

layer heights are higher than both the radiometer and MERRA

A half hourly mean of RWP UBL heights is taken for years 2007 – 2014 and the half hour of greatest boundary layer height evolution happens between 8:00am and 8:30am. The hour of greatest boundary layer height collapse is between 7:00pm and 7:30pm. To determine the hour that the boundary layer emerges into the sensible region above the RWP lowest range gate, a time series of half hourly mean SNR values for 2007 to 2014 is constructed for the lowest range gate. Two peaks appear: one at 8am and the other at 7pm. Therefore due to the limitations of the instrument and the algorithm it is recommended that the boundary layer height product be constrained to the hours of 8am to 7pm.

References

- [1] Angevine, W. M. W. A. B. A. S. K., 1994: Boundary-layer depth and entrainment zone characterization with a boundary-layer profiler. *Boundary Layer Meteorology*, **68**, 375-385.
- [2] Molod, A., H. Salmun, and M. Dempsey, 2015: Estimating Planetary Boundary Layer Heights from NOAA Profiler Network Wind Profiler Data. *Journal of Atmospheric and Oceanic Technology*

Acknowledgement

This study was supported and monitored by National Oceanic and Atmospheric Administration (NOAA) under NOAA CREST Grant # NA11SEC4810004. The statements contained within the manuscript/research article are not the opinions of the funding agency or the U.S. government, but reflect the author's opinions.

K-Nearest Neighbor Approach for Developing Gridded Snow Product in Russia

Lawrence Vulis^{1*}, Naresh Devineni², Sean R. Helfrich³ and Cezar Kongoli⁴

¹*Earth Systems Science and Environmental Engineering, City College of New York, New York, NY, 10031*

²*Department of Civil Engineering, City College of New York, New York, New York 10031*

³*National Oceanic and Atmospheric Administration, National Ice Center, Suitland, MD, 20746*

⁴*University of Maryland, Earth Systems Science Interdisciplinary Center*

*correspondence to Lawrence Vulis (lvulis000@citymail.cuny.edu), 160 Convent Ave, New York, NY, 10031

Abstract

Snow Depth (SD) is an important element of predicting land-surface albedo in snow covered regions, and so becomes a key factor of land-surface energy balance models such as those used in operational weather forecasting. We developed a k-nearest neighbors algorithm to understand historical snow depth climatology on a 1-km resolution grid, using Mahalanobi's distance on spatial and physical predictors such as elevation and surface air temperature, from USGS 1-km resolution digital elevation maps and WorldClim 1-km resolution surface air temperature grids. The KNN grid is currently developed over the former Soviet Union and Alaska. Coefficients of Determination were mostly significant, ranging from 0.5 to 0.9, with better results in winter and fall, but poorer results in the summer. Further work on integrating additional data-sets to include more of the Northern Hemisphere is in progress, as well as introducing forecasting capabilities on a lower-resolution grid. The results can be used for present models such as NOAA's Interactive Multisensor Snow and Ice Mapping System Blended Snow Depth product, to improve NOAA's snow and in turn weather forecasting capabilities.

Introduction

Snow depth (SD) is an important factor for farmers and meteorologists. Snow will melt in high elevation regions and provide freshwater for agriculture, industry, and domestic use downstream¹. The National Oceanic and Atmospheric Administration's (NOAA) National Centers for Environmental Prediction (NCEP) uses the snow cover data provided by the National Ice Center (NIC) to provide weather forecasting and climate modelling². Snow depth affects surface albedo, affecting the land surface energy balance³. The Interactive Multisensor Snow and Ice Mapping System (IMS) Blended Snow Depth Product used by the NOAA/National Ice Center (NIC) is based on Optimal Interpolation (OI) method originally developed by Brasnett⁴ for Canadian Meteorological Center's Snow Depth

Analysis over the Northern Hemisphere and modified to ingest (in addition to in-situ data) satellite derived SD, as well as a regional elevation-SD relationship^{5,6}.

The goal of this work is to provide a look at the SD climatology in the Northern Hemisphere over the second half of the 20th century, as an improvement to the NOAA IMS-BSD. This work would also assist in improving accuracy over high-elevation regions, as well as bringing a better understanding of SD climatology. The improvement to the IMS-BSD will be useful in upgrading IMS-BSD to a 1-km resolution, as well as improving NOAA's operational weather forecasting capabilities.

Methodology

The major improvement in progress to the IMS-BSD is improving the

climatological aspect, by developing a gridded climatology of 1950-2000 mean monthly mean SD at 1-km resolution over the Northern Hemisphere. The results of the work over Russia are being presented here. The grid was generated using a k-Nearest Neighbors (kNN) regression, with 589 in-situ stations providing SD and temperature observations, and the WorldClim dataset providing gridded mean temperature observations⁷. The kNN generated grid values by measuring the Mahalanobi's distance of 4 predictor parameters (Latitude, Longitude, Elevation, and Temperature), of each grid point with all the stations and then selecting the k neighbors which are closest. The SD observations at the k neighbors are then given probability weights and 1000 weighted SD values are simulated for the station, and the median is selected as the simulated SD value.

Results and Conclusions

Results over Russia indicate that winter months tend to show more accurate results, while summer and late spring months are not as accurate. The coefficient of determination (R^2), the root-mean squared error (RMSE), and a within interquartile range metric are reported. The R^2 varied from .46 to .61 in the winter and fall, and RMSE varied from 2.3 to 17 cm in the same months. R^2 varied from -.03 to .25 in the summer, while RMSE varied from 1.25 to 3.90 cm. There is still under-prediction at high-elevations, which may be alleviated with the introduction of remotely-sensed data or error correction. The introduction of predictors that reflect properties not currently being modelled, such as slope or aspect may also be useful. An alternative regression methodology using local polynomial regression which has better extrapolation capabilities is also being tested.

References

1. Balk, B. & Elder, K. Combining binary decision tree and geostatistical methods to estimate snow distribution in a mountain watershed. *Water Resour. Res.* (2000). doi:10.1029/1999WR900251
2. Helfrich, S. R., McNamara, D., Ramsay, B. H., Baldwin, T. & Kasheta, T. Enhancements to, and forthcoming developments in the Interactive Multisensor Snow and Ice Mapping System (IMS). in *Hydrological Processes* (2007). doi:10.1002/hyp.6720
3. Ghatak, D., Gong, G. & Frei, A. North American temperature, snowfall, and snow-Depth response to winter climate modes. *J. Clim.* **23**, 2320–2332 (2010).
4. Brasnett, B. A Global Analysis of Snow Depth for Numerical Weather Prediction. *Journal of Applied Meteorology J. Appl. Meteor.* **38**, 726–740 (1999).
5. Helfrich, S. R., Li, M., Kongoli, C., Nesdis, N. & Nic, O. NOAA NIC Snow Analysis and Blended Products. in (2013).
6. Kongoli, C. & Helfrich, S. A multi-source interactive analysis approach for northern hemispheric snow depth estimation. (2015).
7. Hijmans, R. J., Cameron, S. E., Parra, J. L., Jones, P. G. & Jarvis, A. Very high resolution interpolated climate surfaces for global land areas. *Int. J. Climatol.* **25**, 1965–1978 (2005).

Acknowledgement

This study was supported and monitored by National Oceanic and Atmospheric Administration (NOAA) through the Educational Partnership Program with Minority Serving Institutions Undergraduate Scholarship Program. The statements contained within the manuscript/research article are not the opinions of the funding agency or the U.S. government, but reflect the author's opinions.

Planetary Boundary Layer Turbulence Characterization

Ivan Valerio¹, Mark Arend¹, Fred Moshary¹, Stephen Nufeld²

¹*Department of Electrical Engineering at CCNY and NOAA CREST*

Abstract

Observing atmospheric air flow dynamics can reveal useful patterns for understanding its thermodynamic processes. The planetary Boundary Layer (PBL) can be further studied by measuring vertical transport of aerosols under different synoptic conditions. The Coherent Doppler Lidar at the City College of New York has been operated during both winter and summer periods and the results are analyzed. A parameter of interest is the index of refraction structure constant, which is considered to be a measure of turbulence and represents fluctuations in the index of refraction. Data obtained from the Doppler Lidar is compared to other instruments to expose similarities and differences and how the network of instruments observe the planetary boundary layer dynamics.

Introduction

The Coherent Doppler Lidar located at the City College of New York measures the motion of aerosols in the planetary boundary layer relative to the instrument. This device uses fiber optic technology to produce low energy pulses, which are used to build a vertical profile of this part of the atmosphere. Additionally, cases were chosen to include data where other variables such as temperature can be extracted. These instruments include a backscatter LIDAR, which operates at wavelengths of 1064 nm, 532 nm, and 355 nm, and a Microwave radiometer. Both of these are located and operated at the City College of New York.

The Doppler Lidar operates at wavelength 1542 nm, and emits a pulse strength of 14 microjoules, making this device eye-safe. Tests of interest is the comparison of various cases with similar magnitudes of aerosol concentration in order to discern the connection between turbulence and the Refractive Index Structure Constant. This parameter is used to simulate the effects of turbulence in the retrieval of our signal. Understanding how this parameter changes as a function of the wind in the PBL could provide insight on how to better retrieve

relative intensity profiles of this part of the atmosphere.

Experiments and Conclusions

We recorded data for a wide variety of cases that span the time of 6 months. The defining feature that was searched for was a consistent and measurable effect of measured vertical wind components to the signal strength measured by the Doppler LIDAR.

The expectation was to find a change in the detection of aerosols in regions of the atmosphere where vertical wind components were more prominent. This can be analyzed using the relative intensity measurements obtained with the Doppler LIDAR, as well as measuring any changes in the maximum distance reached in the atmosphere. The structure constant is a measure of the effects of turbulence on LIDAR SNR and can be an indication of wind in the PBL^[1]. As the level of turbulence increases, the scattered light by the aerosols are affected and the return signal is affected by the change in index of refraction.

There was no significant change in signal strength as a result of the increase vertical motion of aerosols. Further work will be required to study the effects of vertical wind on the device's Signal-to-Noise Ratio (SNR).

Additional work might include observing the effects of measured relative intensity and perform a deeper comparison of the results from this instruments with other LIDARs in the region.

References

[1] Kameyama, S., et al. "Compact all-fiber pulsed coherent Doppler lidar system for wind sensing." *Applied Optics* 46.11 (2007): 1953-1962.

Acknowledgement

This study was supported and monitored by National Oceanic and Atmospheric Administration (NOAA) under Grant # NA11SEC4810004. The statements contained within the manuscript/research article are not the opinions of the funding agency or the U.S. government, but reflect the author's opinions.

The Dynamics of Water Storage Over Lake Eyre, Australia Observed by Satellite Data

^{1,2} Obeng Kwaku Buo, ² Kibrewossen Tesfagiorgis

¹ Louis Stokes Alliance for Minority Participation Program

² Borough of Manhattan Community College

City University of New York, New York, NY

ABSTRACT

This study investigated the dynamics of water storage over Lake Eyre, Australia using Polarization Ratio Variation Index (PRVI) values from The Advanced Microwave Scanning Radiometer (AMSR-E) and precipitation rate from the Tropical Rainfall Measuring Mission (TRMM). Lake Eyre, the largest lake in Australia and 18th largest in the world is an ephemeral lake that fills up on rare occasions. Satellite microwave data such as PRVI values from AMSR-E are sensitive to surface change which helps to monitor soil surface wetness from space to detect inundation, hence, in this study the PRVI values were used to observe the water storage variation in Lake Eyre. We examined monthly satellite precipitation rate from TRMM and PRVI from AMSR-E for the time frame of three years (2008-2010) to analyze the links between rainfall rate and water storage dynamics in the Lake.

INTRODUCTION

Water Storage plays a very important role within the global water cycle and on climates, particularly in regions where the coupling between land surface and the atmosphere is theorized to be essential such as Australia (Koster et al., 2004). The use of satellites like the Tropical Rainfall Measuring Mission (TRMM) to measure precipitation over a particular region, prevents greater room for uncertainties. With proper knowledge on TRMM based precipitation data, we can design models in which will allow us to accurately measure rainfall rate, allowing proper warning to regions that are at highest risk overflow and thus place proper measure to store water for other purposes

In the same way, microwave data provide information about a particular target twice a day at a resolution 48 km in the window channels. Because of daily time resolution, microwave data are suitable to study short and long term hydrological dynamics. Particularly, the window channels (microwave channels less than 89 GHz frequency) in the microwave range play important role as they are sensitive to surface variations such as soil wetness. A

great knowledge of the Advanced microwave satellite like the AMSR-E will enable us produce Polarized Ratio Variation Index (PRVI) values which are used for measuring inundation with the help of the TRMM data.

1. METHODS AND MATERIALS

1.1. DATA DESCRIPTION

There are two different satellite data used in this study; the Tropical Rainfall Measuring Mission (TRMM) and the Advanced Microwave Scanning Radiometer (AMSR-E) which are both monitored, operated and managed by NASA.

AMSR-E, one of the six sensors aboard AQUA are used to see water storage over Lake Eyre, Australia. Using the AMSR-E, we were able to achieve high resolution data that are essential for our study. The AMSR-E provided us with a dual polarized six-frequency band data. Most of these bands are appropriate for monitoring inundation, soil moisture and flooding due to their sensitivity to surface change. For the study, we used the 37 GHz frequency

band Polarization Ratio Variation Index (PRVI) to observe water storage variation within the lake. The PRVI is defined as the normalized anomaly in polarization ratio

$$PR = \frac{T_{bv} - T_{bh}}{T_{bv} + T_{bh}}$$

which accounts for the differences between the bare and the wet soil regarding emissivity at Vertical (v) and Horizontal (h) polarizations (Temimi, et al., 2011).

$$PRVI_i = \frac{PR_i - \mu_{PR}}{\sigma_{PR}}$$

Where PR is the polarization ratio, T_{bv} is the 37 GHz vertically polarized AMSR-E brightness temperature, T_{bh} is the 37 GHz horizontally polarized AMSR-E brightness temperature. PRVI is the polarization ratio variation index for i in the historical standard deviation for the month of i .

Three years (2008-2010) of monthly satellite precipitation data from TRMM was used for our study. Global TRMM data was downloaded from NASA's website in Hierarchical Data Format (HDF). The purpose of the TRMM dataset was to provide us with monthly global precipitation over our study period. We collected the level-3 of the monthly data from the TRMM Online Visualization and Analysis System (TOVAS)-TRMM 3 Monthly Product. It is one of the newest models of the Multi Satellite Precipitation Analysis (TMPA) with 5% higher consistency in results. It provided us with data that made the study more accurate, hence giving us a high resolution data of $0.25^\circ \times 0.25^\circ$ (Huffman et al., 2014). The downloaded global monthly precipitation data for our three year study period is processed to our study domain, Australia.

1.2. MATLAB APPLICATION

MATLAB is a high-level technical computing language that allows us to manipulate, open, and load files allowing for images and data analysis. With the

help of MATLAB we were able to 'untar' and run series of codes to visualize TRMM and AMSR-E data. We did the same for the watershed data for the Lake Eye Catchment. We further cut the Lake Eye Catchment and run it on the previous plot images obtained from TRMM to obtain our final analysis of the precipitation rate over our study area.

4. CONCLUSION

The TRMM and the AMSR-E were used to analyze the links between rainfall rates and the storage dynamics in the lake. The rationale of our research was to determine the water storage capacity of Lake Eyre. With the help of the TRMM and AMSR-E data we were able to find the average precipitation and its links with primary water storage capacity of the lake. We examined monthly satellite precipitation rate from TRMM and PRVI from AMSR-E for the time frame of three years (2008-2010) to analyze the links between rainfall rate and water storage dynamics in the Lake.

REFERENCE

- Huffman, George J., and David T. Bolvin. "TRMM and other data precipitation data set documentation." *NASA, Greenbelt, USA* (2013): 1-40.
- Koster, Randal D., Dirmeyer, P. A., Guo, Z., Bonan, G., Chan, E., Cox, P., ... & Yamada, T. "Regions of strong coupling between soil moisture and precipitation." *Science* 305.5687 (2004): 1138-1140.
- Temimi, M., Lacava, T., Lakhankar, T., Tramutoli, V., Ghedira, H., Ata, R., & Khanbilvardi, R. "A multi-temporal analysis of AMSR-E data for flood and discharge monitoring during the 2008 flood in Iowa." *Hydrological Processes* 25.16 (2011): 2623-2634.

5. ACKNOWLEDGEMENTS

This project was made possible by the Research Experience for Undergraduates in the Louis Stokes Alliances for Minority Participation program funded by the National Science Foundation. Special thanks to National Aeronautics and Space Administration in also providing rainfall data from the Tropical Rainfall Measuring Mission Satellite 3B42v7 and 3B43v7.

THEME III

HEALTHY OCEANS

**Marine fisheries, habitats, and biodiversity are sustained within
healthy and productive ecosystems**

Using the position of digestive contents relative to chlorinated hydrocarbon (CHC) concentrations in the liver to map CHC movement through the smooth dogfish (*Mustelus canis*)

Tyler Plum¹, Olivia Skeen², and Eric May³

¹West Virginia University, Research Experience for Undergraduates

²University of Maryland Eastern Shore, NOAA LMRCSC

³University of Maryland Eastern Shore, NOAA LMRCSC

Abstract

Many studies have found that organic pesticides, especially chlorinated hydrocarbons, are absorbed by organisms through bio accumulation in most marine ecosystems, usually in food chain bioaccumulation and magnification. Sharks are one example of a commercially and recreationally valuable organism that could be affected by these contaminants, as they are at a greater threat from bio accumulation, being top level predators. It is therefore important to understand how these chlorinated hydrocarbons are absorbed from their diet, and how they move as digestion occurs. To test this, we sampled a number of smooth dogfish, *Mustelus canis*, and attempted to correlate the results of gut content position analyses at the time of death to chlorinated hydrocarbon concentrations in the liver. Chlorinated hydrocarbon concentrations were expected to spike at different points in digestion, and by comparing the results of multiple shark diet analyses, which were sacrificed at varying stages of digestion, to their liver concentrations, it was assumed a conceptual map of how these chemicals are absorbed during digestion could be created. Assuming elasmobranch digestion was similar to teleost digestion, it was hypothesized that liver concentrations would be highest when large volumes of content are found within the sharks spiral valve, or lower intestine, which usually have high nutrient absorption. In reality, no chlorinated hydrocarbons were found in any of the liver samples, a highly unexpected event. It is assumed that either 1) chlorinated hydrocarbons are absorbed at a continuous rate from the liver into the bodily tissues (i.e. muscle), leaving them virtually absent from the liver, or 2) that the sharks are not absorbing chlorinated hydrocarbons into their body or liver because they are excreted as waste at a rate that does not allow adequate time for absorption.

Introduction

Many studies in recent years have shown that organic chemicals and toxins in marine ecosystems have a tendency to bio-accumulate throughout the trophic levels [3]. It is also well known that elasmobranchs generally occupy these high trophic niches [2]. This often results in sharks, rays and other elasmobranchs having the highest concentrations of organic chemicals [1]. However, while these are carcinogens, there is little information available about the rate at which these organisms suffer malignant tumors or other effects from these

carcinogenic toxins [4]. They also only exhibit signs of reproductive and endocrine effects upon extremely high levels of chemical concentrations [5]. Thorough studies of the effects of these chemicals in elasmobranchs have greatly increased our body of knowledge about these interactions; however, few studies exist that investigate how these chemicals travel throughout the body, and virtually none represent a model that can be applied to all elasmobranchs. Crucial to our understanding of how these multiple processes effect chemical travel in elasmobranchs is an understanding of the

exposure to chemicals in the digestive process.

In order to understand how chemicals travel through the body of elasmobranchs, we must understand how these chemicals travel from the digestive track, through the liver, and whether they are offloaded out again in the short colon. Using a model elasmobranch, the smooth dogfish, *Mustelus canis*, which is abundant on the Atlantic coast in summer, we will examine both the stomach contents and the concentrations of CHCs in the liver. By examining the stomach contents position comparatively to CHC concentrations in the liver at the time of death, where these processes should be effectively frozen in time, we should be able to map the absorption, retention, and excretion pattern and process of elasmobranchs. This could eventually result in a chemical pathway model that could be applied to all sharks. Obtaining this knowledge could potentially bridge the gap between our knowledge of food chain bioaccumulation in sharks and the interesting effects, or lack thereof, of CHCs in many elasmobranchs. This knowledge will also be useful to regulatory bodies by deepening their understanding of the larger anthropogenic threat to sharks, allowing them to take informed steps to conserve elasmobranchs as a vulnerable natural resource.

Experiments and Conclusions

Smooth dogfish, *Mustelus canis*, were harvested by otter trawl in the Delaware Bay by the Delaware Fisheries Service. In total, 64 sharks were sampled, however, only 36 sub-samples of 18 livers have been chemically analyzed at this time. However, digestive data from all 64 sharks have been compiled and the resulting analysis used as a predictor for chlorinated hydrocarbon presence. An attempt was made to correlate the results of gut content position analyses at

the time of death to chlorinated hydrocarbon concentrations in the liver. Chlorinated hydrocarbon concentrations were expected to spike at different points in digestion, and by comparing the results of multiple shark diet analyses, which were sacrificed at varying stages of digestion, to their liver concentrations, it was assumed a conceptual map of how these chemicals are absorbed during digestion could be created. Assuming elasmobranch digestion was similar to teleost digestion, it was hypothesized that liver concentrations would be highest when large volumes of content are found within the sharks spiral valve, or lower intestine, which usually have high nutrient absorption in teleost fish.

In reality, no chlorinated hydrocarbons were found in any of the liver samples, a highly unexpected event. It is assumed that either 1) chlorinated hydrocarbons are absorbed at a continuous rate from the liver into the bodily tissues (i.e. muscle), leaving them virtually absent from the liver, or 2) that the sharks are not absorbing chlorinated hydrocarbons into their body or liver because they are excreted as waste at a rate that does not allow adequate time for absorption. However, butylated hydroxytoluene was found in 35 of 36 sub-samples, which consisted of a total of 18 sharks. While these levels have yet to be quantified with a standard measurement in parts per million, their levels were detectable even when compared on a scaled graph displaying high levels of cholesterol and squalene.

References

- [1] C. E. D. A. e Silva, A. Azeredo, A. D. C. L. Dias, ... J. P. M. Torres, *Mar. Poll. Bull.* **58** (2009) 294.
- [2] E. Cortes, *ICES J. Marine Sci.* **56** (1999) 707

- [3] F. A. Gobas, J. B. Wilcockson, R. W. Russell, G. D. Haffner, *Envir. Sci. & Tech.* **33** (1999) 133.
- [4] G. K. Ostrander, K. C. Cheng, J. C. Wolf, M. J. Wolfe, *Canc. Res.* **64** (2004) 8485.
- [5] J. Gelsleichter, C. J. Walsh, N. J. Szabo, L. E. Rasmussen, *Chemos.* **63** (2006) 1506.

Acknowledgement

This study was supported and monitored by National Oceanic and Atmospheric Administration (NOAA) under The

University of Maryland Eastern Shore Living Marine Resources Cooperative Science Center (LMRCSC) NA11SEC4810002 and the National Science Foundation (NSF) Research Experience for Undergraduates (REU) Program. The statements contained within the manuscript/research article are not the opinions of the funding agency or the U.S. government, but reflect the author's opinions.

Zooplankton Composition in Hampton Roads, VA: Spatio-temporal Variability and DNA Barcoding of Copepoda

Alexandra Salcedo Bauzá¹, Áurea E. Rodríguez² and Deidre M. Gibson²

⁽¹⁾Department of Biology, Hampton University, Hampton, VA 23669,
alexandrasalcedo19@gmail.com

⁽²⁾Department of Marine & Environmental Science, Hampton University, VA, 23669

Introduction

The study of zooplankton biodiversity and distribution is crucial to understand oceanic ecosystems and manage commercially important species. However, mesozooplankton (> 200µm) abundance, diversity and community structure has not been rigorously assessed in Hampton Roads (HR). Monthly plankton samples have been collected since September 2015 with a 0.5m, 200µm mesh net for 3 minutes at 3 study sites located in HR: James River (Site 1), the upper part of the HR estuary (Site 2), and lower Chesapeake Bay (Site 3); physical and chemical parameters were measured simultaneously. Nets were towed in an oblique pattern from the surface to approximately 1.5m and back to the surface. The faunal collection from a filtering cod-end was preserved in 60% ethanol for subsequent identification. When gelatinous zooplankton (ctenophores) became excessive, they were removed from the samples.

Taxonomic identification of zooplanktonic organisms, traditionally performed by expert taxonomists employing optical techniques is time consuming and full of limitations, such as those that appear while studying cryptic species (morphologically indistinguishable species), early developmental stages (eggs and larvae), parts of specimen bodies (e.g. one leg) or semi-digested samples (e.g. gut contents) (Lindeque *et al.*, 2013). In the efforts of studying zooplankton biodiversity, the number and composition of individuals identified by morphological methods can be significantly underestimated (Elias-Gutierrez

et al. 2008). Our approach will be based on molecular genetic techniques.

DNA barcoding aims to provide an efficient method for species-level identifications using species specific molecular tags derived from the 5' region of the mitochondrial cytochrome *c* oxidase (COI) gene (Jungbluth and Lenz, 2013; Pradhan *et al.* 2015); COI gene, a 648 base-pair region, has been adopted as the standard barcode for members of the animal kingdom (Hebert *et al.* 2003). Such techniques can potentially overcome limitations previously discussed as the method does not require morphological identification, while providing an accurate and rapid identification of known species and further discovery of new cryptic organisms. Thus, DNA barcoding will be used to begin a detailed characterization of zooplankton diversity, abundance and community structure in the Hampton Roads Area (HRA). The long term objective of this project is to provide a comprehensive assessment of zooplankton in the Hampton Roads Area (HRA) as a basis for future broad monitoring programs; vital for a better understanding and management of ecologically and commercially important species.

Experiments and Conclusions

Quantitative analyses were performed to determine zooplankton taxonomic composition and abundance, while DNA barcoding of mitochondrial cytochrome *c* oxidase I (COI) gene was used to characterize species composition. Zooplankton samples were thoroughly

mixed, aliquots were taken twice from each sample and zooplankton was examined by morphological analysis and identified to lowest possible taxonomic level. DNA extractions were performed using the Genra Puregene Tissue Kit and Qiagen DNEasy. Mean average zooplankton abundance was estimated from two subsamples drawn using a Stemple pipette, counted under a dissecting microscope. Analyses of Variance ANOVA of abundance were performed to examine similarity among stations and season collections. Correlations of zooplankton abundance with physical parameters were performed. Significant negative correlation between salinity and meroplankton ($r = -.670$, $p < .05$) and salinity and total zooplankton ($r = -.705$, $p < .05$) was observed for the study period. So far, the three study sites have shown noticeable differences in planktonic community. In addition, September 2016 samples revealed high abundance and diversity of both holoplankton and meroplankton (decapod and cirriped larvae) community, which decreased drastically the following months coinciding with the appearance of *Mnemiopsis leidyi* ctenophores in October 2016.

Species identified by BLAST search include *Acartia tonsa*, *Paracalus parvus* and *Undinula vulgaris* copepods. Zoea stage larvae identified were of *Eurypanopeus depressus* (Flatback Mud Crab) and *Dyspanopeus sayi* (Mud crab). Cyprid stages of cirripedia (barnacles) were identified as *Amphibalanus improvisus* (Bay barnacle). Fish eggs were identified as from *Opistonema oglinum* (Atlantic Thread Herring), found at the offshore stations while, *Anchoa mitchilli* was found at both stations. For the study period total zooplankton abundance ranged from 10,780 Ind/m³ in May 2016 at the James River station to 60 Ind/m³ in October at the Hampton River estuary station. Higher abundances for May were dominated by cirriped larvae

mini kit according to manufacturer's protocol while DNA quantity and purity was measured using the Thermo Scientific™ Nanodrop Lite Spectrophotometer; integrity of extracted DNA was assessed by gel electrophoresis.

(barnacles), accounting for the significant increase in overall zooplankton abundance in Mar-May 2016, driving differences in meroplankton abundance overall. Lowest abundances observed in October 2015 coincided with high abundance of large ctenophores. September showed high abundance of copepods (mainly *Acartia tonsa*), dominating the holoplankton component; thus zooplankton abundance was driven by holoplankton. Ichthyoplankton was found only in June 2015, was absent in the fall and winter, it was observed again in April and May. Fish egg samples were barcoded; species identified include *Opistonema oglinum* (Atlantic Thread Herring) at the outer station and *Anchoa mitchilli* (Bay anchovy) at the inner stations (James River and Hampton River estuary).

Significant differences in Meroplankton between sites were found ($P < 0.05$). Significant differences were found for months for meroplankton and total zooplankton. Our results indicate that major differences in our study are related to meroplanktonic (larval forms) organisms. Salinity seemed to be the major force driving meroplankton abundance. We observed low abundances of total zooplankton with high occurrences of the ctenophore, *Mnemiopsis leidyi*

Acknowledgement

This project is supported and monitored by the National Science Foundation (NSF) (Award #'s 1459510 & 1459293) and the NOAA Living Marine Resources Science Cooperative Center (LMRCSC) award # NA11SEC4810002.

A molecular approach to study the in situ diet of the pelagic tunicate *Thalia democratica* (Salpida, Thaliacea) in the South Atlantic Bight (SAB)

A. Natalia B. López-Figueroa¹, B. Deidre M. Gibson², C. Aurea E. Rodríguez-Santiago², D. Tina Walters³ and E. Marc Frisher³

¹Hampton University, Department of Biology

²Hampton University, Department of Marine and Environmental Science

³University of Georgia, Skidaway Institute of Oceanography

Abstract

Salps are pelagic tunicates that play a crucial role in marine planktonic food webs. It has been suggested that salps may become essential in the health of the Future Ocean. The salp, *Thalia democratica*, has been abundantly found off southeastern United States in the upper mixed layer, and is considered a key predator in shelf communities. Wild *T. democratica* will be collected seasonally during day cruises along the Georgia-Florida portion of the South Atlantic Bight (SAB) using a 202 μ m tucker trawl. Laboratory-based feeding studies have shown that *T. democratica* has a preference for microzooplankton (20 to 200 μ m) such as dinoflagellates and nanoflagellates. However, it remains a challenge to estimate their in situ diet and role in the trophic web without experimental bias. Hence, we seek to quantify the in situ gut contents of wild caught *T. democratica* with a molecular gut profiling approach by using a salp-specific peptide nucleic acid (PNA) PCR blocker. The PNA-PCR will be used to quantify consumption of specific prey species in guts. Additionally, zooplankton quantitative analysis and DNA barcoding will be used to compare prey present in the water column with salp gut content.

Introduction

Salps are tubular animals that swim continuously by rhythmic muscular contractions; these (in contrast to other thaliaceans) produce current across the feeding filter [1]. Among the fastest growing metazoans on earth, they can shortcircuit traditional food webs through their ability to continuously filter-feed on a range of particles over 3 orders of magnitude in size [4]. Also, they can form a deflection of the microbial loop by consuming small microbes and packaging them into large fecal pellets. This trait makes them able to feed on different types of microplankton [3]. Therefore, salps are an ecologically and biogeochemically important class of gelatinous zooplankton.

Thalia democratica occurs abundantly off southeastern United States [3]. *Thalia* has a wide distribution across the world oceans, from Antarctica to the mid-Atlantic; they are considered key predators in shelf communities. Thaliacean blooms, dominated by the aggregate stage of salps, have been reported for at various times of year but were mostly found between February and August. As recorded by Deibel and Paffenhöfer, the patches of thaliaceans studied in the SAB between 1976 and 1981 were closely associated in time and space with intrusions of cool, high nutrient water originating from aphotic depths of the Gulf Stream. In fact, research on gelatinous organisms is only a small fraction of resource management needs for fisheries, ocean weathering forecasts, and assessment of pollution.

Experiments and Conclusions

The proposed study includes the collection of salps throughout the year, during day cruises from up to four days, aboard the R/V Savannah (Home Port SkIO). The samples will be collected seasonally along the Georgia-Florida portion of the South Atlantic Bight (SAB). Most thaliacean species occur in the open ocean, a few of the most abundant live in continental shelf waters [3]. Hydrographic transects will be composed of a Conductivity, Temperature and Depth (CTD) cast and plankton net tows with a 202 μ m Trucker trawl will be carried out when the shelf intrusion is located.

The strategy is to search for intrusions by making CTD surveys. Intrusions are identified by evidence of low temperature and high relative fluorescence, which is a proxy for chlorophyll. When intrusion water is located, a profile of the water column is taken to characterize the water column and samples are collected for on board experiments. Concurrently, the tucker trawl will collect salps and zooplankton at two different depths (surface and bottom) in the presence of a bloom. The combination of the Trucker trawl and CTD will aid in determining the abundance and distribution of animals associated to the scattering layers. Hence, this will illustrate a more thorough profile from different depths at the sampling sites.

Preserved zooplankton samples are subjected to quantitative analysis at the laboratory to assess the amount of zooplankton species present in the different water columns. The organisms are morphologically identified using a Motic dissection microscope following the Woods Hole Oceanographic Institution (WHOI) zooplankton identification guide. Two 2ml aliquots will be taken from each sample and will be poured into a Bogorov chamber for

quantitative analysis. Species identification will be confirmed using DNA barcoding. DNA barcoding is the derivation of short DNA sequence(s) that enables species identification, recognition, and discovery in a particular domain of life. The primary purpose of DNA barcoding is to identify an unknown specimen in terms of known classification. Therefore, DNA barcoding will complement (but not supplant or invalidate) existing taxonomic practices [2]. DNA extractions will be conducted using the DNeasy spin column kit by QIAGEN© and polymerase chain reaction (PCR) products obtained will be tagged with primers that have broad taxonomic coverage.

To assess the salp diet in situ, salps will be subjected to a Peptide Nucleic Blocker (PNA) PCR. PNA is synthetic oligonucleotide that is specific to the *T. democratica* sequence and when it is used in a PCR reaction. The structure of the PNA is analog to the one of DNA, but instead of having a phosphodiester backbone it has a peptide back bone. The PNA has a stronger binding capacity than the DNA, hence the PNA would fail as genetic material because it is unable to separate easily like DNA (i.e. DNA is able to be separated and replicated). Therefore, the PNA works as an effective blocker because it inhibits the DNA polymerase from replicating. The difference in their backbone leads to two key properties: (1) DNA-PNA bond has a higher hydrothermal stability than DNA-DNA bond and, (2) It won't be digested by the exonuclease activity that is associated by the DNA polymerase activity because of the absence of the 5'-hydroxyl group. Essentially, the PNA blocks copies of the salp from being amplifying during the different cycles of the PCR, allowing the other DNA present to be amplified such as prey items. When the PNA-PCR is conducted, an exponential amplification will be obtained for the prey

DNA throughout the cycles whereas the salp PNA will not amplify.

In essence, by combining both field and molecular analysis we will identify the salp diet in situ matching metazoan prey present in the water column and salp gut content. We will obtain a profile and location of diverse zooplankton taxa present at the SAB.

References

- [1] Bone, Q. (1998). *The biology of pelagic tunicates*. Oxford University Press.
- [2] Bucklin, A., Steinke, D., & Blanco-Bercial, L. (2011). DNA barcoding of marine metazoa. *Annual Review of Marine Science*, 3, 471-508.
- [3] Deibel, D., & Paffenhöfer, G. A. (2009). Predictability of patches of neritic salps and doliolids (Tunicata, Thaliacea). *Journal of Plankton Research*, 31(12), 1571-1579.
- [4] Henschke, N., Everett, J. D., Baird, M. E., Taylor, M. D., & Suthers, I. M. (2011). Distribution of life-history stages of the salp *Thalia democratica* in shelf waters during a spring bloom. *Marine Ecology Progress Series*, 430, 49-62.

Acknowledgement

This project is supported and monitored by the National Science Foundation (NSF) (Award #'s 1459510 & 1459293) and the NOAA Living Marine Resources Science Cooperative Center (LMRCSC) award # NA11SEC4810002. Also, we would like to thank Dr. Indu Sharma from the Department of Biology and Dr. Luisel Rickssanti from the Cancer Research Center at Hampton University for their collaboration. Also, Kenya Bynes (undergraduate research assistant) and Lauren Lambole (graduate researcher) for their assistance in the field and laboratory.

Effect of benzo[α]pyrene exposure on clutch size and embryonic development of the daggerblade grass shrimp *Palaemonetes pugio*

Coral Thompson¹, and Sue C. Ebanks²

¹*Savannah State University, Marine Sciences Program, M.S. Candidate*

²*Savannah State University, Department of Marine and Environmental Sciences, Assistant Professor*

Corresponding Author:

Sue C. Ebanks

*Savannah State University
3219 College St., Box 20600
Savannah, GA 31404
ebankss@savannahstate.edu*

Abstract

The daggerblade grass shrimp *Palaemonetes pugio* inhabits estuaries along the East and Gulf coasts of the United States and is a link between trophic levels. Benzo[α]pyrene is a polycyclic aromatic hydrocarbon (PAH) and a component of crude oil. This and other PAHs enter estuaries by a variety of pathways and may have negative effects on the inhabitants, including grass shrimp. The purpose of this experiment was to determine the effect of benzo[α]pyrene on reproduction in the daggerblade grass shrimp *Palaemonetes pugio*. Male and female pairs were exposed to 0, 3, and 6 $\mu\text{g/L}$ of benzo[α]pyrene until the female became ovigerous. The female was then placed in clean seawater for 7 d. 10 of 45 female shrimp became ovigerous in each concentration. Overall, 3 of 11 embryonic stages were identified in this study. Average mortality increased with increased concentration: $1.1 \pm 1.92\%$, $2.2 \pm 3.85\%$, and $8.9 \pm 3.85\%$ at 0, 3, and 6 $\mu\text{g/L}$ of benzo[α]pyrene, respectively. Overall clutch size was largest in 0 $\mu\text{g/L}$ (139.5 ± 80.86 eggs/shrimp) and developmental rates were faster in 0 $\mu\text{g/L}$ with 63% of embryos developing to a late stage, VIIB. Future studies should include determining whether eggs are viable and if larval development is affected by short-term exposure to benzo[α]pyrene.

Introduction

Palaemonetes spp. are a large proportion of the resident members of the coastal marsh environment, are an important food source for numerous species including the mummichog *Fundulus heteroclitus*, heron, and red drum *Sciaenops ocellatus* [1, 2, 3], and have been studied for the possible effects of oil spills on marine organisms [4, 5] because they are bioindicators for potential toxins [6]. In 1968, benzo[α]pyrene, also known as 3,4 benzopyrene, was found to be

in crude oil ranging in amount from 450-1800 mg per ton of oil [7]. Heavyweight molecular PAHs were found in higher concentrations in mysids and euphausiids that come in contact with sediment than in a crab that does not often come in contact with sediment [8]. Rainbow trout eggs and alevins exposed to 0.08-0.21 $\mu\text{g/L}$ of BaP had chronic effects that included morphological abnormalities [9]. Invertebrates, such as the water flea *Daphnia pulex*, are sensitive to BaP exposure with 96-h LC_{50} of $5\mu\text{g/L}$ [9].

In this experiment, we investigated the lethal and sublethal effects of short-term exposure to benzo[α]pyrene on reproduction in adult daggerblade grass shrimp *Palaemonetes pugio*. We studied the ovigerity in the female grass shrimp after exposure to different concentrations of the toxicant. We also studied the development of embryos belonging to females exposed to benzo[α]pyrene to determine if there were sublethal effects on the offspring.

Experiments and Conclusions

Adult male and female daggerblade grass shrimp (>20 mm) *Palaemonetes pugio* were collected from Country Club Creek, Georgia during low tide using dip nets. The lengths of all females used in each trial were within 8 mm of each other. Five male and five female shrimp were placed in each tank. The shrimp pairs were separated into 3 tanks, all without sand: control (0 $\mu\text{g/L}$ BaP), low concentration (3 $\mu\text{g/L}$ BaP), and high concentration (6 $\mu\text{g/L}$ BaP). The females in each tank were allowed 3 wks to become ovigerous. Once a female was carrying eggs on her ventral surface, she was removed from the tank and placed in an individual container with clean seawater for 7 d. After 7 d, the eggs were removed using stainless steel forceps and counted to determine the clutch size. The eggs were examined under a dissecting microscope and the developmental stage was determined using Romney and Reiber [10].

The major findings of this experiment were that mortality rates were higher in shrimp exposed to benzo[α]pyrene and that eggs developed slower when exposed to benzo[α]pyrene. This could be due to the lethal and sublethal effects of the toxicant. In another study, there was an effect of caffeine and sulfamethoxazole on embryo development in the daggerblade grass shrimp [11]. Mortality was highest when shrimp were exposed to a mixture of chemicals [11].

In this experiment, a total of 8 shrimp died in the greatest concentration of 6 $\mu\text{g/L}$ and only 1 shrimp overall died in the lowest concentration (0 $\mu\text{g/L}$). While shrimp in all 3 concentrations had similar clutch sizes, a higher percentage of eggs were in the later stage in the lowest concentration of 0 $\mu\text{g/L}$. These findings indicate that benzo[α]pyrene may increase the time necessary for embryos to develop and hatch. It may also decrease the reproductive fitness of the adult grass shrimp by increasing mortality. Future studies should include determining the effect of benzo[α]pyrene exposure on hatch rates and viability of the larval hatchlings.

References

- [1] R.T. Kneib, *American Zoologist*. **26** (1986) 259.
- [2] W. Post, *Waterbirds*. **31** (2008) 179.
- [3] A.T. Humphries, M.K. La Peyre, G.A. Decossas, *PLoS ONE*. **6** (2011) 1.
- [4] A.F. Roth, D.M. Baltz, *Estuar. Coast*. **32** (2009) 565.
- [5] R.M. Moody, J. Cebrian, K.L. Heck, *PLoS ONE*. **8** (2013) e58376.
- [6] P.B. Key, E.F. Wirth, M.H. Fulton, *Environ. Bioindicators*. **1** (2006) 115.
- [7] M. Blumer, *Boston College Environ. Affairs Law Rev.* **1** (1971) 54.
- [8] P. Baumard, H. Budzinski, P. Garrigues, J.C. Sorbe, T. Burgeot, J. Bellocq, *Mar. Pollut. Bull.* **36** (1998) 951.
- [9] Canadian Council of Ministers of the Environment, *Can. Environ. Quality Guidelines*. **1299** (1999) 1.
- [10] A.L. Romney, C.L. Reiber, *Crustaceana*. **86** (2013) 16.
- [11] R.N. Garcia, K.W. Chung, M.E. DeLorenzo, M.C. Curran. *Environ. Toxicol. Chem.* **33** (2014) 2120.

Acknowledgement

This study was supported and monitored by National Oceanic and Atmospheric Administration (NOAA) under Grant – Living Marine Resources Cooperative Science Center Grant # NA06OAR4810163, National Science Foundation GK12 Ocean Literacy Program (DGE-0841372), and the

Department of Education Title VII Grant (P382G090003). The statements contained within the manuscript/research article are not the opinions of the funding agency or the U.S. government, but reflect the author’s opinions.

Population Ecology of Weakfish in the Maryland Coastal Bays

Shynna Dale, Rebecca Peters, and Paulins Chigbu

¹Alabama A&M University

²Department of Natural Sciences, University of Maryland Eastern Shore, Princess Anne, MD 21853

Abstract

Weakfish, *Cynoscion regalis*, is a marine fish of the drum family Sciaenidae. Weakfish are a common inshore species occurring between cape code, Massachutes, and southern Florida.. Spawning areas, then a return migration in the late fall to overwintering grounds (Nesbit1954). Weakfish availability to fisheries also fluctuates seasonally due to migratory nature of the species. Data was collected from 1990 to 2012 to assess the abundance of weakfish in the Maryland Coastal Bays by the Maryland Department of Natural Resources. This data will be analyzed to determine the annual and seasonal variations in abundance, biomass, and size of weakfish found in the Maryland Coastal Bays. The information provided from this study will help improve management plans for this commercially and recreationally harvested. Therefore, I propose to analyze this data set to provide insight on the annual and seasonal variations in abundance and biomass, distribution, size of weakfish, weakfish reproduction, and geographically specific characteristics.

Introduction:

According to Centers for Quantitative Fisheries Ecology, weakfish are a member of the Sciaenidae family. The Sciaenidae family includes the drums as well as sea trouts. To produce their distinctive sounds, Sciaenid's rapidly flex these sonic muscles against their swim bladder. Sciaenid sound reproduction may take two forms, drumming with the sonic muscles, and chattering with the pharyngeal jaws (Burkenroad 1931, fish and mowbray 1970). Weakfish can be found in Chesapeake Bay, which is home to an important population of weakfish. Weakfish is the state fish of Delaware bay in New Jersey, calls itself the " Weakfish Capital of the World". This is why information on this species is important to the Mid-Atlantic region.

The habitat ecology of the adult weakfish remains poorly understood, although they comprise an important ecological and economic portion of estuarine environments

(Turnure, Jason 2010). Sciaends reach sexually maturity very early in their lives, typically at just 10 percent of their potential life span. When the Sciaenids reach sexually maturity they have prodigious reproduction. They are usually found in shallow water along open sandy shores and in larger bays and estuaries, including salt marsh creeks. They can also be found up in a river mouths, but not in freshwater. Weakfish are called weakfish because of their weak mouths that can tear if you try to lift them into the boat without using a net (New York State Fishing Regulations 2015).

Juvenile weakfish represents significant component of the South Atlantic Shrimp trawl by catch (Vaughn et al. 1994). Juvenile weakfish also represent a significant component of the South Atlantic Shrimp trawl by catch (Vaughn et al. 1991). Juveniles recruit heavily to areas <20 ppt but occur throughout the estuary from June to October

(Paperno 1991). Weakfish are dark olive green above with back and sides burnished with purple, lavender, green, blue, gold or copper and marked with a large number of small black, dark green, or bronze spots. They feed on a wide variety of prey such as crabs, amphipods, mysid and decapod shrimps, squids, shelled mollusks and annelid worms (Blouch and Schneider 1807). The main predators of weakfish are older weakfish and bluecrab (Maurer and Bowman 1975).

Weakfish are an abundant finfish found within the Maryland Coastal Bays, however information on the seasonal variation in abundance and biomass is lacking. "Maryland Coastal Bays consist of the mainland and barrier islands. The coastal bay is important because it can be a lot of nursery for juvenile species that may be ecologically imperative. Certain species are protected by the various structures which serve as hiding areas," (Sexton 2015).

Materials and Methods

Data for the present studies were obtained from the Maryland Department of Natural Resources Trawl Surveys carried out annually from April to November between 1990 - 2012.. Samples were collected from 20 sites along the coastal Bays. The trawl samples were used for these studies. The dimensions for the trawl were given as 4.9m of semi balloon trawl with 3.18m of stretch mesh and cod end of 1.27 m of stretch mesh inner liner, (Bolinger et al. 2007).

Data Analysis

Catch per unit effort (CPUE) will be used as an index of abundance and will be estimated as
 Number of fish caught/ number of trawls per site

Data will be analyzed using simple Bar charts and line graphs to show mean seasonal and spatial differences in Weakfish abundance. Weakfish biomass will be estimated using the equation:

$$W = a * L^b$$

Where L is Total Length,

a and b are constants representing the slope and intercept in the regression relationship between Length and Weight estimates of *C. regalis* and will be obtained from the Fish base web site

Analysis of Variance (ANOVA) will be used to investigate statistical significant differences in abundance and biomass of the species. The relationship between fish abundance and environmental variables will be investigated using regression equation. The size structure of Atlantic menhaden over seasons and years will be determined using a histogram.

References:

- 1] Shepherd, Gary R., Nevi Brunswick, and Northeast Fisheries Center. "Reproduction of Weakfish, *Cynoscion regalis*, in the New York Bight and Evidence for Geographically Specific Life History Character; sti'cs." *Fishery Bulletin US* 82 (1984): 501-511.
- [2] SHEPHERD, GARY, and B. Grimes. "GEOGRAPHIC AND HISTORIC VARIATIONS IN GROWTH OF WEAKFISH, *CYNOSCIONREGAUS*, IN THE MIDDLE ATLANTIC BIGHT." *Fishery Bulletin* 81.4 (1983).
- [3] Turnure, Jason T. *Estuarine habitat ecology of adult weakfish (Cynoscion regalis): a multi-scale approach*. RUTGERS THE STATE UNIVERSITY OF NEW JERSEY-NEW BRUNSWICK, 2010.
- [4] Connaughton, Martin A., and Malcolm H. Taylor. "Seasonal and daily cycles in sound production associated with

- spawning in the weakfish, *Cynoscion regalis*." *Environmental Biology of Fishes* 42.3 (1995): 233-240.
- [5] Thorrold, Simon R., et al. "Accurate classification of juvenile weakfish *Cynoscion regalis* to estuarine nursery areas based on chemical signatures in otoliths." *Marine Ecology Progress Series* 173 (1998): 253-265.
- [6] Lankford Jr, T. E., and T. E. Targett. "Suitability of estuarine nursery zones for juvenile weakfish (*Cynoscion regalis*): effects of temperature and salinity on feeding, growth and survival." *Marine Biology* 119.4 (1994): 611-620.
- [7] Sexton, Margaret. "Maryland Coastal Bays lecture." Field trip.,. 6 June 2015. Lecture
- [8] "Weakfish." Weakfish. N.p., n.d. Web. 11 June 2015.
- [9] Bricker, Suzanne. Smdcoastal (n.d.): n. pag. [Http://ccma.nos.noaa.gov/stressors/pollution/eutrophication/eutrocards/smdcoastal.pdf](http://ccma.nos.noaa.gov/stressors/pollution/eutrophication/eutrocards/smdcoastal.pdf). Web.
- [10] "Weakfish *Cynoscion Regalis* (Bloch and Schneider) 1801." Weakfish. N.p., n.d. Web. 11 June 2015. N.p., n.d. Web.
- [11] Pincin, Jennifer. "Trends and Abundance Indices of Fishes in Maryland's Coastal Bays during 1972-2009." W31673 (n.d.): n. pag. Web. Vol. *Cynoscion Regalis to Estuarine Nursery Areas* (n.d.): n. pag. Web
- [12] "Florida Fish and Wildlife Conservation Commission." N.p., n.d. Web.

Analysis of Stranding Demographics, Inorganic Contaminants and Cytotoxicity in Bottlenose Dolphins (*Tursiops truncatus*) from Coastal Maryland

Audy Peoples¹, Cindy Driscoll², Amanda Wechsler², and Maurice Crawford¹

¹Department of Natural Sciences, University of Maryland Eastern Shore, Princess Anne, MD 21853 (email: ajpeoples@umes.edu)

²Maryland Department of Natural Resources, Fish & Wildlife Health Program, NOAA Cooperative Oxford Laboratory, Oxford, MD 21654

Introduction

Marine mammals face a variety of threats around the globe and the International Union for the Conservation of Nature (IUCN) has found that 25% of all marine mammal species are at risk of extinction [1]. Disease, environmental pollutants, anthropogenic interactions (e.g. fisheries bycatch and boat strikes) and climate change are some of the factors that threaten the viability of marine mammal populations. To better understand how these threats impact marine mammal populations, the Maryland Department of Natural Resources created the Stranding Response Program (MD DNR

Results and Conclusions

Since 1990, there have been a total of 442 marine mammals stranded in Maryland coastal waters and these strandings were composed of 26 different species. The bottlenose dolphin (*Tursiops truncatus*) was found to strand more frequently (n=188, 42.7%) than any other marine mammal followed by the harbor porpoise (*Phocoena phocoena*) (n=85, 19.2%). These data also revealed that most strandings occurred between March and September (n=366, 82.8%). In terms of the locations of the strandings, most (n=380, 86%) occurred on the Atlantic Coast of Maryland as opposed to the strandings (n=62, 14%) that were found in the Chesapeake Bay and its tributaries. The results also showed that for the bottlenose dolphin the sex ratio of stranded animals was

SRP) and this program has been collecting data on marine mammals stranded in Maryland. For this study we analyzed over twenty-five years of marine mammal stranding data to identify trends and determine factors that contribute to stranding. In addition, we measured contaminant loads of stranded animals and are currently conducting toxicity studies. These analyses will be useful in developing management strategies for marine mammal populations and help NOAA Fisheries meet its mandates under the Marine Mammal Protection Act.

skewed towards males ($X^2_{.05(1)} = 5.63, p = .02$).

Prior to 2013, there were never more than 30 animals stranded in a given year, however during the 2013 Unusual Mortality Event (UME), there was a record number of 81 marine mammal strandings; of which 72 were bottlenose dolphins. This UME ended in 2015 and its cause has been attributed to a morbillivirus virus.

Seventy-one out of a total of 442 strandings (16.1%) indicated some type of human interaction. Fifty-three or 74.6% of these human interactions involved fisheries, such as nets, lines, hooks or impression marks from nets and lines. The species most commonly associated with human interactions was the harbor porpoise, with 39.4% of total occurrences. The bottlenose dolphin accounted for 26.7% of human interaction

occurrences. Fifty percent of the cases noted with human interaction occurred in Worcester County, which includes some of the most popular tourist destinations in Maryland (e.g. Ocean City and Assateague Island).

We collected tissue samples from the carcasses and analyzed them for inorganic contaminants. In particular, for bottlenose dolphins, we found higher levels of mercury (Hg) in the livers (mean = 29.29 µg/g, n=37) than in the kidney (mean = 3.6 µg/g, n=32). Also three (8%) of the liver samples tested had concentrations of Hg above 100 µg/g. This is noteworthy because work by Wagemann and Muir [2] determined that Hg levels over 100 µg/g may cause hepatic damage. However, none of the three animals with such high levels showed any evidence of hepatic stress. We are currently using cytotoxicity tests to investigate this further and examine how selenium may to detoxify mercury in bottlenose dolphin tissues.

References

- [1] Davidson, A. D., A. G. Boyer, H. Kim, S. Pompa-Mansilla, M.J. Hamilton, D.P. Costa, and J. H. Brown, Proceedings of the National Academy of Sciences **109** (2012) 3395.
- [2] Wagemann, R. and D. Muir, Canadian Technical Report of Fisheries and Aquatic Sciences, **1279** (1984), 4.

Acknowledgement

This study was supported and monitored by National Oceanic and Atmospheric Administration (NOAA) under Grant – (Living Marine Resources Cooperative Science Center) Grant # NA11SEC4810002. Partial support was provided by National Science Foundation (Award # 1505261) to M. Crawford. The statements contained within the manuscript/research article are not the opinions of the funding agencies or the U.S. government, but reflect the authors' opinions.

The Use of Probiotics in Shrimp Production

Jasmine Smalls*, and Dr. Dennis McIntosh

*Delaware State University, Department of Agriculture and Natural Resources
1200 N. DuPont Hwy, Dover, DE 19901
Jsmalls2156@gmail.com*

Introduction

Shrimp production is a major food production and economic sector of the aquaculture industry worldwide. Before the introduction of probiotics, farmers used a wide range of chemicals to treat disease symptoms and to improve the production of shrimp, which led to various problems ranging from ecological disturbances to disease outbreaks (Lakshmi et al. 2013).

Currently, probiotics, which are generally defined as microorganisms that have beneficial effect on animals and humans, are being used as alternatives to antimicrobials. Further, probiotics are believed to enhance the immune system of shrimps (Rengpipat et al. 2000). Taking into account that shrimp production has only become a commercial industry fairly recently, starting in the 1970s (Boyd and Clay 1998), it is logical to conclude that this growth is in response to market demand for shrimp and other aquaculture species, which are relatively cheap and a plentiful source of protein (Lakshmi et al. 2013).

Growth and survival are two major factors that dictate shrimp aquaculture productivity (Immanuel et al. 2007); the application of probiotics can improve both (Wang et al. 2008). In essence, probiotics have become an alternative to antibiotics to help secure a healthier aquatic environment. Not only do probiotics have the ability to improve immune system function, they can improve water quality, enhance growth, prevent disease outbreaks, aid in reproduction, reduce stress, increase digestibility of feed, and boost

survival rates of aquatic species (Cruz et al. 2012).

Exposure to elevated or low temperatures can trigger the expression of Heat Shock Proteins (HSPs) in both aquatic species and plants (Rungrassameea et al. 2010; Anderson et al. 1994; Sabehat et al. 1998). HSPs are produced in the hepatopancreas as well as other tissues. A major role of HSPs is that they aid in the process of repairing denatured proteins resulting from stress (Tomanek 2010). As such, these proteins are an essential component of maintaining homeostasis within an organism and its environment (Qian et al. 2012). HSPs are grouped into functional families based on their molecular weight (Parsell and Lindquist 1993; Feder and Hofman 1999). The initial discovery and description of HSPs were made by Rungrassameea et al. (2010) from *Drosophila busckii* (Ritossa 1962), though HSPs have since been found in the cells of all other studied organisms from bacteria to humans.

Experiments and Conclusions

Because of these factors, we are looking at conducting two experiments. In the first experiment we will analyze the effect of three novel probiotics on growth and survival of post-larval white shrimp. Fifteen 2-L polycarbonate containers will be used for this experiment, with experimental containers divided into five treatment groups (three probiotics plus two controls). Each experimental container will be filled with 1-L conditioned seawater and maintained at 28°C. One hundred and fifty post-larval shrimp will be used for this experiment. Shrimp will be

divided into 15 groups of 25 PL and placed into the 2-L polycarbonate experimental containers in a random order.

The main objective of the second experiment is to determine if these novel probiotics effect the expression of heat shock proteins in juvenile shrimp after being exposed to environmental stress. Two hundred and forty juvenile shrimp (~0.7 g each) will be used for this experiment. Shrimp will be divided into 12 groups of 30 and randomly placed into the prepared 19-L experimental containers. Shrimp in the experimental containers will be sampled in two phases: exposure and recovery. During the exposure period, four shrimp from each treatment container will be sampled at four time points (0, 2, 4, and 6 hours of exposure).

Data sets from both experiments will be analyzed with SPSS (IBM Corp. IBM SPSS Statistics for Windows, Version 23. Armonk, NY). A one-way ANOVA will be used to test for differences among treatments in FCR, survival rates, and growth. A Repeated Measures ANOVA will be used to test water quality parameters and the differences among treatments in temperature. During the course of the first study, shrimp performance will be monitored by analyzing growth and survival rates, in which growth and survival rates will be used as a dependent variables and probiotics will be used an independent variable. During the course of the second study, the expression of HSPs will be monitored by analyzing the hepatopancreas when exposed to different temperature units, in which temperature will be used as dependent variables and probiotics will be used an independent variable. During the course of this study shrimp performance will be monitored by analyzing the expression of heat shock proteins, in which protein expression will be used as a dependent variables and probiotics along with temperatures will be used an independent variable.

References

- [1] J. V. Anderson, Q. B. Li, D. W. Haskell, & C. L. Guy, *Plant Physiology*. **104**(4), (1994) 1359-1370.
- [2] C. E. Boyd, & J. W. Clay, *Scientific American*. **278**(6), (1998) 58-65.
- [3] M. P. Cruz, , A. L. Ibáñez, O. A.M. Hermosillo, & H. C. Ramírez Saad, *ISRN microbiology*. 1-13, (2012).
- [4] M.E. Feder , G.E. Hofmann, *Annu. Rev. Physiol*. **61**, (1999) 243–282.
- [5] Immanuel, G., Citarasu, T., Sivaram, V., Babu, M. M., & Palavesam, A, *Aquaculture International*. **15**(2), (2007) 137-152.
- [6] B. Lakshmi, B.Viswanath, & D. V. R. Sai Gopal, *Journal of pathogens*. (2013) 1-13.
- [7] D. A. Parsell, & S. Lindquist, *Annual review of genetics*. **27**(1), (1993) 437-496.
- [8] Z. Qian, X. Liu, L.Wang, X. Wang, Y. Li, J. Xiang, & P. Wang, *Comparative Biochemistry and Physiology Part C: Toxicology & Pharmacology*. **156**(3), (2012) 211-220.
- [9] S. Rengpipat, S. Rukpratanporn, S. Piyatiratitivorakul, & P. Menasaveta, *Aquaculture*. **191**(4), (2000) 271-288.
- [10] F. Ritossa, *Experientia*. **18**(12), (1962) 571-573.
- [11] W. Rungrassamee, R. Leelatanawit, P. Jiravanichpaisal, S. Klinbunga, & N. Karoonuthaisiri, *Developmental & Comparative Immunology*. **34**(10), (2010) 1082-1089.
- [12] A. Sabehat, S. Lurie, & D. Weiss, *Plant Physiology*. **117**(2), (1998) 651-658.
- [13] L. Tomanek, *The Journal of experimental biology*. **213**(6), (2010) 971-979.
- [14] Y. B Wang, J. R. Li, & J. Lin, *Aquaculture*. **281**(1), (2008) 1-4.

Acknowledgements

This study was supported and monitored by National Oceanic and Atmospheric Administration (NOAA) and the Aquaculture Research and Demonstration Facility, under the Living Marine Resources Cooperative

Science Center (LMRSC) Award # NA11SEC4810002 The statements contained within the manuscript/research article are not the opinions of the funding agency or the U.S. government, but reflect the author's opinions.

The Effects of Hypoxia and Increased Temperature on the Behavior of Larval Estuarine Fish

Keith Leonard¹, Gulnihal Ozbay¹, and Stacy Smith¹

¹Department of Agriculture and Natural Resources, Delaware State University, 1200 N. DuPont Highway, Dover, DE 19901
keithleonar@gmail.com

Introduction

Mid-Atlantic estuaries, such as the Delaware and Chesapeake Bays, are very important and productive ecosystems that act as nursery habitat for many commercially and ecologically valuable species, such as weakfish (*Cynoscion regalis*), bay anchovy (*Anchoa mitchilla*), and menhaden (*Brevoortia tyrannus*) [1]. Despite their importance, many estuaries exhibit human induced eutrophication that often results in hypoxic (less than 3 mg/L O₂) or anoxic waters (less than 0.2 mg/L O₂)[2]. At less lethal levels of hypoxia, fish are subject to metabolic and physiological impairments such as higher ventilation rates, stunted growth, and lower reproductive success. Many fish species reduce activity and increase respiration in order to decrease their

oxygen use and increase absorption. They also suffer from impaired sensory and nervous function that may further inhibit normal movement and make them more vulnerable to hypoxia resistant predators [3,4].

The objective of this study was to determine changes in larval estuarine fish behavior when faced with a threatening stimulus by performing escape response tests on the fish after two-day hypoxia exposure. The escape response test determines how a fish reacts to a threatening stimulus by testing its predatory response reflex as well as its anxiety. This research will give us better insight on the acute effects of hypoxia on anxiety related behaviors of estuarine fish species.

Experiment and Conclusions

The test species used were one-day post hatch mummichog (*Fundulus heteroclitus*). To examine fish behavior when faced with a threatening stimulus, the larval mummichogs were raised under two different treatments for two days before testing their response behavior. Six 19L tanks each held 50 larval mummichog. Two dissolved oxygen (DO) levels, normoxic conditions (~6.5 mg/L DO) and hypoxic conditions (~2 mg/L DO) both at 27 °C, were run in triplicate. Temperature control was achieved through placing all six tanks in a water bath. Nitrogen gas (N₂) bubbled through the water at 20 mL/min displaced oxygen and simulated hypoxic conditions.

After two days, five mummichog from each tank underwent escape tests

utilizing a Zebracube device with camera-based tracking system. Each fish was allowed to acclimate to the test arena within the Zebracube (a 100mL beaker) for 2 minutes. A 440 Hz auditory stimulus sounded for 1 second. The Zebracube software recorded each fish's response by tracking movements using color-coded paths. The paths correlated to the speed the fish was traveling during the response. White paths correlated to a speed between 0-3 cm/sec; green correlated to speeds between 3-20 cm/sec, and red correlated to anything greater than 20 cm/sec. For this study, a red path indicated escape response behavior. The total lengths (mm) and dry weights were taken of all fish used in the study.

Using the Kruskal-Wallis test with a significance level of 0.05, there was no

statistical difference in escape response duration ($p=0.1524$) or distance ($p=0.3135$) between control and treatment. A one-way ANOVA with a significance level of 0.05 showed a significant difference ($p=0.0189$) between total lengths in hypoxia and normoxia, indicating signs of stunted larval growth. The data set collected for the dry weights was too small for statistical analysis. Although mummichog showed behavioral adaptability in hypoxic conditions, their growth rate showed signs of slowing and may indicate developmental impairment in early larval stages.

References

- [1] Able, K.W. 2005. A re-examination of fish estuarine dependence: evidence for connectivity between estuarine and ocean habitats. *Estuarine, Coastal and Shelf Science*, 64, 5-17.
- [2] Bricker, S. B., C. G. Clement, D. E. Pirhall, S. P. Orlando, and D. R. G. Farrow. 1999. National estuarine eutrophication assessment: A summary of conditions, historical trends, and future outlook. National Oceanic and Atmospheric Administration,

Silver Spring, Maryland.

- [3] Breitburg D.L, N. Steinberg, S. DuBeau, C. Cooksey, E.D. Houde.1994. Effects of low dissolved oxygen on predation on estuarine fish larvae. *Mar. Ecol. Prog. Ser.* 104, 235–246.
- [4] Shoji J, R. Masuda, Y. Yamashita, M.Tanaka. 2005. Effect of low dissolved oxygen concentrations on behavior and predation rates on red sea bream *Pagrus major* larvae by the jellyfish *Aurelia aurita* and by juvenile Spanish mackerel *Scomberomorus niphonius*. *Mar. Biol.* 147, 863–868.

Acknowledgement

This study was supported and monitored by National Oceanic and Atmospheric Administration (NOAA) under Grant Living Marine Resources Cooperative Science Center Grant # NA11SEC4810002. The statements contained within the manuscript/research article are not the opinions of the funding agency or the U.S. government, but reflect the author's opinions.

Investigating the Application of Multibeam Sonar and Remotely Operated Vehicles in Fish Population Monitoring on Artificial Reefs

R. Figueroa-Downing and David Hicks

The University of Texas Rio Grande Valley, School of Earth, Environmental, and Marine Science

Introduction

Multibeam sonar (MBS) and remotely operated vehicles (ROVs) have the potential to improve the accuracy and efficiency of fish population monitoring at artificial reefs. Current methods of monitoring fish populations and performing stock assessments on artificial reefs make a great deal of assumptions [1], are highly invasive, and are species-specific in their scope. Both multibeam sonar and ROVs provide a direct, non-invasive means of observing reef communities as a whole that could supplement, or even replace current methods.

MBS operates at high frequencies (usually around 900 kHz) and has a relatively wide field of view (up to 180 degrees). Due to the limitations of previous sonar systems, a great deal of research has been conducted relating the target strength of insonified fish species to their overall length for stock assessment. Yet, with the advent of more advanced systems, the direct measurement of fish length, and therefore biomass, is now possible.

MBS sonar currently faces the obstacle of fish species identification. Little research has been performed regarding the sonar characteristics of different species of fish. However, one recent study found that fish exhibit distinct swim bladder sizes and orientations based on species, and that these differences can be measured via sonar [2]. Such studies suggest that the development of a framework for identifying fish based on sonar images alone is possible.

The purpose of this study is to evaluate the applicability of ROVs and multibeam sonar in fish population monitoring at artificial reef sites. Specifically to 1) determine the accuracy of MBS estimates of fish size (biomass); and 2) determine if sonar characteristics can be used to differentiate fish species.

Experiments and Conclusions

Data was collected for this project at four artificial reef sites off the south Texas coast (Texas clipper PS-1122, South Padre Reef PS-1047, Port Isabel Reef PS-1169L, and Port Mansfield Liberty Ship Reef PS-1070). A Blueview P900-90 sonar unit was mounted onto a VideoRay PRO4 ROV to capture simultaneous video and MBS data. Fish lengths (cm) were estimated from MBS imagery using the Blueview Proviewer software and compared to standard lengths of corresponding fish captured on vertical long lines (VLLs) using linear regression. MBS data was collected from 10 different fish species for principal components analysis (PCA) including fish morphometrics (e.g., mean/max/min reflectivity, area, and perimeter) and MBS operational parameters (e.g., distance from transducer, position in the sonar field of view, and angle of orientation). Twenty MBS variables were ultimately extracted from the imagery using ImageJ software. A principal components analysis (PCA) was used to identify MBS variable combinations that may prove useful in distinguishing individual species.

Red Snapper (*Lutjanus campechanus*) caught on vertical long line were insonified in the water column, then subsequently measured directly. The positive linear relationship between insonified fish length and actual fish standard length was strong ($F = 541.9$, $df = 1, 6$, $P < 0.001$, $R^2 = 0.99$). Simultaneous MBS and video data was collected on 10 different species of reef dwelling fish: Almaco Jack (*Seriola rivoliana*), Atlantic Spadefish (*Chaetodipterus faber*), Barracuda (*Sphyraena barracuda*), Blue Runner (*Caranx crysos*), Crevalle Jack (*Caranx hippos*), Grey Snapper (*Lutjanus griseus*), Lookdown (*Selene vomer*), Red Snapper (*Lutjanus campechanus*), Sheepshead (*Archosargus probatocephalus*), and Grey Triggerfish (*Balistes capriscus*). The 3D PCA ordination of MBS output variables accounted for 75.7% of the variation, with the first factor primarily driven by fish sonar morphometrics (e.g., length of individual, area of highest reflectivity) and distance from the MBS unit explaining 33.3% of the variation, the second factor, driven by derived variable combinations (e.g., swim bladder area / fish length) explaining 29.3% of the variation, third factor primarily driven by angle of incidence explaining 13.1%. The ordination performed surprisingly well in separating the examined species. Amongst these species, Blue Runner showed the greatest similarity between individuals, while

Crevalle Jack, Red Snapper, and Triggerfish demonstrated the greatest variation. Sheepshead, Barracuda, and Lookdown demonstrated moderate similarity with a few outliers.

While the data shows some promise in differentiating fish species, we are still investigating other sonar characteristics in an effort to improve the effectiveness of this framework. We plan on including schooling metrics such as densities of schools and distances between individuals, as well as reflectivity of individuals near or on the reef itself.

References:

- [1] Maunder, M. N. & Piner, K. R. (2015). *ICES Journal of Marine Science* **72**, 7–18
- [2] Benoit-Bird, K. J., Au, W. W., Kelley, C. D. & Taylor, C. (2003). **50**, 221–229.

Acknowledgements

This study was supported and monitored by National Oceanic and Atmospheric Administration (NOAA) under Grant – Environmental Cooperative Science Center (ECSC) Grant # NA11SEC4810001. The statements contained within the manuscript/research article are not the opinions of the funding agency or the U.S. government, but reflect the author’s opinions.

Survival of red deepsea crab *Chaceon quinquedens* Smith, 1879, larvae in cultivation: effects of diet and temperature

Nivette M. Pérez-Pérez¹, Matthew Poach², Bradley Stevens³, Stacy Smith¹, and Gulnihal Ozbay¹

¹*Delaware State University, 1200 N. DuPont Highway, Dover, DE 19901, nivette2p@gmail.com*

²*NEFSC James J. Howard Marine Sciences Laboratory, 74 Magruder Road, Highlands, NJ 07732*

³*University of Maryland Eastern Shore, Maryland Route 822, Princess Anne, MD 21853*

Abstract

Decline in commercial crustacean species (lobsters, king crab, etc.) has caused an increased interest in the harvest of the red deepsea crab *Chaceon quinquedens*. But little is known about this species' general biology, especially conditions required for larval survival. Previous studies had provided conflicting information about their best cultured conditions. This study addressed the effects of combine temperature (9°C and 15°C), diet (rotifers, *Artemia sp.*, algae, and unfed), and cultured system treatments on larval survival. Females were obtained from commercial traps and transported to the NOAA James J. Howard Laboratory. First stage zoea was obtained from females' eggs that hatched in captivity. The flow-through system consisted of two temperature tanks containing 10 buckets each. Inside each bucket, three cylindrical containers with capacity for 10 larvae were held. The recirculating system had two temperature tanks, each containing 12 conical upwellers with capacity for 30 larvae. Larvae were fed and counted daily. Effects of temperature and diet were significant on larvae survival ($p < 0.0001$). Rotifer diet produced higher survival rates at both temperatures. Our finding on the optimal growth conditions of the species will facilitate further research to better understand the ecology, fishery, and impacts of climate variability in their life history.

Introduction

Red deepsea crab (RDSC), *Chaceon (Geryon) quinquedens* Smith 1879, is distributed throughout the continental shelf slope of the Northwest Atlantic Ocean, Gulf of Maine, and Gulf of Mexico. An increased interest in the commercial harvest of the RDSC has been stimulated by the decline in other highly targeted crustacean species (lobsters, king crab, etc.), since the late 1960s-70s [1,2]. The fishery for RDSC is covered by the federal Northeast Fishery Management Plan, but little is known about this species' general biology. Red deepsea crabs have a typical brachyuran life cycle. Larvae are hatched in spring/summer and occur in relatively shallow waters in

comparison with depths occupied by the adults [3]. During the larval development period, they may be more exposed to anthropogenic effects like increase temperatures in surface water or decreasing pH, contributors to climate change and ocean acidification [4].

There is an increased interest in this species as a potential sustainable fishery and aquaculture organism. However, previous research examined several aspects of the species larvae stages, but not to enhance aquaculture conditions, combine environmental factors, explore optimal larvae survival and developmental conditions, or provide detailed protocols for cultivation of the larvae in flow-through and recirculation

systems. Larvae stages were described after keeping them in temperatures between 18-21°C, which accelerated their development [5]. Also, in previous studies larval RDSC was reared at 12°C, 20°C, and 26°C determining that the coldest temperature contributed to developmental abnormalities; survival to first crab stage was best in the higher temperature, and both developmental stage and temperature affected survival [6]. In addition, comparisons made on different temperatures in juvenile crabs' development, 9-15°C resulted as the optimal temperature range for juvenile survival [7]. Larval survival of the red deepsea crab to metamorphosis on diets of rotifer or brine shrimp weren't different, but there was a delay in their development [8].

This study investigates the optimal conditions for peak survival and development of red deepsea crab (RDSC) larvae in a controlled laboratory setting. In the first year, larvae were kept at temperatures of 9°C and 15°C and fed three different diets (rotifers, *Artemia sp.*, and *T. iso*). In the second year, temperatures were 15°C and 20°C with three diets (rotifers, *Artemia sp.*, and combination of the last two). Both years used an additional unfed control group.

Experiments and Conclusions

The *Larvae Feeding System* designs allowed us to systematically contain the red deepsea crab larvae during the feeding experiments and also to measure the effects of diets and temperature, at the NOAA James J. Howard Marine Sciences Laboratory at Sandy Hook, New Jersey. Similar studies measuring the effects of diet and temperature on blue king crab *Paralithodes platypus* showed that larvae survival was significantly different between the diets and temperature and that the time required for development through larvae stages was different [9].

The first year of experiment a *Flow-through Larvae Feeding System* design was

used. The system inflowed 12L/5.1 hrs of UV-filtered seawater (salinity 27‰), directly from the main seawater supply of the building (Sandy Hook Bay, NJ) and distributed it to the experimental buckets. Two separate tanks served as water baths with chillers that kept temperatures at 9°C ± 1°C and 15°C ± 1°C. Each tank contained 10 experimental buckets. Within each bucket 3 smaller containers (750 ml each) held 10 living red deepsea crab larvae. These containers were designed to allow the flow of diets through it, but holding the larvae inside them. Each water bath contained 2 buckets per diet (randomly assigned), for a total of 60 larvae per diet treatment (unfed, rotifers, *Artemia sp.*, and *T. iso*) by each tank. The room for the system was maintained with a light cycle of 12:12 hrs.

During the second year of experiment a *Recirculating Larvae Feeding System* was designed. In this system, two individual temperature tanks with chillers at 15°C ± 1°C and 20°C ± 1°C (water bath), contained 12 custom upwellers each. New temperatures were selected based on the previous information of rapid larvae and juvenile growth [6, 7]. The recirculation system pumped UV-filtered seawater (30‰) from a biofilter water reservoir into the upwellers. Within each upweller a fitted cone mesh with capacity to hold 20 living RDSC larvae, allowed easy access to observe and count the larvae. Each temperature tank contained 3 upwellers per diet (randomly assigned) for a total of 60 larvae per diet (unfed, rotifers, *Artemia sp.*, and combination of the last two). The room for the system was also maintained with a light cycle of 12:12 hrs. To determine the best protocol and condition for optimal larvae survival and development, culture densities, temperatures, feeding, cleaning actions, and concentrations of diets fed to larvae were recorded for both systems daily.

First-year experiments showed that the effects of temperature and diet were

statistically significant on larvae survival ($p < 0.0001$). Larvae raised at 15°C exhibited faster development but lower survival through time than those held at 9°C. Furthermore, the rotifer diet produced higher survival and development rates at both temperatures. It was confirmed that crab larvae weren't feeding on algae and *Artemia* sp. nauplii used were too big for the first stage zoea to consume.

Developing standard operating procedures would facilitate aquaculture operations and development of a sustainable fishery, also providing healthy cultures to conduct experiments on environmental effects. It addresses a complete understanding of the developmental and larval biology of the red deepsea crab *C. quinquedens* and the effects of temperature, salinity, pH, and diets on the early life history. Furthermore, the study parameters and protocols will open new lines of investigation with this species including those of aquaculture and the effects of environmental changes (climate change, ocean acidification).

References

- [1] W. C. Schroeder, Cont. WHOI **947** (1958) 266-282.
- [2] R. L. Wigley, R. B. Theroux, H. E. Murray, Mar. Fish. Rev. 1154 **37** (8) (1975) 1.
- [3] F. W. Steimle, C. A. Zetlin, S. Chang, U.S. Dept. Commerce NMFS-NE-163 (2001) 27.
- [4] P. M. Biesiot, H.M. Perry, J. Mar. Biol. **124** (1995) 407.
- [5] H. C. Perkins, Fish. Bull. **71** (1) (1973) 69.
- [6] M. C. Rosowski, UD-M.S. Thesis (1979) 81.
- [7] W. Van Heukelem, M. C. Christman, C. E. Epifanio, S. D. Sulkin, Fish. Bull. **81** (1983) 903.
- [8] S. D. Sulkin, W. F. van Heukelem, Mar. Ecol. Prog. Ser. **2** (1980) 91.
- [9] B. G. Stevens, K. M. Swiney, L. Buck, J. Shellfish Res. **27** (5) (2008) 1255.

Acknowledgement

This study was supported and monitored by National Oceanic and Atmospheric Administration (NOAA) under Living Marine Resources Cooperative Science Center (LMRCSC) Grant # NA11SEC4810002 and the NOAA EPP/MSI Graduate Research and Training Scholarship Program (GRTSP). The statements contained within the manuscript/research article are not the opinions of the funding agency or the U.S. government, but reflect the author's opinions.

Condos and Connectivity: Developing an Interdisciplinary Approach to Guide Caribbean Spiny Lobster (*Panulirus argus*) Fisheries Management within The Bahamas

K. Callwood

University of Miami-RSMAS, Abess Center for Ecosystem Science and Policy

Introduction

In recent years, The Bahamian spiny lobster (*Panulirus argus*) fishery has seen an increase in the use of condos (AKA casitas), artificial habitats used to aggregate lobsters in large numbers for easy capture. Condos have effectively created additional spiny lobster habitat, where the structures tend to be placed in locations with sandy or grassy bottoms instead of near reefs, the ecological habitat of choice for adults. While the use of condos has increased greatly throughout the Caribbean, the ecological, social, and management implications of their use have not been fully evaluated. Few studies have assessed the role of condos on dispersal characteristics [1] or how these characteristics might influence management of the fishery and vice-versa [2,3]. Additionally, to date, none of these studies have incorporated anthropological methods to determine how condo use might impact dispersal and ultimately spiny lobster fishery management.

With these factors in mind, there is a need to not only determine natural patterns of connectivity, but to learn how to sustain them while also protecting the population, especially in the face of changing perspectives and fishing strategies, such as condos. As the construction and addition of these structures continue to occur, so, too, do the questions and concerns about their impacts on the species and the fishery, and what those impacts mean for sustainable management. Moreover, development of management strategies to ensure sustainability of an entire, and potentially Caribbean-wide ecosystem, will be difficult without utilizing interdisciplinary

approaches. Coupling spatially explicit biophysical models with additional tools, such as anthropological research and social science methods, can aid in the assessment of spiny lobster fisheries, allowing for management decisions based on a range of factors (ecological, social, economic, etc.) that result in the design of appropriate, more holistic, strategies.

The purpose of this study is to examine the sustainability of the Bahamian spiny lobster fishery based on the dispersal characteristics of Caribbean spiny lobster. Emphasis is placed on modeling lobster connectivity to predict the spatial scales over which the lobster travel within, and beyond, The Bahamas, and then coupling the connectivity results with anthropological data gathered from Bahamian fishers. This pairing of data allowed for the examination of how these two methodologies can be used to predict locations that might either help to optimize condo placement or identify those locations requiring additional management considerations.

Experiments and Conclusions

The Connectivity Modeling System [4], an open-source coupled biophysical model of Lagrangian transport, was used to simulate the probabilistic connections between spiny lobster populations around the Caribbean. In these simulations, appropriate habitat for both spawning and settlement was contained within 3202 sites at coral reef locations throughout the Caribbean, with 848 of the habitat polygons located in The Bahamas. During interviews conducted over the course of 3 summers, fishers identified 44.7% of these polygons (n=379) as locations where

they have either placed or fished from condos. Survey responses to the question, “Where in The Bahamas is the best place to catch lobster”, returned a variety of answers; these responses were coupled with the locations identified on the habitat map to delineate 5 main areas of condo placement and use within The Bahamas: the Little Bahama Bank (LBB), the Berry Islands and North of Andros (BI), the Tongue of the Ocean (TOTO), the Great Bahama Bank (GBB), and the Jumentos and Ragged Island Chain (JRI).

The connectivity simulations indicate larval exchange does occur between populations in The Bahamas with other Caribbean spiny lobster populations. Although the dispersal kernel (DK) is narrow, at only 200-400 km, with a 25% probability of successful settlement, many particles successfully traveled longer distances, at times reaching beyond 4500 km. This allowed for many of these connections to cross international lines. Despite this, The Bahamas does tend to retain most of its larval exports, suggesting that lobster spawned within The Bahamas settle and thrive there as well. Examining the probabilistic imports and exports for the main areas of condo placement highlights their connections to other local areas within The Bahamas, as well as to populations elsewhere in the Caribbean. These areas also exhibit high levels of domestic connectivity for the region, with each site demonstrating greater rates of recruit survival, with the exception of the GBB area. This data suggests these areas have some importance for maintaining the populations supporting the Bahamian spiny lobster fishery.

Simulations revealed that GBB and BI support habitats with high levels of betweenness centrality, suggesting these locations may have importance for securing connections between the populations within The Bahamas and across the entire Caribbean

network. As such, it may be best to limit habitats in these areas to intense fishing, as this may impact how individuals in the population move throughout the network. However, this is complicated by the presence of high quantities of condos in these locations, as 100% and 61% of the habitat polygons in the BI and GBB, respectively, are also preferred condo placement areas. On the other hand, LBB and BI have the most habitats with large quantities of diverse connections. The high number of unique incoming connections to these areas indicates these populations can be subsidized by others from various locales, ensuring a level of maintenance for the population and also potentially the sustainability of fishing operations within these areas. As such, these areas should have lower priorities for closure. While a large percentage of the LBB habitats (68%) are already condo sites, there may be additional habitats here that can possibly accommodate condos, especially if condo placement is limited in other highly popular areas. TOTO was the one area displaying relatively high levels of self-recruitment, with 29% of its habitats demonstrating a probability for self-recruitment of 0.01 to 0.12, compared to the 4-7% of habitats in the other 4 areas displaying a self-recruitment probability greater than .01. A closer examination of the larval exchange occurring between TOTO and the rest of the network reveals strong connectivity with other Bahamas sites, but relatively low connectivity with other Caribbean habitats. This is supported by TOTO's DK, which is narrower than the DK's for the rest of the Bahamas, and has the highest probability of successful recruits (36%). These characteristics aid in further substantiating the notion that TOTO may be a self-sustaining system essential to the success of the Bahamian spiny lobster population.

The differences in connectivity between these various areas suggest each location be

evaluated individually to determine spatially-dependent management actions, and to effectively develop and implement condo-related policies that will be supported by local communities. This work confirms that the resolution of connectivity has important implications when trying to gain a fundamental understanding of the structure and dynamics of these populations or when trying to determine the appropriate scales at which to implement management strategies [5]. If larvae are mostly retained at local scales, as may be the case for Bahamian spiny lobster populations, then local management alone can be effective; yet, if larvae disperse beyond those scales, as is also the case for Bahamian spiny lobster populations, management will need to scale up appropriately to be effective. This is one of the fundamental issues that continues to plague connectivity research, especially for species like lobster with long pelagic larval dispersals.

Ecosystem based management will be key to managing for connectivity within The Bahamas, where multiple factors are in play. Through the identification of the functional factors within ecosystems, including humans, managers can begin to assess how best to maintain the connections between all the

possible networks. Understanding how all these factors intersect is imperative; this work demonstrates that creating links between various methodologies may serve as one strategy to help achieve this. Additionally, mapping connectivity patterns will assist with the identification of key management priorities and partnerships that can be created between managers and local fishers, and between The Bahamas and other countries.

References

- [1] D. Eggleston, R. Lipscius, Proceedings of the 45th GCFI (1999) 842.
- [2] K. Ley-Cooper, S. De Lestang, B. Phillips, E. Lozano-Alvarez, *Fisheries Manag Ecol* **21** (2014) 264
- [3] O. Gonzalez, I. Wehrtmann, *Lat Am J Aquat Res* **39** (2011) 575.
- [4] C. Paris, J. Helgers, E. van Sebille, A. Srinivasan, *Environ Modell Softw* **42** (2013) 47.
- [5] P. Sale, H. Van Lavieren, M. Ablan Lagman, J. Atema, M. Butler IV, C. Fauvelot, J. Hogan, G. Jones, K. Lindeman, C. Paris, R. Steneck, H. Stewart. *Preserving Reef Connectivity: A Handbook for Marine Protected Area Managers* (2010)

Water Quality Monitoring and Validation from NOAA operational satellite sensor (VIIRS) Data Products in Coral Reef Environments.

William J. Hernandez^{1,2}, Roy A. Armstrong¹, Alan E. Strong, Robert A. Warner⁵, Erick F. Geiger^{2,4}, C. Mark Eakin⁴, Menghua Wang⁴, Maria A. Cardona-Maldonado³, Suhey Ortiz-Rosa¹, Jeremy Kravitz⁶, Myrna J. Santiago³.

¹NOAA-CREST UPR Mayaguez, ²Global Science and Technology Inc., ³NOAA-NCAS UPR Mayaguez, ⁴NOAA/NESDIS/STAR, ⁵NOAA/NOS/NCCOS, ⁶UPR Mayaguez.

*Presenter: William J. Hernandez, william.hernandez@upr.edu

Abstract

Long-term monitoring of water optical properties is required to examine the impact of land-based sources of pollution (LBSP) on coral community structure. A NOAA multi-line office collaboration with CREST-UPRM was established to conduct effective environmental monitoring and develop ecosystem management tools in the Guánica and La Parguera area. NOAA/NESDIS/STAR/CRW products in this effort included the diffuse attenuation coefficient at 490 nm ($K_d[490]$, an index of turbidity) and chlorophyll-*a* (Chl-*a*) estimates derived from the Visible Infrared Imaging Radiometer Suite (VIIRS), combined with regular field campaigns to measure *in situ* $K_d(490)$ values using a Satlantic Hyper-spectral Profiler and surface water collections for chlorophyll *a* extractions. This *in situ* data is essential for satellite products' calibration, validation and algorithm development in near-shore environments. This poster will present preliminary results of these ocean color tools for water quality and the relevant steps to maximize their benefit to coral reef management.

Introduction

LBSP are a major threat to corals that can cause disease and mortality, disrupt critical ecological reef functions, and impede growth, reproduction, and larval settlement. In Puerto Rico, increased sediment loads from watersheds have been linked to degradation of coral reefs due to reduced water quality [1, 2]. The Guánica/Río Loco watershed has been identified by the US Coral Reef Task Force Watershed Partnership Initiative (USCRTF-WPI) as a priority site for the implementation of activities aimed at the reduction of land-based sources of pollution for the protection of the watershed and particularly the coral reef ecosystems [3]. The coral reefs of Guánica have been described as sites with "exceptional vulnerability" to river discharge, industry, sediments resuspension, agriculture and dredging [4].

To establish effective environmental monitoring and ecosystem management tools, a NOAA multi-line collaboration led by NESDIS/STAR/CRW, Educational Partnership Program with CREST-UPRM, and NOS/NCCOS, is developing a suite of coastal ocean color satellite products for watershed managers to monitor runoff from high precipitation events in near real-time. Evaluating the impact of light, temperature and water quality following heavy precipitation events and how these relate to the health of coastal reef communities are the main focus of these efforts. Long term monitoring of water optical properties, temperature and physiological responses to different stressors are required to examine the impact of LBSP on coral reef community structure, diversity, and health.

Experiments and Conclusions

A long-term field sampling is being conducted with simultaneous retrievals of satellite data to evaluate the spatial and temporal variability of inherent and apparent optical properties and water quality parameters at eleven stations in Guanica Bay and La Parguera, southwestern Puerto Rico. The data collected includes profiles of spectral downwelling irradiance and upwelling radiance are obtained using a Satlantic HyperPro profiler equipped with two MicroPro submersible hyperspectral radiometers that provide 148 channels (from 350 to 800 nm). These measurements from the Satlantic are important for deriving the attenuation coefficients of downwelling irradiance (K_d) and the water-leaving radiance (L_w) for validation and calibration of satellite-derived ocean color products. Water-leaving radiance and the above-surface downwelling irradiance were measured using a GER 1500 spectroradiometer to calculate the remote sensing reflectance (R_{rs}). A Hydrosat-6 backscattering sensor is used to obtain the backscattering coefficient (b_b) at six wavelengths. The optical measurements were compared and calibrated with water samples measurements of total suspended solids (TSS), chlorophyll, and colored dissolve organic matter (CDOM) collected at each site. This *in situ* data is essential for satellite products' calibration and validation and algorithm development in near-shore environments. The *in situ* $K_d(490)$ were correlated with VIIRS $K_d(490)$ ($r^2=0.6$) to evaluate sensor performance in coastal environments. Additionally, monthly mean anomalies and seasonal trends were evaluated with local precipitation values for

both Puerto Rico and the USVI region, and the Guánica and La Parguera Virtual Areas (VA's). This VIIRS product time-series analysis will provide information on the spatial and temporal trends in the Guánica and Guánica/La Parguera areas. The VIIRS Chl-*a* values will also be compared with concurrent *in situ* bio-optical and biochemical measurements to evaluate satellite sensor product performance in the VA's. The analyzed data will be made available to local government agencies, watershed coordinators and NGO's that require this information through a web-based mapping application.

References

- [1] J.L. Torres, J. Morelock. Carib. J. Sci. **38**(2002): 222.
- [2] M.C Larsen, R.M.T. Webb. J. Coastal Res. **25**(2009): 189.
- [3] J.F. Carriger, W.S. Fisher, T.B. Stockton, P.E. Sturm. Coastal. Manag. **41**(2013): 19.
- [4] A.G. Warne, R.M.T. Webb, M.C. Larsen. U.S. Geological Survey Scientific Investigations Report (2005).

Acknowledgements

This study was supported and monitored by National Oceanic and Atmospheric Administration (NOAA) under Grants – NOAA EPP/MSI Grant # NA11SEC4810004 for NOAA CREST and Grant # NA11SEC4810003 for NOAA NCAS Center. The statements contained within the manuscript/research article are not the opinions of the funding agency or the U.S. government, but reflect the author's opinions.

Pharmaceuticals and Personal Care Products: Local, National, and Global Challenges

Zakiya Hoyett^{1,*}, Marcia Allen Owens¹, Clayton Clark II², Michael Abazinge¹

¹ *School of the Environment, Florida Agricultural and Mechanical University, 1515 Martin Luther King, Jr. Blvd., FSH – Science Research Center, Tallahassee, FL 32304, USA*

² *Department of Civil and Environmental Engineering, Florida Agricultural and Mechanical University – Florida State University College of Engineering, 2525 Pottsdamer Street, Tallahassee, FL 32310, USA*

* Presenting and corresponding author: *Email address:* Zakiya.Hoyett@famou.edu

Abstract

The occurrence of pharmaceuticals and personal care products (PPCPs) in sewage treatment plant effluents, surface waters, seawaters, ground water, and some drinking waters has led to an increasing concern about the impact of these chemicals on the aquatic environment. This has also resulted in the evolution of environmental risk assessment (ERA) strategies for such compounds over the past decade and although regulations are in effect or planned in several developed countries, there is no global standard for conducting ERAs. The overall purpose of this research was to execute a reconnaissance survey for PPCPs in two unlike bays on the gulf coast of Florida using a modified version of EPA Method 1694, a widely accepted ex-situ detection method for these contaminants. The statuses of these contaminants were observed at a presumably pristine site, Apalachicola Bay, and a significantly degraded site, Tampa Bay. Sulfamethoxazole (SMZ), a common sulfonamide used as an antibiotic in animals and humans, exists in both bays in concentrations ranging from 3.4 – 8.9 ng/L. Carbamazepine (CBZ), an anticonvulsant and mood-stabilizing drug, was discovered in Tampa Bay only at a concentration of 7.4 ng/L. Additionally, a review of ERA guidelines for PPCPs developed by the United States Food and Drug Administration (US FDA), European Union European Medicines Evaluation Agency (EU EMEA), and Japan are presented. The methods of each protocol are compared and contrasted, thereby highlighting the strengths and weaknesses of each approach.

Introduction

Pharmaceuticals and personal care products (PPCPs) are among a group of chemicals termed “contaminants of emerging concern” (CECs). CECs are not necessarily new pollutants as they may have been present in the environment for several years, but their presence and significance are only now being evaluated [1]. Due to their medical properties, PPCPs have an inherent biological effect; furthermore, they behave as persistent pollutants because of their continual infusion into the aquatic ecosystem [2-4]. Such

pollutants may have potentially devastating effects on the aquatic environment, more specifically, in coastal and marine ecosystems. With the increased concern of potential threats triggered by the occurrence of pharmaceuticals and personal care products (PPCPs) in the environment, environmental risk assessment (ERA) strategies for such compounds have considerably evolved over the past decade. Regulations are in effect or planned in several developed countries, however, there

is no global standard for conducting ERAs [5-7].

The overall purpose of this research was to execute a reconnaissance survey for PPCPs in two different bays on the gulf coast of Florida using a modified version of EPA Method 1694, a widely accepted ex-situ detection method for these contaminants. The statuses of these contaminants were observed at a presumably pristine site, Apalachicola Bay, and a significantly degraded site, Tampa Bay. Additionally, risk assessment procedures for PPCPs employed by the United States Food and Drug Administration (US FDA), European Union European Medicines Evaluation Agency (EU EMEA), and Japan were compared, addressing the similarities and distinctions of the three approaches. In order to further highlight the variations between the three ERAs, the protocols were carried out using actual environmental concentrations of sulfamethoxazole (SMZ), a common sulfonamide used as an antibiotic in animals and humans, in selected US bays.

Experiments and Conclusions

The sites investigated for this baseline survey were Apalachicola Bay, a presumably pristine site located along the pan-handle of Florida, and Tampa Bay, a significantly degraded Florida estuary along the Gulf of Mexico. Five sampling sites were chosen in each bay as an attempt to characterize the water and/or sediment represented throughout the entire bay area. Following sampling methods suggested by EPA Method 1694, duplicate samples for this study were collected at a depth of approximately one to two meters in early December of 2011, during the high river flow season in Florida. Liter aliquots of water samples were extracted using solid-phase extraction (SPE) procedures with hydrophilic lipophilic balanced (HLB) extraction disks then

analyzed using liquid chromatography tandem mass spectrometry (LC-MS/MS).

Sulfamethoxazole (SMZ), a common sulfonamide used as an antibiotic in animals and humans, was found in both bays in concentrations ranging from 3.4 – 8.9 ng/L and carbamazepine (CBZ), an anticonvulsant and mood-stabilizing drug, was discovered in Tampa Bay only at a concentration of 7.4 ng/L. The occurrence of PPCPs varies across regions and coastlines due to diverse sources and distinct water transport and circulation, however, finding a substance with such significant potential impacts in a presumably pristine bay could have a devastating effect in the future on the health of the bay system [8]. As the scope of the problem evolves, innovative research is essential to increase the available data on these contaminants and their occurrence in the environment. Furthermore, there is a definite need for a finely honed ERA procedure that will ensure more effective regional, national, and global regulation of these PPCPs.

References

- [1] Daughton CG. (2001).
- [2] Harada A, Komori K, Nakada N, Kitamura K, Suzuki Y. *Wate. Scie. Tech.* **58** (2008) 1541.
- [3] Ferrari B, Mons R, Vollat B, Fraysse B, Paxéaus N, Giudice RL, Pollio A, Garric J. *Envi. Toxi. Chem.* **23** (2004) 1344.
- [4] Van der Oost R, Beyer J, Vermeulen NPE. *Envi. Toxi. Phar.* **13** (2003) 57.
- [5] European Agency for the Evaluation of Medicinal Products. CPMP/SWP/4447?00 draft corr. Available from <http://www.emea.eu.int/pdfs/human/swp/444700en.pdf>. (2003).
- [6] United States Food and Drug Administration. CMC6, July, Revision 1. Office of Training and Communications. Rockville, MD. (1998).

- [7] Yamashita N, Yasojima M, Nakada N, Miyajima K, Komori K, Suzuki Y, Tanaka H. *Wate. Scie. Tech.* **53** (2006) 65.
- [8] Singh S.P., Azua A., Chaudhary A., Khan S., Willett K.L., Gardinali P.R. *Ecot.* **19** (2010) 338.

Administration (NOAA) under the Environmental Cooperative Science Center at Florida Agricultural and Mechanical University – Grant # NA11SEC4810001. The statements contained within the manuscript/research article are not the opinions of the funding agency or the U.S. government, but reflect the author’s opinions.

Acknowledgement

This study was supported and monitored by National Oceanic and Atmospheric

Protocol Development for Environmental Stressors on Reproduction and Larval Development in the Daggerblade Grass Shrimp *Palaemonetes pugio*

Vanessa Foster¹, Coral Thompson², and Sue C. Ebanks³

¹*Savannah State University, Marine Sciences Program, Undergraduate Student*

²*Savannah State University, Marine Sciences Program, M.S. Candidate*

³*Savannah State University, Department of Marine and Environmental Sciences, Assistant Professor*

Corresponding Author:

Sue C. Ebanks

*Savannah State University
3219 College St., Box 20600
Savannah, GA 31404
ebankss@savannahstate.edu*

Abstract

Daggerblade grass shrimp *Palaemonetes pugio* are small semi-transparent shrimp, typically found in brackish water estuaries on the East & Gulf coasts of the United States, including waterways in Savannah, GA. Reproduction in *P. pugio* occurs March-October, with females producing multiple broods. Once a female becomes gravid, the ovary is dark and more clearly seen. Eggs then drop to the shrimp pleopods (shrimp status: ovigerous) and remain there until hatching. Objectives of this project were to determine the effects of different field-collected sediments on ovigerous shrimp behavior, embryo development and hatching, and characteristics of newly hatched shrimp. All shrimp and water were from Country Club Creek. Sediments were collected from 3 diverse sites in 2 estuaries: Tom Thumb (TT; Wassaw Sound), Country Club Creek (CCC; Wassaw Sound), and Moon River (MR; Ossabaw Sound). Males and gravid females were placed in a holding tank with appropriate site sediment. Once control females became ovigerous, they were placed in individual chambers containing CCC sediment but treatment females were placed in individual chambers with sediment from MR or TT. Data from these experiments will help establish a protocol for bioassays to test the effects of environmental stressors on *P. pugio* reproduction.

Introduction

Daggerblade grass shrimp *Palaemonetes pugio* are small semi-transparent shrimp, and are year-round inhabitants of brackish marsh and seagrass ecosystems. The life span of the daggerblade grass shrimp is approximately 6-13 months with the juveniles reaching maturity after about two months [1]. Their spawning season spans from February until October [1]. Before spawning, the ovary of the female darkens as it becomes full of

unfertilized eggs and is easily visible. Then the female molts, making her receptive to males. Copulation must occur within 7 hours of molting, and after sperm transfer is complete, the fertilized eggs are repositioned and adhere to the ventral surface of the abdomen [1]. The eggs hatch approximately 12 to 60 days after being fertilized and the females can produce multiple broods [1]. This species of grass shrimp is also host to many parasites, including coccidia [2], microsporidians [3], trematodes [4], isopods

[5], and leeches [6]. The most common parasite observed amongst *P. pugio* in the southeast region is the trematode. Despite the prevalence of multiple parasites, they do not appear to negatively impact growth or abundance of *P. pugio* [1]. The purpose of this study was to observe the differences in behavior and embryonic development in ovigerous females exposed to sediments from different sites.

Experiments and Conclusions

Each site is exposed to various degrees of pollution including residential and commercial runoff, which has the capacity to alter the concentration of contaminants in the sediment. To better understand the effect the different sediments have on the organisms that inhabit the location grass shrimp were collected from a control location and placed in tanks with sediment from the different sites in order to observe any differences in behavior and reproductive cycle. Highly infected shrimp (>30 trematodes) were excluded from the experiment to avoid any negative effects on individual behavior such as lethargy, decreased motility, and lack of stamina [7]. Male and gravid female grass shrimp were collected from Country Club Creek, Georgia (32.020498°N, 81.057584°W) using dip nets. The length, weight, and number of trematodes were determined and recorded before shrimp were placed in tanks with sediment from Moon River (31.951214°N, 81.081649°W), Tom Thumb (32.031860°N, 81.014607°W) or Country Club Creek. Five gravid females and five males were placed in each 2.6-L tank. Once the female became ovigerous, the length, weight, and number of trematodes were recorded once more before it was placed in an individual 500-mL chamber with sediment from the same site. Once in the chamber, the female was observed daily for common behaviors (swimming, walking, resting, fanning, and sifting sediments) and the presence/absence

of eggs. Once the female released the eggs, the length and weight were recorded for a final time, which marked the end of the experiment.

For the first trial, the only female to become ovigerous was from the tank containing Moon River sediment but died at day 9, before hatching occurred. In the second trial, 4 females became ovigerous; 2 from the Moon River sediment tank, 1 from the Tom Thumb sediment tank and 1 from the Country Club Creek sediment tank. Of those 4 ovigerous females, the 2 from the Moon River sediment tank released its clutch of eggs 12 days after becoming ovigerous, whereas the two other females released their clutch in 13 days. Based on land use information and sediment analysis of polycyclic aromatic hydrocarbon concentration, we anticipate a correlation between the degree of site-specific human-impact and rates of ovigerity and hatching, with longer times for shrimp to become ovigerous and longer embryonic periods for shrimp exposed to sediments from contaminated sites.

References

- [1] G. Anderson, U.S.A.C.E. Biol. Rep. **82**(1985) 1-30.
- [2] M. Solangi, R. Overstreet, J Parasitol**66**(1980) 513-526.
- [3] R. Overstreet, E. Weidner, Z. Parasitenk**44** (1974) 169-186.
- [4] R. Heard and R. Overstreet, Proc. Helminthol. Soc. Wash. **50** (1983) 170-174.
- [5] G. Anderson, Mar. Biol.**42**(1977) 239-251.
- [6] R. Overstreet, MASGP **78** (1978) 40-45.
- [7] A. Kunz, J Parasitol. **90**(2004) 441-445.

Acknowledgement

This study was supported and monitored by National Oceanic and Atmospheric Administration (NOAA) under Grant –

(Living Marine Resources Cooperative
Science Center) Grant #
NA06OAR4810163. The statements
contained within the manuscript/research
article are not the opinions of the funding
agency or the U.S. government, but reflect
the author's opinions.

Post-nesting movement patterns of the green sea turtle from the East End beaches of St. Croix, USVI

E. Schultz¹ and D. Hoskins^{1,2}

¹Savannah State University, LMRCSC

²NOAA National Marine Fisheries Service

1403 Hammocks View Savannah, GA 31410

emmaschultz25@gmail.com

Abstract

The green sea turtle *Chelonia mydas* is listed as threatened in the United States under the Endangered Species Act of 1973. The main purpose of this study was to investigate post-nesting movement patterns and habitat utilization of green sea turtles that have nested on the East End beaches of St. Croix, USVI. Seven Wildlife Computers® SPOT-352A platform transmitter terminals (PTTs) were attached to female green turtles in August and October 2015. Satellite telemetry data was collected using the Argos system and filtered with the Satellite Tracking and Analysis Tool (STAT) on seaturtle.org. Movement, core use and activity areas, and minimum convex polygons (MCPs) were mapped during the tracked post-nesting periods. Benthic habitat mapping was utilized to investigate habitat utilization during the post-nesting period. Three females remained within the same waters directly surrounding St. Croix during this period, while two females moved to the waters near St. Kitts and Nevis, and one moved to the northwest of Vieques. This is one of the first studies identifying resident green turtles that do not make long distance migrations between nesting and foraging grounds. Future work tracking male green turtles would distinguish if different sexes utilize the same areas after the breeding season.

Introduction

The green sea turtle *Chelonia mydas* is listed as endangered by the IUCN Red List of 2004. The Endangered Species Act now classifies the green turtle species into 11 distinct population segments (DPSs) with most segments being classified as threatened and only three (Mediterranean, Central West Pacific, and Central South Pacific) being listed as endangered. More information needs to be obtained about the foraging, nesting, and movement behaviors of the different green turtle rookeries worldwide to implement the best management practices. The main purpose of this study was to track the post-nesting movements and categorize

the benthic habitat types utilized during this period of female green sea turtles nesting on the East End beaches, including the beaches within Jack, Isaac, and East End Bays, of St. Croix, US Virgin Islands.

Experiments and Conclusions

Seven Wildlife Computers™ SPOT-352A platform transmitter terminals (PTTs) were attached to female green sea turtles on the East End beaches of St. Croix in August and October 2015. The satellite data were collected using the Argos system with Kalman filtering. The females were tracked using the Satellite Tracking and Analysis Tool (STAT) on seaturtle.org and movement patterns were mapped. Locations representing

speeds of more than five kph, locations on land, and locations very spatially different (greater than 120 km) from the last valid location were removed. Kernel density estimation (KDE) was utilized to calculate 50% core use and 95% activity areas during their post-nesting period. Minimum convex polygons (MCPs) were created when KDE could not be completed. Habitat utilization was identified in the core use areas and MCPs using previously created benthic habitat maps.

Female green turtles were tracked between 16-241 d (mean=160.9±10.6) for a total of 1,126 PTT days transmitted before analyses were conducted. Kernel density estimation and a MCP could not be created when less than ten detections of the highest location class were received. Three females were identified as residents of the waters around St. Croix, remaining within the same areas during both their inter-nesting and post-nesting periods. Three females were classified as migrants as two transitioned to the waters near St. Kitts and Nevis during their post-nesting periods and one moved to the waters to the northwest of Vieques.

The major finding of this study was that there are resident and migrant green

turtles on the East End beaches of St. Croix. While conclusions cannot be drawn about the movements of the entire green turtle population from these results, evidence is provided that not all green turtles make long migrations from their nesting to foraging grounds as previously hypothesized. Future work tracking male green turtles would distinguish if different sexes utilize the same areas after the breeding season. Researchers should utilize additional satellite transmitters equipped with depth recorders to monitor dive profiles of both male and female green turtles throughout the Caribbean. Continued collaborative research involving satellite telemetry, genetic analyses, and nest monitoring is vital for protecting this threatened and endangered species.

Acknowledgement

This study was supported and monitored by National Oceanic and Atmospheric Administration under (Living Marine Resources Cooperative Science Center) Grant # NA11SEC481002. The statements contained within the manuscript/research article are not the opinions of the funding agency or the U.S. government, but reflect the author's opinions.

Satellite retrievals of *Karenia brevis* harmful algal blooms in the West Florida Shelf using neural networks and comparisons with other techniques

Ahmed El-habashi¹ and Samir Ahmed^{1*}

¹The City College of New York, NOAA Crest, Optical Remote Sensing Laboratory, Department of Electrical Engineering,
160 Convent Ave, New York, NY 10031, USA; aelhaba00@citymail.cuny.edu
[*ahmed@ccny.cuny.edu](mailto:ahmed@ccny.cuny.edu);

Introduction

A new approach is needed for the detection and tracking of *KB* HABs that frequently plague the coasts and beaches of the West Florida Shelf (WFS) using VIIRS satellite data. Such a monitoring capability for *KB* HABs is important because of their negative impacts on ecology and health. More specifically, high *KB* HABs levels pose a threat to fisheries and human health, and directly affect tourism and local economies [1]. Effective *KB* HABs detection and tracking approaches are needed for use with VIIRS so that NOAA can extend its HABs monitoring capabilities, which previously relied on MODIS-A imagery [2–3]. Unfortunately, VIIRS, unlike its predecessor MODIS-A, does not have a 678 nm channel to detect chlorophyll fluorescence, which is used in the normalized fluorescence height (nFLH) algorithm, or in the Red Band Difference (RBD) algorithm, developed by our CCNY group [3]. Both of these techniques have demonstrated that the *Rrs* 678 nm from the MODIS-A fluorescence band helps in effectively detecting and tracking *KB* HABs in the WFS [3]. To overcome the lack of a fluorescence channel on VIIRS, the alternative approach described here, bypasses the need for measurements of chlorophyll fluorescence, allowing us to extend *KB* HABs satellite monitoring capabilities in the WFS to VIIRS.

The essence of the approach is the application of a standard multiband neural network (NN) inversion algorithm, previously

developed and reported by us, that takes VIIRS *Rrs* measurements at the 486, 551 and 671 nm bands (or 488, 555, and 667 nm for MODIS-A) as inputs, and produces as output the related Inherent Optical Properties (IOPs), namely: absorption coefficients of phytoplankton (a_{ph443}) dissolved organic matter (a_g) and non-algal particulates (a_{dm}) as well as the particulate backscatter coefficient, (bb_p) all at 443 nm. In this work, however, it is only with the NN output of a_{ph443} that we are concerned with and which can be converted to equivalent [*Chla*] using empirical relationships for specific absorption in the WFS which have been determined from *in situ* measurements. For the next step, to obtain *KB* values from the VIIRS NN retrieved a_{ph443} image, we apply additional constraints, defined by (i) low backscatter manifested as a maximum *Rrs*551 value and (ii) a minimum [*Chla*] threshold [3] (and hence an equivalent minimum $a_{ph443min}$ value) both known to be associated with *KB* HABs in the WFS. These two constraining filter processes are applied sequentially to the VIIRS NN retrieved a_{ph443} image. First an image is made of retrieved VIIRS *Rrs*551. A mask is then made of all pixels with $Rrs551 \geq Rrs551max$, the maximum value known to be compatible with the existence *KB* HABs. This mask is then applied, in a filter process hereinafter dubbed F1, to the VIIRS NN retrieved a_{ph443} image to exclude pixels with $Rrs551 \geq Rrs551max$. The residual image, after application of filter process F1, will only show a_{ph443} values that also comply with

$Rrs551 \leq Rrs551max$. Then, in a second filter process, hereinafter dubbed F2, all values of $a_{ph443} \leq a_{ph443min}$ are eliminated. The residual image will now only show a_{ph443} values that are compatible with both criteria for *KB* HABs, and are therefore representative of *KB* HABs, see Figure 1.

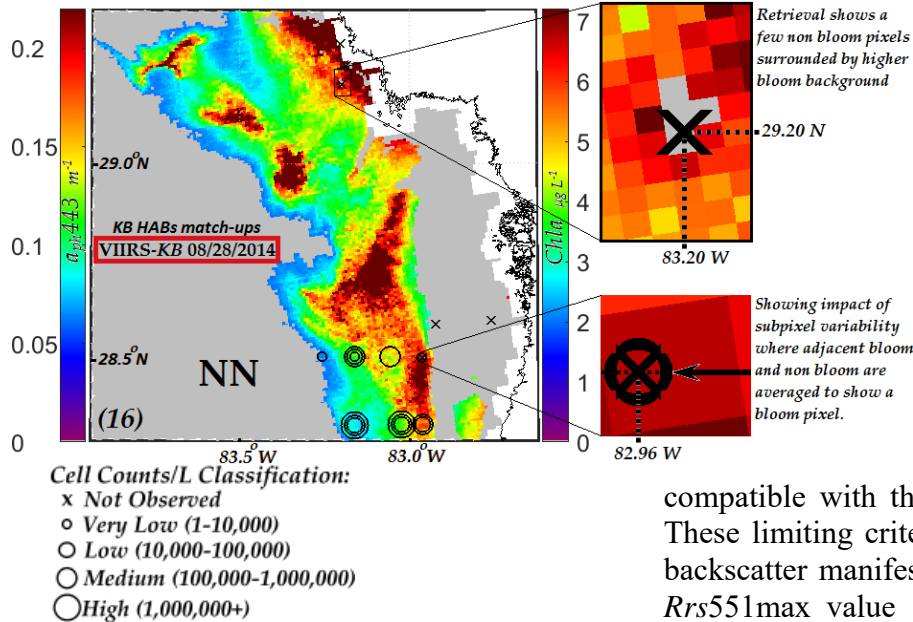


Figure 1. VIIRS-NN *KB* HABs retrievals for blooms date (28 August 2014), showing bloom compatible a_{ph443} and equiv. $[Chla]$ values. Notes image are overlaid with cell counts for this date. White areas represent cloud cover or invalid data.

It will be shown that when both these filter condition are applied to VIIRS NN a_{ph443} retrievals, they can be used to effectively delineate and quantify *KB* HABs in the WFS. The *KB* HABs retrieved in this manner also show good correlations with *in situ* *KB* HABs measurements as well as with nFLH retrievals and other techniques to which the same filtering criteria have been applied, confirming the viability of the approach.

Experiments and Conclusions

Detection of *KB* HABs in the WFS have been aided in the past by use of the 678 nm MODIS-A fluorescence band for retrievals using nFLH and RBD techniques. The lack of a fluorescence channel on the successor VIIRS satellite provided the impetus for the NN work reported here. In this approach, NN

algorithms using Rrs values from the 486, 551 and 671 nm VIIRS bands are used to retrieve an image of a_{ph443} values in the WFS. Then, as detailed above, the additional limiting constraints are applied, in two filter processes, F1 and F2 to eliminate from that image all a_{ph443} pixels which are not

compatible with the existence of *KB* HABs. These limiting criteria are defined by (i) low backscatter manifested as a maximum VIIRS $Rrs551max$ value [3] and (ii) the minimum $[Chla]$ and hence equivalent minimum (a_{ph443}) values that are known to be associated with *KB* HABs in the WFS. Thus, through the implementation of filter processes F1 and F2, all pixels in the VIIRS NN retrieved a_{ph443} image that are incompatible with *KB* HABs are eliminated. The residual image then shows only retrieved a_{ph443} values and their equivalent $[Chla]$ values that are consistent with the existence of *KB* HABs. The specific limiting values for maximum $Rrs551$ and minimum a_{ph443} used in the filter processes were based on published data, reinforced and refined by inspections of retrieval results against available *in situ* data. The retrieved values of a_{ph443} and equivalent $[Chla]$ retrieved using these filter limits, were then compared both qualitatively and quantitatively both against other satellite retrieval techniques and *in situ* measurements limited for in-shore retrievals, where the more complex waters with increased non-algal

particulate scattering interfere with the fluorescence signal making its interpretation more difficult. Comparisons were also made between the NN technique and retrievals using OCI/OC3 and the RGCI for [*Chla*] retrievals. Again, these comparisons showed reasonable correlations in open ocean waters, but confirmed difficulties with retrievals in more complex inshore waters. Further work is also needed on our NN *KB* retrieval technique before we can properly evaluate its capabilities for in-shore retrieval and compare them more rigorously with those of MODIS-A nFLH, OCI/OC3 and RGCI.

Finally, the critical test for the viability of *KB* HABs satellite retrieval techniques is the comparison of their ability to match retrieved values with concurrent in situ measurements. We therefore sought to extend the range of available in situ comparisons. This was done by seeking all available match-ups between VIIRS NN aph443 (and equivalent [*Chla*] retrievals) and in situ *KB* cell count measurements for the period 2012–2015. These comparisons showed that when the window between in situ observations and satellite measurements was reduced from daily, to 1 h and 0.5 h, the correlations greatly improved for the VIIRS NN and VIIRS RGCI retrievals against in situ match-ups. These showed respectable $R^2 = 0.82$ and $R^2 = 0.70$ respectively for the 0.5 h window. The comparisons also supported the choice of values for the F1 and F2 filter processes. Comparisons were also made comparing VIIRS NN retrievals identifying *KB* HABs, and in situ *KB* cell counts measured on the same date for 3 specific bloom events. All three confirmed the viability of the VIIRS NN retrieval approach, with no apparent false negatives or positives. Comparisons with other NN retrieval techniques are not so straightforward. Several of the previously reported NN techniques have used in situ measurements of IOPs, including sea surface temperatures and other physical parameters as

inputs to NNs for bloom prediction, apparently with some success. The more directly comparable NN technique reported, is the NN algorithm product for [*Chla*] retrievals in Case 2 waters from the MERIS satellite, which is no longer operational. This appears to give comparable results, in European waters, to OCI/OC3 retrievals in open waters, and possibly higher accuracies in coastal waters. This MERIS algorithm does not appear to have been tested for *KB* retrievals in the WFS. Tests of historical data for such retrievals may yield interesting results.

In conclusion, results to date with the VIIRS NN technique appear promising. However, more match-ups, including more detailed considerations of observation times and their connections to false positives or negatives, sample depths, distance to observation pixel centers and sub-pixel variability and impact of complex in-shore waters need to be studied. More comprehensive statistics need to be obtained on the overall efficacy of the approach and its comparisons to other techniques

References

- [1] NOAA's National Ocean Service. Harmful Algal Blooms. Available online: <http://oceanservice.noaa.gov/hazards/hab> (accessed on 9 March 2015).
- [2] Soto, I.M.; Cannizzaro, J.; Muller-Karger, F.E.; Hu, C.; Wolny, J.; Goldgof, D. Evaluation and optimization of remote sensing techniques for detection of *Karenia brevis* blooms on the West Florida Shelf. *Remote Sens. Environ.* **2015**, *170*, doi:10.1016/j.rse.2015.09.026.
- [3] Amin, R.; Gilerson, A.; Gross, B.; Moshary, F.; Ahmed, S. MODIS and MERIS detection of dinoflagellate blooms using the RBD technique. *Proc. SPIE* **2009**, *7473*, 747304.

Acknowledgement

This work was partially supported by grants from NOAA through NOAA CREST Grant# NA11SEC481004, and NOAA JPSS. We would like to thank the NASA Ocean Color Processing Group for satellite imagery. We

also thank NOAA HABSOS and Florida Fish and Wildlife Conservation Commission's Fish and Wildlife Research Institute (FWRI) groups for making *in situ* KB data available to us.

Diet analysis of Red Snapper, *Lutjanus campechanus*, on natural and artificial reefs in the western Gulf of Mexico

¹Charles H. Downey, ¹Rachel A. Brewton, ¹Jennifer J. Wetz, ²Matthew J. Ajemian, and ¹Gregory W. Stunz

¹ *Harte Research Institute, Texas A&M University-Corpus Christi, 6300 Ocean Dr., Corpus Christi, TX 78412-5869*

² *Florida Atlantic University, Harbor Branch Oceanographic Institute*

Introduction

Red Snapper (*Lutjanus campechanus*) is a species of snapper native to the western Atlantic, including the Gulf of Mexico, where it is one of the most popular and economically important reef fish in the Gulf of Mexico [1]. The species inhabits deep waters, staying near the bottom associating with hard substrates, either natural or artificial. Spawning is thought to occur in the northern Gulf of Mexico from April through September with peak spawning during the summer months [2]. Currently Red Snapper is overfished and has been since 1994 [2]. However, populations appear to be recovering in the western Gulf of Mexico [3, 4].

The availability of hard-bottom could be critical to the productivity of several important federally managed species in the Gulf of Mexico, such as Red Snapper. Early studies suggest long term residence of Red Snapper around natural hard bottom structure. There is evidence that Red Snapper may associate with artificial structures over long periods of time, however, in some areas Red Snapper exhibit low site fidelity to artificial structure [5, 7]. The function and effect of such artificial structures on the population of Red Snapper and other reef associated fish is largely unknown. Debate is ongoing especially in relation to categorizing artificial structures as essential fish habitat and increased fishing pressure at these sites [6].

Experiments and Conclusions

Red Snapper were collected throughout the year using Gulf-wide standardized vertical longline sampling following the Southeast Area Monitoring and Assessment Program (SEAMAP). Several different sites for each of the structure types will be targeted with a focus in the months April through October. Collected individual were kept on ice until returning to the lab where the fish were weighed (g). Standard length (SL), fork length (FL), and total length (TL) were measured in mm for each fish. The fish were dissected for otoliths, gonads, tissue samples and stomach contents.

Stomachs removed from sacrificed individuals were placed in 10% formalin then transferred to 70% ethanol after 48 hours. The contents were be removed, sorted and identified to the lowest possible taxon (LPT), counted and weighed. Frequency of occurrence (FO), percent by number, and percent composition by weight were calculated for each prey type. Using these parameters, the Index of Relative Importance was calculated. LPT, using the various parameters, was compared by PERMANOVA and MDS plots to determine any differences in the diet composition among Red Snapper collected from natural and artificial habitats in the western Gulf of Mexico.

References

- [1] Camber, C.I. 1955. A survey of the Red Snapper fishery of the Gulf of Mexico, with special reference to the Campeche Banks. Florida Board of Conservation Technical Series 12: 1-64.
- [2] Gallaway, B.J., S.T. Szedlmayer, and W.J. Gazey. 2009. A life history review for Red Snapper in the Gulf of Mexico with an evaluation of the importance of offshore petroleum platforms and other artificial reefs. *Reviews in Fisheries Science*. 17: 48-67.
- [3] GMFMC. 2010. Final Regulatory Amendment to the Reef Fish Fishery Management Plan to Set Total Allowable Catch for Red Snapper. Gulf of Mexico Fishery Management Council, Tampa, FL. 261 pp.
- [4] GMFMC. 2012. Final regulatory amendment to the fisher management plan for the reef fish resources of the Gulf of Mexico: Revise fall recreational fixed closed season and set 2012 and 2013 quotas for Red Snapper. Gulf of Mexico Fishery Management Council, Tampa, FL. 62 pp.
- [5] Peabody, M.B. and Wilson, C.A. 2010. Fidelity of Red Snapper (*Lutjanus campechanus*) to petroleum platforms and artificial reefs in the northern Gulf of Mexico. U.S. Dept. of the Interior, Minerals Management Service, Gulf of Mexico OCS Region, New Orleans, LA. OCS Study MMS 2006-005. 64pp.
- [6] Powers, S.P., J.H. Grabowski, C.H. Peterson, and W.J. Lindberg. 2003. Estimating enhancement of fish production by offshore artificial reefs: uncertainty exhibited by divergent scenarios. *Marine Ecology Progress Series* 264: 265-277.
- [7] Szedlmayer, S.T. and R.L. Schroeffer. 2005. Long-term residence of Red Snapper on artificial reefs in the northwestern Gulf of Mexico. *Transactions of the American Fisheries Society* 134: 315-325.

Acknowledgement

This research was made possible in part by a grant from BP/The Gulf of Mexico Research Initiative, C-IMAGE, and in part by NOAA MARFIN Grant Number: NA14NMF4330219. The statements contained within are not the opinions of the funding agency or the U.S. government, but reflect the author's opinions.

Reducing Discard Mortality in the Northwestern Gulf of Mexico Red Snapper Fishery

Alex Tompkins¹, Judd Curtis¹, Greg Stunz¹

¹ *Harte Research Institute at Texas A&M University – Corpus Christi*

Introduction

Discard mortality in Red Snapper (*Lutjanus campechanus*) may be one impediment towards a rapid stock recovery for this economically important Gulf of Mexico fishery. Red Snapper are highly susceptible to pressure-related injuries (i.e., barotrauma) that compromise survival after catch-and-release, resulting in a high discard mortality rate (Rummer 2007). Barotrauma intensity and subsequent mortality is affected by many variables, with the most important being capture depth (Gitschlag and Renaud 1994, Burns et al. 2004, Alós 2008, Hannah et al. 2008, Brown et al. 2010, Campbell et al. 2010, Curtis et al. 2015).

Various tools have been employed by fishery managers to reduce discard mortality. In 2008, the GMFMC enacted Amendment 27, which required fishermen fishing for federally managed reef fish to carry a venting tool onboard (GMFMC 2007). Soon after the amendment went into effect, studies began to emerge that challenged the effectiveness of venting deep-water fish, eventually leading to the rescinding of the requirement (Wilde 2009, Scyphers et al. 2013). An alternative option to venting, and one that requires less knowledge of fish physiology to operate successfully, is to rapidly recompress the fish by manually returning it to depth. Devices designed to complete such a task are commonly referred to as descender devices. Various descender devices are available to the public and allow anglers to release fish at predetermined depths in the water column or at the seafloor. Simple descender devices can be manually constructed using large barbless fishing hooks attached upside-down to a rope, while others, like SeaQualizers™, are complex devices that allow the user to set the device to release the fish at a predetermined

depth. Previous studies suggest descender devices are successful in reducing discard mortality in other deep-water demersal fish such as snappers, groupers, emperors, and rockfish (Jarvis and Lowe 2008, Sumpton et al. 2010), but literature examining the feasibility of descender devices in the Red Snapper fishery is lacking.

Experiments and Conclusions

To determine the relationship between capture depth, barotrauma impairment intensity, and post-release survival, we tagged Red Snapper with ultrasonic acoustic transmitters to estimate catch-and-release mortality. 300 fish were released at five incremental depths ranging from 30 to 70 m, and of those 300, 15 were tagged at each depth. The number of visible barotrauma symptoms was recorded and converted into an impairment score to compare with survival. Twenty Red Snapper from each depth treatment were released at 1/3 depth, 2/3 depth, or the bottom using two different rapid recompression devices, the SeaQualizer™ and the Blacktip Catch & Release Recompression Tool™. GoPro cameras were used to observe release behavior and predict survival rates. Estimates from this study can be integrated into stock assessment models to achieve better calculations of overall mortality and inform managers on effective release methods to maximize survival in discarded Red Snapper. Data collection is currently taking place, therefore, the presentation of data will not be possible until the time of the conference.

References

- [1] Rummer, J. L. 2007. Factors affecting catch and release (CAR) mortality in fish: Insight into CAR mortality in red snapper

- and the influence of catastrophic decompression. *Red Snapper Ecology and Fisheries in the U.S. Gulf of Mexico* 60(August):123–144.
- [2] Gitschlag G. R., M. L. Renaud. 1994. Field experiments and survival rates of caged and released red snapper. *North American Journal of Fisheries Management* 14:131–136.
- [3] Burns, K. M., R. R. Wilson, and N. F. Parnell. 2004. Partitioning release mortality in the undersized red snapper bycatch: Comparison of depth vs. hooking effects.
- [4] Alós, J. 2008. Influence of anatomical hooking depth, capture depth, and venting on mortality of painted comber (*Serranus scriba*) released by recreational anglers. *ICES Journal of Marine Science* 65(9):1620–1625.
- [5] Hannah, R. W., S. J. Parker, and K. M. Matteson. 2008. Escaping the surface: the effect of capture depth on submergence success of surface-released Pacific rockfish. *North American Journal of Fisheries Management* 28(3):694–700.
- [6] Brown, I., W. Sumpton, M. McLennan, D. Mayer, M. Campbell, J. Kirkwood, A. Butcher, I. Halliday, A. Mapleston, D. Welch, G. A. Begg, and B. Sawynok. 2010. An improved technique for estimating short-term survival of released line-caught fish, and an application comparing barotrauma-relief methods in red emperor (*Lutjanus sebae* Cuvier 1816). *Journal of Experimental Marine Biology and Ecology* 385(1-2):1–7.
- [7] Campbell, M. D., R. Patino, J. Tolan, R. Strauss, and S. L. Diamond. 2010. Sublethal effects of catch-and-release fishing: Measuring capture stress, fish impairment, and predation risk using a condition index. *ICES Journal of Marine Science* 67(3):513–521.
- [8] Curtis, J. M., M. W. Johnson, S. L. Diamond, and G. W. Stunz. 2015. Quantifying delayed mortality in discarded Red Snapper using acoustic telemetry. *Marine and Coastal Fisheries: Dynamics, Management, and Ecosystem Science*:434–449.
- [9] GMFMC (Gulf of Mexico Fishery Management Council). 2007. Final amendment 27 to the reef fish fishery management plan and amendment 14 to the shrimp fishery management plan. GMFMC, Tampa, Florida.
- [10] Wilde, G. R. 2009. Does Venting Promote Survival of Released Fish? *Fisheries* 34(January):20–28.
- [11] Scyphers, S. B., F. J. Fodrie, F. J. Hernandez, S. P. Powers, and R. L. Shipp. 2013. Venting and Reef Fish Survival: Perceptions and Participation Rates among Recreational Anglers in the Northern Gulf of Mexico. *North American Journal of Fisheries Management* 33(6):1071–1078.
- [12] Jarvis, E. T., and C. G. Lowe. 2008. The effects of barotrauma on the catch-and-release survival of southern California nearshore and shelf rockfish (*Scorpaenidae*, *Sebastes* spp.). *Canadian Journal of Fisheries and Aquatic Sciences* 65(7):1286–1296.
- [13] Sumpton, W. D., I. W. Brown, D. G. Mayer, M. F. McLennan, a. Mapleston, a. R. Butcher, D. J. Welch, J. M. Kirkwood, B. Sawynok, and G. a. Begg. 2010. Assessing the effects of line capture and barotrauma relief procedures on post-release survival of key tropical reef fish species in Australia using recreational tagging clubs. *Fisheries Management and Ecology* 17(1):77–88.

Acknowledgement

This study was made possible by the National Fish and Wildlife Foundation. The statements contained within are not the opinions of the funding agency or the U.S. government, but reflect the author’s opinions.

Salinity Responses of Oyster Reefs to Freshwater Inflow in Apalachicola Bay NERR, Florida

¹Duc N Le, and ²Wenrui Huang

^{1,2}Florida A & M University, Environmental Cooperative Sciences Center (NOAA-ECSC)
FAMU-FSU College of Engineering, 2525 Pottsdamer Street Tallahassee, FL 32310

¹le_du@eng.fsu.edu, ²whuang@eng.fsu.edu

Abstract

Introduction

Outdated water management practices and water usage threaten the ACF River Basin. Managed by the US Army Corps of Engineers, the ACF River Basin could face economic and environmental damage due to this interstate water dispute (Alabama, Georgia, and Florida) ultimately affect Florida's fisheries located in the Apalachicola Bay, one of the more diverse and productive ecosystems [1]. Thirty-five percent of the nutrient-rich freshwater of the ACF River Basin flows down the Apalachicola River discharging into the Eastern Gulf of Mexico supporting Florida's multi-billion dollar fisheries as well as the livelihoods of local fishing communities often carried on by multi-generations of fishermen along the Gulf Coast of Panhandle Florida. The excessive water consumption upstream may be a contributing factor to NOAA declaring a fishery disaster on the Apalachicola Bay in 2013; the yields from commercially successful staples of crab, shrimp, finfish, and oysters that usually dominate this region have been declined. Due to water demands, freshwater inflow discharging into the Apalachicola Bay has been kept artificially set at drought levels for extended periods during dry conditions. Hence, the natural flow of the Apalachicola River is affected by the allocation from the dams and locks upstream putting the estuary health at danger. Years of litigation have yet found a way to protect the rivers, floodplains and the Apalachicola Bay.

Affecting the Apalachicola Bay downstream, the ACF River Basin is one of the more endangered river systems in the US due to water management practices. With the change in freshwater inflow, native species living in the estuarine ecosystems of the Apalachicola Bay must be able to respond quickly to drastic changes in salinity in order to survive. These native species usually live in either freshwater or saltwater environments but due to the driving forces that create the mixing of the fresh and ocean waters, several species have to adapt to periods of transition that occur within their estuarine ecosystems. Most species cannot tolerate the rapid changes in salinity that occurs during each tidal cycle in an estuary. Unlike most vegetation within estuarine ecosystems, many animals that live in Apalachicola Bay must change their behavior according to the surrounding waters' salinity in order to survive. Oysters are among the many that need to do this. Oysters in Apalachicola Bay can live in the brackish waters of estuaries by adapting their behavior to the constantly changing salinity within this environment. During low tides when they are exposed to low-salinity water, oysters close up their shells and stop feeding. Isolated in their shells, oysters switch from aerobic respiration in which they breathe oxygen through their gills to anaerobic respiration, which does not require oxygen. Many hours later, when the high tides return and the salinity and oxygen levels in the water are considerably higher, the oysters open their shells and return to feeding

and breathing oxygen [2]. Salinity varies from one location to another within the estuary. They are influenced by tidal effects, volume of fresh water flowing into the estuary as well as contributing wind effects. Estuarine salinity levels are generally highest near the mouth of a river where the ocean water enters, and lowest upstream where freshwater flows in. Salinity levels usually rise during the summer when higher temperatures increase levels of evaporation in the estuary.

Salinity is an important indicator for water quality and ecosystem health. Estuarine organisms have different tolerances and responses to salinity changes. Many bottom-dwelling species such as oysters tolerate some change in salinity, but salinities outside an acceptable range will negatively affect their growth and reproduction, and ultimately, their survival in this sensitive environment. The increase of salinity in the Apalachicola Bay may have major repercussions on this biodiverse estuarine ecosystem. Oyster populations have been an indicator for a healthy ecosystem in coastal regions including assessments for how estuarine ecosystems respond to changes in freshwater inflow. Freshwater inflow into estuaries is a major contributing factor influencing oyster abundance. During periods of low freshwater discharge, estuarine salinity levels increase making oysters more vulnerable to predation and disease. Conversely, it has been suggested that during high freshwater inflow, oyster populations may experience an increase in mortality due to long periods of low salinity. This preliminary study presents an application of the artificial neural network (ANN) to assess salinity variation responding to the multiple driving forces of freshwater inflow, tides, and wind effects into the Apalachicola Bay in Florida at specific locations particularly those in oyster reefs. Parameters in the ANN model were trained until the model predictions of salinity matched well

with the observations. Then, the trained model was verified by applying the ANN model to a complementary but independent data set. Though the results indicate that the model is capable of correlating the non-linear time series of salinity to the multiple driving forces, this study suggests that salinity in estuaries such as the Apalachicola Bay are still difficult to model. To validate the results of the ANN model, an optimum range was observed comparing various flow scenarios in response to how salinity may affect oyster productivity. Salinity remains difficult to model even sophisticated three-dimensional numerical models that are available to provide detailed results to environmental problems would need to calibrate and verify large amounts of observation data for ecological applications which takes a large amount of effort under a number of predetermined assumptions [3].

References

- [1] Livingston RJ. Historical relationships between research and resource management in the Apalachicola River estuary. *Ecol. Appl.* 1991;1:361–382.
- [2] Sumich, J.L. 1996. *An Intro to the Biology of Marine Life* (sixth edition). Dubuque, IA: Wm. C. Brown.
- [3] Huang, W. and S. Foo, 2002. Neural network modeling of salinity variation in Apalachicola River. *Journal of Water Research. International Water Association.* Vol. 36, pg 356-362.

Acknowledgement

This study was supported and monitored by National Oceanic and Atmospheric Administration (NOAA) under Grant – Environmental Cooperative Sciences Center (ECSC) Grant # NA11SEC4810001. The statements contained within the manuscript/research article are not the opinions of the funding agency or the U.S. government, but reflect the author’s opinions.

Persistent Impacts to the Deep Soft-Bottom Benthos four years after the Deepwater Horizon Event

Paul A. Montagna¹, Jeffery G. Baguley², Jeffery L. Hyland³, Cynthia Cooksey³

¹*Texas A&M University-Corpus Christi, Harte Research Institute*

²*University of Nevada-Reno, Department of Biology*

³*NOAA/NOS, National Centers for Coastal Ocean Science*

Abstract

In September-October 2010, three to four months after the Deepwater Horizon blowout was capped, a zone of moderate and severe impacts to deep-sea soft-bottom benthos was identified that extended over an area of 172 km². The impact was a loss of -53.7% of macrofauna family diversity and -38.3% of meiofauna major taxa diversity in the most severely impacted zone. The area was resampled in May-June 2011 and May-June 2014 to determine if the identified effects were persisting. The sampling design compared 19 stations in the impact zone to 13 stations in the reference zone that were sampled in all years. While there are some signs of recovery in 2011 and 2014 in terms of abundance, there is evidence of persistent, statistically significant impacts to both macrobenthic and meiobenthic diversity because the relative losses of biodiversity are largely the same as in 2010. A loss in diversity has been shown to correlate with a loss of deep-sea ecosystem services because these fauna serve vital functional roles in the deep-sea (including: biomass production, sediment bioturbation and stabilization, organic matter decomposition and nutrient regeneration, and secondary production and energy flow to higher trophic levels). The persistence of significant biodiversity losses four years after the wellhead was capped indicates that full recovery of ecosystem services has yet to occur.

Introduction

The Deepwater Horizon (DWH) blowout at the Macondo well drilling site occurred in the northern Gulf of Mexico on April 20, 2010. The spill, which occurred at a water depth of 1525 m, in Mississippi Canyon Block 252, released approximately 3.19 million barrels (507 million liters) of oil over a 3-month period [1]. Ryerson et al. [2] has estimated that a majority of the oil was removed by cleanup operations, other natural mechanisms, or was present at the surface in oil slicks, but up to 35% of the hydrocarbons were trapped and transported in persistent deep-sea plumes. The large volume of oil trapped in the deep-sea plumes indicates that large amounts of oil were likely transported to offshore, deep-water sediments. It is now known that this

transport could occur via several potential pathways e.g., sinking of dispersed oil droplets that were absorbed onto suspended particles, incorporation of oil droplets into copepod fecal pellets, transport of oil-laden particles, sinking of heavier oil burn residues that resulted from burning oil during the Oil Spill Response activities, or settling of oil-mud complexes from the injection of drilling mud during the failed top-kill operations. In addition, drill cuttings, drill fluids, and other containment fluids, commonly used during offshore oil-drilling operations [3], were likely released from the well blowout and deposited to the bottom after the blowout.

In September-October 2010 two DWH Response cruises (aboard RV Gyre and RV Ocean Veritas) were deployed to sample

sediments for the purpose of determining if substantial amounts of oil were on the deep-sea floor. Initial results from analysis of 65 deep-water (>200 m) stations demonstrated significant impacts to the macrofauna (benthic invertebrates > 300 μm in size) and meiofauna (benthic invertebrates between 45 and 300 μm in size) based on a spatial interpolation of a principal components analysis (PCA) of combined benthic and abiotic variables [4]. The PCA produces a first principal component (PC1) axis that accounts for the largest possible variance in the data attributable to oil-spill impacts. The new PC1 variable was mapped in a geographic information system (GIS) to identify the footprint of DWH-related benthic impacts. The most severe reductions in macro- and meiofaunal abundance and diversity occurred within 3 km of the wellhead, and covered an area approximately 24 km^2 . Moderate impacts were observed in an area of 148 km^2 that had elliptical shape, which extended up to 17 km towards the southwest and 8.5 km towards the northeast of the wellhead. Thus, the total area that was adversely impacted covered 172 km^2 . Adverse benthic effects were strongly correlated with concentrations of total petroleum hydrocarbons, polycyclic aromatic hydrocarbons, and barium, as well as distance to the wellhead, but there were no correlations with distance to hydrocarbon seeps. Thus, the observed correlations of biological effects were most likely due to the oil spill and not natural hydrocarbon seepage.

A study was initiated in May 2011 and May 2014 to determine the effects of the DWH oil spill on sediments and benthic fauna in the deep-sea of the Gulf of Mexico. This study was performed under the direction of the DWH Natural Resource Damage Assessment (NRDA) Deepwater Benthic Communities Technical Working Group (NRDA Deep Benthic TWG). The purpose of the study was to assess potential spatial and temporal impacts of the DWH oil spill on sediments

and benthic fauna in deep-water areas of the Gulf.

Experiments and Conclusions

The objective of this NRDA study was to resample 32 stations that were sampled in 2010 and statistically compared the data to test for persistence of impacts or alternatively any signs of recovery from the oil spill. The stations were divided into two groups based on previously identified impacts [4]: 1) the impact zone with 20 stations that had severe and moderate impacts, and 2) a reference, or non-impact, zone with 12 stations. An OISL mega-multicorer was used to collect 12 sediment core samples with each deployment. Cores from each drop were apportioned for analysis of macrofauna, meiofauna, hydrocarbons, metals, pore-water chemistry (Eh, sulfides, ammonia), and other basic sediment properties (total carbon, total organic carbon, total inorganic carbon, total nitrogen, grain size). The method details are described in Montagna et al. [4].

Concentrations of chemical contaminants e.g., total petroleum hydrocarbons (TPH), total polycyclic aromatic hydrocarbons (total PAHs), barium, and selected natural habitat characteristics (depth, sediment grain size, and total organic carbon (TOC)) did not change over time.

Macrofauna appeared to recover in 2011 because abundances in the impact zone were higher than in the non-impact zone, but impact abundances decreased to below reference in 2014. The increase in 2011 was due to a large bloom of pioneering species with low diversity, which means the sites were actually exhibiting traits of a succession stage of a disturbed ecosystem. Diversity has not recovered at all, having lower, parallel responses in the impact zone in 2011 and 2014 than the non-impact zone.

Meiofauna appeared to recover in 2011 because the nematode:copepod ratio (N:C), an indicator of disturbance decreased to the

background level. As with macrofauna, the (N:C) rose in 2014 indicator recovery was not occurring. Abundance was always higher in the impact zone because of a bloom of nematodes, which indicates disturbance. Taxa richness has not recovered at all, having lower, parallel responses in the impact zone in 2011 and 2014 than the non-impact zone.

Macrofauna and meiofauna community structure exhibited year-to-year differences, but the difference between the impact and non-impact zone did not change over time. Stations within the impact zone clustered together, and had distinctly different structure than stations within the non-impact zone.

In conclusion, the deep-sea footprint of the oil spill can be defined with high concentrations of oil and drilling mud indicators, and low diversity of macrofauna and meiofauna. There was a wide-spread oil footprint on the bottom of the deep sea, which was consistent with deep-sea plume trajectories. Macrofauna and meiofauna diversity has not recovered after four years. Community structure differences from background still persist.

In the future, we will continue the times series. We have 2015 samples and 2016 samples are planned. We are also comparing DWH with the 1979 Ixtoc spill. In addition, we are trying to identify genomic responses to the DWH event using high-throughput biological assays for oil spills, and develop genomic methods to assess benthic communities.

References

- [1] DWH Natural Resource Trustees (2016) <http://www.gulfspillrestoration.noaa.gov/>

[wp-content/uploads/Chapter-2_Incident-Overview_508.pdf accessed 5 April 2016.](#)

- [2] Ryerson TB, Camilli R, Kessler JD, Kujawinski EB, Reddy CM, Valentine, DL Atlas E, Blake DR, de Gouw J, Meinardi S, Parrish DD, Peischl J, Seewald JS, Warneke C. (2012) Proc. Natl. Acad. Sci. U.S.A. **109**: 20246-20253.
- [3] Neff JM, Rabalais NN, Boesch DF (1987). Chapter 4, pp. 149-174, in Boesch DF, Rabalais NN, editors, Long-Term Environmental Effects of Offshore Oil and Gas Development, Elsevier Applied Science, NY.
- [4] Montagna PA, Baguley JG, Cooksey C, Hartwell I, Hyde LJ, Hyland JL, Kalke RD, Kracker LM, Reuscher M, Rhodes ACE (2013) Plos One 8(8)/e70540: 1-8.

Acknowledgement

This study was partially supported British Petroleum (BP) and by National Oceanic and Atmospheric Administration (NOAA) under Grant DG133C06NC1729 from NOAA's Office of Response and Restoration (ORR) via subcontract 1050-TAMUCC from Industrial Economics (IEC), and a Grant from NOAA's Office of Education, Educational Partnership Program award (NA11SEC4810001) via a subcontract from Florida A& University. Any opinions, findings, conclusions, recommendations, or statements contained within the manuscript/research article are those of the author(s) and do not necessarily reflect the view of the U.S. Department of Commerce, National Oceanic and Atmospheric Administration.

Carbon Storage in Northern Gulf of Mexico Salt Marshes and Mangroves

Lauren Hutchison*¹, David Yoskowitz¹, Just Cebrian², and Aaron Macy²

¹*Harte Research Institute, Texas A&M University- Corpus Christi*

²*Dauphin Island Sea Lab, University of South Alabama*

Abstract

Mangroves are expanding their range northward in the northern Gulf of Mexico due to increasing temperatures and decreases in the frequency and duration of freezes [1, 2]. With a 2°C to 4°C increase in mean annual minimum temperature, 95-100% of salt marshes in Texas and Louisiana will be vulnerable to displacement by mangroves [3]. This projected transition of habitat types could have cascading ecosystem effects, affecting the supply and resiliency of ecosystem services.

In order to assess potential changes in the provision of ecosystem services, we conducted a meta-analysis of carbon storage in salt marshes and mangroves in the northern Gulf of Mexico. Preliminary results from our research suggest that there is not enough data on mangrove carbon storage in the northern Gulf of Mexico to make statistical comparisons between total carbon storage of salt marshes and mangroves. Based on our research, we suggest prioritizing research on mangrove carbon storage in the northern Gulf of Mexico, particularly in areas where mangroves are documented to be expanding into salt marsh habitat.

Introduction

Mangroves are expanding their range northward in the northern Gulf of Mexico due to increasing temperatures and decreases in the frequency and duration of freezes [1, 2]. With a 2°C to 4°C increase in mean annual minimum temperature, 95-100% of salt marshes in Texas and Louisiana will be vulnerable to displacement by mangroves [3]. This projected transition of habitat types could have cascading ecosystem effects, affecting the supply and resiliency of ecosystem services.

Experiments and Conclusions

In order to assess potential changes in the provision of ecosystem services, this study presents results of a meta-analysis of carbon storage in salt marshes and mangroves in the northern Gulf of Mexico. To conduct the analysis, carbon storage was divided into three components (aboveground biomass, belowground biomass and soil carbon) and

estimated per component. Additionally, the variability of carbon storage in relation to geographical location and dominant plant type was assessed.

Preliminary results from our research suggest that there is not enough data on mangrove carbon storage in the northern Gulf of Mexico to make statistical comparisons between total carbon storage of salt marshes and mangroves. However, we were able to determine that the average value of the soil carbon component of salt marshes was slightly lower (but not significantly lower) than that of mangroves. Further, we determined that each carbon storage compartment of salt marshes in the northern Gulf of Mexico was significantly different from each other. The belowground biomass and soil carbon in the top 20cm of salt marsh sediment was approximately three and four times greater (respectively) than aboveground biomass. Thus, the carbon stored below ground in the roots, rhizomes and soil

of salt marshes is approximately seven times greater than the carbon stored in aboveground biomass. When extrapolated to the estimated depth of total soil carbon in northern Gulf of Mexico marshes, this value is much greater.

Findings from this study: 1) enhance understanding of how coastal habitats are functioning in the northern Gulf of Mexico; 2) provide data needed to model changes in blue carbon as a result of climate change; and 3) identify data gaps and research needs within coastal marshes in the northern Gulf of Mexico. Based on our research, we suggest prioritizing research on mangrove carbon storage in the northern Gulf of Mexico, particularly in areas where mangroves are documented to be expanding into salt marsh habitat.

References

- [1] C.L. Perry, I.A. Mendelsohn, *Wetlands*. **29** (2009) 396-406.
- [2] N. Saintilan, N. Wilson, K. Rogers, A. Rajkaran, K.W. Krauss, *Global Change Biology*. **20** (2014) 147-157.
- [3] M.J. Osland, N. Enwright, R.H. Day, T.M. Doyle, *Global Change Biology*. **19** (2013) 1-13.

Acknowledgement

This material is based upon work supported by the National Oceanic and Atmospheric Administration, Educational Partnership Program, U.S. Department of Commerce, under Agreement No. NA11SEC4810001. Any opinions, findings, conclusions, or recommendations expressed in this publication are those of the author(s) and do not necessarily reflect the view of the U.S. Department of Commerce, National Oceanic and Atmospheric Administration.

A Study of Nutrient Impacts on HAB Biotxin Concentrations in Apalachicola Bay and Grand Bay National Estuarine Research Reserve

Shareena Cannonier

Florida A&M University, School of the Environment
1515 S Martin Luther King Jr. Blvd, FSH Science Research Center
Tallahassee, Florida 32307 |Email: shareena1.cannonier@famuedu

Michael Abazinge, Florida A&M University michael.abazinge@famuedu

Charles Jagoe, Florida A&M University, chjagoe@gmail.com

Steve Morton, Research Oceanographer, NOAA/NOS, Marine Biotoxins Program

331 Fort Johnson Road, Charleston, SC 29412 |steve.morton@noaa.gov

Abstract

Harmful algal blooms (HABs) are the overgrowths of algae that can cause harm by the production of toxins or by biomass accumulation in the marine environment. Algal growth and toxin production is influenced by the availability of sunlight, carbon-dioxide, and nutrients. Other sources include temperature, salinity, wind, water-depth, and the types of predators grazing on them. The goal of this study is to determine HAB biotoxin concentration in two NERR sites: ANERR and GNERR and to determine the correlations to water column nutrient concentrations. Concentrations will be determined using Solid Phase Adsorption Tracking (SPATT) bags to access the amount of dissolved biotoxin levels of domoic acid in seawater. The SPATT bag method involves the passive adsorption of biotoxins onto porous resin filled pouches, which are deployed for two weeks in the water column using embroidery hoops, rope, and carabiners to suspend the bags. Nutrient and other data will be obtained from the System-Wide Monitoring Program (SWMP) developed by the NERR sites. Dissolved biotoxin extracts will be measured using Light Chromatography-Mass Spectrometry/bioassays. Quantitative analysis of the data will be used to access the differences between the two sites.

In order to validate the SPATT bag method, a spiking protocol will be utilized to assess the efficiency of the porous resin. Variables such as salinity, humic acid, and domoic acid concentrations will be tested in deionized water, artificial salt water, and estuarine water collected from both GNERR and ANERR. Using 1L Erlenmeyer flask with stoppers, SPATT bags will be exposed to the various treatments for 2 weeks and LC-MS will be used to measure toxin uptake, while spectrophotometry will be used to measure humic acid levels.

Changes in the Earth's climate will impact the production of HABs. This study is important in sharing more information on some factors that influences HAB production. This framework will add value to the greater scheme of maintaining healthy oceans.

References

- Anderson, D.M., (2007). The Ecology and Oceanography of Harmful Algal Blooms: Multidisciplinary Approaches to Research and Management. IOC Technical Series 74, UNESCO 2007. . IOC/2007/TS/74.
- Anderson, D.M., B. Reguera, G.C. Pitcher, and H.O. Enevoldsen. (2010). The IOC International Harmful Algal Bloom Program: History and science impacts. *Oceanography* 23(3):72–85, doi:10.5670/oceanog.2010.25.

Edmiston, H. (2008). A River Meets the Bay. Apalachicola National Estuarine Research Reserve. Retrieved from http://coast.noaa.gov/data/docs/nerrs/Reserves_APA_SiteProfile.pdf

Lane, Jenny Q., C. Meiling Roddam, Gregg W. Langlois, and Raphael M. Kudela. "Application of Solid Phase Adsorption Toxin Tracking (SPATT) for Field Detection of the Hydrophilic Phycotoxins Domoic Acid and Saxitoxin in Coastal California." *Limnology and Oceanography-Methods* 8 (November 2010): 645–60. doi:10.4319/lom.2010.8.645.

Liefer, Justin D., Alison Robertson, Hugh L. MacIntyre, William L. Smith, and Carol P. Dorsey. "Characterization of a Toxic Pseudo-Nitzschia Spp. Bloom in the Northern Gulf of Mexico Associated with Domoic Acid Accumulation in Fish." *Harmful Algae* 26 (June 2013): 20–32. doi:10.1016/j.hal.2013.03.002.

Acknowledgements

The project is supported by NOAA EPP/MSI Grant #NA11SEC481001. The author would like to thank Steve Morton, NOAA .

Assessment of fish health parameters of *Morone americana* (White Perch): A fish health index in the Choptank River, MD

D. Bell¹, Dr. M. Abazinge¹, Dr. C. Jagoe¹, Dr. L. Gonsalves², M. Matsche²

¹Florida Agricultural and Mechanical University

²Cooperative Oxford Laboratory

Abstract

The assessment of fish health can be an effective tool in gaining an insight into the health of a fish population. Fish health assessments also allow researchers to make inferences about the health of the water ecosystems in which sampled fish inhabit. The use of the fish health assessment index allows for a quick analysis of a large population of fish which require minimal use of equipment and researchers need little to no training to perform the assessment. In addition to being a quick way to analyze fish health the health assessment index is also very customizable. The HAI allows for the integration of additional health metrics such as bacteriology, hematology, and histology which are utilized to provide a diverse array of health parameters. Assessing multiple areas of health help reveal important health condition drivers in a fish population. The health of *Morone americana* (white perch) was assessed in the Choptank River and its tributaries in Maryland. The current study focuses on assessing the health status of white perch in regards to method of capture, temporal, and spatial changes through the use of the HAI. Also, a flow cytometry protocol was developed to rapidly quantify and differentiate white blood cells from red blood cells in white perch. The data from flow cytometry will aid in obtaining an idea of the blood cell populations in white perch and help to analyze the relative ratios of white blood cells, which may be important as an additional health metric in the HAI.

Introduction

Biological organisms are extensively utilized in research as indicators of ecosystem health¹⁻⁴. These “bioindicators” can be instrumental in the assessment of population health and provide insights into the relative health of the environment in which the organism inhabits. Due to spending the entirety of their life in a given ecosystem, bioindicators inherently accumulate imprints from biotic and abiotic stressors present in a system. Accumulation of environmental stressors on an organism can in turn cause health abnormalities which can be measured through the use of health metrics. In aquatic systems, fish are excellent bioindicators because they interact with various aspects of

their environment and can be captured easily for analysis.

Health metrics can consist of any tools or methodology which are used to assess the health of an individual. Health metrics are used to test for the presence or absence of any abnormality. The assessment of these health metrics allows researchers to evaluate the health conditions of organisms. The purpose of this study is to characterize the health of white Perch in the Choptank River using a system called the Health Assessment Index (HAI).

Experiments

Fish samples were collected from various areas along the Choptank River and its surrounding tributaries. Fish capture

underwent health assessment analysis using the health metrics of the HAI (gross pathology, hematology, histology, bacteriology and flow cytometry). Semi quantitative analysis of health metrics were used to make an index system based around reference values that are categorized according to severity of lesion (0=none, 10=mild, 20=moderate, 30=severe). Scores are tallied up amongst health metrics and combine to create the final HAI score. A lower final HAI score indicates a healthy fish while a higher score indicates a health impacted fish. The final HAI score was then used to compare the mean health of fish population in respect to different seasons, locations, and methods of capture.

Initial results suggest that white perch from the Choptank River had a significantly higher mean HAI score in 2014 than in 2015. Fish were found to have higher HAI score in the Spring season than in the Fall and Summer. In terms of location, fish sampled closer to more develop areas exhibited higher mean HAI scores. The mean HAI of fish capture by trawl netting was significantly higher to fish caught by hook and line. These results suggest that a multi-parametric approach to fish health assessment such as the HAI can be effective as a means of assessing the health of a large number of fish in a relatively short amount of time. Also, results suggest that white perch in the Choptank River change in response to time and location. Further research will help uncover which environmental factors influence the health of the fish species.

References

- [1] 1. Rice CD, Kergosien DH, Adams SM. Innate immune function as a bioindicator of

pollution stress in fish. *Ecotoxicol Environ Saf.* 1996;33(2):186-192. doi:10.1006/eesa.1996.0024.

- [2] 2. Galal TM, Farahat EA. The invasive macrophyte *Pistia stratiotes* L. as a bioindicator for water pollution in Lake Mariut, Egypt. *Environ Monit Assess.* 2015;187(11):701. doi:10.1007/s10661-015-4941-4.
- [3] 3. Findik O, Cicek E. Metal concentrations in two bioindicator fish species, *Merlangius merlangus*, *Mullus Barbus*, captured from the West Black Sea coasts (Bartın) of Turkey. *Bull Environ Contam Toxicol.* 2011;87(4):399-403. doi:10.1007/s00128-011-0373-1.
- [4] 4. Beg MU, Al-Subiai SN, Al-Jandal N, Butt SA, Beg KR, Al-Husaini M. Seasonal effect on biomarkers of exposure to petroleum hydrocarbons in fish from Kuwait's marine area. *Mar Pollut Bull.* September 2015. doi:10.1016/j.marpolbul.2015.09.017.

Acknowledgement

This research is supported by NOAA ECSC grant number NA11SEC481001. Thanks to NOAA ECSC for support during summer internship at the Cooperative Oxford Laboratory. Thanks to Dr. Lonnie Gonzalvez, Mark Matsche, Kevin Rosemary and Amanda Weschler for mentorship and guidance during my time at the laboratory. Thanks to the Cooperative Oxford Laboratory for a wonderful summer internship experience. Lastly, a special thanks to my supervisory committee, family, and friends for the continued support through my academic journey

High resolution measurements of changes in molecular composition of crude oil undergoing degradation by native microbes from the Gulf of Mexico

G. Hitz,¹ C. Jagoe,¹ A. Chauhan,¹ E. Hilinski,² E. Johnson,¹ and R. Gragg¹

¹ *School of the Environment, Florida Agricultural and Mechanical University, Tallahassee, Florida, 32307*

² *Department of Chemistry and Biochemistry, The Florida State University, Tallahassee, Florida, 32306*

Abstract

The ability of microbes to degrade crude oil in marine systems is well known. However, a detailed understanding of the changes in molecular composition of crude oil undergoing bacterial degradation is lacking. A pilot project was done using a pure strain of *Pseudomonas aeruginosa* isolated from Apalachicola Bay, FL, capable of using Macondo oil as the sole source of carbon and energy. In this study, a model light, sweet crude oil was incubated in replicate microcosms with *P. aeruginosa* over 20- and 40-day periods. Changes in molecular composition of the oil will be characterized using ultra-high resolution Fourier transform-ion cyclotron resonance mass spectrometry (FT-ICR MS), capable of resolving tens of thousands of components present in the oil. Simultaneously, gene copy numbers of predominant biodegradative gene classes (oxygenases, hydroxylases, decarboxylases etc.) will be assayed and correlated with changes in molecular composition of oil across various time points and treatments. This pilot study serves as a precursor to a dissertation research project to investigate in detail the changes in molecular composition of various types of crude oils (light sweet, medium, and heavy sour) during and after biodegradation by representative in-situ microbial communities present in the Gulf of Mexico.

Introduction

The ability of microbes to biodegrade crude oil is well known. For example, Thomas [1] investigated various bacterial strains from an oyster reef in Apalachicola Bay, Florida. Twenty-three strains of *Pseudomonas aeruginosa*, an important hydrocarbon degrader in the Gulf of Mexico, were isolated. One strain, *P.aeruginosa* strain WC55, biodegraded $42.7 \pm 2.7\%$ of crude oil during the exposure period. This finding was consistent other studies showing bacteria from *Pseudomonadaceae* family are able to degrade crude oil. The Thomas study estimated the percentage of crude oil biodegraded by various bacterial isolates; however, it did not attempt to chemically

characterize the crude oil fractions before or after bacterial degradation.

Other recent studies involving microbial degradation of oil have characterized crude oil using various analytical techniques including gas chromatography and mass spectrometry, or a combination of both methods. For example, Kostka [2] while measuring bacterial community response in beach sands utilized GC-MS to conduct FL-PRO and SW846 8270C LL methods to perform a chemical analysis of weathered oil petroleum hydrocarbon ranging from C8 to C40. Dubinski [3], investigating the succession of hydrocarbon-degrading bacteria post-DWH spill, used an Agilent GC/FID and GC/MS. Beazley [4], while studying

microbial communities in coastal salt marshes impacted by DWH spill, used a Fourier transform infrared spectroscopy (FTIR) and gas chromatography-mass spectrometry (GCMS) to conduct various analysis.

To date, researchers have not used the ultra-high resolution of a Fourier transform ion cyclotron resonance mass spectrometry to determine the complex molecular compositional changes occurring in a spectrum of crude oil from microbial degradation in the northern Gulf of Mexico across low and high bioproductive season.

As a follow-on study to the Thomas [1] paper, a pilot project was designed to understand in more detail how *P.aeruginosa* alters the molecular composition of crude oil as it utilizes the carbon as an energy source (degradation). A light, sweet crude oil, was used as the carbon energy source for *P.aeruginosa*. As a pre-treatment baseline, the crude oil sample was characterized using Fourier transform ion cyclotron resonance mass spectrometry (FT-ICR MS).

Experiments and Conclusions

A sample of 1.25 mL (112mg) of a light, sweet crude oil and 1.25 mg of an isolated bacterial strain *P. aeruginosa* (concentration 1%) was added to 125 mL of Bushnell-Haas growth medium [5] in a 250-mL Erlenmeyer flask (microcosm). The microcosms were incubated for 20 and 40 day periods and held at 30°C at 150 rpms to simulate northern Gulf of Mexico summer conditions. Optical density readings were collected to monitor bacterial growth. Microcosms were centrifuged to removed *P. aeruginosa* and crude oil was further separated by neutral, acidic, and basic extractions. Pre-treatment and post-treatment, extracted crude oil samples were sent to the The Ion Cyclotron Resonance Facility, The National High Magnetic Field Laboratory, Tallahassee, Florida, for analysis with the use of +/- electropray ionization FT-ICR MS.

Comparison of pre-treatment and the various post-treatment crude oil samples will show changes in the molecular composition of the crude oil from *P.aeruginosa* biodegradation.

This pilot study will serve as a precursor to a dissertation research project that investigates in more detail the changes in molecular composition of various types of crude oils (light, medium, and heavy) under degradation from various in situ microbial communities present in the Gulf of Mexico. Four brackish sample sites are being considered at Terrebonne Bay, LA, Barataria Bay, LA, Apalachicola Bay, FL, and Cedar Key, FL. The Louisiana sites were selected to represent areas that have been exposed to long-term oil pollution from production activities and accidents, particularly the 2010 Deepwater Horizon spill. The Florida samples sites represent areas that have not been exposed to oil and gas operations.

References

- [1] Thomas IV, J. C., Wafula, D., Chauhan, A., Green, S. J., Gragg, R., & Jagoe, C. (2014). *Front Microbiol*, 5.
- [2] Kostka, J. E., Prakash, O., Overholt, W. A., Green, S. J., Freyer, G., Canion, A., . . . Huettel, M. (2011). *Applied and Environmental Microbiology*, 77(22), 7962-7974.
- [3] Dubinsky, E. A., Conrad, M. E., Chakraborty, R., Bill, M., Borglin, S. E., Hollibaugh, J. T., . . . Andersen, G. L. (2013). *Environmental science & technology*, 47(19), 10860-10867.
- [4] Beazley, M. J., Martinez, R. J., Rajan, S., Powell, J., Piceno, Y. M., Tom, L. M., . . . Zhou, J. (2012). *PloS one*, 7(7), e41305.
- [5] Bushnell and Haas (1941). MgSO₄ 0.2 g/L, CaCl₂ 0.02 g/L, KH₂PO₄ 1 g/L, (NH₄)₃PO₄ 1 g/L, KNO₃ 1 g/L, and FeCl₃ 0.05 g/L, pH 7.1, and salinity of 20 ppt.

Acknowledgement

This study was supported by The Environmental Biotechnology Laboratory, School of the Environment, Florida Agricultural and Mechanical University,

Tallahassee, Florida, and The Ion Cyclotron Resonance Facility, The National High Magnetic Field Laboratory, Tallahassee, Florida.

Effects of light on vertical migration patterns of *Chrysaora quinquecirrha* Ciara C. Schnyder

Margaret Sexton

University of Maryland Eastern Shore, UMES Research Experience for Undergraduate Program

Abstract: It is desirable to be able to track the distribution patterns of jellyfish in order to help reduce the negative effects that the jellyfish are producing globally. Being able to track where the jellyfish are benefits the fisherman, nuclear power plant operations, swimmers, and local bay areas. A significant concern in the Chesapeake Bay is the high abundance of the scyphozoan *Chrysaora quinquecirrha* medusae, known as sea nettles. *C. quinquecirrha* is known to appear in high abundance in a narrow range of temperature and salinity in the mesohaline portion of the Bay and its tributaries. This characteristic allows for predictions of timing and location of medusa occurrence. However, there is a high degree of unpredictability at the beginning of the season. In order to gain a better understanding of the beginning of the medusa bloom, it is necessary to understand earlier life stages. Here we focus on the ephyra stage, the first free swimming stage. Medusae are known to be negatively phototactic, but the vertical swimming behaviors of ephyrae are unknown. Vertical swimming behavior can affect horizontal position in the estuary due to the interactions of two-layer estuarine flow. We hypothesized that ephyrae would exhibit similar vertical swimming behaviors. We exposed ephyrae to light and dark conditions in the laboratory and observed vertical swimming behavior. Results of this experiment showed that ephyrae did not behave significantly differently under different light conditions.

Introduction

All across the world, jellyfish populations are becoming more troublesome. Jellyfish are concerning for swimmers, fishers, aquaculture and nuclear power plant operations [3]. Jellyfish are getting caught in fishing nets and ruining the quality of catch, as well as clogging up nuclear power plants around the world. Tracking the distribution patterns of the jellyfish ephyra stage, will may help reduce the effects that the jellyfish are producing globally. Being able to track where the jellyfish are going to be will benefit the fisherman, nuclear power plant operations, swimmers and local bay areas. Fisherman will be able to minimize their catching of jellyfish by knowing where they are going to be throughout the seasons. Swimmers will be able to swim and know the whereabouts of the jellyfish and try to avoid them better. Nuclear power plant operations will have a better chance of detecting and deflecting the jellyfish

from clogging their operations [2]. The more information gathered with regards to the jellyfish will benefit the world. By having a good definition of the oyster larvae swimming behaviors, they were able to predict the vertical swimming behaviors. If the methods in this experiment were applied to *Chrysaora quinquecirrha*, we would be able to predict the horizontal dispersal patterns of the sea nettles by using the models, but we would need to have information regarding the vertical migration behaviors of ephyrae and medusae.

Discussion

The ANOVA test results indicated that there was no consistent significant difference between the height and pulsation rate of the light and dark treatments. According to Schuyler and Sullivan (1997), *Chrysaora quinquecirrha* medusae are negatively phototactic and when light is blocked they migrate in random directions. C.

quincecirra medusae have different diel vertical migration patterns because they are related to changes in light levels [1]. When exposed to light, *C. quincecirra* ephyrae showed no consistent significant difference, that would explain the vertical migration patterns. Since there was no consistent significant difference, ephyrae are not phototactic and have different diel vertical migration patterns than the medusae.

References

[1] Purcell, Jennifer E., et al. "Temperature, salinity and food effects on asexual reproduction and abundance of the scyphozoan *Chrysaora quincecirra*." *Marine ecology. Progress series* 180 (1999): 187-196.
[2] Purcell, Jennifer E., Shin-ichi Uye, and Wen-Tseng Lo. "Anthropogenic causes of jellyfish blooms and their direct consequences for humans: a review." *MARINE ECOLOGY-PROGRESS SERIES*- 350 (2007): 153.

[3] Schuyler, Qamar, and Barbara K. Sullivan. "Light responses and diel migration of the scyphomedusa *Chrysaora quincecirra* in mesocosms." *Journal of Plankton Research* 19.10 (1997): 1417-1428.

[4] Sexton, Margaret A. (2012). Factors Influencing Appearance, Disappearance, and Variability of Abundance of the Sea Nettle, *Chrysaora quincecirra* in Chesapeake Bay (Unpublished doctoral dissertation). University of Maryland College Park, Maryland

Acknowledgements

This work is supported by the UMES REU program, which is funded by NSF award number and the NOAA Living Marine Resources Cooperative Science Center Grant #NASEC11481002

Can Other Crustaceans be a Host to a Fatal Blue Crab Virus?

Chiamaka Nnah¹, Eric Schott²

¹University of Maryland Eastern Shore, ¹30655 Student Services Center Lane
¹cannah@umes.edu

²University of Maryland Center for Environmental Science, ²Institute of Marine and
Environmental Technology, 701 E Pratt St, Baltimore, MD 21202, ²schott@umces.edu

Abstract

In Maryland, the blue crab supports a \$60 million/year fishery industry. Blue crabs are found along the coastal bays and throughout the Chesapeake Bay. In 2009, it was discovered that many blue crabs in soft crab production systems were dying with infections of a virus, CsRV1. Although this virus is non-infectious towards humans, it raises the question of how the Blue crabs are contracting the deadly virus. Wild blue crabs also harbor the virus, but it is not known how blue crabs are contracting this virus. Blue crabs feed on smaller crabs such as *Panopeus* and *Hemigrapsus*. The virus is transmissible through cannibalism. This raises the question of whether CsRV1 can infect other crustaceans in the blue crab food web. We collected *Panopeus* and *Hemigrapsus* from the wild, to inject them with the CsRV1 virus. The goal of this experiment is to determine whether *Panopeus* and *Hemigrapsus* are capable of being a host of the disease, if so this could be a reason why the blue crabs are contracting the virus. With our results, we concluded that both *Panopeus* and *Hemigrapsus* can carry the CsRV1. This finding has lead us to suggest that the blue crabs could potentially contract this disease through feeding on *Panopeus* and *Hemigrapsus*. With further analysis we can ultimately determine the origin of the CsRV1.

Introduction

The importance of blue crab, *Callinectes sapidus*, to the ecology and economy of Atlantic and Gulf states is far reaching. The blue crab is a key link between the benthic and pelagic food webs and supports a commercial harvest valued at approximately \$200 million dockside (\$4 million for soft and peeler crabs) (2010-2011 NMFS / NOAA Current Fishery Statistics No. 2011). The fishery defines a way of life for thousands of commercial crabbers from Delaware Bay to the Gulf of Mexico, and employs thousands more who participate in related on-shore activities. The blue crab also supports a substantial recreational fishery that extends as far north as Massachusetts. For example in NJ, the recreational harvest was equivalent to 41% of the commercial blue crab harvest from 2005-2007 (NJ Division of Fish

and Wildlife). Blue crab abundance fluctuates unpredictably over time and space; recruitment and predation are significant factors, but are highly variable and have unquantified effects on abundance. Other sources of mortality are not well understood, but there is also an increasing appreciation for the role of disease in shaping population size (e.g., Marty et al. 2003; Stentiford et al. 2012). The variability in crab numbers, and the lack of knowledge about its causes, is recognized by the Chesapeake Bay Stock Assessment Committee (CBSAC) in the 2013 CBSAC Report (Turner 2013), which lists among the "Critical data and analysis needs" the study of "other sources of incidental mortality", and mentions disease specifically (8. CRITICAL DATA AND ANALYSIS NEEDS). We do not know whether crustaceans other than the blue crab can be infected by the RLV virus.

However, in an intriguing preliminary study conducted by an LMRCSC-supported summer intern (Kahil Simmonds) in 2013, we discovered that green crabs (*Carcinus maenas*, a portunid, like *C. sapidus*) can be experimentally infected (by injection) with RLV (3 out of 15 recipient green crabs infected, with no sign of disease). This is a significant finding that bears confirmation, and raises the possibility that *C. maenas* and other crustaceans sympatric with *C. sapidus* may also carry the virus. This lead us in trying to infect other smaller crabs such as Asian crab and the mud crab to see if they can be a potential host.

Experiments and Conclusions

This objective will consist of collection of crustaceans, preservation at -20°C, and extraction of RNA to be used in PCR-based assays to detect the virus. The PCR assay to be used is an improvement of the published method (Bowers et al. 2010), that is 100 fold more sensitive (Flowers et al. in preparation). The goal is to assess 37 crustaceans from Ocean City, MD. Twelve mud crabs and twenty-five Asian crab, to be injected with the virus than re-confirm that RLV is present at the time of sampling (typical prevalence is 10-50%).

Crustaceans will stored frozen (-20°C) until they are dissected and RNA extracted from homogenized muscle (asian crab, blue crab) or viscera (mud crab) (bead beater method, Savant FastPrep). RNA will be extracted using commercial reagents (Trizol) and procedures routine in the Schott lab. RNA quality will be assessed by spectrophotometry and gel electrophoresis. The RNA genome of the virus will be detected by reverse

transcription PCR using the primers Set1 For TGC GTTGGATGCG-AAGTGACAAAG and Set1 Rev GCGCCATACCGAG-CAAGTTCAAAT. Viral load will be quantified by comparison to a standard curve (10e1 to 10e6 copies) Rt-qPCR conducted on purified RLV genomic dsRNA, and expressed in gene copied per milligram host tissue. Based on data, we concluded that the Asian crab and mud crab can be potentially suspect in the blue crab contracting the disease.

References

- [1] Bowers, H. A., G. Messick, A. Hanif, R. Jagus, L. Carrion, O. Zmora, and E. J. Schott. 2010. Using the physicochemical properties of double stranded RNA to discover a reo-like virus from blue crab (*Callinectes sapidus*) *Dis Aquat Org.* 93:17-23.
- [2] Flowers, E.F., Simmonds, K., Hanif, A.H., Schott, E.J. *In preparation.* Assessment of a fatal virus of the blue crab *Callinectes sapidus*, along the US Atlantic and Gulf coasts.
- [3] Johnson, P. 1977. A viral disease of the blue crab, *Callinectes sapidus*: Histopathology and differential diagnosis. *J Invertebr Pathol.* 29:201-209.

Acknowledgement

This study was supported and monitored by Institute of Marine Environmental Technology (IMET)- University of Maryland Center for Environmental Science and NOAA Living Marine Resources Cooperative Science Center (LMRCSC)-University of Maryland Eastern Shore Grant number NA11SEC481002

More Regulation for Healthier Oceans: A look at the Magnuson- Stevens Fishery Conservation and Management Act (MSA)

Leara Morris-Stokes

Florida Agricultural and Mechanical University College of Law
leara1.morris@famu.edu
201 Beggs Avenue
Orlando, Florida 32801

Abstract

The Magnuson-Stevens Fishery Conservation and Management Act (MSA) is the code of law that governs vulnerable marine fishery stocks in the federal waters of America. The MSA was created in an effort to cease overfishing, eliminate by catch, and replenish fishery stocks in the nation. Healthier oceans are achieved under the MSA through the use of national standards, Fishery Management Plans (FMP), and the best available scientific information available. For more than forty years the MSA has achieved success restoring fishery stocks, but not without challenges and disparagement. The changes in climate and urbanization support that the MSA needs to transition from being driven by specific fishery stocks to ecosystem based. With more regulation and oversight the MSA can yield a wider range of success.

Introduction

More than 70% of the earth's surface is covered by water, which makes the need for healthy oceans vital. Billions of people rely on the ocean as a source of protein on their dinner plates. (Nations, 2000) A healthy and clean ocean is of dire importance. Phytoplankton near the surface waters of the ocean absorbs the carbon dioxide (Co2) in the atmosphere created by humans. The carbon is released as oxygen, which allows clean air to breath and sustains the circle of life. (Abate, 2015) Phytoplankton are relied upon as a major food source too many small fish, which are a food source to larger fish humans rely upon for protein. Ensuring a variable fisheries stock keeps the ocean healthier, which in term makes us all healthier. Through the efforts of Senators Warren Magnuson and Ted Stevenson the MSA was enactment by Congress in 1976. The MSA although amended several times is the catalyst to keeping the nation's oceans healthy.

Methods

Prior to 1976 foreign and domestic commercial fishing exploited and nearly depleted the nation's fishery stocks due to unregulated over fishing and by catch. Maintaining an abundant fishery stock is important to maintain healthy oceans. Foreign vessels in U.S. waters removed important fishery stock including New England Cod, Gulf Red Snapper, and Pacific Whiting. (Magnuson,1977) The national standards, the MSA enforced fishing quotas; vessel restrictions, and created a legal framework to ensure fishing guidelines and procedures are followed in an effort to rebuild and sustain optimum yield of fishery stocks. To accomplish its objectives regions of the country were divided into eight councils to manage fishery. (Sustainable Fisheries Act, 1996) Under the MSA each Council is responsible for the creation of Fishery Management Plans, convene committees and advisory panels, develop scientific and statistical research, set annual catch limits, and implement rebuilding plans.(NOAA)

Discussion

Four decades after the enactment of the Magnuson-Stevens Fishery Conservation and Management Act there still is a need for increased regulation, more oversight, and accurate science based fisheries data. Specific stocks have garnished significant success such as the Gulf Coast Red Snapper. The Red Snapper stock has replenished and yielded positive results. Conversely, the Atlantic Salmon, which has been prohibited since 1987 under the MSA, has not replenished. The stock has failed to rebuild to the extent that in 2000 it was listed under the Endangered Species Act (ESA). (NOAA, 2016) Currently, the primary focus of the MSA is the reduction of overfishing and sustaining the optimum yield on specific fishery stocks. Focusing solely on specific fishery stocks is not an inclusive approach considering all stocks are not included. Other factors such as Climate Change, urbanization, migratory fish patterns, and invasive species are presently unaccounted. The changes in climate support that the MSA needs to transition from specific fish stocks to ecosystem based. (Abate, 2015)

Conclusion

Since its inception in 1976 the Magnuson-Stevens Fishery Conservation and Management Act successfully laid the foundation to replenished specific fishery stocks in the federal water. To achieve healthier oceans it is not enough to simply restrict fishing zones and cap the amount of fish that are removed from the oceans. The need for more regulation, government oversight, and stringent legal repercussion such as fines are necessary to deter violators of America's Fishery Act. Accounting for changes in climate, including cutting edge scientific technology, and transitioning to a broader ecosystem based strategy would not only strengthen the MSA it would create healthier oceans.

References

- [1] (NOAA), N. O. (n.d.). *NOAA Fisheries, Regional Fishery Management Council*. Retrieved July Saturday, 2016, from NOAA Fisheries: <http://www.fisheries.noaa.gov/sfa/management/councils/index.html>
- [2] Abate, R. S. (2015). Climate Change Impacts on Ocean and Coastal Law. In R. S. Abate, *Climate Change Impacts on Ocean and Coastal Law* (pp. 28-9). New York: Oxford University Press.
- [3] Magnuson, W. G. (1977). The Fishery Conversation and Management Act of 1976: First Step Toward Improved Management of Marine Fisheries. *Washington Law Review*, 427.
- [4] (2000). State of the Worlds Fisheries and Aquaculture. In U. Nations. Rome, Italy: UN.
- [5] NOAA. (2016, July). *NOAA Atlantic Salmon*. Retrieved July Sunday, 2016, from NOAA: <http://www.fisheries.noaa.gov/pr/species/fish/atlantic-salmon.html>
- [6] Sustainable Fisheries Act. (1996). *Public Law*, 104-297.

THEME IV
Resilient Coastal Communities and
Economies

**Coastal and Great Lakes communities are environmentally and
economically sustainable**

Simulating Dust Emission and Biota Transport from Playa Systems using a Wind Tunnel

Jose Rivas¹, Thomas E. Gill², Elizabeth J. Walsh¹, R. Scott Van Pelt³

¹ *Biological Sciences, University of Texas-El Paso, El Paso, TX 79968 jarivas@utep.edu*

² *Geological Sciences, University of Texas- El Paso*

³ *USDA -Agricultural Research Service, Big Spring, Texas*

Abstract

Ephemeral wetlands are ideal sources for dust emission, as well as repositories for dormant stages of aquatic invertebrates. An important component of invertebrate dispersal and colonization to new areas is the ability to be entrained into the atmosphere. Here, we control the wind erosion process in a wind tunnel to test entrainment of diapausing stages of brine shrimp, clam shrimp, tadpole shrimp, fairy shrimp, *Daphnia*, and the rotifers *Brachionus plicatilis* and *B. calyciflorus* into the air by saltation.

Introduction

As the environment changes due to changes in climate or weather patterns or cyclic changes in seasonality, aquatic invertebrates must adapt to these potentially harmful changes. Therefore, organisms that inhabit ephemeral wetlands and playas rely on the production of dormant stages for the survival of the population during times of environmental stressors [1]. Resting stages can survive for many seasons and sediment egg banks can accumulate with these stages. These egg banks play a major role in the success of aquatic invertebrate communities [2].

Ephemeral wetlands, playa systems, and dry river basins serve as a significant source of dust in many ecosystems [3]. As soil particles begin to move, saltation, bombardment, collision, and entrainment of these particles cause lofting of smaller dust particles into the atmosphere. It is through these processes that dormant stages of aquatic invertebrates can be easily transported long distances.

Our previous work has shown that invertebrate resting stages can be transported along with dust however, not much research has focused on how these

stages are dispersed by erosion processes of ephemeral wetlands. In this study we use a wind tunnel housed at the United States Department of Agriculture- Agricultural Research Service located Big Spring, Texas to simulate erosion and dust generation of a desiccated wetland containing invertebrate propagule banks.

Experiments and Conclusions

Diapausing stages of seven species of aquatic invertebrate propagules were obtained. Tadpole shrimp (*Triops longicaudatus*), water fleas (*Daphnia magna*), clam shrimp (*Eulimnadia* cf. *texana*), and fairy shrimp (*Streptocephalus* sp.) were purchased from Arizona Fairy Shrimp (www.arizonafairyshrimp.com) while brine shrimp (*Artemia salina*) were obtained from Carolina Biological Supply Co. Diapausing embryos of two rotifer species, *Brachionus plicatilis* and *B. calyciflorus*, were purchased from Florida Aqua Farms (<http://florida-aqua-farms.com>). Twenty-one soil trays were assembled at the United States Department of Agriculture, Agricultural Research Service (USDA-ARS) facility at Big Spring, TX. Approximately 1.0 kg of sterilized Pullman clay loam soil, a

Southern Great Plains soil typical of playas and with high wind erodibility, was evenly distributed into the collection area. After soil was added, propagules were scattered throughout the collection area and mixed within the top 2 mm of soil. The entire soil area was wetted with distilled water and the pans were placed in sunlight to dry. This process allowed the soil to form polygonal crusts as it dried, simulating natural playa sediment structure. A second experiment was conducted to attempt to quantify propagule transport by coating the propagules with a fluorescent solution and proceeding as in the initial experiment.



Figure 1. Suction type wind tunnel located at the USDA-ARS, Big Spring, TX

Dust was generated in a wind tunnel [Figure 1] by releasing sand grains to bombard the soil, acting as saltator material similar to wind-entrained natural sands. Aeolian sediment was collected from three

transfer section for coarse sediment, the pan subtending a settling chamber for finer saltation-sized sediment, and two paper filters for suspension-sized sediment. These sediment collection sections also ideally

Organism	Transfer Section (coarse sized sediment)		Pan Subtending Section (Fine saltation-sized sediment)		Filter (suspension-sized sediment)	
	Present	Hatched	Present	Hatched	Present	Hatched
<i>Artemia salina</i>	+++	+++	+++	+++	++	++
<i>Streptocephalus sp.</i>	+++	+++	+++	+++	++	++
<i>Triops longicaudatus</i>	++	-	+++	+++	++	-
<i>Eulimnadia texana</i>	+++	-	+++	-	+	++
<i>Daphnia magna</i>	+	+	+++	+++	+	-
<i>Brachionus plicatilis</i>	+++	+	+++	+	+++	+
<i>Brachionus calyciflorus</i>	+++	+	+++	+	+++	+

Table 1. Wind tunnel location where propagules were collected. Plus signs represents recovery of diapausing stage in that section while a minus sign indicated an absence.

points in the sediment collection system; the represent transport distance from source

areas that include distance in meters, tens to hundreds of meters, and kilometers for the three sections respectively.

Approximately 1.8 to 2.0 g of these wind-transported sediments collected from the wind tunnel were rehydrated with 75 mls of the appropriate media and observed daily for one month to monitor hatching of viable propagules.

Preliminary results from both experiments indicate that all organisms collected in sediment recovered from all three sections of the wind tunnel [Table 1]. This provides evidence that propagules of a variety of aquatic invertebrates can be entrained into the atmosphere by the saltation-bombardment mechanism, which is the primary mechanism of dust emission. Each organism was successfully hatched from its dormant stage demonstrating that viability of organisms also is retained during wind transport after bombardment.

By simulating dust emission in a controlled system, we have demonstrated the transport of seven species of aquatic invertebrates commonly found in temporary waters. This study establishes aeolian transport (known to ecologists as anemochory) as a viable method of the dispersal of resting stages of arid land

aquatic invertebrates and a viable pathway for successful colonization of new habitats, and further gives credence to viable aquatic invertebrate resting stages being transported by dust storms.

References

- [1] L. Brendonck, De Meester, L. (2003), *Hydrobiologia*, 491:65-84.
- [2] E.J. Walsh, L. May, R.L. Wallace. (2016), *Hydrobiologia*, ROTIFERA XIV: 1-12.
- [3] J.M. Prospero, P. Ginoux, O. Torres, S.E. Nicholson, T.E. Gill, (2002), *Reviews of Geophysics*, 40:2-1.

Acknowledgement

This study was supported by the National Oceanic and Atmospheric Administration (NOAA) under NOAA Office of Education, Educational Partnership Program with Minority Serving Institutions (EPP/MSI) through cooperative agreement # NA11SEC4810003 – NOAA Center for Atmospheric Sciences (NCAS). The statements contained within the manuscript/research article are not the opinions of the funding agency or the U.S. government, but reflect the author's opinions.

Benthic Invertebrate Communities at Five South Texas Banks

M. Cooksey¹ and D. Hicks¹

¹*School of Earth, Environmental, and Marine Sciences, University of Texas – Rio Grande Valley*

Introduction

Scattered on the continental shelf off of the South Texas coast, between the Brazos-Colorado and Rio Grande deltas in the northwestern Gulf of Mexico, lie a series of hard bottom banks which are remnants of coral-algal reefs that perished approximately 10,000 years ago [1]. The hard bottom structures, which now lie between the 60 to 80 m isobaths with crest depths ranging from 58 to 70 m, are now collectively known as the South Texas Banks. Mesophotic reefs like the South Texas Banks are understudied and consequently, are often underprotected habitats. In 2008, the South Texas Banks were identified as a possible site of a Marine Protected Area (MPA), however, the banks were removed from consideration for protections because not enough information about the relic reefs was available.

This study aims to investigate and quantitatively describe the epifaunal communities of five hard bottom banks found off the coast of South Texas: North Hospital, Hospital, Southern, Big Adam, and Mysterious Banks.

Experiments and Conclusions

Exploratory video footage of the ocean floor was collected using an underwater remotely operated vehicle (ROV) (Triggerfish T4H, Deep Ocean Engineering) on the University of Texas Rio Grande Valley's research cruise aboard the *M/V Fling* in September 2014. Videos were divided into two minute segments and five frames were selected at random from segments until a total of 50 suitable frames from each bank were collected (where sufficient frames were found). A grid with 100 crosshairs was overlaid onto each image

and the subject under each crosshair was identified, resulting in percent cover. Benthic organisms observed in the videos were identified to the lowest possible taxon using morphological characteristics from video surveys and opportunistically collected specimens.

Big Adam Bank had the lowest biodiversity and biotic cover of all the observed South Texas Banks. Only 26.0% of the frames contained floral cover and 46.0% of frame grabs at Big Adam Bank contained one of the seven observed faunal species. *Stichopathes* spp. accounted for the majority (76.9%) of the faunal percent coverage with the remaining comprised of sparse tube and encrusting sponges.

Due to high turbidity, only 35 frame grabs from Mysterious Bank video footage were considered suitable for analysis. These frame grabs indicated that Mysterious Bank has a similarly low biodiversity to that of Big Adam, with 95.6% of benthic cover lacking macrobiota. However, where corals occurred, Mysterious Bank had the highest density of antipatharians (1.87 ind/m²) and octocorals (3.29 ind/m²) and the lowest algal coverage (0.3% of images), of the five studied banks. No scleractinians or other non-sponge invertebrate species were recorded from any of the frame grabs.

Of the 25 frames grabs collected at Hospital Bank, 90.0% of benthic coverage lacked macrobenthos. Algae (40.8%) and sponges (34.7%) made up the majority of biotic coverage at Hospital Bank. Only eight frame grabs contained a coral species, and while coral density was low overall, representatives of the orders Antipatharia, Octocorallia, and Scleractinia were observed

(comprising 1.2%, 0.04% and 0.04% of total benthic coverage, respectively).

Forty flora and fauna categories were observed at North Hospital Bank, including seven species/categories that were not recorded at other banks during this study. Although abiotic cover made up 60.2% of benthic coverage, North Hospital had the highest algal cover of the five banks (28.2%). Corals made up a total of 13.0% of biotic benthic cover, due to the presence of antipatharians, octocorals, and scleractinians.

At Southern Bank, flora and fauna covered 44.9% of the sea floor, with algae making up the dominant biotic cover type. Encrusting sponges (46.0%), antipatharians (23.2%) and crinoids (6.7%) made up the majority of macrofauna cover. Antipatharians dominated the coral cover at Southern Bank (75.7%), primarily because of the coverage provided by *Stichopathes* spp. (47.3%), *A. furcata* (22.9%) and *A. atlantica* (21.9%). Scleractinians provided 22.7% of the coral cover, due to *M. brueggemani* (83.8%) and *A. fragilis* (10.0%). Octocorals only comprised of 1.7% of the coral cover.

To compare the communities at the five banks, square-root transformed and standardized species abundance data in a Bray Curtis similarity matrix was used in an ANOSIM test and a metric multidimensional scaling (MDS) ordination with 95% bootstrap regions generated from 150 bootstrap averages for each bank. The species that characterized each bank were identified using SIMPER analysis. All of the banks had significantly different benthic biotic communities. The largest differences in benthic communities were found between North Hospital and Mysterious Banks ($R=0.754$, $p=0.001$) and Southern and Mysterious Banks ($R=0.701$, $p=0.001$). Big Adam Bank and Mysterious Bank contained the most similar mesophotic benthic communities amongst the studied banks, but there were still significant differences

observed ($R=0.314$, $p=0.002$). These differences among benthic biotic communities were driven particularly by the higher abundance of *Stichopathes* spp. at Mysterious Bank (3.4% overall coverage vs. 0.6% at Big Adam Bank) and higher coverage of foliose algae species at Big Adam Bank (2.3%) than Mysterious Bank (0.3%).

This research represents the first quantitative description of the benthic invertebrate communities of these five South Texas, but more research could be conducted to further investigate species that are either difficult to see or identify in ROV footage, particularly with biological sample collection during ROV dives. Despite the inherent caveats involved in such broad sampling with an ROV, the collected sample sizes were sufficient to be able to detect differences between the benthic communities at the banks, and the results of this study can be applied to future characterization attempts. The biological information from this study provides critical insight regarding the range of diversity across these five South Texas Banks at a high enough resolution that they may be included for consideration of habitat protection should the need arise again.

References

[1] R. Rezak, T.J. Bright, D.W. McGrail, Reefs and Banks of the Northwestern Gulf of Mexico::their geological, biological, and physical dynamics. (1985) 259.

Acknowledgement

This study was supported and monitored by National Oceanic and Atmospheric Administration (NOAA) under Grant – Environmental Cooperative Science Center (ECSC) Grant # NA11SEC4810001. The statements contained within the manuscript/research article are not the opinions of the funding agency or the U.S. government, but reflect the author's opinions.

Improved Remote Sensing Tools for Monitoring Marine Ecosystem Health

R. Foster¹, A. Ibrahim², A. Gilerson¹, A. McGilloway¹, A. El-habashi¹, C. Carrizo¹, M. Ottaviani¹, S. Ahmed¹

¹*Optical Remote Sensing Laboratory, The City College of the City University of New York, 160 Convent Ave, NY, NY 10031*

²*NASA Goddard Space Flight Center / Universities Space Research Association, Code 616, Greenbelt, MD 20771*

Introduction

The ability to estimate the inherent optical properties of the coastal ocean is extremely important for monitoring the health of coastal ecosystems. Traditional remote sensing methods are not able to estimate the particulate attenuation (c_p) of a water body, which is a critical parameter for estimating the amount and type of suspended particles in the ocean. Through recent research conducted at NOAA-CREST, use of the polarized nature of light in addition to traditional remote sensing methods allow the retrieval of c_p , but this retrieval requires knowledge of the polarization state of light within the water body. The present work investigates a method of determining the underwater polarized light field from above surface observations. A hybrid approach combining vector radiative transfer simulations and the Monte Carlo method is used to determine the optical transfer functions for polarized light through wind-driven ocean surfaces. Transfer functions for surface-reflected skylight and upward transmission of light through the sea surface are computed for the visible wavelengths for many common field conditions. The findings are validated with in-situ polarimetric measurements acquired during the NASA Ship Aircraft Bio-Optical Research (SABOR) campaign. Comparisons with direct subsurface measurements indicate excellent agreement with above surface estimates even in high winds.

Experiments and Conclusions

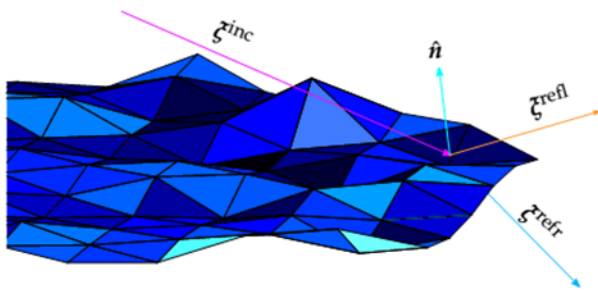
HyperSAS-POL, developed at the City College of New York, is a heavily modified



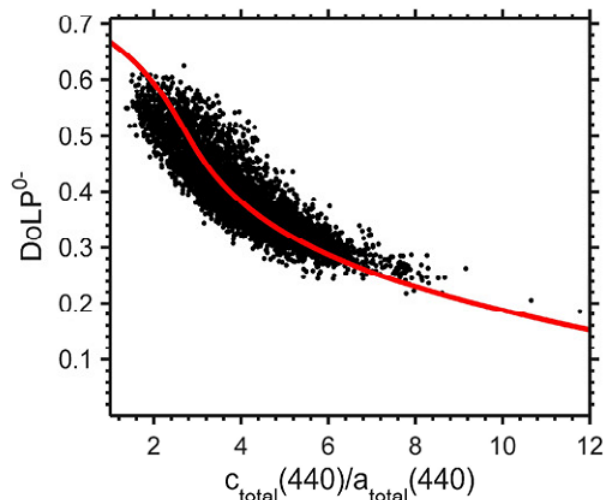
HyperSAS system produced by Satlantic, Canada. The commercially available HyperSAS system consists of a set of 3 HyperOCR radiometers. One points downward toward the water at a 40° angle from nadir ($\theta_v = 50^\circ$), while the second points upward at a 40° angle from zenith ($\theta_v = 140^\circ$). The final radiometer is a sensor which measures downwelling irradiance (E_d). Each

HyperOCR is able to produce a hyperspectral measurement in the 300-900 nm regime, 3.3 nm spacing between channels, and 10 nm full-width half-maximum channel bandwidth. The full angle field of view is nominally 3° in air. The sensor integration time changes with ambient lighting conditions, but can vary between 128 and 2048 ms.

HyperSAS-POL is able to maintain a constant relative solar azimuth angle (ϕ_r) regardless of the orientation of the research vessel to which it is attached. By design the system is set to maintain, by order of preference, $\phi_r = 90^\circ, 270^\circ, 135^\circ, \text{ or } 225^\circ$, to minimize the presence of Sun glint in the measurements. 16 To achieve this, the system receives a continuous stream of information from the research vessel, including the current GPS coordinates, the heading of the research vessel, and the current time and date. This information is used to compute the current solar azimuth and solar zenith angle, followed by the required change in sensor azimuth to maintain the closest possible ϕ_r given above. At any given moment, the ship structure makes some of the relative azimuth angles listed above impossible to achieve, so the system chooses the closest ϕ_r possible given the current situation. A movement command is issued to the pointing system (MDrive 34ac, Schnieder Electric, USA), which performs the actual movement through a geared sprocket fixed to the instrument frame. Additionally, HyperSAS-POL is equipped with a weatherproof IP camera which takes photos of the sky every minute to qualitatively assess the cloud conditions during measurement.



In order to obtain and validate the submarine polarized light field from above the surface, we need to know two transfer functions for a wind-blown sea surface: the reflection of polarized sky light from the sea surface, and the upward transmission of polarized light from below the sea surface to above. The former is needed to arrive at the polarized remote sensing reflectance (\mathbf{R}_{rs}) from above surface observations, and the latter is required for computing \mathbf{R}_{rs} from the radiance just below the surface (a product of the radiative transfer code). The matrices were computed for various common viewing conditions via a hybrid combination of Monte Carlo simulations and vector radiative transfer codes.



The relationship between the water attenuation to absorption ratio (c/a) and the Degree of Linear Polarization (DoLP) has been previously explored by our laboratory. In this work we utilize this relationship to calculate the particulate absorption spectra of data acquired during the SABOR campaign and compare it to *in-situ* measurements. The SABOR cruise included continuous measurements of particulate attenuation via a flow-thru system, which when added to the attenuation of pure water and non-algal particulates yields the total attenuation. Retrieval of the particulate attenuation coefficient is not possible using scalar remote

sensing methods, and thus this polarimetric method provides a new way of monitoring the suspended material content of coastal environments, a critical parameter required for monitoring the health of marine ecosystems.

References

- [1] Foster, R., A. Ibrahim, A. Gilerson, A. El-Habashi, C. Carrizo and S. Ahmed, Proc. SPIE 96130W, 2015
- [2] Ibrahim, A., A. Gilerson, T. Harmel, A. Tonizzo, J. Chowdhary and S. Ahmed, Optics Express 20(23): 25662-25680, 2012

- [3] Harmel, T., A. Gilerson, A. Tonizzo, J. Chowdhary, A. Weidemann, R. Arnone and S. Ahmed, Applied Optics 51(35): 8324-8340, 2012

Acknowledgement

This study was supported and monitored by National Oceanic and Atmospheric Administration (NOAA) under Grant – (Cooperative Remote Sensing Science and Technology Center, NOAA-CREST) Grant # NA11SEC4810004. The statements contained within the manuscript/research article are not the opinions of the funding agency or the U.S. government, but reflect the author’s opinions.

A Survey of Arm Length and Regeneration Abundance in the Forbes Sea Star *Asterias forbesi* in Wassaw Inlet, GA, USA

Rebecca Noel Thublin_1 and Sue C. Ebanks_2

¹*Savannah State University, Marine Sciences Program, M.S. Student*

²*Savannah State University, Department of Marine and Environmental Sciences, Assistant Professor*

Corresponding Author:

Sue C. Ebanks

*Savannah State University
3219 College St., Box 20600
Savannah, GA 31404
ebankss@savannahstate.edu*

Abstract

In benthic environments, the sea star is a keystone species. However, it is extremely hard to keep in the laboratory for any amount of time, making experiments challenging. The purpose of this study was to determine whether there was a change in size distribution and prevalence of regeneration over time for Forbes sea stars *Asterias forbesi* at Wassaw Inlet, Savannah, GA, USA. Sea stars were collected via otter trawl. Four trawls, each lasting 8-15 minutes, were conducted on 15 Oct 2015, 9 Dec 2015, and 2 Feb 2016. Once in the laboratory, the arm lengths were measured and regeneration was noted. Sea stars were kept under different conditions like different bioloads and feeding practices to establish the best husbandry practices for maximum survival and minimal stress. Seventy stars were collected on 15 October, 115 on 9 December, and 69 on 2 February. The percent of sea stars regenerating was 10.1%, 6.5%, and 11.4%, respectively. Average arm length by date was 3.51 ± 0.640 , 5.75 ± 0.860 , and 7.07 ± 0.813 cm, respectively. Average arm length increased dramatically over the 3 trawl dates, which may indicate a pattern of migration. Future studies should be conducted to determine other optimal husbandry techniques for this species.

Introduction

Sea stars contribute to the diversity of the benthos by acting as the apex predator [1, 2]. The removal of the ochre sea star *Pisaster ochraceus* caused the species diversity to decrease from 15 different species to 8 [1]. Without the presence of the main predator, prey species, specifically bivalves in the case of sea stars, were allowed to take over most of the benthos. However, this change may not be permanent. The removal of the Forbes sea star *Asterias forbesi* in Raritan Bay caused a

temporary surge in Northern quahog *Mercenaria mercenaria* populations [2]. After a couple of years, the quahog numbers began to decline again, possibly due to competition amongst conspecifics in the absence of their main predator. Therefore, even though sea stars prey on commercially-important bivalves, they are essential in keeping bivalve populations healthy and at their maximum potential over time.

Successful prey selection by the sea star is affected by sea star arm length, with bigger

stars eating larger prey [3]. Therefore, sea star size is a key parameter when assessing potential prey selection. Another important characteristic of their life history is frequency of regeneration. Once an arm is fully regenerated, there is no apparent physical evidence of any trauma (personal observation). Therefore, one cannot tell if a fully grown arm has been regenerated or not. Furthermore, frequency of regeneration can be nearly 50% in natural populations. In a cumulative study of 205 benthic habitats, Lindsay [4] found that the average maximum incidence of injury was 47% for sea stars. The purpose of the present study was to determine the frequency of regeneration and the change in average arm length of the Forbes sea star in Wassaw Inlet from October 2015 to May 2016.

Experiments and Conclusions

Trawls were conducted bimonthly in Wassaw Inlet (32° 55.0818" N, 81° 55" W), GA on 15 Oct 2015, 9 Dec 2015, 2 Feb 2016, 29 Mar 2016, and 25 May 2016. Four trawls were conducted of the same 1 nmi. area at a speed of 1-2.5 knots off the R/V Margaret C. Robinson. The sea stars were collected via a large otter trawl with 5 cm mesh size. Salinity, temperature, and dissolved oxygen (DO) were measured at the site using a YSI Pro 2030 multimeter. Water was sampled at the surface and collected at depth using a 2-L Niskin bottle. The water quality parameters were measured each trip to record the natural environmental ranges in which the stars were found. Any sea stars caught were distributed amongst three 45-L coolers and brought back to the laboratory. Three coolers were used to reduce bioload and maximize survivorship. A protocol was developed for determining arm length. Arms were numbered 1-5 with 1 being the arm directly across from the madreporite, and the subsequent arms numbered continuing clockwise around the sea star. The measurements of arms 1 and 4 were averaged

to give the radius of each star. The radii were then averaged for each trawl date. Sea stars that were regenerating were not included in the means presented.

Salinity (range: 25.8-32.7 ppt) was fairly constant throughout the months, but temperature fluctuated (13.2-23.5°C). However, there was not a difference in water parameters measured between surface water and water at depth. We saw a significant increase in arm length from October (3.5 ± 0.64 cm) to March (8.01 ± 1.04 cm) and then a decrease again in May (6.9 ± 0.54 cm). In October, 70 sea stars were collected and average arm length was 3.5 ± 0.64 cm. Of those 70 stars, 10.12% were regenerating. The most sea stars ($n = 115$) were caught in December, with an average arm length of 5.8 ± 0.86 cm and a regeneration frequency of 6.45%. Sixty-nine sea stars were caught in February. The average arm length for those was 7.1 ± 0.81 cm, and the frequency of regeneration was 11.39%. On 29 March, 71 sea stars were caught, with an average arm length of 8.0 ± 1.04 cm and regeneration frequency of 4.23%. Finally, only 8 sea stars were caught in May. They had an average arm length of 6.9 ± 0.54 cm and a 25% regeneration frequency.

The changes in arm length across sampling dates were too great to be due to growth rate. Therefore, this could possibly be because of a migration of the sea stars farther off shore in the colder months. This type of migration is documented in some sea stars and is well-accepted to be common practice for most coastal species [5]. These data may indicate that smaller sea stars move farther offshore in the winter than larger ones, which is why the larger ones were still collected in Wassaw Inlet. Additionally, the regeneration frequencies of the sea stars caught at our site, which is located adjacent to a National Wildlife Reserve and is only accessible via boats, were much lower than established values [4]. This could be due to a lack of

direct human disturbance, a main cause of sea star arm loss. Also, birds, another main predator of the sea star, would not be able to reach the sea stars in this location [6]. Further studies using dyeing techniques could be beneficial to better determine if the sea stars are actually moving offshore [7].

References

- [1] R. T. Paine. *Am. Nat.* **100** (1966) 65.
- [2] C. L. Mackenzie and R. Pikanowski. *Mar. Fish. Rev.* **61** (1999) 66.
- [3] M. Baeta and M. Ramon. *Mar. Biol.* **160** (2013) 2781.
- [4] S. M. Lindsay. *Integr. Comp. Biol.* **50** (2010) 479.
- [5] B. Pabst and H. Vincentini. *Mar. Biol.* **48** (1978) 271.
- [6] I. C. Wilkie. *Mar. Biodiv. Rec.* **3** (2009) 10.1017.

- [7] A. S. Martinez, M. Byrne, and R. A. Coleman. *Meth. Ecol. Evol.* **4** (2013) 993.

Acknowledgement

This study was supported by National Oceanic and Atmospheric Administration (NOAA) under Grant – Living Marine Resources Cooperative Science Center Grant # NA06OAR4810163 and National Science Foundation (NSF GK-12 Award #DGE-0841372). The statements contained within the manuscript/research article are not the opinions of the funding agency or the U.S. government, but reflect the author’s opinions. Special thanks go to Dr. C. Hintz and Dr. J. Carroll for their insight and help throughout this study. Also, thank you to Capt. S. Smith for driving the boat and helping with our bimonthly trawls and to the many students and interns that have volunteered their time to aid in collection and data analysis, especially C. Parrish and C. Thompson.

Wetland Land Use/ Land Cover (LULC) Changes: Case Study from Grand Bay National Estuarine Research Reserve (NERR)

Eric M. Gulledge¹, Ranjani W. Kulawardhana¹, Taimei T. Harris¹, Fengxiang X. Han² & Paul B. Tchounwou¹

¹Department of Biology, Jackson State University, Jackson, MS 39217

²Department of Chemistry, Jackson State University, Jackson, MS 39217

Abstract

Coastal habitats of the Gulf of Mexico have been recognized as increasingly vulnerable to changing climate and human disturbances. The Gulf of Mexico's wetlands have experienced significant declines in recent decades and projections are expected to further increase the rate and magnitude of wetland loss [1]. The goal of our study is to assess the land cover changes in the GB NERR wetland extent and its adjacent landscape over the last decade. Our study area, the Grand Bay NERR is one of the largest estuarine ecosystems and is a representative of wetland habitats of the Mississippi coast. We implemented a remote sensing based approach using Landsat 7 & 8 imagery to map land cover classes and to evaluate their changes over the last decade (from 2005 to 2015). LULC classes were mapped and identified using supervised-unsupervised classifications performed on Landsat 7 image of May 2003 and Landsat 8 image of May 2015. We identified seven major LULC classes within our study area. Our analyses based on the total areal extent under each LULC class reveal that these LULC classes have not been changed significantly over the study period. However, further analyses are necessary to evaluate any changes in the spatial patterns and the relative distribution of the wetland LULC as well as the upland areas of the wetland boundary .

Introduction

Grand Bay NERR, a 7446 ha estuary, is located in southeastern Jackson County Mississippi. This region includes the Louisianian biogeographic region and is located in the Mississippi Deltaic subregion. Grand Bay consists hosts several different wetland habitats which together forms a large intact coastal watershed. Grand Bay over the past decade has experienced significant changes over the past decade due to anthropogenic activity, catastrophic events and natural environmental phenomenon. There is a need to evaluate the changes to Grand Bay after events such as the BP Oil spill, phosphorus spill, Hurricane Katrina, and shoreline erosion [2].

Remote sensing techniques have been used to determine the biological extent of wetlands for the past 25 years. Remote sensing

techniques used for wetland change is one of the most commonly used techniques to evaluate the change in environment. Remotely sensed data provides the primary data source for wetland change detection. The data provides an accurate account of land classes and their changes over time.

Experiments and Conclusions

The aim of this research project was to assess the land cover change from 2005 to 2015 and to estimate the percent change among parameters. Satellite imagery was acquired from 2005 and 2015. A supervised classification was performed using ERDAS software to classify the classes of the two datasets. The area was classified into seven main classes: water, forest, tidal marsh, high marsh, shrubbery, and constructed area. A comparison was developed by estimating the total hectares of each parameter for both

datasets and comparing them to each other. The results reveal a slight change but not a significant change in the tidal marsh, bare and constructed area. The tidal marsh decreased by 321.93 hectares from 2003 to 2015, which was less than a 4% change. There was an increase in the constructed area from 2003 to 2015. The surrounding built-up areas are growing businesses and communities.

References

[1] Nicholls, R.J. 2004. Coastal flooding and wetland loss in the 21st century: changes under the SRES climate and socio-economic

scenarios. *Global Environmental Change*, 14:69-86.

[2] Evans, Eric D., Yerramilli Anjaneyulu, and Paul B. Tchnouwou. "Effects of Hurricane Katrina on land cover within the Grand Bay National Estuarine research reserve in Mississippi, USA." *Environmental and Food Safety and Security for South-East Europe and Ukraine*. Springer Netherlands, 2012. 173-188.

Acknowledgement

This work was supported by the NOAA ECSC Grant# NA11SEC4810001.

Decomposition of Black Mangrove (*Avicennia germinans*) leaf litter: calibrating estuarine indicators of functional recovery.

Leticia Contreras*, Alejandro Fierro-Cabo, and Carlos E. Cintra Buenrostro
University of Texas Rio Grande Valley (UTRGV), School of Earth, Environmental, and Marine Sciences

*Presenter and corresponding author. UTRGV. One West University Blvd. Brownsville, TX 78520. leticia.contreras01@utrgv.edu

Introduction

The continued loss of estuarine and wetland habitats due to natural and anthropogenic disturbance has triggered increasing efforts to restore them. Assessing recovery for estuaries using taxonomic-based metrics and community derived structural variables turns difficult due to biota well adapted to stress as a response to high spatial and temporal variability. The ability to tolerate natural stress also applies to anthropogenic stress, thus changes in structural metrics may not suffice to detect the effects of human intervention whether is degradation or restoration.

Functional characteristics including ecosystem processes such as litter decomposition and nutrient transformations have been considered as potentially more robust ecological indicators than community derived metrics. It has been demonstrated that rates of mass loss of submerged litter are affected by stressors such as increased acidity and nutrient concentrations. Functional characteristics can thus provide useful insight on estuarine ecosystem status, and can be utilized for developing a complementary or standalone assessment tool.

In a recent study, measurements of in situ decomposition and concurrent nitrogen (N) dynamics of black mangrove (*Avicennia germinans*) leaf litter effectively discriminated among four south Texas estuarine sites with different known disturbances. Potential use of these metrics as estuarine functional indicators requires an understanding of how they are affected by driving environmental variables.

Thus, a series of experiments under controlled conditions (i.e. microcosm) are being

conducted to determine the influence of salinity, temperature, water turbulence, and N availability on mass loss rates and N dynamics of decomposing black mangrove leaf litter. Results presented here focus on mass loss in order to verify the alternative hypothesis that these environmental variables can accelerate or repress this part of the litter decomposition process in estuaries.

Microcosm experiments

Experimental treatment levels were selected based on the ranges of environmental variables observed in the south Texas estuaries previously studied. Experimental units consisted of aquaria filled with 56 l of estuarine water. A known amount of dried black mangrove leaf litter collected from one local mangrove was placed in litter bags. For each experiment, each aquarium included 10 litter bags of which two were retrieved every 3, 7, 14, 30, and 60 days. Ash free dry weight of the remaining contents of the litter bags was recorded. The factorial salinity and temperature experiment had a completely randomized design, including three levels of salinity (S): low (20‰), medium (43‰), and high (66‰), and two temperature (T) levels: low (20°C) and high T (31°C). The experimental set up for the water turbulence experiment required the placement of a wave maker in the treatment with turbulence, and no modifications for the no- turbulence treatment. Regular monitoring was done to ensure water movement. In order to assess the effects of N availability, ammonium sulfate was used to

establish four N levels in the water: 1.5 mg/L, 3.0 mg/L, 4.5 mg/L, and 0 mg/L (control). The water turbulence and N availability experiments are currently in progress.

Results and conclusions

Results for the S and T experiment indicate that higher T and lower S promoted the greatest mass loss after 60 days, about 48%, whereas litter decomposing in lower temperature and higher salinity lost only about half this amount. A two-way repeated measures ANOVA showed significant differences among salinity and temperature treatments, and a significant interaction between salinity and temperature treatments (S: $F_{0.05}(2, 35) = 9.5$, $p = 0.005$; T: $F_{0.05}(1, 35) = 10.3$, $p = 0.02$; S x T $F_{0.05}(2, 35) = 9.2$; $p = 0.05$). Increased salinity seems to slow decomposition, but the effect is variable and depends on water temperature, which explains the observed interaction effect. Preliminary

results point at water turbulence considerably increasing mass loss of leaf litter compared to the no turbulence treatment, and availability of N having a variable effect on litter mass loss. The use of mass loss derived metrics as functional indicators should consider its application on estuarine sites with a similar salinity regime and comparable water temperatures.

Acknowledgement

This study was supported and monitored by National Oceanic and Atmospheric Administration (NOAA) under Grant – Environmental Cooperative Science Center (ECSC) Grant # NA11SEC4810001. The statements contained within the manuscript/research article are not the opinions of the funding agency or the U.S. government, but reflect the author's opinions.

**Impacts of natural- and human-induced disturbances on Estuarine Wetland Ecosystems:
Case study from Grand Bay National Estuarine Research Reserve (NERR), Mississippi,
USA**

Ranjani W. Kulawardhana¹, Taimei T. Harris¹, Eric M. Gullett¹, Fengxiang X. Han², & Paul B. Tchounwou¹

¹*Department of Biology, Jackson State University, Jackson, MS 39217*

²*Department of Chemistry, Jackson State University, Jackson, MS 39217*

Abstract

The goal of this study was to understand impacts of natural and human-induced disturbances on wetland LULCC of the Grand Bay NERR, Mississippi, USA. Specific objectives were to: 1) evaluate and quantify LULCC within estuarine wetland extent and its immediate surrounding from 2003 to 2015; 2) understand if the changes observed were due to the errors associated with classification algorithms and/ data rather than actual change on ground; and 3) to evaluate the impacts of shoreline change (as affected by rising sea levels and shore line erosion), and increased human disturbances (as reflected in upland LULC conversions) on wetland LULCC. We applied a remote sensing based LULC change modelling approach using medium- to very high-resolution remote sensing data (Landsat and Worldview 3 data, respectively). LULC maps were verified using ground observations and were used to derive LULCC maps that we used to map and evaluate spatial extents of the changes in each LULC class. Our findings indicated that the GB NERR wetland extent has remained nearly constant over the past decade (i.e. marsh extent has decreased by 4%). Expansion of upland area (forests) has mainly contributed to this shrinking of marsh extent. Further, comparisons between two LULC maps did not revealed any signs of marsh submergence or subsidence along the shoreline and thus indicated no quantifiable effects of sea level rise on marsh vegetation and wetland LULC. However, given the data limitations used in this study, (i.e. 30 m resolution of Landsat data) it is possible that our LULCC modelling approach may not have detected some fine scale changes (i.e. changes of <30m extent) resulting from sea level rise. Our findings also indicate that the GB NERR remains as intact wetland ecosystem with minimal or no disturbances in terms of LULC conversions over the study period. However, further analyses would be necessary to evaluate vegetation health and condition of the wetland extent for complete understanding on the impacts of multiple stressors including land conversions and water pollution in the upper catchment area.

Introduction

Estuarine wetland ecosystems serve many ecosystem products and services. Among many others, their role as future terrestrial carbon sinks remains crucial¹ in particular under climate change scenarios. These resource rich, high productive environments

are however under a number of threats. Conversion of wetlands to other land uses that include commercial, urban, and open water² due to submergence and/ subsidence^{3,4}; and 2) climate change, in particular, sea level rise⁵ and increases in hurricane intensity and frequency⁶ are recognized as the most

significant threats. Over the recent past, several studies examined coastal wetland losses due to the effects of these multiple stressors^{2,7,8}. Their findings indicate that the rate of wetland loss have been rapidly increased over the past few decades. For example, in the Eastern United States alone the average rates of wetland loss were about 59, 000 and 80,000 acres per year during the periods from 1998 to 2004 and 2004 to 2009, respectively. While the majority of this loss occurred in freshwater wetlands that included both tidal and non-tidal, nearly 60 percent of this loss was attributed to the causes relating to both human activity and natural processes. Coastal wetlands, especially estuarine and marine wetlands, are naturally altered by high energy events such as erosion and inundation from sea level rise and storms. The impacts of these processes may be magnified by climate change and shoreline armoring. Estuarine wetlands typically protect the coastline from erosion and flooding, but if sea level increases and development prevents inland migration of wetlands, more wetlands will be converted to open water. However, the status and condition of these wetland ecosystems in particular their ability to sustain under changing climate conditions and increasing human disturbances vary largely depending on specific conditions and multiple stressors that affect each of the wetland ecosystems. Thus, it is important to evaluate how different wetland ecosystems have been affected by these multiple stressors and over time.

In this study we hypothesized that wetland vegetation in particular the amount of vegetation cover, their health and condition changes over time and space in response to the effects of these multiple stressors; and 2) these changes are recorded in remotely sensing data as wetland Land Use Land Cover Changes (LULCC) and thus quantifiable using multi-temporal remotely sensed data. The goal of this study was to understand impacts of natural and human-induced disturbances on

wetland LULCC of the Grand Bay NERR, Mississippi, USA. Specific objectives were to: 1) evaluate and quantify LULCC within estuarine wetland extent and its immediate surrounding from 2003 to 2015; 2) understand if the changes observed were due to the errors associated with classification algorithms and/ data rather than actual change on ground; and 3) to evaluate the impacts of shoreline change (as affected by rising sea levels and shore line erosion), and increased human disturbances (as reflected in upland LULC conversions) on wetland LULCC.

Experiments and Conclusions

To evaluate wetland LULCC we applied a remote sensing based LULCC modelling approach using medium- to very high-resolution remote sensing data (Landsat and Worldview 3 data, respectively). LULCC analyses were evaluated using Landsat data acquired in May 30, 2003 & May 23, 2015 while Worldview 3 data acquired in May 03, 2015 were used for the accuracy assessment and verification of LULC classification approach. LULC maps of 2015 were also verified using ground observations.

Our findings from LULCC analyses indicate the wetland extent has remained nearly constant over the past decade. For example, the marsh extent (low and high marshes) has decreased by 4% while the expansion of upland area (forests) has mainly contributed to this shrinking of marsh extent. Comparisons between two LULC maps did not revealed any signs of marsh submergence or subsidence along the shoreline and thus indicated no quantifiable effects of sea level rise on marsh vegetation and wetland LULC. However, given the data limitations used in this study, (i.e. 30 m resolution of Landsat data) it is possible that our LULCC modelling approach may not have detected some fine scale changes (i.e. changes of <30m extent) resulting from sea level rise. Our findings also indicate that the GB NERR remains as intact

wetland ecosystem with minimal or no disturbances in terms of LULC conversions over the study period. However, further analyses would be necessary to evaluate vegetation health and condition of the wetland extent for complete understanding on the impacts of multiple stressors including land conversions and water pollution in the upper catchment area

References

- [1] Chmura, G.L., Anisfeld, S.C., Cahoon, D.R., Lynch, J.C., (2003). Global carbon sequestration in tidal, saline wetland soils. *Glob. Biogeochem. Cycles* 17, 1111
- [2] T.E. Dahl and S.M. Stedman. 2013. Status and trends of wetlands in the coastal watersheds of the Conterminous United States 2004 to 2009. U.S. Department of the Interior, Fish and Wildlife Service and National Oceanic and Atmospheric Administration, National Marine Fisheries Service. (46 p.)
- [3] Craft, C., Clough, J., Ehman, J., Joye, S., Park, R., Pennings, S., Guo, H., Machmuller, M. (2009). Forecasting the effects of accelerated sea-level rise on tidal marsh ecosystem services. *Front. Ecol. Environ.*, 7, 73-78
- [4] White, W.A., Tremblay, T.A., (1995). Submergence of wetlands as a result of human induced subsidence and faulting along the upper Texas Gulf coast. *J. Coast.Res. Res.* 11, 788-807
- [5] Nicholls, R. J., Hoozemans, F. M., Marchand, M. (1999). Increasing flood risk and wetland losses due to global sea-level rise: regional and global analyses. *Glob. Env. Change*, 9, 69-87
- [6] Turner, E. R., Baustian, J. J., Swenson, E. M., Spicer, J. S. (2006). Wetland Sedimentation from Hurricanes Katrina and Rita. *Science*, 314, 449-452
- [7] Army Corps (U.S. Army Corps of Engineers - 2009). Mississippi Coastal Improvements Program (MsCIP), Hancock, Harrison, and Jackson Counties, Mississippi comprehensive plan and programmatic environmental impact statement. <<http://www.ms Cip.usace.army.mil>>
- [8] NOAA. (2010). Programmatic framework for considering climate change impacts in coastal habitat restoration, land acquisition, and facility development investments.

Acknowledgement

This study was supported by National Oceanic and Atmospheric Administration Environmental Cooperative Science Center (NOAA ECSC) Grant # NA11SEC4810001. The statements contained within the manuscript/research article are not the opinions of the funding agency or the U.S. government, but reflect the author's opinions.

Spatial Patterns and Temporal Dynamics of *Juncus roemerianus* Dominated Wetland Vegetation Characteristics and Carbon Stocks of Grand Bay National Estuarine Research Reserve (GBNERR), Mississippi, USA

Taimei T. Harris¹, Ranjani W. Kulawardhana¹, Eric M. Gullett¹, Fengxiang X. Han²,
and Paul B. Tchounwou¹

¹ Dept. of Biology, *Jackson State University*, Jackson, MS 39217

² Dept. of Chemistry, *Jackson State University*, Jackson, MS 39217

Abstract

Wetlands serve as important carbon sinks for atmospheric carbon. However, their role in the terrestrial carbon cycle is under-estimated, mainly due to the lack of reliable and timely estimates on their carbon stocks. Depending on their dense vegetation, algal activity and soils as wetlands experience high productivity in the ecosystem, they have a high capacity to sequester and store carbon. Within this background, this study was implemented with the goal of evaluating the carbon storage ability of the Grand Bay National Estuarine Research Reserve (GBNERR) of Mississippi, USA. Our specific objectives were to: 1) study spatial patterns and temporal dynamics; and 2) to evaluate factors affecting spatial variability of vegetation characteristics and carbon stocks of *Juncus roemerianus* (Black needlerush) dominated wetland habitats of GB NEER. Extensive field sampling from May 11, 2015 to September 24, 2015 was conducted to collect vegetation measurements on plant height, density, moisture, and biomass and carbon contents. Spatial patterns were evaluated using geospatial analytical techniques. *J. roemerianus* of our study area are characterized by relatively taller plants (mean plant height of 134 ± 21 cm), which is characteristic of the low marsh vegetation of this region, while the mean live shoot density is relatively low (mean of 354 per m²). Marsh vegetation of our study area is characterized by high productivity with a mean plant biomass density of 767 g per m², while the dead biomass accumulations over the marsh surface accounts for 60% of the total biomass indicating contributions from the previous season's growth.

Keywords: wetlands, vegetation characteristics, carbon, GBNERR

Introduction

Coastal wetlands supply useful products such as peat, and perform valued functions such as water purification and carbon storage [11]. Vegetated inter-tidal wetlands play an important role as carbon stores (*Wetlands and the carbon cycle*). Despite their small proportion of land extent, wetlands constitute as much as 25 percent of global terrestrial carbon [9]. Coastal wetland ecosystems such as salt marshes can sequester and store large amounts of carbon due to their rapid growth rates and slow

decomposition rates which contribute to a net annual carbon sink. Undisturbed wetlands are inclined to act as important carbon sinks due to their dense vegetation, algal activity, and soils characterized by very high carbon storage ability [10]. However, their capacity to absorb and sequester carbon varies widely depending on the site specific characteristics relating to vegetation, soil factors, climatic, & terrain [2].

All wetlands are capable of sequestering and storing carbon through photosynthesis and accumulation of organic matter in soils,

sediments, and plant biomass [3]. However, these rates vary substantially, both spatially and temporarily [4]. Castillo et al. [1] conducted an extensive review on salt marsh biomass that suggests studies that can capture significant variations in salt marsh biomass accumulation rates. Studies have linked elevation as an important factor in determining spatial distribution of salt marsh vegetation communities [5] [8] [6] [7].

This research is significant because the role of wetlands in the global carbon cycle requires further research, particularly on variants of wetland plants and their function as both sources and sinks of greenhouse gases (carbon). While recognizing the complex processes that occur in wetlands, wetland plants grow at a more expeditious rate than they decompose, contributing to a net carbon. According to the National Oceanic and Atmospheric Administration (NOAA) coastal wetland ecosystems (salt marshes, mangroves, and sea grass beds) can store large quantities carbon for two main reasons: Their plants usually grow a lot each year, and in the process, capture (or sequester) large amounts of carbon dioxide (CO₂) and their soils are largely anaerobic (without oxygen) so carbon that gets incorporated into the soils decomposes very slowly and can persist for hundreds or even thousands of years (carbon storage).

Experiments and Conclusions

Field sampling was conducted from May 11, 2015 through September 24, 2015. The time of the year was selected to match with the growing *Juncus Roemerianus*. This study used extensive field measurements on above ground vegetation characteristics (plant height, density, moisture, and biomass) and carbon estimates. Castillo et al. [1] proposed random sampling to be an appropriate

sampling method for pervasive and mature salt marsh communities. In this study, we applied systematic random sampling to incorporate spatial variations resulting from environmental and elevation gradients across the study area. Fifteen transects extending from water lines to uplands were randomly selected across the study area Northeast (Site 1), Middle (Site 2), & Southwest (Site 3) locations. Fifteen to forty sample plots of 65 cm x 65 cm area quadrants were selected along each transect for the collection of plant height, density, moisture, and biomass measurements once a month (every two weeks).

These vegetation characteristics revealed noticeable variations in their spatial distributions over the marsh extent characterized by localized patches of low and high biomass accumulations. These findings therefore indicate the necessity of further analyses to evaluate the factors that contribute to these spatial variations in vegetation characteristics including their productivity and thus the ability to sequester atmospheric carbon.

References

- [1] J. Castillo, A. Rubio-Casal, E. Figueroa, Sciyo.Com. (2010) 183.
- [2] J. Colletti, C. Hinz, R. Vogwill, M. Hipse, Ecol. Mod. **249** (2013) 3.
- [3] Y. Gao, G. Yu, N. He. Science. Direct. **57** (2013) 366.
- [4] R. Kulawardhana, S. Popescu, R. Feagin, Rem Sen of the Environ. (2014).
- [5] K. McKee, W. Patrick, Estuar. **11** (1988) 143.
- [6] J. Morris, P. Sundareshwar, C. Nietch, B. Kjerfve, D. Cahoon, Ecol. **83** (2002) 2869.
- [7] S. Mudd, S. Fagherazzi, J. Morris, D. Furbish, Eco of Tidal Mar. (2004) 165.

- [8] [National Oceanic and Atmospheric Administration \(NOAA\) National Ocean Service.](#)
- [9] S. Pennings, R. Callaway, *Ecol.* **73** (1992) 681.
- [10] J. Wang, S. Dodla, *LA Agr Magazine.* (2013).
- [11] Wetlands and the carbon cycle, (2014).
- [12] J., Zedler, S. Kercher, *Environ Resour.* **30** (2004) 39.

Acknowledgement

This study was supported and monitored by National Oceanic and Atmospheric Administration (NOAA) Environmental Cooperative Science Center (ECSC) at Jackson State University, Grant # NA11SEC4810001. The statements contained within the manuscript/research article are not the opinions of the funding agency or the U.S. government, but reflect the author's opinions.

A framework for conducting riverscape genetics studies

Chanté Davis¹, Flitcroft, R.L.², and Banks, M.A.¹.

¹*Oregon State University Department of Fisheries and Wildlife, 2030 Marine Science Dr., Newport, OR 97365*

²*US Forest Service, Pacific Northwest Research Station, Corvallis Forestry Sciences Lab*

Abstract

Research in landscape genetics has provided new insight into the role of past events in shaping present genetic diversity, and the effectiveness of conservation measures on observed genetic variation. Recent publications have provided designs for conducting landscape genetic studies and improving statistical methods for analyzing landscape effects on genetic variation, but in this context the river functions only as a feature on the landscape rather than as the landscape itself. Aquatic ecologists continue to develop conceptual models for understanding riverine landscapes (riverscapes) by including the physical habitat, processes that produce and maintain those habitats, and the inherent physical structure of the stream network. We present a framework for the design of a riverscape genetics study. In the riverscape framework we describe how to establish a sampling design while considering the spatial scale, and unique hydrologic characteristics of freshwater habitats. We describe analytical tools that are available for the integration of genetic and spatial environmental data in aquatic environments. Our framework provides a first step toward the formation of theory, analytical tools, and methods for the developing field of riverscape genetics.

Introduction

Application of molecular tools in ecology has expanded and improved our ability to characterize patterns of genetic diversity, assess levels of hybridization, and improve management and conservation strategies. While we have progressed a great deal, we still lack a basic understanding of the processes that drive genetic diversity and evolutionary responses in organisms. Within molecular ecology, the field of landscape genetics has emerged as a way to advance our understanding of the processes that are driving patterns of genetic structure in terrestrial habitats through integration of spatial statistics, population genetics, and landscape ecology¹⁻³. While much of landscape genetics research is conducted on terrestrial systems, marine and freshwater ecologists also approach community dynamics from a perspective of habitat heterogeneity⁴⁻⁶. Traditionally landscape geneticists treat

bodies of water as features on the landscape, elements that are linked to terrestrial habitats, and barriers to gene flow⁷⁻⁹. Only recently aquatic systems have been modeled as landscapes in their own right with heterogeneous and diverse patches within them¹⁰⁻¹⁶. From this “riverscape” perspective, we describe how to establish a sampling design while considering the spatial scale, and unique hydrologic characteristics of aquatic habitats.

Water is the major homogenizing force in freshwater and estuarine aquatic habitats creating and maintaining linkages throughout the network of available habitats based on the directionality of flow. Terrestrial systems do not have a force that uniformly impacts habitat context in a similar way. The forces that drive the distribution of habitats within marine and

freshwater are directly linked to the frequency, duration, timing, or rate of change of water discharge¹⁷⁻¹⁹. In freshwater systems the seasonal and temporal variation in discharge creates discrete habitat patches, continuous gradients, and fragmentation across the landscape. The resulting heterogeneous environment forms selective pressures that, in combination with genetic drift, lead to adaptation of life history traits.

Over the past quarter century the way we think about spatial heterogeneity in aquatic environments has transformed. Empirical research has identified a greater complexity of habitat arrangements leading to improved models that include network structure, temporal environmental heterogeneity, hydrodynamic forces and hierarchical structure²⁰. Processes, like perturbation, disturbance, and flow hydrology have been identified as variables that maintain this great complexity of habitat¹⁸. Aquatic systems are indeed as complex as terrestrial systems but the processes that underlie the complexity are fundamentally different and require a new suite of theoretical frameworks to deal with them.

We present a framework for the design of a riverscape genetics study. We describe analytical tools that are available for the integration of genetic and spatial environmental data in aquatic environments. The eight-step framework we developed outlines the workflow for conducting analysis that may lead to understanding of processes underlying genetic patterns in freshwater landscapes. The steps are: 1) Define a study objective, 2) understand organismal life history and establish an appropriate scale for research to be conducted, 3) develop a robust sampling design that will produce sufficient spatial resolution 4) conduct genetic analysis, 5) conduct riverscape or spatial aquatic landscape analysis 6) Integrate genetic and riverscape data 7) develop riverscape genetics theory and finally, 8) applications for

management. We hope that this framework will encourage continued development of analytical tools and theory that will enrich understanding of aquatic systems and improve our ability to manage and conserve them.

Conservation of species requires that we understand how gene flow is impacted by geographic and environmental characteristics. Geographic distance and environmental variables are correlated and identifying how each factor impacts genetic variation is difficult at best. Nonetheless, the ability of conservation and management to ensure long-term viability of populations is dependent on understanding how the processes described effect natural genetic connectivity. Our framework provides a step toward the formation of theory, analytical tools, and methods for the application of landscape genetics research in aquatic habitats.

References

- [1] Manel, S., Schwartz, M. K., Luikart, G. & Taberlet, P. *Trends in ecology & evolution* **18** (2003) 189-197.
- [2] Holderegger, R. & Wagner, H. H. Landscape Genetics. *BioScience* **58** (2008) 199-207.
- [3] Segelbacher, G. *et al.* *Conservation Genetics* **11** (2010) 375-385.
- [4] Le Pichon, C. *et al.* *Environmental management* **37** (2006) 322-335.
- [5] Johnson, L. B. & Host, G. E. *Journal of the North American Benthological Society* **29** (2010).
- [6] Steel, E. A. *et al.* *Living Rev. Landscape Res* **4** (2010) 1-60.
- [7] Wang, I. J., Savage, W. K. & Shaffer, H. B. *Molecular ecology* **18** (2009) 1365-1374.
- [8] Trumbo, D. R., Spear, S. F., Baumsteiger, J. & Storfer, A. *Molecular ecology* **22** (2013).
- [9] Watts, A. G. *et al.* *Frontiers in Genetics* **6** (2015) 275.

- [10] Kanno, Y., Vokoun, J. C. & Letcher, B. H. *Molecular ecology* **20** (2011) 3711-3729.
- [11] Hopken, M. W., Douglas, M. R. & Douglas, M. E. *Molecular ecology* (2012), 1-16.
- [12] Ozerov, M. Y., Veselov, Alexey E., Lumme, J., Primmer, Craig R. & Moran, P. *Journal of Fisheries and Aquatic Sciences* **69**, (2012) 1947-1958.
- [13] Landguth, E. L., Cushman, S. A., Murphy, M. A. & Luikart, G. *Molecular ecology resources* **10** (2010) 854-862.
- [14] Landguth, E. L. *et al. Ecological Applications*, **19** (2013).
- [15] Pilger, T. J., Gido, K. B., Propst, D. L., Whitney, J. E. & Turner, T. F. *Conservation Genetics* **16** (2015) 875-888.
- [16] Le Pichon, C., Tales, E., Gorges, G., Baudry, J. & Boet, P. *J Freshwater Ecol* **31** (2016) 1-19.
- [17] Junk, W. J., Bayley, P. B. & Sparks, R. E. *Canadian Journal of Fisheries and Aquatic Sciences* **106** (1989) 17.
- [18] Poff, N. L. *et al. BioScience* **47** (1997) 15.
- [19] Rolls, R. J., Leigh, C. & Sheldon, F. *Freshw Sci* **31** (2012) 1163-1186.
- [20] Vannote, R. L., Minshall, W. G., Cummins, K. W., Sedell, J. R. & Cushing, C. E.. *Canadian Journal of Fisheries and Aquatic Sciences* **37** (1980) 130-138.

Acknowledgement

Funding for this research was provided by CTSI, the Coastal Oregon Marine Experimental Station (COMES), the Living Marine Resources Cooperative Science Center (LMRCSC #NA11SEC4810002) and NOAA/EPP/MSI Graduate Research Training Fellowship.

New VIIRS Satellite Ocean Color Products for Management of Land-Based Sources of Pollution over Coral Reefs

Alan E. Strong^{1,2}, Menghua Wang³, C. Mark Eakin¹, Erick F. Geiger^{1,2}, Robert A. Warner⁷, William Skirving^{2,5}, Gang Liu^{1,2}, Scott F. Heron^{2,5}, Kyle V. Tirak^{1,2}, Michael Ondrusek³, William J. Hernandez^{2,6}, Maria Cardona-Maldonado⁴, *Roy A. Armstrong^{4,6}, and Jacqueline L. De La Cour^{1,2}

¹ NOAA/NESDIS/STAR Coral Reef Watch, College Park, MD 20740, U.S.A.

² Global Science & Technology, Inc., Greenbelt, MD 20770, U.S.A.

³ NOAA/NESDIS/STAR, College Park, MD 20740, U.S.A.

⁴ NCAS at University of Puerto Rico, Mayaguez 00680, Puerto Rico

⁵ NOAA Coral Reef Watch-ReefSense, Townsville, Queensland 4817, AUS

⁶ NOAA-CREST, City College, New York, NY 10031, U.S.A.

⁷ NOAA/NOS/NCCOS Silver Spring, MD 20910, U.S.A.

* = Presenter, roy.armstrong@upr.edu

Abstract

A NOAA multi-line office collaboration led by NESDIS/STAR/CRW, EPP/MSI with CREST and NCAS at UPRM, and NOS/NCCOS, is developing a suite of coastal ocean color satellite products for watershed managers to monitor runoff from high precipitation events in near real-time. Evaluating the impact of light, temperature and water quality following heavy precipitation events and how these relate to the health of coastal reef communities are the main focus of these efforts. The NOAA/STAR/CRW products of interest, the diffuse attenuation coefficient at 490 nm (K_d [490]) and chlorophyll *a* (Chl-*a*), derived from the *Visible Infrared Imaging Radiometer Suite* (VIIRS), are essential for assessing land-based sources of pollution.

Introduction

Land-based sources of pollution (LBSP) are a major threat to corals that can cause disease and mortality, disrupt critical ecological reef functions, and impede growth, reproduction, and larval settlement. NOAA's Coral Reef Watch (CRW) program and the NESDIS Ocean Color Team are developing new products to monitor LBSP over coral reef ecosystems using the Visible Infrared Imaging Radiometer Suite (VIIRS) onboard the S-NPP satellite. From VIIRS, near-real-time satellite products of Chlorophyll-*a* and $K_d(490)$ are being developed for three U.S. Coral Reef Task Force priority watershed sites - Ka'anapali (West Maui, Hawai'i), Faga'alu

and Vatia Bays (American Samoa), and Guánica Bay (Puerto Rico). In many cases managers and stakeholders do not have appropriate monitoring tools to evaluate these water quality parameters and establish best management practices.

Experiments and Conclusions

Long-term monitoring of water optical properties, temperature and physiological responses to different stressors is required to examine the impact of LBSP on coral reef community structure, diversity, and health. Field sampling is being conducted for simultaneous retrievals with satellite data and to evaluate the spatial and temporal variability

of biogeochemical properties. Current efforts in Guanica and La Parguera include the sampling of inherent and apparent optical properties and water quality at eleven stations. Profiles of spectral downwelling irradiance and upwelling radiance were obtained using a Satlantic HyperPro profiler equipped with two MicroPro submersible hyperspectral radiometers that provide 148 channels (from 350 to 800 nm). These measurements from the Satlantic are important for deriving the attenuation coefficients of downwelling irradiance (K_d) and the water-leaving radiance (L_w) for validation and calibration of satellite-derived ocean color products. Water-leaving radiance and the above-surface downwelling irradiance were measured using a GER 1500 spectroradiometer to calculate the remote sensing reflectance (R_{rs}). A Hydrosat-6 backscattering sensor is used to obtain the backscattering coefficient (b_b) at six wavelengths. The optical measurements were compared and calibrated with water samples measurements of total suspended solids (TSS), chlorophyll, and colored dissolve organic matter (CDOM) collected at each site. Current efforts for West Maui include the establishment of partnerships with the University of Hawaii Maui College, where students will be conducting field measurements and sampling as well as laboratory analysis. A transect was taken along West Maui in May 2016 to provide a baseline on the sampling procedures to be performed in that location. NOAA will be providing additional laboratory and field instrumentation for the students to use for the Ocean Color project. We have also established additional partners in Hawaii (Big Island) for additional *in situ* water mass data for calibration / validation. Initial discussions for Faga'alu and Vatia, American Samoa sites have begun with Kelley Anderson-Tagarino (American Samoa Community College) and Mia Comeros from the Environmental

Protection Agency (EPA) American Samoa. These collaborations will be further enhanced as the third year of the Ocean Color project progresses. Additional instrumentation that includes a spectroradiometer will be added for these efforts to provide cal/val data for VIIRS satellite products.

These *in situ* data are essential for satellite products' calibration and validation and algorithm development in near-shore environments. Matching large rainfall events to satellite-derived measurements for inspection by reef managers led to the development and refinement of the three priority watersheds and associated "Virtual Areas". Daily and weekly data composites will be analyzed for major rainfall events. VIIRS climatology, time-series and retrospective reports are important to identify critical periods of time for these events as well as monitoring the effectiveness in the implementation of sediment reduction measurements in the drainage basin. The analyzed data will be made available to local government agencies, watershed coordinators and NGO's that require this information through networked web mapping application. This poster will present preliminary results of these ocean color tools for water quality and the relevant steps to maximize their benefit to coral reef management.

Acknowledgements

This study was supported and monitored by National Oceanic and Atmospheric Administration (NOAA) under Grants # NA11SEC4810004 for NOAA CREST and NA11SEC4810003 NOAA NCAS Centers. The statements contained within the manuscript/research article are not the opinions of the funding agency or the U.S. government, but reflect the author's opinions.

Satellite Data Products for Coral Reefs in Southwestern Puerto Rico: In Situ Water Quality Measurements for Data Validation

*Suhey Ortiz-Rosa¹, William J. Hernandez^{1,2}, Roy A. Armstrong^{1,4}, Maria A. Cardona-Maldonado³, Jeremy Kravitz^{1,3} and Myrna J. Santiago⁴

¹NOAA-CREST UPR Mayagüez, ²Global Science and Technology Inc., ³UPR Mayagüez,

⁴NOAA-NCAS UPR Mayagüez

*Presenter: Suhey Ortiz-Rosa, suhey.ortiz@upr.edu

Abstract

Visible Infrared Imager Radiometer Suite (VIIRS) products and water quality data are being used to monitor land-based sources of pollution (LBSP) in southwestern Puerto Rico. This project is an effort to trace LBSP impacts on coral reef areas identified as local action strategies sites in Puerto Rico. We measure field optical properties and analyze water samples to improve satellite retrievals in this area using VIIRS. The chlorophyll-*a* concentration, total suspended solids (TSS) and colored dissolved organic matter (CDOM) values are compared to the corresponding satellite-derived products. A chlorophyll gradient was found from Gúanica Bay to La Parguera Natural Reserve. The values decreased offshore and towards La Parguera increasing again at nearshore waters. Preliminary data show chl-*a* ranging from 0.1 to 1.9 µg/L, TSS 15 to 33 mg/L and CDOM₄₁₂ 0.01 to 0.45 m⁻¹. We found unexpected high CDOM at some offshore sites where biogeochemical processes are responsible for *in-situ* CDOM production. These offshore high values, which have not been previously reported for this area, were likely driven by the presence of *Trichodesmium spp.* and *Sargassum spp.*, which were observed at these stations.

Introduction

Studies on spatial and temporal changes in chlorophyll-*a* and turbidity has been used as a proxy to determine coral reef health. These key parameters are essential for coral reef and water quality monitoring. We also measured Chromophoric Dissolved Organic Matter (CDOM) as part of the VIIRS calibration/validation activities. Chlorophyll values are indicative of phytoplankton biomass and can be related to nutrient inputs and outputs into aquatic ecosystems. Turbidity and CDOM are related to water clarity and also impact light transmittance into coral reef ecosystems. Turbidity has been reported as a major factor impacting the reefs from Gúanica to La Parguera. CDOM and chlorophyll have not been studied at large temporal and spatial

scales at this area. We explored the use of remote sensing to monitor land-based sources of pollution (LBSP) as well as chlorophyll and CDOM dynamics in southwestern Puerto Rico.

Experiments and Conclusions

We sampled eleven stations from Gúanica Bay to La Parguera including Bioluminescent Bay and two offshore sites. Sampling dates were planned to coincide with Landsat 8 overpasses unless cloudy conditions were encountered. A Satlantic Hyperpro Profiler was used to measure downwelling irradiance and calculate spectral attenuation coefficients.

For Chlorophyll-*a* measurements, water samples (triplicates) were taken from surface waters in 500 ml amber glass bottles, kept in the dark at 4°C and filtered through 0.7µm fiberglass filters during the same day. The filters were kept in dark conditions at -20°C until analyses or soaked in 90% acetone for 48 hours. Fluorometric analysis was conducted with a Triology™ Fluorometer (Turner Design) using non-acidification and acidification methods. For acidification, 2 drops of 10% HCl were added to the sample and fluorescence was measured again. Fluorescence was determined in relative fluorescence units (RFU) and converted to µg/L units using a chl-*a* standard according to Strickland and Parson (1972) [1]. Total Suspended Solids (TSS) was reported in mg/L using triplicate sea-surface filtered water samples. A SCUFA (Turner Design) instrument was used to measure turbidity and Chl fluorescence as ancillary data. CDOM measurements were based on duplicated surface water samples following the procedure described in Ortiz-Rosa (2010) [2].

Chlorophyll-*a* values ranged from 0.08 to 1.91µg/L, decreasing offshore, with higher values at Gúanica Bay (1.9 µg/L) and Bioluminescent Bay (1.2 µg/L). Unusual high Chl-*a* values (0.89 \pm 0.31 and 0.39 \pm 0.07 µg/L) were found at Gúanica offshore sites, possibly related to the presence of *Trichodesmium spp.* and *Sargassum spp.* In general, chl-*a* values are within the range previously reported for this area. Satellite-derived 10-year data (MODIS) for La Parguera area showed Chl-*a* average values ranging from 0.08 to 0.72 mg/m³ [3]. A positive linear regression was found between Kd₄₉₀ from the *in situ* Atlantic data and chl-*a* ($R^2 > 0.8$). Additional cloud-free imagery is required to validate VIIRS data products.

Turbidity in coral reefs influences calcification rates, photosynthesis and

decreasing light penetration [4]. TSS values ranged from 15 to 33 mg/L showing a low correlation with Kd₄₉₀ ($R^2 = 0.15$). However, SCUFA turbidity data showed a positive correlation with Kd₄₉₀ ($R^2 = 0.68$).

The absorption coefficient of CDOM₄₁₂ ranged from 0.01 to 0.45 m⁻¹. Values higher than 0.1 m⁻¹ were measured at the Gúanica offshore station on February and March 2016. These relatively high values are unexpected for clear, oceanic waters. In this case, we assume that autochthonous sources of CDOM are influencing the signal. The presence of *Trichodesmium spp.* is the likely source of this signal and not runoff from terrigenous sources from Gúanica Bay. We found unexpected values of TSS, chl-*a* and CDOM at some of the sampling sites. Additional retrievals for VIIRS data calibration/validation will provide insights into the influence of land-based sources of pollution in the biochemistry of surface waters in this area and their potential impact on coral reef ecosystems.

References

- [1] J.D. Strickland and T.R. Parson, Bull Fisheries Research Board Canada **167** (1972) 311
- [2] S. Ortiz-Rosa, MSc. Thesis, University of Puerto Rico-Mayagüez (2010)
- [3] G. García-Moliner, PhD Dissertation, University of Puerto Rico-Mayagüez (2013)
- [4] E. Otero, Caribbean Journal of Sciences **45** (2009) 168

Acknowledgements

This study was supported by National Oceanic and Atmospheric Administration (NOAA) under Grants # NA11SEC4810004 for NOAA CREST and # NA11SEC4810003 for NOAA NCAS Centers. Thanks to CARICOOS for the use of laboratory facilities, E. Troche, G. Gomez and T. Moya for laboratory assistance and E. Otero for the use of the SCUFA

instrument and helpful suggestions. The statements contained within this manuscript are not the opinions of the funding agency or the U.S. government, but reflect the author's opinions.

Improving coral reef science and management through collaborative efforts from NOAA Educational Partnership Program

William J. Hernandez^{1,2}, Maria Cardona-Maldonado³, Roy Armstrong^{1,2}, Portia Caldwell⁴, Endia Casely⁴, Charles Jagoe⁴, Marlene Kaplan⁵, William Skirving^{2,6,7}, Alan E. Strong^{2,7}, Robert A. Warner⁸.

¹NOAA-CREST UPR Mayaguez, ²Global Science and Technology Inc., ³NOAA-NCAS UPR Mayaguez, ⁴Florida A&M University, ⁵NOAA Office of Education/EPP, ⁶Coral Reef Watch-ReefSense, ⁷NOAA/NESDIS/STAR, ⁸NOAA/NOS/NCCOS

Abstract:

NOAA's Office of Education, Educational Partnership Program with Minority Serving Institutions (EPP/MSI) offers opportunities for student's participation in various projects submitted by NOAA scientists that are associated with four focused centers and corresponding NOAA line offices. The projects were focused on coral reef health from various research perspectives and the results of these collaborative efforts have established a quantitative assessment framework for evaluating the effectiveness of coral reef protection, recovery activities and initiatives by applying the best available technology.

Introduction

NOAA's Office of Education's Educational Partnership Program with Minority Serving Institutions (EPP/MSI) allows NOAA mentor scientists to submit opportunities for student participation. Once selected, the NOAA opportunity is circulated among students associated with four focused centers and corresponding NOAA line offices; the Environmental Cooperative Science Center (ECSC) / National Ocean Service (NOS), the NOAA Center for Atmospheric Science (NCAS) / National Weather Service (NWS), the Cooperative Remote Sensing Science and Technology (CREST) / National Environmental Satellite Data and Information Service (NESDIS), and the Living Marine Resources Cooperative Science Center (LMRCSC) / National Marine Fisheries Service (NMFS). We present four examples of successful partnerships between NOAA coral science projects in Hawai'i and Puerto Rico and EPP/MSI students and how these projects address the goals of bridging science to management and policy. These examples also

show how students can be integrated into science projects as key team members.

Experiments and Conclusions

The projects were focused on coral reef health from various research perspectives. Biomarkers and FIRE instrument were used for *in vitro* stressed corals and *in vivo* larval bundles from Kaneohe Bay and Pearl Harbor, Oahu. These were focused in evaluating the utility of Fluorescence Induction and Relaxation (FIRE) measurements, as a tool to assess photosystem responses to stressors in the symbiotic zooxanthellae living in corals from collected larvae exposed to pyrene, benzene, and gasoline. In addition, larvae exposed to bunker C, diesel fuel, copper and increased temperature were also analyzed using the FIRE instrument, which proved to be more sensitive to some stressors when compared with biomarkers. Another coral reef project was focused in using ocean color remote sensing and *in situ* measurements to monitor land-based sources of pollution to the coral reef areas. This multi-site ocean color project (PI Dr. Alan Strong) monitors land

runoff by using NOAA's operational satellite sensor, VIIRS and its derived products to provide monitoring tools for watershed managers for Guanica/La Parguera, Puerto Rico; West Maui, Hawaii [1]; and Fagalu, American Samoa [2]. The field sampling is being conducted for simultaneous retrievals with satellite data and to evaluate the spatial and temporal variability of biogeochemical properties and inherent and apparent optical properties. We are using a networked GIS project to allow a coordinated effort and data comparison and calibration between the different watersheds. A local implementation of the global Light Stress Damage (LSD) product is being conducted in southwest Puerto Rico. This algorithm is designed to use data from satellite-derived products for both temperature and solar radiation and their effects in coral reefs [3]. These efforts are part of a multi-agency initiative for the validation and calibration of NOAA's LSD algorithm. A temporal analysis of historical radiation and temperature data is currently being conducted at La Parguera, southwestern Puerto Rico in order to assess the forecasting capacity of the LSD algorithm.

In addition to the current research results, graduate students have received their Master degrees (2) and Doctoral degrees (1) using the project data for their research. Also, additional undergraduate and graduate students with support from NOAA EPP/MSI and other programs are currently working on this research as part of their projects. The results

of these collaborative efforts have established a quantitative assessment framework for evaluating the effectiveness of coral reef protection, recovery activities and initiatives by applying the best available technology.

References:

- [1] NELHA <http://nelha.hawaii.gov/>
- [2] Ocean Color <http://coralreefwatch.noaa.gov/satellite/research/oceancolor.php>
- [3] LSD <http://coralreefwatch.noaa.gov/satellite/lsd/index.php>
- [4] Aswani, S., P.J. Mumby, A.C. Baker, P. Christie, L.J. McCook, R.S. Steneck, R.H. Richmond. 2015 Scientific frontiers in the management of coral reefs. *Frontiers in Marine Science* 2, Article 50: 1-13.

Acknowledgements

The authors wish to thank Dr. H. Putnam (HIMB), and also the Navy ESTCP FIRE project team. This study was supported and monitored by National Oceanic and Atmospheric Administration (NOAA) under Grants # NA11SEC4810004 for NOAA CREST and NA11SEC4810003 for NOAA NCAS Centers. The statements contained within the manuscript/research article are not the opinions of the funding agency or the U.S. government, but reflect the author's opinions.

Evaluation of Oyster (*Crassostrea virginica*) Density and Slope at Natural and Restored Oyster Reefs in Coastal Georgia

P. Clower, T. Taubenheim, D. Hoskins

Savannah State University, NOAA Living Marine Resources Cooperative Science Center

Abstract

Oyster reefs have been restored along the east coast in an effort to recover the population of eastern oysters that used to be so abundant. These restored reefs have been monitored to assess what restoration methods work best. The purpose of this study was to determine whether the reef slope at these oyster reefs affected oyster density and to compare the mean oyster density between upper and lower sections of natural and restored reefs. Data were collected at low tides during the summer and assessed using SAS software (Cary, N.C.). The majority of variation in oyster density was not attributed to reef slope ($R^2 = 0.0197$). Oyster density differed significantly between the upper and lower sections of natural reefs ($p = 0.0002$). However, the difference between upper and lower sections of restored reefs was not statistically significant ($p=0.9302$). While slope did not impact oyster density significantly, choosing a location with a moderate slope is ideal. Natural reefs in coastal Georgia generally have a greater abundance of live oysters in the upper sections of reef, and in this study the majority of restored reefs are exhibiting this characteristic with the exception of a couple of sites. Future sampling of these restored sites will allow comparable timelines to observe the success or failure of restored oyster reefs.

Introduction

The Eastern Oyster (*Crassostrea virginica*) is the most prominent oyster in Georgia. Several decades ago, around 1980, the oyster fishery on the east coast crashed. In 1950, the eastern oyster catch from the Atlantic Ocean consisted of 25,348.9 metric tons and dropped to 2,675.5 metric tons in 2013 [1]. This loss was attributed to disease, habitat destruction, and overharvesting. The past few decades have consisted of efforts to restore the oyster population to its pre-crash level. Oyster reefs of the Savannah River estuary and surrounding areas generally consist of small patches of reef that occur throughout the marsh, along creek and river beds. This project is part of a larger effort to monitor these reefs since 2011 and to observe the success and changes of restored reefs.

The eastern oyster (*Crassostrea virginica*), ranges from the Lawrence River in Canada to the Gulf of Mexico [2]. *C. virginica* is reef forming, and depending on the tidal and

temperature differences, each reef system grows at different rates and different sizes, and can either be found in rivers, creeks, and throughout marshes depending on these factors [3]. Maturation of oysters can be affected by location, tides, temperature, and predation. Depending on these factors, it can take between one and five years for an oyster to mature [3]. The eastern oyster provides various benefits to the environment, including water filtration, food source, and shoreline stabilization to prevent erosion [4]. Oyster reefs provide an important habitat for many of species. One study conducted on an oyster reef in South Carolina observed over 87 resident and 60 transient species associated with the study [5]. Monitoring the Oyster reef is necessary to observe whether restored or constructed reefs are functioning and able to sustain themselves like natural oysters reefs.

Experiments and Conclusions

Nineteen oyster reef sites along the coast of Georgia have been monitored by the Savannah State Benthic lab since 2011. This project involved assessing 11 sites that were monitored in June and July of 2015 during low tide. At each oyster reef, three transects were measured perpendicular to the shoreline and subdivided into 1-m² quadrats. Within each quadrat the percentage of *Spartina*, shell (dead oyster, and other shells), live oyster, mud, and barnacles were recorded to the nearest 5 percent. The rugosity, or layout, of the reef was then measured using a 2-m metal chain that was laid horizontally across the quadrat and the distance covered is recorded. This information was then used in a modified equation ($R = 1 - \frac{D}{200}$) to calculate the rugosity of the reef. R is rugosity, D was the distance covered by the placed chain, and 200 is the length of the chain in centimeters. Reef height was measured from the sediment surface to the tallest point on the chain that was used for rugosity, using a metal ruler. Elevation was then measured by placing a laser level at the marsh edge and the height from the sediment surface to the laser is measured using a metal ruler. The rugosity and reef height of the oyster reef was collected haphazardly, human choice. A total of 20 measurements were made for rugosity and height, using the same method as before only at random, with 10 of these measurements focused in the upper half of the reef and 10 in the lower half of the reef. Then the density of the reef was measured. A total of six 0.25-m² quadrats, with three in the upper half of the reef and three in the lower, were randomly placed onto the reef and the number of live oysters, recently dead oysters, mussels, and clams are counted. Then up to 30 oysters are measured in millimeters, if applicable (some quadrats may not contain thirty live oysters), within the quadrat and recorded. A linear regression was used to assess the effect of reef slope on total oyster density (oysters/m²). A 2-

way ANOVA was used to test for interaction between reef site and reef section, and a 1-way ANOVA was used to assess the difference between upper and lower reef at individual sites. A 1-way ANOVA was also used to compare upper and lower sections of reef at natural and restored sites as a whole.

Slope did not affect oyster reef density in either the natural or restored reef sites. A 2-Way ANOVA was used to test for interaction between site and reef section and the interaction was significant ($p < 0.0001$). Therefore, reef sections were assessed at individual sites. The density of the restored reefs did not differ significantly ($p = 0.9302$) between the lower (207 oysters/m² ± 49) and upper reefs (213 oysters/m² ± 36), while the density of the natural reefs was significantly higher ($p = 0.0002$) in the upper reef (217 oysters/m² ± 30) than lower reef (33 oysters/m² ± 10). The restored reefs showed almost equal density among the lower and upper portions of the reef. When individual sites were assessed, mean density was significantly higher ($p = 0.0060$ and $p = 0.0009$; respectively) in the upper section at Turner's Creek (269 oysters/m² ± 38) and Moon River (164 oysters/m² ± 14) than the lower section (40 oysters/m² ± 20 and 25 oysters/m² ± 6; respectively). There were only two restored sites among nine that showed a significant difference between the upper and lower sections of reef. Density was significantly greater ($p = 0.0050$ and $p = 0.0078$; respectively) in the lower sections of Priest Landing (84 oysters/m² ± 8) and MAREX Moderate (760 oysters/m² ± 77). None of the other sites showed a statistically significant difference between the lower and upper sections.

References

- [1] Nat. Fish. Ser., Fish. Stat. Div. 2015.
- [2] V.S. Kennedy, MD Sea Grant. 1996.
- [3] L.D. Coen, M.W. Luckenbach. Eco. Eng. 15 (2000) 323-343.

- [4] L.D. Coen, Mar. Ecol. Prog. Ser. 341 (2007) 303-307. (Cooperative Agreement # NA11SEC4810002). The statements contained within the manuscript/research article are not the opinions of the funding agency or the U.S. government but reflect the author's opinions. This study also was supported by the SSU Bridge to Science in Marine Sciences Program (NSF-OCE 1156525 and NSF-OCE 1460457).
- [5] L.D. Coen, M.W. Luckenbach, D.L. Breitburg. Amer. Fish. Soci. Symp. 22 (1999) 438-454.

Acknowledgements

This study was supported and monitored by National Oceanic and Atmospheric Administration (NOAA) under the Living Marine Resources Cooperative Science Center

The 2014-2016 Global Coral Bleaching Event: Preliminary Comparisons Between Thermal Stress and Bleaching Timing and Intensity

Andrea M. Gomez¹, C. Mark Eakin², Jacqueline L. De La Cour^{2,4}, Gang Liu^{2,4}, Erick F. Geiger^{2,4}, Scott F. Heron^{3,4}, William J. Skirving^{3,4}, Kyle V. Tirak^{2,4}, Alan E. Strong^{2,4}, Kyle C. McDonald¹, Ana Carnaval¹
Email: Andrea.gomez@noaa.gov

¹*Ecosystem Science Lab and NOAA-CREST, City College of New York, New York, NY 10031, U.S.A.* ²*NOAA/NESDIS/STAR Coral Reef Watch, College Park, MD 20740, U.S.A.*

³*NOAA/NESDIS/STAR Coral Reef Watch-ReefSense, Townsville, Queensland 4817, Australia*

⁴*Global Science & Technology, Inc., Greenbelt, MD 20770, U.S.A.*

Introduction

Coral reefs cover less than 1% of the ocean floor yet contain a tremendous amount of biodiversity, providing habitat for over 25% of all known marine species (Burke *et al.* 2008). Tragically, at least 75% of Earth's coral reefs are currently threatened by natural and anthropogenic impacts (Burke *et al.* 2011). Rising ocean temperatures have increased the frequency of coral bleaching events. Multiple recent El Niño events have exacerbated the damage to corals from global warming. The extremely strong El Niño in 1997/98 triggered a global coral bleaching event that destroyed about 16% of the world's coral (Wilkinson 2000). Even during a mild El Niño year (2010), elevated ocean temperatures caused mass bleaching of reefs in many parts of the world (Heron *et al.* 2016b).

Currently during another record-strength El Niño event, another global bleaching event has been underway since mid-2014. The National Oceanic and Atmospheric Administration's (NOAA) Coral Reef Watch (CRW) is undertaking an effort to collect and document reports of the severity and extent of the ongoing bleaching event. CRW is collating bleaching data (including reports of no bleaching) from collaborators for the period 2014 through at least 2016. *In situ* bleaching observations are compared with CRW's satellite measurements of bleaching thermal stress to test CRW's thermal stress monitoring

products, including the Coral Bleaching HotSpot and Degree Heating Week products. This presentation explores the timeline of record thermal stress and bleaching occurring globally from 2014-2016 based on the comprehensive *in situ* bleaching observations CRW has collected to date. Preliminary results from comparisons of bleaching patterns with CRW's satellite products will be discussed for coral reef regions around the globe.

Experiments and Conclusions

Qualitative and quantitative spreadsheets were developed for collaborators to report coral bleaching. A bleaching event log was created to keep track of *in situ* observations of coral bleaching or no bleaching. Reports were collated and used to produce an ESRI story map and other communication tools.

CRW plans to continue monitoring, documenting and reporting on the current bleaching event. A global bleaching database of this event is also being developed. NOAA Coral Reef Watch's Four-Month Outlook indicates more bleaching could occur in the northern Indian Ocean, parts of the Coral Triangle and Southeast Asia, and the central to eastern tropical Pacific during June-September 2016. Bleaching is likely to return to the Caribbean and be particularly severe in the western Pacific Ocean. This global coral bleaching event may unfortunately continue into 2017.

References

[1] Burke L, Bryant D, McManus J, Spalding M (2008) Reefs at Risk. World Resources Institute (WRI): p56.

[2] Burke L, Reytar K, Spalding M, Perry A (2011) Reefs at Risk Revisited. Washington DC, World Resources Institute (WRI), The Nature Conservancy, World Fish Center, International Coral Reef Action Network, UNEP World Conservation Monitoring Centre and Global Coral Reef Monitoring Network: p114.

[3] Heron, SF, Eakin CM, vanHooidek R, Maynard JA (2016b) Coral Reefs. In Laffoley D and Baxter J (eds.) *Explaining ocean warming: causes, scale, effects and consequences*, International Union for the Conservation of Nature. In press.

[4] Wilkinson, C (2000) Status of Coral Reefs of the World: 2000. Australian Institute of Marine Science, Townsville, Australia.

Acknowledgement

This research is fully funded and supported by The National Oceanic and Atmospheric Administration – Cooperative Remote Sensing Science and Technology Center (NOAA-CREST) and the NOAA GRTSP Fellowship. NOAA CREST Cooperative Agreement #NA11SEC4810004. We would like to thank The City College of New York for the facilities and resources provided. We would also like to thank the NOAA Environmental Visualization Lab for helping to produce the ESRI Story Map. The statements contained within the manuscript/research article are not the opinions of the funding agency or the U.S. government, but reflect the author's opinions.

Offshore Oil Rig Decommissioning and Rigs-to-Reefs Programs in the Gulf of Mexico: Current Status and Strategies, and a Review of Decommissioning Cost Estimation

Elena Kobrinski

6300 Ocean Drive, Unit 5869, Corpus Christi, Texas 78412 elena.kobrinski@tamucc.edu
Harte Research Institute for Gulf of Mexico Studies

Abstract

Rigs-to-reefs programs are gaining popularity in the United States due to the release of the Idle Iron policy (2010) which cast light on many oil rig platforms being left 'idle' in the Gulf of Mexico. The goal of this study is to determine the reasoning behind idle structures, and how recent communication with regulatory agencies determined that requirements for cost estimation are placing pressure on the federal government to potentially cover decommissioning costs at the conclusion of the lease contract. Research objectives include: 1. What the most effective role is for rigs-to-reef programs to play in addressing the idle iron list, 2. How financial issues are inhibiting successful structural removal procedures, and how these issues are affecting rigs-to-reefs programs, and 3. How a public website and survey may provide transparency among all parties, providing a means of communication between stakeholders and the federal government to address problems in decommissioning operations that are currently not well understood. The research will also include a review of the United States decommissioning strategy, incorporating international perspectives and global case studies. Expected achievements in data collection and analysis include insight into how to update federal and state policies to assist decommissioning process efficiency moving forward.

Introduction

With over 5,000 active leases, almost 3,000 platforms and approximately 33,000 miles of oil- or gas-related pipelines, the Gulf of Mexico continues to be the most extensively developed hydrocarbon producing area in the world [2, 4]. As the global market faces decommissioning approximately 6,500 oil rig platforms by 2025 [1] it is clear that this region could greatly benefit from global collaboration.

The focus of this study is to research the national perspective on the United States decommissioning strategy in the Gulf of Mexico, taking a closer look at the recent interest in the development of various state rigs-to-reefs programs. The objective is to determine the reasoning behind idle or abandoned structures in the Gulf of Mexico,

and how oil and gas leasing sales and cost estimation play a role. Preliminary research and personal communication has determined that the current financial climate in offshore oil and gas decommissioning in the Gulf of Mexico is placing additional pressure on the federal government at the conclusion of the lease contract, and potentially impacting the funding of state supported rigs-to-reefs programs [3, 5].

This research study will address the intricate features associated with this issue in three chapters. The first chapter will provide an overview of oil exploration and extraction history, including legal, policy issues associated with decommissioning. Environmental, navigational and safety concerns associated with decommissioning

will be discussed. Current status in the Gulf of Mexico and California will be reviewed, with an exploration of global case studies. A focus will be on decommissioning cost estimation and the influence on rigs-to-reefs programs, specifically how current financial negotiations are influencing donations on the state level. The main question answered in this chapter will be what the most effective role is for rigs-to-reef programs to play in managing the idle iron list as a part of the “Idle Iron policy”, a policy released from the federal government in 2010 to address idle structures in the Gulf of Mexico.

The second chapter will synthesize and summarize data specific to the Idle Iron policy regarding abandoned and relinquished structures, from both a technical and financial perspective, with an emphasis on understanding the financial landscape of the leasing sales Five Year Program cycles (BOEM 2016 www.boem.gov). The goals of this chapter are three-fold: (1) to shed light on how to best manage and remove the existing idle iron infrastructure from a technical and financial perspective (2), how to create a regulatory landscape that secures financial assurance for structural decommissioning (removal or reefing) in the future and (3), how financial issues are inhibiting successful structural removal procedures, and how these issues are affecting rigs-to-reefs programs.

The third chapter will present a website with an associated survey that will be internally developed and revised as information is gained through the proposed research. Once the website is launched, it will provide education and a survey that will evaluate perceptions about current and relevant issues regarding offshore energy and

decommissioning strategies in the Gulf of Mexico. Survey results will be further developed into a predictive model. The goal of chapter three is to glean light on the complex issues that the nation faces in regard to current and future offshore oil and gas exploration in the Gulf of Mexico, and how education and collaboration could assist in addressing these issues by providing transparency among the government, stakeholders, and the public. It will conclude with recommendations and ideas for future research.

Experiments and Conclusions

Scientific experiments will not be conducted as this dissertation is a study of existing regulations and policies at the federal and state level in regard to decommissioning, with conclusions providing insight into how those regulations and policies may be improved. However, information obtained from a database provided by Earth Science Associates, coupled with more information following research into financial records will shed light on the reasoning behind relinquished leases and abandoned structures that will assist in providing suggested guidance in the management of existing infrastructure in the Gulf of Mexico.

Furthermore, the goal of the website and the results of the associated survey will contribute to the overall picture of what the best possible solutions are for effective management of oil and gas exploration on the Outer Continental Shelf, and will become valuable when providing recommendations at the conclusion of the study.

References

- [1] Booth, D. (2011). Environmental Scientists Urge That Decommissioned Oil Rigs Be Transformed Into Artificial Reefs. [www.forbes.com](http://www.forbes.com/sites/alexknapp/2011/04/13/environmental-scientists-urge-)
<http://www.forbes.com/sites/alexknapp/2011/04/13/environmental-scientists-urge->

[that-decommissioned-oil-rigs-be-transformed-into-artificial-reefs/](#)

- [2] BOEM (Bureau of Ocean Energy Management) 2016 www.boem.gov
- [3] BSEE (Bureau of Safety and Environmental Enforcement) Personal Communication, March 2015.
- [4] Kaiser, M.J. (2009). An update on the cost of decommissioning in the Gulf of Mexico, 2003 – 2008. *International Journal of Oil, Gas and Coal Technology*, 2, 89-120.
- [5] TWPD (Texas Parks and Wildlife Department) Personal Communication, 2015.

Acknowledgement

This material is based upon work supported by the National Oceanic and Atmospheric Administration, Educational Partnership Program, U.S. Department of Commerce, under Agreement No. NA11SEC4810001. Any opinions, findings, conclusions, or recommendations expressed in this publication are those of the author(s) and do not necessarily reflect the view of the U.S. Department of Commerce, National Oceanic and Atmospheric Administration.

Evaluating the Eastern Mosquitofish (*Gambusia holbrooki*) as a bioindicator species for endocrine disrupting chemicals.

Queriah Simpson¹ and Paulette C. Reneau²

¹Florida A&M University, School of the Environment

²Florida A&M University, Department of Biological Sciences, Corresponding author

Introduction

The use of xenotoxic chemicals has grown considerably with approximately 100,000 compounds currently being produced on an industrial scale and about 2000 new chemical species are introduced and released into the environment each year [1]. Chemical contamination is nearly ubiquitous in surface and ground water resulting from industrial products and processes and agricultural chemicals. Close to 800 chemicals are known or suspected to be capable of interfering with hormone receptors, hormone synthesis or hormone conversion. Some of the attributable effects of these environmental pollutants include a reduced fertility, hatchability and viability of exposed offspring, as well as impaired hormone activity and altered sexual behavior. Among the various effects documented is endocrine disruption – the alteration of the normal endocrine system by chemicals that mimic hormones or compounds that alter the synthesis, metabolism and activity of native hormones [2]. The Fenholloway River is a blackwater stream located in the Econfina Fiver Basin of northern Florida. It is 36 miles long and the Buckeye Florida pulp mill is the major point source discharge to the Fenholloway River. Since 1954, the Fenholloway River has received over 50 million gallons of effluent daily from the pulp mill, which has impacted the hydrology and water quality of the river [3]. Several studies have provided evidence that the pulp-derived phytosteroids in the paper mill effluent accumulate in river sediment where microbes convert them into

androstenedione and other bioactive steroids. Theses have been shown to act as endocrine disrupting chemicals (EDCs), mimicking natural hormone action by either agonizing/antagonizing hormonal effects, modifying hormone receptor structure, or recognizing/blocking hormonal binding sites. Data have shown that as much as 100% of the river water below the paper mill is effluent [3]. The study investigated the effects of pulp mill effluent on the live-bearing, Eastern mosquitofish – *Gambusia holbrooki*. The hypothesis tested was that fish exposed to pulp mill effluent regulate the expression of genes associated with reproduction and metabolism differently that those in a non-impacted site. The transcriptional activity of two key genes - vitellogenins (Vtg) and cytochrome P450 (cP450) – were quantified.

Experiments and Conclusions

Live fish were collected from the impacted river (Fenholloway River) and a nonimpacted river (Econfina River). All fish were sexed by determining the presence or absence of a urogenital papilla. Fish were flash frozen in liquid nitrogen. The anal fin of female fish were assessed for elongation under a stereoscopic microscope and documented. Livers and gonads of female fish were dissected and total RNA was extracted. The tissues were analyzed for Vtg and cP450 expression using quantitative real time PCR. Female fish exposed to the pulp mill effluent showed elongation of anal fins. Expression levels of hepatic Vtg and gonadal Vtg were low compared to non-impacted fish.

Conversely, expression levels of hepatic and gonadal cP450 were high compared to non-impacted fish. Endocrine disrupting chemical-related effects involve a direct increase in cP450 but a decrease in the relative expression of Vtg in both gonadal and hepatic tissues. The androgen exposure not only results in morphological changes but also results in decreased reproductive health.

References

- [1] M. Younes, Chemosphere 39(1999) 1253.
- [2] J. A. McLachlan, Endc. Rev. 22 (2001) 319.

- [3] FDEP, (2000) Tallahassee, FL.

Acknowledgement

This study was supported and monitored by National Oceanic and Atmospheric Administration (NOAA) under Grant – Environmental Cooperative Science Center Grant # NA11SEC4810001. The statements contained within the manuscript/research article are not the opinions of the funding agency or the U.S. government, but reflect the author’s opinions.

Polarization characteristics of light in water and their impact on the TOA radiances.

Carlos Carrizo, Gilerson, A., Foster R., Al-Habashi, A., Ottaviani, M.
NOAA CREST

Satellites, such as MODIS and most recently VIIRS make routinely “Ocean Color” measurements, intended as the collection of the spectrally dependent reflectance of the underlying water body. These measurements are used to retrieve the Inherent Optical Properties of the water, which can be parameterized as a function of the concentrations of phytoplankton, Color Dissolved Organic Matter, and mineral and non-mineral particulate hydrosols. However, the water-leaving radiance only accounts for less than 10% of the total TOA signal, with the remaining 90% coming from the atmospheric scattering, both molecular (Rayleigh) and particulate (Mie).

Recently, our CREST group has been investigating the (spectral) impacts of varying water conditions on the polarization state of the water-leaving radiance. These impacts and the polarizing effects of the atmosphere yield a partially polarized signal to the TOA. While MODIS and VIIRS satellite sensors are not designed to be polarization dependent, they exhibit, small, but still appreciable sensitivity to the polarization on the TOA radiances. Even when this sensitivity may seem small to be considered as part of the data processing routines of satellites such as VIIRS and MODIS, future mission can be affected if a proper correction of this effect is not taken into account.

Figure 3 below shows the impact of 10.5 mg/m^3 of Chlorophyll (common of coastal waters) to the TOA radiances for wavelengths in the visible and Near-IR. In most cases scalar treatment underestimates the TOA radiance with respect to more accurate vector radiative transfer (VRT) simulations. Relative differences higher than 10% are encountered at all modeled geometries when water constituents are added in excess (i.e. maximum concentration among typical values) and generally with higher values at shorter wavelengths.

Negative relative differences in the mid-visible for large concentrations of Chlorophyll are explained by larger absorption. Generally, decreasing absorption implies increasing scattering, which leads to depolarization. Negative relative differences for larger concentrations of CDOM and Chlorophyll in the blue-green are due to increased absorption and polarization.

Vector vs. scalar: Chlorophyll (10.5 mg/m³)

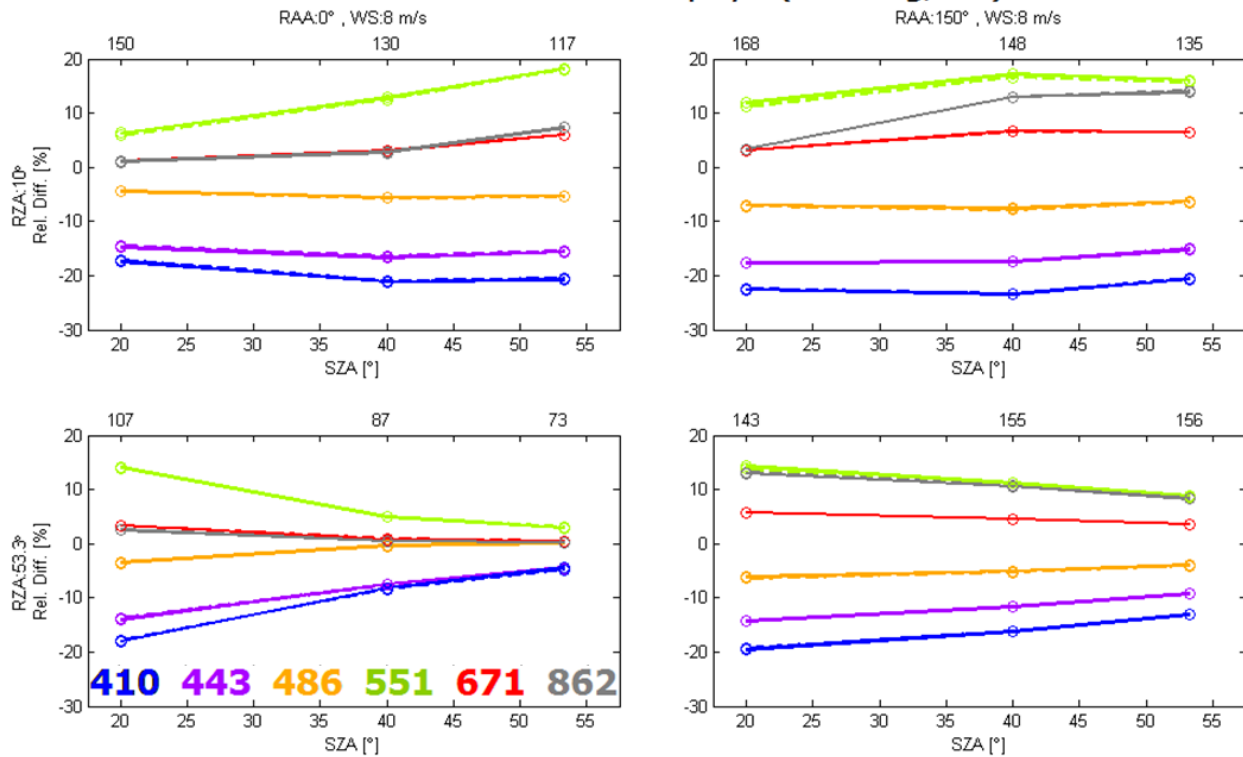


Figure 3: Impact of Chlorophyll concentration to TOA radiances.

Acknowledgement: This study was supported and monitored by National Oceanic and Atmospheric Administration (NOAA) under the NOAA Cooperative Remote Sensing Science and Technology Center Grant # NA11SEC4810004. The statements contained within the manuscript/research article are not the opinions of the funding agency or the U.S. government, but reflect the author’s opinions.

Urban Flooding Index Based on NYC311 Reporting Database

Sina Kashuk, PhD¹; Michael Grossberg, PhD²; Masoud Ghandehari, PhD³; and Reza Khanbilvardi, PhD⁴

¹NOAA-CREST Center, The City College of New York, CUNY, skashuk@ccny.cuny.edu

²NOAA-CREST Center, The City College of New York, CUNY, grossberg@cs.ccny.cuny.edu

³Center for Urban Science and Progress, NYU, Masoud@nyu.edu

⁴NOAA-CREST Center, The City College of New York, CUNY, khanbilvardi@ccny.cuny.edu

Abstract

Flooding is a major and often common yet complex environmental problem in urban environments. Its causes are manifold and its impact range from minor to cataclysmic. Yet because of the complexity in the urban topography, it is difficult to maintain flood maps over time. Flooding, for example of a building basement, may be invisible is often be satellite based measurement, street cameras, or even civil monitoring systems. Crowd-sourced reporting provides a new way through use of NYC311 data. However, it is very difficult to use NYC311 data because we need to separate the inherent variability of reporting bias from the underlying phenomena. In this study, NYC311 calls were used to locate the areas of the city most vulnerable to flooding. A novel algorithm was presented to produce Urban Flooding Index (UFI), a spatial distribution of complaints which factor out reporting bias across New York City's five boroughs. The proposed methodology created a robust and reliable tool to extract information from a noisy open dataset. The results presented in this paper provide insights into which locations in the city are most vulnerable to flooding events.

Introduction

Flooding is most important, complex and common disasters that occur in the United States. It can manifest as a cataclysmic event from storm surge or flash flood. Or it could cause lots of very expensive damage over time. Seawater is amazingly corrosive. Water rusts and weakens reinforced concrete. Flooding can come from weather, change in underground rivers, damaged infrastructure, sea-level-tidal rise and many other factors. It also is invisible because satellites can see it but it may not be visible at all. A basement or underground shopping area may experience flooding but it may not be visible from the surface. In addition, cascading phenomena with adverse socioeconomic impacts may result, including loss of revenue from businesses, and repercussions to the well-being of local

inhabitants, agriculture, and environment. With increasing climate change and variability of weather extremes, and with a rising number of reported flood events and a growing population, the effects of flooding have become an expanding concern worldwide [1,2].

In order to assess future risks of flooding events and their impact on infrastructure, historical flood magnitudes need to be determined. However, direct measuring flood magnitude is not possible due to complexity of historical system and lack of high spatial resolution of sensor network in the urban areas. Therefore, when this direct measurement is not available, meteorological and hydrological predictive model are used as the best alternative. However, these models typically do not have the spatial or temporal resolution to provide flood risk data for assessment,

especially at the local scale. Moreover, these model are not well implemented in urban areas due to the complexity of urban hydrology systems and infrastructure such as drainage system [3].

In these study we examine the potential of using community reporting to measure impact of flooding on infrastructure. NYC311 call center is used as example of community reporting. “311” is the US Federal Communications Commission code assigned for non-emergency contact that allows residents of many cities to make requests for government services [4]. In New York City, NYC311 was launched in March 2003 as a toll-free non-emergency call center. NYC311 now encompasses a range of channels to exchange information, including a short message service, online portal, social media, and smartphone apps [5]. These service requests are then forwarded to the assigned agency which will inspect the incident and take further action as needed. All of requests are stored and publicly available on the NYC open data portal (<https://nycopendata.socrata.com>) by service type (“descriptor”) and responsible agency with fine-grained information on the date, time, and geographic coordinates, and location of issue reported. For example, a complaint about a pothole would be assigned to the Department of Transportation and filed as street condition for the service type. Most flood-related complaints are channeled through New York City Department of Environmental Protection [NYC DEP], which is in charge of the storm water drainage systems and can be considered as multiple service types such as sewer backup and street flooding.

Experiments and Conclusions

When considering NYC311 open data, the first question to ask is why these contacts, which include reports or complaints about incidents, are made. The primary reasons are either because of the objective existence of the problem or because of the local citizens’

tendency to report the problem. Minkoff (2015) studied these two causes under names ‘condition’ and ‘contacting propensity’ and connected them to a series of socioeconomic variables [6]. By understanding the impact of each socioeconomic variable on ‘contacting propensity’, the effects of the ‘contacting propensity’ could be mitigated. NYC311 contacts can also be used to measure or to indicate other concepts, such as community engagement, political participation, and social well-being [7,8,9].

In this study, we aim to use NYC311 flooding-related calls to determine the spatiotemporal frequency of flooding in a locality. The main challenges are: (1) spatial aggregation and (2) untangling condition and contacting propensity. (1) Different levels of spatial aggregation can be used, from borough level to zip code level to even census tract level. If the resolution is too coarse we are not able to find the neighborhood with most problems. If the resolution is too fine, then we face the challenge of data starvation. In this study, rather than using any specific spatial level of aggregation, such as zip code aggregation, we used Kernel Density Estimator (KDE) to create density of calls at any given location.

(2) In order to extract the objective existence of the problem from the calls, spatial variation contacting propensity (in other words, the likelihood that a person in the area would call NYC311 to report the existing condition) has to be measured. To overcome this challenge, we proposed a robust algorithm that calculates spatial variation of contacting propensity. Later, this can be used as a normalizer to calculate actual flooding condition in each point of time and space, which we define as the Urban Flooding Index (UFI).

In order to use community reporting, in this case NYC311 calls, to locate the areas of the city most vulnerable to flooding, the spatial

density of complaints was mapped throughout the city. Using the top 25 most frequent complaint types, the overall propensity of calling was estimated and mapped. This map was then used to normalize the flood-related complaints map, creating the Urban Flooding Index map. Finally, the UFI map was compared with the elevation map. Low elevations tended to correlate with high frequency of flooding conditions, independent of tendency to call NYC311. Moreover, the monthly UFI tended to correlate with monthly rainfall intensity.

UFI has a vast variety of applications. The results of this study beget numerous other questions. Perhaps most obviously, the question of why specific neighborhoods are more vulnerable to flooding should be investigated. This would in turn allow for the definition of short and long term plans to reduce the vulnerability of these regions.

The applications of UFI could also have broader reach beyond flooding. For example, one can look at different neighborhoods with similarly high UFIs and examine them for similarities in the socioeconomic characteristics. This may help to point out systemic inequalities in terms of resource distribution. As an example, are neighborhoods where a high proportion of people live near the poverty line less likely to have the roads cleaned, leading to catch basin blockages and as a result flooding.

References

- [1] Cohen, B. (2006). Urbanization in developing countries: Current trends, future projections, and key challenges for sustainability. *Technology in society*, 28(1), 63-80.
- [2] Ashley, R. M., Balmforth, D. J., Saul, A. J., & Blanksby, J. D. (2005). Flooding in the future—predicting climate change, risks and responses in urban areas. *Water Science and Technology*, 52(5), 265-273.
- [3] Djordjević, S., Saul, A. J., Tabor, G. R., Blanksby, J., Galambos, I., Sabtu, N., & Sailor, G. (2012). Experimental and numerical investigation of interactions between above and below ground drainage systems. *Water Science and Technology*, 67(3), 535-542.
- [4] Nam, T., & Pardo, T. A. (2013). Identifying success factors and challenges of 311-driven service integration: a comparative case study of NYC311 and Philly311. In *Proceedings of the 46th Hawaii international conference on system sciences*.
- [5] Buzz, the official newsletter of NYC311, (2015), volume one, issue one. Retrieved from http://www1.nyc.gov/portal/apps/311_literatures/3-1-1/311NewlsetterMARCH2015.pdf
- [6] Minkoff, S. L. (2015). NYC 311 A Tract-Level Analysis of Citizen–Government Contacting in New York City. *Urban Affairs Review*, 1078087415577796.
- [7] Lerman, A. E., & Weaver, V. (2014). Staying out of sight? Concentrated policing and local political action. *The ANNALS of the American Academy of Political and Social Science*, 651(1), 202-219.
- [8] O'Brien, D. T., Gordon, E., & Baldwin, J. (2014). Caring about the community, counteracting disorder: 311 reports of public issues as expressions of territoriality. *Journal of Environmental Psychology*, 40, 320-330.
- [9] Trump, K. S., & White, A. (2015). Research Note: The Promises and Pitfalls of 311 Data.

Acknowledgement

The writers gratefully acknowledge the assistance our colleagues Gregory Dobler, Federica Bianco, Tim Savage, Tarendra Lakhankar, Filip Mlekicki, Milad Aghamohamadnia, Ali Hamidi, and Liron Shimrony.

High Temporal and Spatial Resolution Study of Morphological Response to Beach Management

Melanie Gingras^{1*}, James C. Gibeaut¹, Michael Starek² and Philippe Tissot²

¹*Harte Research Institute, Texas A&M-Corpus Christi, 6300 Ocean Drive, Corpus Christi, TX 78412*

²*Conrad Blucher Institute, Texas A&M-Corpus Christi, 6300 Ocean Drive, Corpus Christi, TX 78412*

Abstract

North Padre Island is a barrier island trending northeast to southwest along the southern portion of the Texas Gulf Coast which is a predominantly erosional microtidal, wave- and storm-dominated coast. The Texas Open Beaches Act permits vehicular traffic and provides for grooming conducted by the gulf cities. A growing concern has become the impact of grooming actions on both the health of wildlife and beach morphology. The goal of this study is to observe and monitor how grooming activities influence the moveable sand bed of the natural beach and a maintained beach on a relatively short time scale using a Terrestrial Laser Scanner (TLS). The TLS will perform scans every three days on a maintained beach and on an unmaintained beach. The point clouds will be transformed into Digital Elevation Models (DEMs) that will be differenced using map algebra to identify morphological changes between them. The sediment movement monitored by this time series of DEMs will determine how the beach is responding management practices, indicate whether or not these practices are harmful or disruptive to natural processes, and provide important insights into small-scale processes for modeling sediment transport and morphodynamics.

Introduction

The Texas Open Beaches Act (1959) provides for public access to all Gulf of Mexico beaches between the mean low tide line and the vegetation line. According §§61.062 of the Texas Natural Resources Code, it is the responsibility of the local governments of beach communities to clean and maintain public beaches. In a very broad sense, cleaning and maintaining refers to the removal of any hazards that may pose a threat to personal health or safety. In the proposed areas of study, Mustang Island and North Padre Island, beach maintenance is performed by the City of Corpus Christi, City of Port Aransas, and Nueces County. Maintenance in these areas includes beach grooming to

remove *Sargassum*, bolster dunes, and enhance accessibility. The type and frequency of maintenance is directly dependent upon the deposition rate of *Sargassum* on the beach and the priority assigned to the beach area by the municipality that maintains it as outlined by the City of Corpus Christi USACE Permit No. SWG-2006-00647 and from the City's Adaptive Beach Maintenance Plan [1]. In general (excluding Special Events Maintenance), from April to November, maintenance involves the removal of seaweed and sand which is subsequently relocated either to the foredune area and placed on the surface or to just landward of the mean tide line (MTL), in a shallow trench and buried. From November to April, sand is collected

from immediately in front of the dune and redistributed over the beach into a drivable 2” layer [2]. Since maintenance is both a costly and unnatural process and the Texas coast is vulnerable to submergence from sea level rise, subsidence, dam-related sediment restriction, and extreme weather events, studying the morphological and ecological consequences of maintenance is vital to both city planning and conservation efforts.

Studies are ongoing since there is a definite paucity of data regarding the possible repercussions of beach management but a few previous studies of maintained and unmaintained beaches have emerged bearing controversial results regarding changes to animal communities, vegetation, and beach morphology as direct consequences of management practices. A study by Dugan et al [3] found significant losses of shorebird prey that was linked to changes in bird community structure on groomed beaches in California. A more recent study by Smith, Harrison, and Rowland [4] in Australia found shorebird prey to be robust and found no lasting difference in infauna or bird community structure on groomed versus ungroomed beaches, which corroborated the findings of two Texas studies: one conducted in 1997 by the Padre Island National Seashore [5] and one conducted by HDR Engineering Inc in 2013 [6, 7]. A study in 2010 by Dugan and Hubbard [8] found that vegetation on groomed beaches is sparser and less diverse but this may not be a direct product of grooming but rather the secondary consequences suffered by a well-traveled beach [9, 10, 11]. However, some studies indicate that grooming may directly impact sediment transport by enhancing the amount of unconsolidated sand, which may influence backshore and foreshore dune elevation, bury vegetation, and elevate the number of blowouts produced during extreme events [8, 10, 12, 13, 14, 15, 16, 17]. The most recent study was completed in 2015 by the Harte Research Institute for Gulf of

Mexico Studies under the Coastal Erosion and Planning Response Act (CEPRA). It used quarterly dune surveys from September 2008-March 2015 to monitor seasonal beach changes, which remained unchanged over the years, LiDAR to compile digital elevation models (DEMs) to compute volumetric changes in dunes from 2005-2010, which were inconclusive due to anomalous jetty influence, and two vegetation surveys from December 2014 and July 2015, which corroborated Dugan and Hubbard’s findings in 2010. The inconclusiveness of the various beach management studies and the physical vulnerabilities of the study area necessitate further study of these practices to determine what impact, if any, maintenance has on the Texas coast.

The purpose of this project is to determine minute variations in sediment volume and beach morphology that result directly from beach management practices and to outline practices for continued high resolution monitoring. This detailed study, may allow beach managers to tailor beach management practices to best suit the current environment to promote beneficial changes to the beach and will provide detailed information for continued high-resolution monitoring as well as baseline data for modeling and extrapolation of future changes. The objectives for this study include 1) gathering high temporal and spatial resolution surveys to create detailed DEMs of various maintained and unmaintained beaches; 2) analyzing short-term volumetric changes in morphology of all surveyed beaches; 3) assessing the differences (if any) between sediment transport on groomed versus ungroomed beaches ; 4) determining if there is a way to improve beach management to foster healthy dune morphology and beach ecology; and 5) outlining practices for future high-resolution studies.

Experiments and Conclusions

A Riegl VZ 400 TLS will be utilized to conduct scans at a high maintenance site and a low to no maintenance site every three days for one month. Depending on weather, an initial test survey will be completed in June 2016 and the surveys for this study will occur throughout the month of July 2016 when maintenance and beach frequenting are at a maximum. The data collected from each survey will be statistically analyzed in Rstudio and point cloud data will be interpolated to generate digital elevation models (DEMs) using ArcGIS, LAStools, and Matlab AI applications. DEMs will be compared by differencing the before and after surfaces to generate a series of change surfaces which can be monitored through time and compared to determine the influences of natural physical processes and decipher management influences on sediment transport and beach morphology.

It is the expectation of this author that there will be differences in morphology and sediment volumetric changes between maintained and unmaintained beach. It is expected that the maintained beach will exude wider and flatter morphology with fewer bedforms present due to their destruction by scraping and vehicular traffic. It is equally likely that the maintained beach will experience more sediment loss from numerous sediment-loosening anthropogenic influences concomitant of vegetation destruction and burial by maintenance. Additionally, it is unlikely that vegetation will advance on maintained beaches due to constant scraping and vehicular traffic and the vegetation that is present is unlikely to have high diversity due to an inability of many plants to cope with the many anthropogenic disturbances. On the other hand, the natural beach is more likely to contain undisturbed aeolian and aqueous bedforms and accrete more sediment due to fewer sediment-loosening disturbances and superior vegetation growth and diversity.

References

- [1] The City of Corpus Christi, and Watershore Beach Advisory Committee. 2011. "Corpus Christi Gulf Beach Adaptive Management Plan."
- [2] Gibeaut, J., Del Angel, D., Lord, A., Luper, B., Lumb, L., Anderson, M. 2015. *Mustang and North Padre Island Beach Maintenance Impacts and Recommendations for Best Management Practices*. Harte Research Institute for Gulf of Mexico Studies, Texas A&M-Corpus Christi.
- [3] Dugan, J.E., D.M. Hubbard, M.D. McCrary, and M.O. Pierson. 2003. "The Response of Macrofauna Communities and Shorebirds to Macrophyte Wrack Subsidies on Exposed Sandy Beaches of Southern California." *Estuarine, Coastal and Shelf Science* 58: 25–40.
- [4] Smith, Stephen D.A., Matthew A. Harrison, and Jennifer Rowland. 2011. "The Effects of Beach Scraping on the Infauna of New Brighton Beach, Northern, NSW." A report for Byron Shire Council. Coffs Harbour: National Marine Science Centre, Southern Cross University.
- [5] Engelhard, T., and K. Withers. 1997. "Biological Effects of Mechanical Beach Raking in the Upper Intertidal Zone on Padre Island National Seashore, Texas." Center for Coastal Studies, Texas A&M University-Corpus Christi.
- [6] HDR Engineering, Inc. 2013a. "Habitat Monitoring Effort Report Year 3 (January 1, 2012-December 31, 2012)." Report submitted by the City of Port Aransas to the US Army Corp of Engineers as per conditions of the USACE permit SWG-2007-01847, prepared by HDR Engineering, INC. Corpus Christi, TX.
- [7] HDR Engineering, Inc. 2013b. "Habitat Monitoring Effort Report Year 4 (January 1, 2012-December 31, 2012)." Report submitted by the City of Corpus Christi to

- the US Army Corp of Engineers as per conditions of the USACE permit SWG-2006-00647, prepared by HDR Engineering, INC. Corpus Christi, TX.
- [8] Dugan, J. E., and D. M. Hubbard. 2010. "Loss of Coastal Strand Habitat in Southern California: The Role of Beach Grooming." *Estuaries and Coasts* 33 (1): 67–77.
- [9] Grunewald, R., and H. Schubert. 2007. "The Definition of a New Plant Diversity Index for Assessing Human Damage on Coastal dunes—Derived from the Shannon Index of Entropy H'." *Ecological Indicators* 7 (1): 1–21.
- [10] Houser, C., B. Labude, L. Haider, and B Weymer. 2013. "Impacts of Driving on the Beach: Case Studies from Assateague Island and Padre Island National Seashores." *Ocean & Coastal Management* 71: 33–45.
- [11] McAtee, Jerry W., and D. Lynn Drawe. 1981. "Human Impact on Beach and Fore-dune Microclimate on North Padre Island, Texas." *Environmental Management* 5 (2): 121–34. doi:10.1007/BF01867332.
- [12] Lancaster, N., and A. Baas. 1998. "Influence of Vegetation Cover on Sand Transport by Wind: Field Studies at Owens Lake, California." *Earth Surface Processes and Landforms* 23 (1): 69–82.
- [13] Nordstrom, Karl F., Nancy L. Jackson, and Katherine H. Korotky. 2011. "Aeolian Sediment Transport across Beach Wrack." *Journal of Coastal Research*, 211–17.
- [14] Nordstrom, Karl F, Nancy L Jackson, Katherine H Korotky, and Jack A Puleo. 2011. "Aeolian Transport Rates across Raked and Unraked Beaches on a Developed Coast." *Earth Surface Processes and Landforms* 36 (6): 779–89.
- [15] Nordstrom, K. F, U. Gamper, G. Fontolan, A. Bezzi, and N. L. Jackson. 2009. "Characteristics of Coastal Dune Topography and Vegetation in Environments Recently Modified Using Beach Fill and Vegetation Plantings, Veneto, Italy." *Environmental Management* 44 (6): 1121–35.
- [16] Hesp, P. 2002. "Foredunes and Blowouts: Initiation, Geomorphology and Dynamics." *Geomorphology* 48 (1-3): 245–68.
- [17] Conaway, C. A, and J. T Wells. 2005. "Aeolian Dynamics along Scraped Shorelines, Bogue Banks, North Carolina." *Journal of Coastal Research* 21 (2): 242–54.

Acknowledgement

This study was supported and monitored by National Oceanic and Atmospheric Administration (NOAA) under the NOAA Environmental Cooperative Science Center chapter at Texas A&M Corpus Christi Grant # NA11SEC4810001. The statements contained within the manuscript/research article are not the opinions of the funding agency or the U.S. government, but reflect the author’s opinions.

Ecosystem response to freshwater inflow: determining a link between freshwater pumping regimes, salinity, and benthic macrofauna

Elizabeth A. Del Rosario*, Paul A. Montagna

Texas A&M University-Corpus Christi, Harte Research Institute for Gulf of Mexico Studies

Corresponding author: Elizabeth Del Rosario

Address: 6300 Ocean Drive, HRI Suite 311, Corpus Christi, TX 78412

Email: edelrosario@islander.tamucc.edu

Introduction

The Nueces River Basin is one of the 15 major river basins in Texas, and is an important water supply for the Nueces-Rio Grande Coastal Basin area. The construction of two large reservoir dams in the Nueces River Basin has reduced the amount of freshwater reaching the Nueces Estuary by 99% from that of its historical flows [1, 2, 3]. The reduction of freshwater to the marsh has created a reverse estuary condition, where lowest salinity values are near Nueces Bay and the highest are in the upper delta. The City of Corpus Christi has been required to provide not less than 185 million cubic meters (151,000 acre-feet) of water per year to the Nueces Estuary by a combination of releases, spills, and return flows to maintain ecological health and productivity of living marine resources [4]. The City constructed a pump station and pipeline to convey up to 3.7×10^6 m³ (3,000 acre-feet) of freshwater directly into the Nueces Delta at Rincon Bayou. Inflow into Rincon Bayou is dependent upon pumped inflow with salinity and depth regimes in the Nueces Delta being controlled through management release actions. Haphazard pumping release, along with drought conditions, cause the salinity in Rincon Bayou to fluctuate from fresh to hypersaline, and hypersaline to fresh in very short time periods [5].

Experiments and Conclusions

The presence of benthos was represented by indicator species that were determined by the most numerically dominant species: *Streblospio benedicti*, Chironomidae larvae, and *Laeonereis culveri*. The biological responses of the indicator species to three physical variables (salinity, temperature, and depth) were examined using SAS 9.3 software and Microsoft Excel 2010. The optimal ranges in Rincon Bayou during the current study were determined by combining the ranges for the indicator species. The optimal salinity was between 1 and 15 psu for biomass and 1 and 14 psu for abundance, and the optimal depth range between 0.05 m and 0.2 m (2-7.9 inches).

There are several management recommendations that can be made for Station C in Rincon Bayou: 1) to improve ecological stability: inflows should be a trickle, not a flood, releases should be continuous and not haphazard, only one pump should be used at a time, and releases should not be dependent on pass-through requirements; 2) to maximize ecological function: salinity should be maintained under 20 psu, and water depth should be maintained between 0.05 m and 0.2 m; 3) to maintain ranges: inflows rates on the order of ≥ 0.00102 m³/s (0.084 acre-feet/day) are required to maintain salinities ≤ 20 psu, inflows on the order of ≤ 0.689 m³/s (48.261 acre-feet/day) are required to maintain a depth ≤ 0.5 m, and inflow on the order of 0.41 m³/s (28.72 acre-feet/day) will obtain an optimal

value for both salinity at 2.2 psu and depth at 0.2 m (7.9 inches).

References

- [1] HDR Engineering Inc. 2001. Water Management Strategies: Coastal Bend Water Plan. Corpus Christi (Texas).
- [2] Bureau of Reclamation (BOR). 2000. Concluding report: Rincon Bayou demonstration project [Internet]. Volume II: Findings. Austin (Texas): United States Department of the Interior, Bureau of Reclamation, Oklahoma-Texas Area Office. Available from: <https://archive.org/details/rinconbayoudemon00unit>
- [3] Irlbeck MJ, Ward GH. 2000. Analysis of the historic flow regime of the Nueces River into the Upper Nueces Delta, and of the potential restoration value of the Rincon Bayou Demonstration Project. Volume II: Appendix B. Austin (Texas): United States Department of the Interior, Bureau of Reclamation.
- [4] Texas Commission on Environmental Quality (TCEQ). 1992. Agreed order establishing Advisory Council to Special Condition B, Certificate of Adjudication No. 21-3214; City of Corpus Christi, et al. [Internet]. (March 4, 1992). Available from: http://tceq.com/assets/public/implementation/water/1992_agreedorder.pdf

- [5] Montagna PA, Adams L, Chaloupka C, DelRosario E, Gordon A, Herdener M, Kalke RD, Palmer TA, Turner EL. 2015. Effects of pumped flows into Rincon Bayou on water quality and benthic macrofauna [Internet]. Corpus Christi (Texas): Coastal Bend Bays & Estuaries Program project 1417. CBBEP-101. 46 p. Available from: <http://www.cbbep.org/manager/wp-content/uploads/CBBEP-1417-Final-Report.pdf>

Acknowledgement

This study was partially supported by the National Oceanic and Atmospheric Administration (NOAA) under Grant – Educational Partnership Program (EPP) Environmental Cooperative Science Center (ECSC) Grant # NA11SEC4810001. The statements contained within the manuscript/research article are not the opinions of the funding agency or the U.S. government, but reflect the author’s opinions.

The study was partially supported by Coastal Bend Bays & Estuaries Program grant numbers 1417 and 1617, and Texas Water Development Board Interagency Agreement number 1548311787 to Montagna. Partial support was also provided by the Harte Research Institute (HRI).

Resilience in the face of sea level rise: What do people value?

David Yoskowitz¹ and James Gibeaut¹

¹Harte Research Institute, Texas A&M University-Corpus Christi, 6200 Ocean Drive, Corpus Christi, TX 78411

Introduction

Sea level rise poses potential threats to not only built infrastructure but also to natural resources that provide numerous ecosystem services from which humans benefit. As sea level rises it is likely that the quality and distribution of our natural assets will change as well. For example, wetland losses or marked vegetation changes can result from accelerated sea level rise, which in turn can lead to significant changes in the provision of ecosystem services. In this study we assess the impact of sea level rise on ecosystem service resilience and the value that people place on it. Our study site is the greater Houston metropolitan area, home to over 6 million people.

One of the more important changes taking place along the Texas coast is sea level rise and more specifically, relative sea level rise in the Galveston Bay region. Sea level rise is not a hypothetical phenomenon, it is happening. The instrumental record for Galveston's Pier 21 has recorded a 0.60 meter increase in relative sea level over the last 100 years. To assess the potential impact that sea level rise may have on the region, this report will focus on two scenarios of sea level rise and the associated socio-economic impact for the next 100 years.

The three county region that surrounds Galveston Bay, and that will be impacted by relative sea level rise, is dynamic and heterogeneous. This region is significantly large in many respects. It totals over 2,700 square miles and has over 46,000 census blocks. The region has a combined population of 4.1 million, employment level of over 2 million and total personal income of \$183.2

billion. This region makes up 18% of Texas employment and population, and 20% of the households. The city of Houston, in the northwestern corner, is a large metroplex with a diversified economy that includes a major port and energy industry along with a large medical complex and numerous other diversified economic activities. Galveston, the city and county, has a mix of tourism, petrochemical industry and agriculture as the main economic drivers, and Chambers County is dominated by agriculture.

Low-lying coastal areas infrastructure and their stock is at an increasing risk to damage from sea-level rise inundation, extreme astronomical tides, storm surge flooding, hurricanes, and other storm events. This risk continues to increase due to the continuing growth of coastal cities and tourism. Damage cost estimations due to increasing sea level are often substantial [1, 2](Bates et al. 2008, Fitzgerald et. al. 2008).

Results

We model two scenarios of relative sea level rise for 100 years and an Ike level storm (100 year storm event): 1) 0.69 meters and, 2) 1.5 meters. For each of these scenarios we estimate the impact on the following variables: 1) displaced population (number of households); 2) expected number of buildings impacted, 3) building related economic loss, 4) industrial, hazardous, superfund, solid waste sites, and 5) water treatment plants.

Shoreline change is the position of the shoreline as it retreats landward or advances seaward as it reacts to the changes in sea level, storm occurrence, wave directions and heights, and sediment supply. Since shoreline change is caused by variable processes a

shoreline with a statistical trend of retreat over 70 years may experience periods of stability and advance seaward during other periods.

The rates for Galveston have been computed using shoreline data sets from 1930-2000. The area on the southwest side of Galveston Island, less than two miles from San Luis Pass is very dynamic due to processes associated with the San Luis Pass tidal delta. During 1995-2000 this area experienced shoreline advance in tens of meters, this is indicated (by examination of past shoreline positions) as a temporary situation and equally large amounts of retreat are likely in the future.

Projecting the socio-economic impact of sea level rise on the Galveston Bay region 100 years into the future is challenging. There are many confounding variables on the social and economic side of the equation as well as environmental. However, it is possible to illustrate what the impact would be if today's socio-economic characteristics were transported 100 years into the future or, impose the various sea level rise scenarios of 100 years onto today's economy. At the very least we get a sense of what we would face if nothing changed as it relates to the socio-economic characteristics of the region. Given the length of time (100 years) and uncertainty with regards to economic development, strong assumptions for the modeling process have to be made. They are: 1) Mitigation, adaptation, or resiliency measures that might take place to address relative sea level rise are not considered, and; 2) The socio-economic impact is based on the current conditions.

In order to calculate the socio-economic impact of sea level rise we utilize the Federal Emergency Management Agency's (FEMA) HAZUS- Multi-Hazard (MH) MR3 ArcGIS Extension. HAZUS-MH provides a risk-based approach to disaster management, risk mitigation, emergency preparedness, response, and recovery by identifying and displaying hazards and vulnerabilities.

HAZUS is a risk assessment tool for analyzing potential losses from flood, hurricane winds, and earthquakes. It allows users to develop loss estimation studies of hazard-related damage before or after disaster occurs using community datasets that come with the software including essential facilities, lifelines, general building stock, and demographic data

For the region, almost 99,000 households would be displaced under the 1.5m scenario. For Galveston County alone, 78% of the current number of total households would be displaced under the 0.69m scenario and 93% under the 1.5m scenario households. This would equate to about 1.3% of all the households in Texas and equivalent to the entire city of Corpus Christi (year 2000).

Over 75,000 structures are impacted to some degree in the region under the 1.5m scenario. Once again the regional impact is dominated by what happens in Galveston County, but Harris and Chambers are not exempt from the impact. The economic loss estimates for buildings are significant. Regional impact approaches \$12.5 billion dollars. To put that figure in perspective, it would equal 1% of Texas gross state product (2008).

Just as important as the socio-economic impact of sea level rise, is the impact on public facilities and industrial sites as it relates to waste storage or treatment. The environmental impact of an inundated waste treatment or holding facility could be significant under our two scenarios. Under the 0.69 meter scenario a total of 23 sites would be threatened or impacted. Most prominently waste water treatment plants but also 3 superfund sites. Under the 1.5 meter scenario a total of 33 sites would be impacted or threatened with 16 of those being wastewater treatment plants and 9 being solid waste sites. In order to protect the public from the potential environmental and health impacts, government agencies at all levels will be

required to expend resources on moving, mitigating, or protecting these sites. Finally, if Hurricane Ike were to come ashore with the sea level 0.69 meters higher, it would have caused an additional \$1.7 billion in damages, for a total of \$16.8 billion for the three counties only. That is equivalent to 1.3% of gross state product for Texas. The additional damage is also equivalent to the sum of the median income of 35.7 thousand Texas households.

References

- [1] Bates, B.C., Z.W. Kundzewicz, S. Wu and J.P. Palutikof, Eds., 2008: Climate Change and Water. Technical Paper of the Intergovernmental Panel on Climate Change, IPCC Secretariat, Geneva, 210 pp.
- [2] FitzGerald, Duncan M., Michael S. Fenster, Britt A. Argow, and Ilya V. Buynevich (2008). Coastal Impacts Due to Sea-Level Rise. Annual Reviews Earth and Planetary Science. **36**:601-647.

Using Radar Remote Sensing to Map Wetlands in the Chesapeake Bay For the Purpose of Understanding Carbon Cycling Processes

A. Brian Lamb¹, B. Maria Tzortziou¹ C. Kyle McDonald¹

¹The City College of New York, 160 Convent Ave, New York, NY 10031

Author Emails: blamb25@gmail.com, mtzortziou@ccny.cuny.edu, kmcdonald2@ccny.cuny.edu

Presenter Address: 3463 60th Street Woodside, NY, 11377

Abstract

Wetlands play a key role in Earth's carbon cycle. However, wetland carbon cycling exhibits a high level of spatiotemporal dynamism, and thus, is not as well understood as carbon cycling in other ecosystems. Accurate characterization of wetland ecosystem parameters (vegetation communities, inundation, salinity and tidal regimes) is of particular importance for understanding these carbon dynamics. Especially since a significant portion of wetland carbon transport is hydrologic rather than gaseous. Here, we use radar remote sensing to map and study wetlands within the Chesapeake Bay. The Chesapeake Bay is the largest estuary in the US with more than 1,500 square miles of tidal wetlands, across a range of tidal amplitudes, salinity regimes, and soil organic matter content levels. We seek to understand how this spatiotemporal variability impacts carbon cycling.

We have been using Sentinel-1 and ALOS PALSAR-1/PALSAR-2 observations to characterize vegetation and inundation dynamics with the future goal of characterizing salinity gradients and tidal regimes. Our initial results indicate that Sentinel-1 C-band radar is able to effectively separate open water targets from low-biomass vegetation (e.g. marsh grasses) based on backscatter. While PALSAR L-band radar more effectively separates vegetation of varying biomass based on backscatter (e.g. marsh grasses vs. mature trees). Because the aforementioned radar

satellites take multiple observations per year, they provide observations that are crucial in understanding vegetation seasonality and wetland inundation/flood regimes, something that wetlands maps produced at even a yearly interval don't do.

In addition to utilizing differences in radar backscatter, radar polarization differences and ratios are particularly effective at distinguishing between vegetated and non-vegetated areas. Utilizing these principles, we have been characterizing various wetland types using supervised classification techniques including: Random Forest, Maximum Likelihood, and Minimum Distance. The Random Forest classification approach has been demonstrated as particularly effective in wetlands mapping [1]. In addition to using radar backscatter, we have also been using positional parameters to perform these classifications. The National Wetlands Inventory has been used as training and validation data. Ideally, the techniques we outline in this research will be applicable to the characterization of wetlands in coastal areas outside of the Chesapeake Bay.

References

[1] Clewley, D., Whitcomb, J., Moghaddam, M., McDonald, K., Chapman, B., & Bunting, P. (2015). Evaluation of ALOS PALSAR Data for High-Resolution Mapping of Vegetated Wetlands in Alaska. *Remote Sensing*, 7(6), 7272–7297

Acknowledgement

This study was supported and monitored by

National Aeronautics and Space Administration (NASA) Grant #NNH13ZDA001N. The statements contained within the manuscript/research

article are not the opinions of the funding agency or the U.S. government, but reflect the author's opinions.

Electrospun Chitosan and Cyclodextrin Nanofibers For Oil Absorption

De'Marcus Robinson-

Florida A&M University School of the Environment

Co: Authors Dr. Nelly Mateeva Florida A&M University Chemistry Department

Presenters Email: demarcus1.robinson@fam.u.edu

Co Author: nelly.mateeva@fam.u.edu

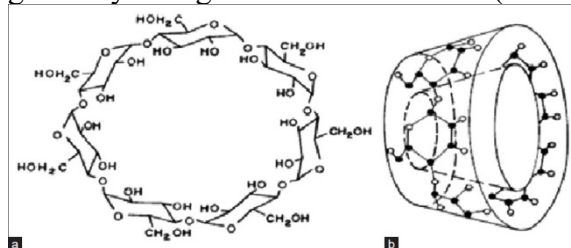
Introduction

Finding new ways to clean up oil spills in the ocean quickly and efficiently is not only vital to us, but also extremely vital for the organisms that use the ocean as a source of food, and a place to call home. During the Deep Horizon Oil Spill that leaked 200 million gallons of crude oil into the Gulf of Mexico. Corexist, one of the Horizon Oil Spill Cleanup technologies used during the oil spill, was used to disperse the oil into smaller droplets so microbes could degrade the oil. Corexist ended up causing more harm than good, and the oil leaked into the ocean for a total of eighty-seven days. Oil Skimmers, Boom, and Barriers were also used to clean the oil.

The presented study deals with utilization of novel materials based on electrospun fibers, for absorption and cleaning of oil spills. Cyclodextrins are known to be good absorbing materials for non-polar oily substances. Applying them in form of powder or solution however will be costly and collecting the absorbed material will require additional time and efforts. The suggested composite material is a porous structure based on a polymer matrix. The material also incorporates an absorbing substance, the cyclodextrin, and a surfactant to modify the generally poor solubility of the material.

β-Cyclodextrin is an oligosaccharide 7-membered sugar ring consisting of a hydrophobic central cavity and a hydrophilic outer surface. The cyclodextrins are shaped into a truncated cone rather than a cylinder and have a strong intermolecular hydrogen bond resulting in its low solubility in water.

Cyclodextrin is produced from starch and is generally regarded as safe (GRAS).



Sodium Lauryl Sulfate (SLS) ($\text{CH}_3(\text{CH}_2)_{11}(\text{OCH}_2\text{CH}_2)_n\text{OSO}_3\text{Na}$) is a surfactant and detergent that is found in many cleaning and personal care products like shampoos, and lipsticks. Polyethylene oxide (PEO) is a polyether compound, a product of a reaction of ethylene oxide and water and is synthesized by suspension polymerization.

The main objective of this research is to produce nanofiber based composite material for effective oil absorption.

Methods

Materials

All materials and solvents were purchased from Sigma Aldrich and were used without further purification. The materials were electrospun on an in-house assembled instrument.

Experimental

Different amounts of β-cyclodextrin were suspended in ethanol and a surfactant (10 – 70 mg) were added to increase the solubility. A solution of PEO in chloroform was prepared separately and the two mixtures were combined prior to the electrospinning. The mixture was stirred at room temperature for 10

¹ Figure 1. Chemical structure of β-Cyclodextrin **A** is the outer structure and **B** is the inner structure

min and electrospun using 16 gauge needle, at a rate of 0.8 mL/h. The applied voltage was 20 V and the distance to the receiving plate was 12 cm. The amounts of polymer, cyclodextrin, and surfactant were changed in different experiments while the electrospinning conditions remained the same.

Discussion and Conclusion

The morphology of the produced fibers depends on the relative ratio of the α -CD, PEO, and surfactant, as well as on the overall concentration of the solution. This is mainly related to the viscosity, but also to the electrical conductivity of the starting mixture. The white, cotton candy like material was 3-dimensional, with most of the fibers building 2-3 cm above the surface of the plate. The fiber size and structure were characterized by Scanning Electron Microscopy and Fourier Transform Infrared Spectroscopy (FTIR). Oil absorption testing is pending and the results will be related to the overall structure and composition of the matrix.

References

- [1] "Properties Of Graphene." *Graphenea*. N.p., n.d. Web. 05 Dec. 2015.
- [2] Zang, Wang. "Electrospinning β -cyclodextrin/poly(vinyl Alcohol) Nanofibrous Membrane for Molecular Capture." N.p., Aug. 2011. Web. 6 Mar. 2015.
- [3] Dang, Lei. " β -Cyclodextrin-based Oil-absorbents: Preparation, High Oil Absorbency and Reusability." N.p., Feb. 2011. Web. Mar. 2015.
- [4] Adebajo, M. O., R. L. Frost, J. T. Kloprogge, O. Carmody, and S. Kokot. "Porous Materials for Oil Spill Cleanup: A Review of Synthesis and Absorbing Properties." *SFX by Ex Libris Inc.* N.p., Sept. 2003. Web. 05 Mar. 2015.
- [5] Atta, Ayman M., Witold Brostow, Tea Datashvili, Rasha A. El-Ghazawy, Haley E. Hagg Lobland, Abdul-Raheim M. Hasan, and Jose M. Perez. "Porous Polyurethane Foams Based on Recycled Poly(ethylene Terephthalate) for Oil Sorption." N.p., 6 Sept. 2012. Web. Mar. 2015.

Long-term changes in seagrass distribution using a high-spatial resolution satellite image, historic aerial photography and field data

Mariana C. León-Pérez¹, Roy A. Armstrong², and William J. Hernandez³

¹*University of Puerto Rico Mayagüez Campus, Bio-Optical Oceanography Laboratory*

Introduction

The seagrass habitat constitutes a highly productive and ecologically valuable marine community [1]. They provide sediment stabilization and serve as nurseries and feeding grounds for a diverse number of organisms [1-5]. Past and present natural and anthropogenic factors have influenced the decline of seagrass areas worldwide [3, 4, 6]. Given the magnitude of seagrass loss, continued monitoring and adaptive management is crucial for the long term persistence of the seagrass ecosystem.

In a scenario of global climate change and increasing anthropogenic disturbances, there is a need to establish a baseline reference of seagrass distribution in order to better understand seagrass dynamics at different temporal scales. In the absence of long-term monitoring programs in Puerto Rico, historical aerial photography represents the longest record of data for studying seagrass dynamics. This study aims to estimate the long-term spatial changes in seagrass distribution at Caja de Muertos Island Nature Reserve, Puerto Rico. This study was divided into two phases. The first phase was focused on the creation of an accurate and current seagrass benthic habitat map for Caja de Muertos Island, while the second phase aimed to reconstruct the historic distribution of seagrass at the study area.

Methods and Conclusions

The benthic habitat map was created using a 2014 WorldView-2 satellite image and by integrating a combination of mapping techniques, including an Object-Based Image

Analysis (OBIA). A total of 164 sampling sites were used to calibrate and validate the map. Vertical spectral profiles of downwelling irradiance were measured using a Satlantic HyperPro spectroradiometer and used to calculate spectral attenuation coefficients (K_d) at two sites on the North and West of the island.

For the second phase of the study, an OBIA approach and a visual interpretation were used to assess seagrass changes using a recent high-spatial resolution satellite image and historical aerial photography from 1950 to 2014. Four zones with continuous data for the studied period were analyzed.

Benthic habitats, including seagrass, were mapped with an overall accuracy of 82.76%. The dominant seagrass species were *Thalassia testudinum*, and *Syringodium filiforme*, which were mainly located in the West and North of the island. Light availability was not a limiting factor for seagrass colonization at the study area. The time series analysis revealed an overall increase in seagrass extent of 64% over the studied period. This increase was mainly driven by an increase in the patchy seagrass cover, which was also the most persistent cover for the 64-year period. This result contrasts with many reports documenting a worldwide reduction in seagrass area [4]. Differences in seagrass extent were observed both between zones and between years, which were mainly related to the influence of natural factors.

This is the first study in Puerto Rico which assesses the spatial distribution of seagrass in a time scale of over six decades. Additionally, the method presented here

represents an alternative technique to map and monitor seagrass distribution in the absence of long-term in situ monitoring data. The data provided could be used in future management decisions within the Reserve and as a baseline to compare future changes in seagrass distribution.

References

- [1] J.C. Zieman, R.T. Zieman, U.S. Fish Wildl. Serv. Biol. Rep. **85** (1989) 155.
- [2] R. Costanza, R. d'Arge, R. de Groot, S. Farber, M. Grasso, B. Hannon, K. Limburg, S. Naeem, R.V. Oneill, J. Paruelo, R.G. Raskin, P. Sutton, M. van den Belt, Nat. **387** (1997) 253-260.
- [3] C.M. Duarte, Environ. Conserv. **29** (2002) 192-206.
- [4] R. Orth, T. Carruthers, W. Dennison, C. Duarte, J. Fourqurean, K. Heck, A.

Hughes, G. Kendrick, W. Kenworthy, S. Olyarnik, F. Short, M. Waycott, S. Williams, Bioscience **56** (2006) 987-996.

- [5] M. Wacott, C.M. Duarte, T.J.B. Carruthers, R.J. Orth, W.C. Dennison, S. Olyarnik, A. Fourqurean, K.L. Heck, A. Hughes, G. Kendrick, W. Kenworthy, F. Short, S. Williams, Proc. Natl. Acad. Sci. **106** (2009) 12377-12381.
- [6] F. Short, S. Wyllie-Echeverria, Environ. Conserv. **23** (1996) 17.

Acknowledgement

This study was supported by National Oceanic and Atmospheric Administration (NOAA) Cooperative Remote Sensing Science and Technology Center (CREST) under Grant NOAA/EPP Grant # NA11SEC4810004 and by the Puerto Rico Sea Grant College Program.

Estimate CDOM and DOC in estuarine waters in the Chesapeake Bay and the Gulf of Mexico from ocean color

Fang Cao*, Maria Tzortziou

The City University of New York-City College of New York, New York, NY 10031

*Corresponding author (fcaony@gmail.com)

Introduction

Tidal wetlands and estuaries are dynamic features of coastal ocean and play critical roles in the global carbon cycle. Exchanges of dissolved organic carbon (DOC) between tidal wetlands and adjacent estuaries have important implications for carbon sequestration in tidal wetlands as well as biogeochemical cycling of wetlands derived material in the coastal zones. Recent studies demonstrated that the chromophoric dissolved organic matter (CDOM), as the optically active fraction in DOC, can be derived from ocean color observations and also can be a proxy to accurately retrieve DOC in some coastal waters. Herein we developed ocean color algorithms to estimate DOC and CDOM from ocean color based on a synthesis of existing field observations collected in the Chesapeake Bay (GEO-CAPE CBODAQ field campaign, July 11-20, 2011) and the Gulf of Mexico (GoMex field campaign, Sep. 09-22, 2013).

To better quantify the carbon flux between the interfaces of tidal wetlands and their adjacent estuaries, satellite data with high spatial resolution are required to provide a synoptic view of the dynamic processes. We pursued to generate remote sensing reflectance at 645 nm (R_{rs645}) from MODIS-Aqua, with a spatial resolution of 250 m during these two field campaigns, using the approach proposed by D. Aurin [1]. This provides promising tools to further estimate carbon budget between tidal wetlands-estuaries interfaces from space.

Results from this work will benefit of quantifying long term carbon fluxes from satellite observations in the US estuaries.

Experiments and Conclusions

Retrievals of CDOM absorption and CDOM absorption spectral slope, $S_{275-295}$, were based on least square multiple linear regressions (MLR) relating $a_{CDOM}(\lambda)$ and $S_{275-295}$ to multiple remote sensing reflectance (R_{rs}) bands across the spectrum measured by different satellite ocean color sensors (namely, MODIS-Aqua and MERIS). Dissolved organic carbon concentrations were, then, estimated based on the tight relationship between the DOC-specific CDOM absorption and CDOM absorption spectral slope. Remote sensing retrievals of CDOM, $S_{275-295}$ and DOC were applied to satellite-retrieved R_{rs} from MODIS-Aqua (1-km resolution at nadir) and MERIS (full resolution, 300 m resolution at nadir). The relative error (mean absolute percent difference; MAPD) for the MLR retrieval of $a_{CDOM}(280)$ was 34%, for a large dynamic range (0.5-9.8 m^{-1}). The MADP for DOC was 33% (values in the range of 88-220 $\mu mol/L$). The MADP for the spectral slope $S_{275-295}$ was 8.6% and values ranged from 0.018 nm^{-1} to 0.048 nm^{-1} .

Our results in the Chesapeake Bay highlight the importance of freshwater inputs (tributaries and Susquehanna) and wetlands (e.g., Blackwater Refuge marshes along the western shoreline) as sources of strongly absorbing, DOC-rich, and low spectral slope dissolved organic matter. In the Gulf of Mexico, strong gradients from the shoreline to offshore waters were observed, in good agreement with field observations (e.g., results

from NASA's GoMex campaign). The impact of the Mississippi outflow and coastal wetlands (e.g., Marsh Island) on CDOM optical properties (absorption magnitude and shape) and DOC gradients was also captured in the MERIS satellite imagery.

To better quantify the carbon flux between the interfaces of tidal wetlands and their adjacent estuaries, satellite data with high spatial resolution are required to provide a synoptic view of the dynamic processes. We generated remote sensing reflectance at 645 nm (R_{rs645}) from MODIS-Aqua, with a spatial resolution of 250 m using the approach proposed by D. Aurin (Aurin et al., 2013). Retrievals were applied to the Chesapeake Bay estuarine waters and Gulf of Mexico coastal environment. This approach provides a

promising tool to further estimate carbon budget between tidal wetlands-estuaries interfaces from space.

References

- [1] D.A. Aurin, A. Mannino, B.A. Franz, Remote Sensing of Environment, 137 (2013), pp. 212–225

Acknowledgement

Financial supports from NASA (Carbon Cycle Science MarshCycle program NNX14AP06G and Carbon Cycle Synthesis project NNX14AM37G) are greatly acknowledged. We thank M. Ondrusek, Z-P. Lee, A. Mannino for contributing ocean color and CDOM data to the SeaBASS.

Surface Modification of Polyethersulfone Membrane to Control Organic Fouling.

Efosa Igbiginun*, Yaolin Liu, Ramamoorthy Malaiasamy, Kimberly Jones, and Vernon Morris*

*Department of Chemistry**
Department of Civil and Environmental Engineering
Howard University

ABSTRACT

Humic acid is a complex organic carbon nutrient found in coastal waters that aids the proliferation of algae-bloom causing micro-organisms, and also forms precursors of carcinogenic disinfection by-products. This study presents a nano-composite membrane filtration system that has the potential of reducing the high concentration of humic acid in surface water, and controlling of organic fouling most likely to occur on the membrane surface during surface water treatment. Through a three-step surface modification technique, a thin film of allylamine-modified graphene oxide polymer was chemically attached onto a commercial microfiltration polyethersulfone (PES) membrane. The surface modification approach produced a nano composite membrane with improved surface chemistry and anti-organic fouling properties. The modified membrane showed better resistance to humic acid fouling and rejection compared to unmodified PES membrane.

Introduction

The use of microfiltration (MF) membrane in water/wastewater treatment is limited by two factors: hydrophobic surface and relatively low rejection rates on contaminants.^{1, 2, 3} The hydrophobic nature of MF membranes is strongly linked to membrane fouling, where hydrophobic organic particles or microbes are attracted to the membrane surface through hydrophobic-hydrophobic interaction.⁴ Consequently, the fouled MF membranes result into high energy consumption with low membrane life time and low water quality. Surface modification of these membranes via chemical functionalization with graphene oxide GO nanosheets has been explored to address the problem of organic fouling during water treatment. In this study, different concentrations (2, 4, and 6wt. %) of GO were synthesized and used to modify a polyethersulfone (PES) MF membrane pretreated with amino functional groups. The resulting GO composite membrane is stable and possesses a typical ultrafiltration (UF) membrane properties based on water flux and

MWCO. The 4wt% GO membrane was selected for the anti-fouling study because it showed low water flux decline and high humic acid rejection compared to the other GO formulations.

Experiments and Conclusions

Graphene oxide nanosheets were produced from chemical oxidation of graphite powder using the Hummers' method. The GO nano sheets synthesized were confirmed using the FT-IR and Raman spectroscopy. Polyethersulfone micro filtration membranes (0.1 μ m) were pre-treated via UV induced graft polymerization of allylamine on the PES membrane active surface. Then, solutions of 1,3,5-tricarbonyl trichloride, TMC (cross-linker) dissolved in hexane and GO dispersed in acetonitrile were spin coated onto the surface of the polyallylamine modified PES membrane, respectively. The surface morphology and roughness of the modified membrane were observed using the scanning electron microscopy and the atomic force microscopy, respectively. The anti-fouling and rejection performance of the GO-modified

membrane against humic acid, modeled as the organic foulant, was investigated in cross flow filtration system. The anti-fouling performance of the GO-4 modified membrane was compared to a commercial ultrafiltration membrane because they both showed similar molecular weight cut-off and water permeability. The addition of graphene oxide nano sheets onto the polymeric membrane surface improved the surface properties of the membrane such as high surface charge, hydrophilicity, and less surface roughness, which contributed in mitigating the adhesion of humic acid onto the surface of the GO-modified membrane. This study has demonstrated a simple approach of covalently attaching GO onto PES membrane surface to reduce organic foiling during water treatment. The GO modified membrane did not only showed higher resistance to organic fouling and rejection but also improved pure water flux recovery after hydraulic cleaning when compared to unmodified commercial UF membrane.

References

- [1] Van der Bruggen, B.; Manttari, M.; Nystrom, M. *Separation and Purification Technology* **2008**, *63*, 251-263.
- [2] Vatanpour, V.; Madaeni, S. S.; Khataee, A. R.; Salehi, E.; Zinadini, S.; Monfared, H. A. *Desalination* **2012**, *292*, 19-29.
- [3] Maximous, N.; Nakhla, G.; Wan, W.; Wong, K. *Journal of Membrane Science* **2009**, *341*, 67-75.
- [4] Lee, S. Y.; Kim, H. J.; Patel, R.; Im, S. J.; Kim, J. H.; Min, B. R. *Polym. Adv. Technol.* **2007**, *18*, 562-568.

Acknowledgement

This material is based upon work supported by the National Science Foundation (NSF) and the Environmental Protection Agency (EPA) under NSF Cooperative Agreement EF-0830093, Center for the Environmental Implications of NanoTechnology (CEINT)

and the National Oceanic and Atmospheric Administration, Office of Education, Educational Partnership Program Award # NA11SEC4810003. Any opinions, findings, conclusions or recommendations expressed in this material are those of the author(s) and do not necessarily reflect the views of the NSF or EPA. This work has not been subjected to EPA review and no official endorsement should be inferred. Its contents are solely the responsibility of the award recipient and do not necessarily represent the official views of the U.S. Department of Commerce, National Oceanic and Atmospheric Administration.

Onsite Bioremediation of Hydrocarbons Using Anaerobic Processes.

Brian Wartell and Michel Boufadel
Center for Natural Resources Development and Protection (NRDP)
John A. Reif, Jr. Dept. Civil and Environmental Engineering
The New Jersey Institute of Technology
Room 426 Colton Hall
323 MLK Blvd, Newark, NJ 07102-1824
Ph: 973-596-6079
<http://nrdp.njit.edu>; baw9@njit.edu

Abstract

Hydrocarbon contamination from offshore oil spills and onshore hydrocarbon releases occupy large portions of North Jersey coastal waters. The contamination could result both from natural events, such as Hurricane Sandy and anthropogenic activities, such as leaking tanks. Oil pollution can be deep within the sediment due to subsequent sedimentation after the oil binds to sediments in the water column and sinks to the bottom of the water body. And while oil components biodegrade aerobically readily (within a year), deeply buried oil could reside in an anaerobic environment (i.e. lacking oxygen) for decades. The organisms present in these environments are largely anaerobic bacteria and archaea, and research has shown that they have the ability to degrade certain oil components (alkanes and single ring aromatics) in the laboratory. However, they have not been shown to readily biodegrade the polycyclic aromatic hydrocarbons (PAHs), which are very toxic and mutagenic. Thus, there is much interest in their removal due to their potentially harmful effects to both environmental and human health. The PAHs average around 5% of the oil total oil mass.

Introduction

Technologies for cleanup include oxidation techniques such as ozone or persulfate as a pretreatment to anaerobic degradation. The oxidation techniques allow for the fragmenting and decomposition of larger complex molecules that allow for easier utilization by the organisms present. It is a technique that has been used widely for aerobic treatment but only recently as a practical part of anaerobic solutions.

Tools to analyze metabolic pathways are key in determining the processes taking place and can include basic identification through machines such as a GC/MS (gas chromatograph/mass-spectrometer) or more complex methods such as hydrogen isotope fractionation. Biodegradation rates and co-metabolic activities of anaerobic organisms are also not well understood and are strongly influenced by the populations present (or added), the electron acceptors, and electron donors that are available.. Sulfate-reduction

techniques can be coupled with methanogenic conditions as well iron-reducing conditions to maximize biodegradation potential, although the extent of interaction and its success is largely debated and still being researched. Nitrate-reduction is also somewhat promising but only seems to work under specific conditions and has a higher likelihood of being inhibited, especially when being paired with sulfate-reducing organisms.

Our investigation aims at creating the optimal conditions for microorganisms to break down the PAHs. We report preliminary results of laboratory studies in flasks and in sediments suggesting variable success in biodegrading the PAHs as well as future initiatives and recent literature findings. Our goal was to modify or discover techniques that can present major cost and environmental benefits in comparison with other techniques, such as dredging the sediments.

We will be investigating degradation conditions, nutrient availability, and oxidation techniques and monitor the types of metabolites produced. In addition, we aim to characterize the predominant populations in hopes of bioaugmenting contaminated sites when needed. While anaerobic PAH degradation research is still somewhat in its infancy, especially for those compounds with 4+ rings, the amount of information provided and suggested to date will function as valuable clues to pave the way to help explore and expedite future breakthroughs.

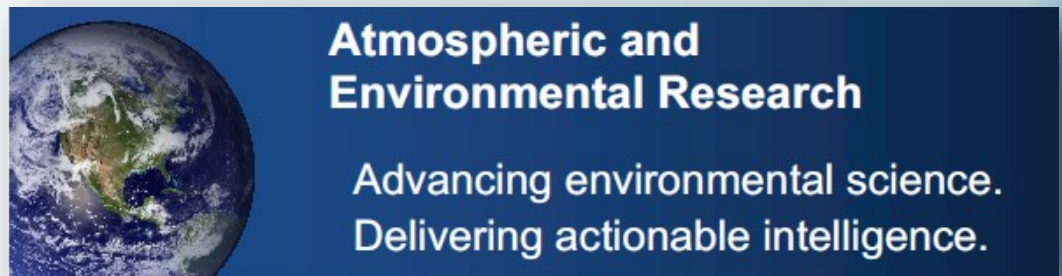
Our preliminary findings suggest that the addition of microorganism or an easy-to-degrade substrate is needed for enhancing the biodegradation of PAHs.

Supporting NOAA's Education Partnership Program with Minority Serving Institution (EPP/MSI) mission to build a strong and diverse STEM workforce; the following are Corporate Sponsors to the EPP/MSI Eighth Biennial Education and Science Forum.



SCIENCE SYSTEMS AND APPLICATIONS, INC.

Science and Technology with Passion



NOAA Educational Partnership Program with Minority Serving Institution (EPP/MSI)

The National Oceanic and Atmospheric Administration (NOAA) Educational Partnership Program with Minority Serving Institutions (EPP/MSI) is increasing programs and opportunities for individuals to pursue applied research and education in atmospheric, oceanic, and environmental sciences and remote sensing technology, in support of NOAA's mission. www.epp.noaa.gov

NOAA Center for Atmospheric Sciences (NCAS), Howard University, DC

Student education and training through research focused on improving the accuracy of weather and climate forecast models. NCAS has developed two primary research themes: Air Quality Forecasting and Analyses and Climate and Weather Forecasting and Analyses. <http://ncas.howard.edu/>

NOAA Cooperative Remote Sensing Science and Technology (CREST), Center, The City University of New York, NY

Student education and training through research that focuses on all aspects of remote sensing, including: sensor development, satellite remote sensing, ground-based field measurements, data processing and analysis, modeling and forecasting. www.noacrest.org

NOAA Environmental Cooperative Science Center (ECSC), Florida A&M University, Tallahassee, FL

Student education and training through innovative courses and degree programs at all levels and by engaging in research in ecological processes, geospatial analysis, integrated social science, integrated ecological assessment and any combination of these in support of environmental decision making. www.ecsc.famu.edu/

NOAA Living Marine Resources Cooperative Science Center (LMRCSC), University of Maryland Eastern Shore, Princess Anne, MD

Students education and training through marine and fisheries sciences, to prepare for careers in research, management and public policy that support the sustainable harvest and conservation of our nation's living marine resources. <https://www.umes.edu/lmrcsc/>

For more information on NOAA CSCs please visit: www.epp.noaa.gov

**NOAA-Cooperative Science Centers are funded by NOAA EPP/MSI Cooperative Agreements
NA11SEC4810001 - 4 (2011-2016)**

Disclaimer: THE NOAA EMBLEM IS A REGISTERED TRADEMARK OF THE U.S. DEPARTMENT OF COMMERCE, USED WITH PERMISSION.



Photo Credit: CCNY Website

Acknowledgement

The NOAA EPP/MSI Forum Executive Committee wishes to acknowledge the outstanding contributions of the many individuals and enterprises that made the Eighth Biennial Education and Science Forum a success. To the participants and all who engaged in the planning through execution phases of the Forum - for whatever part you played - **thank you!** Your unwavering support for the goals of NOAA mission aligned education training and scientific research is greatly appreciated. The collective commitment of all participants to develop a world class diverse next generation STEM workforce is acknowledged.

EPP/MSI Eighth Biennial Education and Science Forum 2016 Proceedings

Copyright© NOAA EPP/MSI and NOAA CREST. All Rights Reserved.

August 2016